THE UNIVERSITY OF CHICAGO

ESTABLISHING A CONSISTENT THEORY OF TRANSPORT IN STRONGLY CORRELATED FERMI SUPERFLUIDS

A DISSERTATION SUBMITTED TO
THE FACULTY OF THE DIVISION OF THE PHYSICAL SCIENCES
IN CANDIDACY FOR THE DEGREE OF
DOCTOR OF PHILOSOPHY

DEPARTMENT OF PHYSICS

BY

RUFUS M. BOYACK

CHICAGO, ILLINOIS
AUGUST 2017

CONTENTS

LIST OF FIGURES vii

ACKNOWLEDGMENTS ix

ABSTRACT x

1 INTRODUCTION 1
1.1 A brief history of gauge invariance and symmetry breaking 1
1.2 Symmetries of BCS theory 4
1.3 BCS-BEC crossover theory 8
1.4 BCS-BEC in spin-orbit coupled topological superfluids 11
1.5 Fulde-Ferrell and pair-density-wave superfluids 13
1.6 Thesis outline 17

2 SIGNATURES OF PAIRING AND SPIN-ORBIT COUPLING IN CORRELATION FUNCTIONS OF FERMI GASES 19
2.1 Introduction 19
2.2 Background theory 21
2.3 Density/current response and f-sum rules 24
2.4 Spin response and f-sum rules 26
2.5 Correlation functions in the helicity basis 27
2.6 Numerical results 28
2.7 Conclusions 30

3 TOPOLOGICAL EFFECTS ON TRANSITION TEMPERATURES AND RESPONSE FUNCTIONS IN THREE-DIMENSIONAL FERMI SUPERFLUIDS 31
3.1 Introduction 31
3.2 Topological superfluids 33
3.3 Fluctuation formalism 34
3.4 Phase diagram 37
3.5 Frequency dependent spin and density response functions 39
3.6 Conclusions 42

4 EXACT CORRELATION FUNCTIONS IN THE CUPRATE PSEUDOGAP PHASE: COMBINED EFFECTS OF CHARGE ORDER AND PAIRING 43
4.1 Introduction 43
4.2 Full vertex and Ward-Takahashi identity 46
4.3 Behavior of the neutron cross section: comparison between pseudogap theories . . 50
4.4 Conclusions 53

5 GAUGE INVARIANT THEORIES OF LINEAR RESPONSE FOR STRONGLY CORRELATED SUPERFLUIDS 54
5.1 Introduction 55
5.2 Correlation effects beyond BCS theory: Ward-Takahashi identity 58
5.2.1 Kubo formulae 58
5.2.2 Full vertex and Ward-Takahashi identity 61
5.2.3 Collective mode vertices 63
5.2.4 Λ^{μ} vertex correction 67
5.3 Alternative approach to Ward-Takahashi: Path integral 71
5.3.1 Gauge-invariant electrodynamics 71
5.3.2 Inconsistency with the compressibility sum rule 74
5.4 Conclusions 77

6 GOING BEYOND THE BCS LEVEL IN THE SUPERFLUID PATH INTEGRAL: A CONSISTENT TREATMENT OF ELECTRODYNAMICS AND THERMODYNAMICS 79
6.1 Introduction 79
6.2 Path integral and mean-field formalism 82
6.3 Response functions at saddle-point level 83
6.4 Beyond saddle point 85
6.5 Compressibility sum rule 87
6.6 Gaussian fluctuations 88
6.7 Amplitude and phase fluctuations 88
6.8 Conclusions 89

7 COLLECTIVE MODE CONTRIBUTIONS TO THE MEISSNER EFFECT: FULDE-FERRELL AND PAIR-DENSITY WAVE SUPERFLUIDS 91
7.1 Introduction 91
7.2 Theoretical formalism 95
7.2.1 Mean-field formalism 95
7.2.2 Electromagnetic response and Ward-Takahashi identity 96
7.2.3 Collective mode vertices 97
7.3 Superfluid density 99
7.3.1 Superfluid density derivation via Kubo formula 99
7.3.2 Superfluid density derivation via equilibrium current 100
7.4 Numerical results 101
7.5 Conclusions 103

8 CONCLUSIONS 105

A SIGNATURES OF PAIRING AND SPIN-ORBIT COUPLING IN CORRELATION FUNCTIONS OF FERMI GASES 109
A.1 Overview of present pseudogap formalism 109
A.2 Green's functions and self energy in the helicity basis 112
A.3 Full vertex and Ward-Takahashi identity 114
A.3.1 Deriving the full electromagnetic vertex 114

A.3.2 f-sum rule and longitudinal sum rule . . . 115
A.4 Spin-spin correlation functions and sum rules . . . 117
A.4.1 General sum rules for spin density-spin density correlation functions . . . 117
A.4.2 Explicit spin-spin correlation functions and sum rules for Rashba SOC . . . 119
A.5 Superfluid density . . . 120

B TOPOLOGICAL EFFECTS ON TRANSITION TEMPERATURES AND RESPONSE FUNCTIONS IN THREE-DIMENSIONAL FERMI SUPERFLUIDS . . . 122
B.1 Derivations of the vertex function $\Gamma(Q,T)$ and coherence factors . . . 122
B.2 Density and spin correlation functions . . . 124

C EXACT CORRELATION FUNCTIONS IN THE CUPRATE PSEUDOGAP PHASE: COMBINED EFFECTS OF CHARGE ORDER AND PAIRING . . . 126
C.1 Inclusion of both charge-density-wave and pair-density-wave effects . . . 126
C.2 Relation between sum rules and the Ward-Takahashi identity . . . 132
C.2.1 f-sum rule . . . 132
C.2.2 Longitudinal sum rule . . . 133
C.3 Spin response functions . . . 134

D GAUGE INVARIANT THEORIES OF LINEAR RESPONSE FOR STRONGLY CORRELATED SUPERFLUIDS . . . 136
D.1 Deriving the full electromagnetic vertex . . . 136
D.2 Collective mode vertices . . . 139
D.3 Specific examples for the Λ^{μ} vertex correction . . . 141
D.3.1 Pairing pseudogap approximation . . . 141
D.3.2 YRZ . . . 141
D.3.3 Particle-only t-matrix . . . 142
D.4 f-sum rule and longitudinal sum rule . . . 147

E GOING BEYOND THE BCS LEVEL IN THE SUPERFLUID PATH INTEGRAL: A CONSISTENT TREATMENT OF ELECTRODYNAMICS AND THERMODYNAMICS 150
E.1 Partition function . . . 150
E.1.1 Saddle point for $A_{\mu} \neq 0$ . . . 152
E.1.2 Beyond saddle point . . . 154
E.2 General response kernel . . . 156
E.2.1 Functional chain rule . . . 156
E.2.2 Gap equation and collective mode vertices . . . 158
E.2.3 Second order fluctuation of $\Delta^{\mathrm{mf}}[A]$ . . . 160
E.3 Proving gauge invariance . . . 161
E.3.1 Useful contraction formulas . . . 162

F COLLECTIVE MODE CONTRIBUTIONS TO THE MEISSNER EFFECT: FULDE-FERRELL AND PAIR-DENSITY-WAVE SUPERFLUIDS . . . 168
F.1 Mean-field formalism . . . 168
F.1.1 Green's functions . . . 168

F.1.2 Mean-field equations . . . 171
F.2 Full vertex and Ward-Takahashi identity . . . 173
F.3 Gap equation and collective mode vertices . . . 175
F.4 Superfluid density derivation via Kubo formula . . . 180
F.4.1 Kubo formula analysis . . . 180
F.4.2 Comparison of bubble term with the literature . . . 182
F.5 Superfluid density derivation via equilibrium current . . . 184
F.5.1 Equilibrium current analysis . . . 184
F.5.2 Vanishing of the superfluid density in directions transverse to Q . . . 188
F.6 Thermodynamic potential and stability criteria . . . 189

BIBLIOGRAPHY . . . 193

LIST OF FIGURES

2.1 Phase diagrams for a degenerate Fermi gas without (a) and with (b) SOC. Plotted is T^* as a function of inverse scattering length, $1/k_F a$, indicating where pairing first sets in, while T_c marks the onset of condensation to the superfluid phase. The plot shows the weakly interacting regime with $1/k_F a < 0$. As spin-orbit coupling is turned on, pairing is enhanced leading to a larger pseudogap region. The inset in (a) indicates the temperature dependence of the component gap parameters (defined in the text) at unitarity, $1/k_F a = 0$. 23

2.2 The spin-spin response function as a function of frequency. Figure 2.2(a) corresponds to a pseudogap phase without SOC. The peak at lower ω reflects thermally excited fermions while the second peak is at ω comparable to the pseudogap energy scale, where pairs are now broken. Since $\lambda = 0$, the spin-spin and density-density correlation functions are the same. In Fig. 2.2(b) the pseudogap is set to zero with fixed $\lambda = 1.2k_F$. The lower energy intra-helicity band peak is enhanced and one observes an SOC-related peak. As shown in the inset, the low-energy threshold reflects the onset of inter-helicity band transitions, while the high-energy endpoint occurs when these transitions are no longer possible. In Fig. 2.2(c), in the presence of both a pseudogap and SOC, one sees a combination of the effects in the previous two panels. Spectral weight is transferred to yield a larger SOC peak, reflecting the gapping of the low energy contributions. All quantities are measured relative to the Fermi energy, E_F, or Fermi momentum k_F. 28

3.1 Phase diagrams for the superfluid temperature T_c and (where shown) the mean-field transition temperature T^*. The $T = 0$ topological phases are indicated by shaded regions in light (dark) blue color with 2 (4)-Weyl points. The top two panels show the dependence on either SOC strength λ (left) or scattering length $1/k_F a$ (right), with other parameters fixed. The lower panels show T_c versus b_z with $\lambda/k_F = 1$ for both panels, $1/k_F a = -1$ on the left and $1/k_F a = 2$ on the right. Dotted lines indicate $\delta\mu = 0$. Once a topological phase is entered the system becomes more BCS-like. . . . 36

3.2 Evolution of the dispersion as the topological transition is crossed by tuning b_z. In the weak pairing limit (top panel), the system smoothly evolves across the transition, whereas for enhanced pairing (bottom panel) there is a more abrupt change in band-structure. In all plots we show constant energy contours $+E_{-1,\mathbf{k}}/E_F$ at unitarity, with $k_\perp$ and $k_\parallel$ in units of k_F. For panels (a)-(c) we set $\lambda/k_F = 0.5$ and the magnetic field $b_z/E_F = 0.4, 0.6, 0.8$, whereas for panels (d)-(f) we set $\lambda/k_F = 1$ and $b_z/E_F = 1.2, 1.7, 1.8$ respectively. Only the left-most figures are in a trivial phase. 39

3.3 Contrast between topological (solid, red) and trivial (dashed, black) phases of the frequency dependent spin-spin [panel (a)] and density-density [panel (b)] correlation functions. Both response functions are calculated at $1/k_F a = 0$ and $\lambda/k_F = 1$, with respective wave-vectors of $\mathbf{q} = 0$ and $\mathbf{q} = 0.5k_F\hat{z}$ for the spin and charge responses. The inset in panel (b) shows the energy contours of $E^{(2,+)}(\mathbf{k}, \mathbf{q})/E_F$ in the topological phase, with $k_\perp$ and $k_\parallel$ in units of k_F. The dashed lines highlight the saddle point Van Hove singularity whose magnitude determines the frequency location of the peak response in panel (b). 41

4.1 Comparison of the spin-density correlation function $\mathrm{Im}\chi_0(Q) = -\mathrm{Im}P_S^{00}(\mathbf{q},\omega)$ for three different values of $\mathbf{q}$ in Amperean, d-wave, and YRZ pseudogap theories. In (a) we have labeled the Van Hove peaks appearing in the d-wave theory, which appear as saddle points in the contour plot of Fig. (4.2). Here we use the band structure given in Ref. [Comin et al., 2014] with $T = 0.01$ and a broadening of $\Gamma = 0.01$. The doping $p = 0.12$ and the chemical potential μ is fixed by the Luttinger sum rule. The band structure and frequency are all normalized by t, and the gap function has an amplitude of $\Delta_0 = 0.15$. For the Amperean theory we use a k_x, k_y-symmetrized Gaussian [Lee, 2014] gap function. 51
4.2 The equal energy contours $E_2(\mathbf{k}) \equiv E_{\mathbf{k}} + E_{\mathbf{k}+\mathbf{q}}$, which appear as the integrand in $\mathrm{Im}\chi_0(\mathbf{q},\omega)$, for both (a) d-wave and (b) the Amperean pseudogap schemes. Here $\mathbf{q} = (\pi,\pi)$. Note there are several energy scales as indicated by the legend. The labels A and B indicate the location of the saddle points of $\mathrm{Im}\chi_0(\mathbf{q},\omega)$. 52

5.1 Feynman diagram for the gap equation $\Delta_{\mathrm{sc}}/g = \Delta_{\mathrm{sc}} \sum_k G_0^{\alpha}(-k)G(k)$. 64
5.2 Self-consistent equation for the collective modes after performing all possible vertex insertions in the gap equation of Eq. (5.6). 64
5.3 Feynman diagrams for the two particle response function $P^{\mu\nu}(q)$, given a self energy of the form in Eq. (5.5). The order of appearance of the diagrams, from top to bottom and left to right, corresponds directly to the order of appearance of terms in Eq. (5.8). The pseudogap approximation corresponds to $\alpha = 0, \Sigma_{\mathrm{corr}}(k) = -\Delta_{\mathrm{pg}}^2 G_0(-k)$, for the YRZ model $\alpha = 1, \Sigma_{\mathrm{corr}}(k) = -\Delta_{\mathrm{pg}}^2 G_0(-k)$, and for the t-matrix model $\alpha = 1, \Sigma_{\mathrm{corr}}(k) = \sum_l t(l)G(l-k)$. 70

7.1 Superfluid density as a function of temperature for the FF phase (a) at unitarity $(1/k_F a = 0)$ and with polarization $p = (n_\uparrow - n_\downarrow)/n$ set to $p = 0.75$, (b) in the near-BCS regime $(1/k_F a = -0.5)$ with polarization $p = 0.4$. The blue curves plot the full expression for n_s^{zz}/n, given in Eq. (7.11), while the red curves plot the bubble contribution alone, given in the first term of Eq. (7.11). The green curves plot n_s^{xx}/n; in this case there are no collective modes and so the bubble and full expressions are equivalent. In agreement with symmetry considerations, for all $T < T_Q$, $n_s^{xx}/n = 0$. 102

C.1 All twenty one Feynman diagrams which contribute to the response functions $P^{\mu\nu}(Q)$. The wavy lines denote either Δ_1 or Δ_2, whereas the dashed lines denote either C_1 or C_2. The various Green's functions are labeled. The order of the Feynman diagrams, from left to right and top to bottom, corresponds to the terms appearing in Eq. (C.13). . 130

F.1 Feynman diagram for the self energy $\Sigma_\sigma(k) = -|\Delta|^2 G_{0,\bar{\sigma}}(-k+Q)$. 174
F.2 Feynman diagrams for the full vertex $\Gamma_\sigma^\mu(k_+,k_-)$ appearing in response functions. . . 174
F.3 Feynman diagram for the gap equation $\Delta/g = \sum_k \Delta G_{0,\downarrow}(-k+Q)G_\uparrow(k)$. 176
F.4 Self-consistent equation for collective mode vertices after performing all possible vertex insertions in the gap equation. 177
F.5 Feynman diagram for the equilibrium current $j^z(Q)$. 185
F.6 Feynman diagrams of the derivative of the equilibrium current, $j^z(Q)$, with respect to Q. For convenience, here $\widetilde{k}_+ = k + Q/2$ has been used. 187

ACKNOWLEDGMENTS

I tender my most sincere thanks to my supervisor, Professor Kathryn Levin, for her guidance and support throughout my graduate studies. I am thankful to my collaborators, Dr. Brandon M. Anderson and Dr. Chien-Te Wu, for their important contributions to our collaborative work. Finally, I thank my thesis committee members: Professor Arvind Murugan, Professor David Schuster, and Professor Savdeep Sethi for their time commitments.

ABSTRACT

A diagrammatic method of obtaining exact gauge-invariant response functions in strongly correlated Fermi superfluids is implemented for several example condensed matter systems of current interest. These include: topological superfluids, high temperature superconductors, and superfluids with finite center-of-mass momentum pairing known as Fulde-Ferrell superfluids. Much of the literature on these systems has focused on single-particle properties or alternatively has invoked simple approximations to treat response functions. The goal is to show that, for this wide class of topical problems, one can compute exact response functions. This enables assessment of the validity of different physical scenarios and allows a very broad class of experiments to be addressed.

The method developed is based on deriving the full electromagnetic vertex, which satisfies the Ward-Takahashi identity, and determining the collective modes in a manner compatible with the self-consistent gap equation. In the condensed phase of a superfluid and a superconductor, where gauge invariance is spontaneously broken, it is crucial to determine the collective modes from the gap equation in a manner which restores gauge invariance. Our diagrammatic framework provides a very general and powerful method for obtaining these collective modes in a variety of strongly correlated Fermi superfluids. We show that a full electromagnetic vertex satisfying the Ward-Takahashi identity ensures the f-sum rule is satisfied and thus charge is conserved.

This diagrammatic method is implemented for both normal and superfluid phases. While there are no collective modes in the normal phase, the Ward-Takahashi identity plays a similarly important role. In particular, for the normal phase we study Rashba spin-orbit coupled Fermi gases with intrinsic pairing in the absence and presence of a magnetic field. Exact density and spin response functions are obtained, even in the absence of a spin conservation law, providing signatures of topological order. Another set of examples studied in the normal phase include a broad collection of models of the cuprate pseudogap. For these cases too, the exact response functions are obtained and signatures of each model are identified. A detailed discussion of the superfluid phase is provided by the study of Fulde-Ferrell superfluids. The generally omitted collective modes are computed and the exact gauge-invariant response is obtained. The first complete calculation of the

superfluid density, incorporating the collective mode contribution and without any assumptions on the size of the gap, is provided. It is found that the amplitude mode causes the superfluid to become unstable at temperatures much lower than the mean-field transition temperature.

As an alternative to the diagrammatic approach, the functional path integral technique for Fermi superfluids is presented. While this approach is widely studied in the literature, it is of restricted utility, in comparison to the diagrammatic approach presented here, due to the inability to perform the functional integral except in very limited cases. A short coming in the current literature is identified, in that the standard method of deriving gauge-invariant electrodynamics leads to a violation of the compressibility sum rule. It is found that to satisfy this sum rule the amplitude mode of the order parameter must be incorporated. A reformulation of the path integral method for Fermi superfluids is derived, which has both gauge-invariant electrodynamics and thermodynamics compatible with the compressibility sum rule, to all orders of approximation.

CHAPTER 1

INTRODUCTION

In this thesis the electromagnetic response of a variety of strongly correlated Fermi superfluids is considered. The overarching theme is that exact gauge-invariant response functions can be calculated by using a diagrammatic approach based on the Ward-Takahashi identity or a functional integral approach based on the path integral, depending on the system under study. The electromagnetic response of these systems exhibits very rich and diverse phenomena, and showcases how many ideas from quantum field theory can be utilized in a condensed matter context. The goal is to use this formalism to study a wide class of topical condensed matter problems and, using the exact response functions, address a very broad class of experimentally accessible transport phenomena.

1.1 A brief history of gauge invariance and symmetry breaking

The first successful microscopic theory of superconductors was proposed by Bardeen, Cooper, and Schrieffer (BCS) in 1957 [Bardeen et al., 1957a,b]. This formalism was based upon earlier work by Cooper [Cooper, 1956], who showed that, in the presence of a net positive attraction, electrons on opposite sides of the Fermi surface favor pairing a bound state with a gapped energy dispersion. Among the many successes of BCS theory was its ability to provide a microscopic derivation of the Meissner effect. When BCS theory was first proposed, however, it was met with some criticism because it was claimed the derivation of the Meissner effect was not gauge invariant [Schafroth, 1958]. The BCS derivation of the Meissner effect was performed in a specific gauge (the Coulomb gauge) and numerous papers were devoted to establishing a gauge-invariant formalism. Of particular importance is the fact [Anderson, 1958, Rickayzen, 1959] that a superconductor has distinct transverse and longitudinal currents, with the collective sound excitations contributing solely to the latter. It is this fact which allows for a gauge-invariant Meissner effect in a gapped energy model of a superconductor, such as BCS theory, in contrast to an insulator, where the same phenomenon is not observed.

In 1960 Nambu [Nambu, 1960], among others, provided a gauge-invariant formulation of BCS theory. The method of Nambu was to treat BCS theory as a Hartree-Fock theory, and by using ideas from quantum electrodynamics he was able to derive the full electromagnetic vertex which satisfies the Ward-Takahashi identity. This approach included the collective excitations, and rendered the BCS derivation of the Meissner effect gauge invariant. Bogoliubov [Bogoliubov, 1958] originally introduced the idea of quasi-particles, which are not eigenstates of electric charge, to describe superconductivity. Nambu pointed out that in such a picture, collective excitations are necessary to restore the gauge invariance of the theory. This relation between symmetry breaking and collective excitations was later described in more generality by Goldstone, Salam, and Weinberg [Goldstone, 1961, Goldstone et al., 1962], which led to Goldstone's theorem. [1] Following this understanding of superconductivity, Nambu and Jona-Lasinio [Nambu & Jona-Lasinio, 1961a,b] developed a model of nucleon masses by way of analogy with BCS theory. In this model global chiral symmetry is spontaneously broken (for massless fermions), in contrast with the spontaneously broken gauge invariance in BCS theory. An intermediate result was this symmetry breaking leads to "pseudoscalar massless bosons". These bosons are now known as Nambu-Goldstone bosons.

Originally, within the high energy physics community, the Goldstone theorem was thought of as an obstacle to overcome, given the apparent lack of massless scalar bosons in Nature. Moreover, the fact that, apart from the photon, Nature has a plethora of massive gauge bosons was also seen as a challenge needing a theoretical explanation. Anderson suggested [Anderson, 1963], by way of analogy, that the Nambu-Goldstone boson present in spontaneous symmetry breaking might "become tangled up with the Yang-Mills gauge bosons". For example, a neutral superfluid spontaneously breaks global $\mathrm{U}(1)$ symmetry, leading to a longitudinal phonon. A superconductor, in the absence of Coulomb effects, similarly has a longitudinal phonon; in the presence of Coulomb interactions, however, this phonon is pushed up to the plasmon frequency and becomes gapped. In this way, the Goldstone theorem is circumvented and a massive excitation results.

1. A global continuous symmetry that is spontaneously broken in a Lorentz invariant theory produces a massless spin-0 boson. That is, there is an excitation for which $\omega \to 0$ as $\mathbf{k} \to \mathbf{0}$. In general, the number of such bosons is equal to the number of broken symmetry generators.

The difficulty in the above analogy, however, is that the Goldstone theorem assumes Lorentz invariance; this was pointed out quite lucidly by Gilbert [Gilbert, 1964]. The above systems are all non-relativistic systems, and so the analogy on how to possibly circumvent the Goldstone theorem needs to be treated with care. In 1964, three seminal papers by Englert and Brout [Englert & Brout, 1964], Higgs [Higgs, 1964], and Guralnik, Hagen, and Kibble [Guralnik et al., 1964] appeared almost simultaneously, providing relativistic models where the Goldstone theorem was circumvented and a massive gauge boson was present in the physical spectrum. This effect, where the Nambu-Goldstone boson arising from the spontaneous breaking of a continuous symmetry, in the presence of a (massless) gauge field, subsequently couples to the gauge field giving it mass, is now known as the Englert-Brout-Higgs-Guralnik-Hagen-Kibble mechanism.[2] It was shown later on by Guralnik, Hagen, and Kibble [Guralnik et al., 1968] that the Goldstone theorem is applicable for a non-relativistic system, provided no long-range interactions, such as Coulomb, are present.

This mechanism can be formulated in a gauge-invariant manner, preserving local gauge invariance which can never be broken. Within this approach the same result arises, namely that of a massive gauge boson, due to the existence of a non-zero vacuum expectation value for the scalar field. In the case of a superfluid or superconductor the order parameter plays an analogous role, with the phase of the order parameter corresponding to the Nambu-Goldstone mode and the amplitude mode corresponding to the Higgs mode. The latter terminology is, strictly speaking, only appropriate for the case where Coulomb interactions are present; in this case there is no Nambu-Goldstone boson in the spectrum, and the amplitude mode of the order parameter is a Higgs mode. Observing these amplitude modes in condensed matter physics is of great current interest. In chapter (7) we show that these amplitude modes have important contributions in non-uniform superfluids.

Much of the original work on gauge invariance in superconductivity was devoted to BCS theory. However, the diagrammatic method implemented in this thesis does not have this restriction.

2. It is important to emphasize that a local symmetry can never be spontaneously broken, because local symmetries are not symmetries at all but rather are redundant mathematical representations of the same state. The above phraseology, of spontaneously breaking local gauge invariance, is the conventional phraseology. The Higgs mechanism can be formulated in a gauge-invariant manner with the same outcome. The fundamental aspect of the Higgs mechanism is the existence of a vacuum expectation value for the symmetry breaking field.

For the cases studied in this thesis exact calculations are possible, avoiding the complicated integral equations present in Nambu's work, which enhances our ability to make quantitative predictions. We conclude by noting the problem of gauge invariance in superconductivity is one of great importance with commonality to similar ideas in high energy physics.

1.2 Symmetries of BCS theory

This section provides a brief review of aspects relating to electromagnetic response in BCS theory. The starting point is the Hamiltonian for a system of electrons interacting through a four-fermion interaction:

$$H = \int dx\, \psi_\sigma^\dagger(x) \left(\frac{\mathbf{p}^2}{2m} - \mu \right) \psi_\sigma(x) + g \int dx\, \psi_\uparrow^\dagger(x) \psi_\downarrow^\dagger(x) \psi_\uparrow(x) \psi_\downarrow(x). \tag{1.1}$$

Here $g > 0$ is an s-wave interaction constant, μ is the chemical potential, and m is the fermion mass. There is an implicit summation over the spin index $\sigma = \uparrow, \downarrow$, the particle coordinates are denoted by $x = (t, \mathbf{r})$, and the fermionic fields $\psi_\sigma^\dagger(x)(\psi_\sigma(x))$ represent creation (annihilation) operators respectively. Only spatial coordinates are integrated over. Throughout $\hbar = c = 1$.

This Hamiltonian has a global $\mathrm{SU}(1,1)$ symmetry with a global $\mathrm{U}(1)_{\mathrm{EM}}$ symmetry subgroup [Guo et al., 2013a, Nambu, 1960]. Let $\alpha \in \mathbb{R}$; then the $\mathrm{SU}(1,1)$ symmetry is generated by

$$\psi_\uparrow \to \cosh\alpha \psi_\uparrow - \sinh\alpha \psi_\downarrow^\dagger, \quad \psi_\downarrow^\dagger \to \cosh\alpha \psi_\downarrow^\dagger - \sinh\alpha \psi_\uparrow, \tag{1.2}$$

$$\psi_\uparrow \to \cosh\alpha \psi_\uparrow + i\sinh\alpha \psi_\downarrow^\dagger, \quad \psi_\downarrow^\dagger \to \cosh\alpha \psi_\downarrow^\dagger - i\sinh\alpha \psi_\uparrow, \tag{1.3}$$

$$\psi_\sigma \to e^{-i\alpha} \psi_\sigma, \quad \psi_\sigma^\dagger \to e^{i\alpha} \psi_\sigma^\dagger. \tag{1.4}$$

The transformation on the third line is the global $\mathrm{U}(1)_{\mathrm{EM}}$ symmetry associated with charge (in the neutral case, particle number) conservation. The generators of these transformations are $-i\tau_1, -i\tau_2, \tau_3$ in the space spanned by the Nambu spinor $(\psi_\uparrow, \psi_\downarrow^\dagger)^\mathsf{T}$, where the τ_i are Pauli matrices. These matrices form a representation for the generators of $\mathrm{SU}(1,1)$, as claimed.

The Hamiltonian in Eq. (1.1) also has a global $\mathrm{SU}(2)$ symmetry with a global $\mathrm{U}(1)_{\mathrm{z}}$ symmetry subgroup. The $\mathrm{SU}(2)$ symmetry is generated by

$$\psi_\uparrow \to \cos\alpha\psi_\uparrow - i\sin\alpha\psi_\downarrow, \quad \psi_\downarrow \to \cos\alpha\psi_\downarrow - i\sin\alpha\psi_\uparrow, \tag{1.5}$$

$$\psi_\uparrow \to \cos\alpha\psi_\uparrow - \sin\alpha\psi_\downarrow, \quad \psi_\downarrow \to \cos\alpha\psi_\downarrow + \sin\alpha\psi_\uparrow, \tag{1.6}$$

$$\psi_\sigma \to e^{-iS_\sigma\alpha}\psi_\sigma, \quad \psi_\sigma^\dagger \to e^{iS_\sigma\alpha}\psi_\sigma^\dagger. \tag{1.7}$$

Here $S_{\uparrow,\downarrow} = \pm 1$. The transformation on the third line is the global $\mathrm{U}(1)_{\mathrm{z}}$ symmetry associated with spin-rotation about the z-axis [Guo et al., 2013a, Nambu, 1960]. The generators of these transformations are τ_1, τ_2, τ_3 in the space spanned by the Nambu spinor $(\psi_\uparrow, \psi_\downarrow)^{\mathsf{T}}$, where the τ_i are Pauli matrices. These matrices form a representation for the generators of $\mathrm{SU}(2)$, as claimed.

The Hamiltonian in Eq. (1.1) cannot be solved exactly. The BCS theory of superfluidity and superconductivity involves making the mean-field approximation for the order parameter Δ:

$$\Delta(x) = g\langle\psi_\uparrow(x)\psi_\downarrow(x)\rangle. \tag{1.8}$$

Note that, the order parameter Δ is not gauge invariant; under the $\mathrm{U}(1)_{\mathrm{EM}}$ transformation Δ transforms as $\Delta \to \Delta e^{-2i\alpha}$. Invoking the mean-field (saddle-point) condition thus spontaneously breaks the global $\mathrm{U}(1)_{\mathrm{EM}}$ symmetry. On the other hand, under the $\mathrm{U}(1)_{\mathrm{z}}$ symmetry the gap Δ is invariant. Thus, the mean-field (saddle-point) condition does not spontaneously break the $\mathrm{U}(1)_{\mathrm{z}}$ symmetry. Ignoring fluctuations, the mean-field Hamiltonian then becomes

$$\begin{aligned} H_{\mathrm{mf}} = &\int dx\, \frac{|\Delta(x)|^2}{g} + \int dx\, \psi_\sigma^\dagger(x)\left(\frac{\mathbf{p}^2}{2m} - \mu\right)\psi_\sigma(x) \\ &+ \int dx\, \left[\Delta(x)\psi_\uparrow^\dagger(x)\psi_\downarrow^\dagger(x) + \Delta^*(x)\psi_\downarrow(x)\psi_\uparrow(x)\right]. \end{aligned} \tag{1.9}$$

This mean-field Hamiltonian can be diagonalized exactly by using a Bogoliubov transformation [Schrieffer, 1964]. If the order parameter Δ is treated as a fixed parameter, then the Hamiltonian in Eq. (1.9) explicitly breaks the global $\mathrm{U}(1)_{\mathrm{EM}}$ symmetry. However, as mentioned above,

the parameter Δ itself is not invariant, and must be transformed to ensure the underlying $\mathrm{U}(1)_{\mathrm{EM}}$ symmetry is preserved. Thus, while the mean-field (saddle-point) condition breaks the global $\mathrm{U}(1)_{\mathrm{EM}}$ symmetry, the Hamiltonian in Eq. (1.9) is still invariant, as required for a symmetry that is spontaneously broken. The $\mathrm{U}(1)_{\mathrm{z}}$ symmetry, however, is not spontaneously broken.

In order to study the electrodynamics of superfluids and superconductors, we need to consider the response to an electromagnetic field with potentials $\mathbf{A}(x)$ and $\Phi(x)$. Incorporating these potentials is done by minimally coupling the Hamiltonian in Eq. (1.9):

$$\begin{aligned} H_{\mathrm{mf}} = & \int dx\, \frac{|\Delta(x)|^2}{g} + \int dx\, \psi_\sigma^\dagger(x) \left(\frac{[\mathbf{p} - e\mathbf{A}(x)]^2}{2m} - \mu \right) \psi_\sigma(x) \\ & + e \int dx\, \Phi(x)\delta n(x) + \int dx\, \left[\Delta(x)\psi_\uparrow^\dagger(x)\psi_\downarrow^\dagger(x) + \Delta^*(x)\psi_\downarrow(x)\psi_\uparrow(x) \right] \\ & + \frac{1}{2} \int dx\, \delta n(x) V(\mathbf{r} - \mathbf{r}')\delta n(x'). \end{aligned} \tag{1.10}$$

For completeness, here we have included the electron-electron Coulomb interaction. The above Hamiltonian accounts for the presence of a uniformly distributed positive background, which ensures the electric neutrality of the system [Arseev et al., 2006]. This gives rise to the density fluctuation operator $\delta n(x) = \psi_\sigma^\dagger(x)\psi_\sigma(x) - n_0$, where n_0 is the electron number density in the absence of the Coulomb interaction, $V(\mathbf{r} - \mathbf{r}') = e^2/|\mathbf{r} - \mathbf{r}'|$.

Due to the $\mathrm{U}(1)_{\mathrm{EM}}$ symmetry discussed earlier, if an external field is added to the Hamiltonian in Eq. (1.1), then the action remains invariant under the following gauge transformation

$$\mathbf{A}(x) \to \mathbf{A}'(x) = \mathbf{A}(x) - \nabla\alpha(x), \tag{1.11}$$

$$\Phi(x) \to \Phi'(x) = \Phi(x) + \frac{\partial\alpha(x)}{\partial t}, \tag{1.12}$$

$$\psi_\sigma(x) \to \psi'_\sigma(x) = \psi_\sigma(x) \exp\left(-ie\alpha(x)\right). \tag{1.13}$$

As mentioned above, in order for the action based on the Hamiltonian in Eq. (1.10) to be invariant under this gauge transformation, the parameter Δ itself must transform. If Δ is treated as a fixed parameter, then under the above gauge transformation, the action is no longer gauge invariant.

This, therefore, brings us to one of the most crucial aspects of the electrodynamics of superfluids and superconductors; the order parameter must always be treated in a self-consistent manner based on Eq. (1.8). In the presence of an external electromagnetic field Δ itself depends on the field and transforms accordingly under Eq. (1.8). Gauge invariance is restored in BCS theory by accounting for the fact that Δ itself changes under a gauge transform; this necessarily leads to collective excitations restoring gauge invariance, as will be shown in chapters (5-7).

By Noether's theorem, the global $\mathrm{U}(1)_{\mathrm{EM}}$ and $\mathrm{U}(1)_{\mathrm{z}}$ symmetries for the mean-field Hamiltonian implies there exists two conserved currents: j^{μ}_{EM} and j^{μ}_{z}, where $\partial_{\mu} j^{\mu}_{\mathrm{EM}} = 0 = \partial_{\mu} j^{\mu}_{\mathrm{z}}$. The explicit forms of these current operators are $j^{\mu}_{\mathrm{EM}}(x) = (n_{\mathrm{EM}}(x), \mathbf{j}_{\mathrm{EM}}(x))$ and $j^{\mu}_{\mathrm{z}}(x) = (n_{\mathrm{z}}(x), \mathbf{j}_{\mathrm{z}}(x))$, where [Guo et al., 2013a]:

$$n_{\mathrm{EM}}(x) = \psi^{\dagger}_{\sigma}(x)\psi_{\sigma}(x), \tag{1.14}$$

$$\mathbf{j}_{\mathrm{EM}}(x) = \frac{1}{2mi}\left[\psi^{\dagger}_{\sigma}(x)\nabla\psi_{\sigma}(x) - \left(\nabla\psi^{\dagger}_{\sigma}(x)\right)\psi_{\sigma}(x)\right]. \tag{1.15}$$

$$n_{\mathrm{z}}(x) = S_{\sigma}\psi^{\dagger}_{\sigma}(x)\psi_{\sigma}(x), \tag{1.16}$$

$$\mathbf{j}_{\mathrm{z}}(x) = \frac{1}{2mi}S_{\sigma}\left[\psi^{\dagger}_{\sigma}(x)\nabla\psi_{\sigma}(x) - \left(\nabla\psi^{\dagger}_{\sigma}(x)\right)\psi_{\sigma}(x)\right]. \tag{1.17}$$

Note that, there is an implicit summation over spin indices. The conservation laws for these current operators leads to sum rules for the many-body correlation functions, a topic which is discussed in much more depth in the appendices for the systems of particular interest.

In chapters (5-7), it will be found that treating the order parameter self consistently is what gives rise to collective mode effects and is how gauge invariance in a superfluid is restored. In particular, two different approaches to restoring gauge invariance, which are equivalent in the BCS limit, based on the above important point will be studied in detail. Chapter (5) provides a diagrammatic approach to including collective modes and restoring gauge invariance, whereas chapter (6) is a functional integral approach based on the path integral.

1.3 BCS-BEC crossover theory

The BCS theory of superfluidity and superconductivity is a successful theory of conventional superfluids and superconductors, such as, for example, ^{3}He and Sn, respectively. As discussed in the previous section, BCS theory is a mean-field theory; its validity and success can be attributed to the fact that conventional superconductors have large coherence lengths. This description can be generalized by allowing attractive interactions of arbitrary strength, which then allows for a smooth evolution from the weakly interacting BCS regime to the strongly interacting Bose-Einstein condensation (BEC) regime. In this scenario attractive interactions cause the fermions to pair and subsequently, due to statistical reasons, they are driven to Bose condense. The conventional BCS theory is a special case of this in which the pair formation and condensation temperatures coincide. The excitement around this BCS-BEC crossover scenario is that it can be studied in ultra cold Fermi gases, and it may also have applicability to short coherence length materials, such as high-temperature superconductors [Chen et al., 2005].

It was noticed by Leggett [Leggett, 1980] that the BCS ground state wave function (at zero temperature) has a greater applicability than originally proposed.[3] Indeed, as the attractive interaction is increased, this wave function is also capable of describing a continuous evolution from BCS-like behavior to a form of Bose-Einstein condensation. The essential requirement is that the fermionic chemical potential and the order parameter are computed self consistently as the interaction strength is varied. Nozières and Schmitt-Rink [Nozières & Schmitt-Rink, 1985] were the first to investigate this crossover scenario at non-zero temperatures, and following this Randeria and collaborators [Randeria et al., 1995] suggested this crossover physics might be applicable to high-temperature superconductors. For a thorough review of applications of BCS-BEC crossover physics to both high-T_c superconductors and ultra cold Fermi gases see Ref. [Chen et al., 2005] and the references cited therein.

To understand BCS-BEC crossover in more detail, consider first the behavior of the zero tem-

3. Early studies by Eagles [Eagles, 1969], in the context of semiconductor superconductors, showed that pairing can occur at a temperature larger than the condensation temperature.

perature chemical potential. In the BCS-like regime, where the interaction strength is weak, the electron energies are very near the Fermi surface, and so the fermionic chemical potential is roughly $\mu \sim E_F$, with E_F the Fermi energy. In the BEC-like regime, where the interaction strength is strong, the system is more bosonic and the Fermi surface is absent with the chemical potential becoming large in magnitude and negative. Thus, for some intermediate interaction strength, the chemical potential is equal to zero. This crossing point at $\mu = 0$ represents a change from a more fermionic to a more bosonic system. The regime between the BCS and BEC limits is a regime where one has a non-Fermi-liquid-like state with a gap which reflects the electron pairing. When one then considers the extension to finite temperature, due to the strong electron binding one expects fermions to form pairs at temperatures even above the transition temperature. Thus there exists bosonic pairs of fermions present in the normal state due to the strong electron binding. These bosonic pairs of fermions are not restricted solely to the normal state, but are also present in the superconducting state; the existence of preformed pairs in the normal state has the counterpart of non-condensed pairs in the superfluid state. What is crucial here is that the onset of a normal state gap (known as a "pseudogap") is not associated with pair condensation in the superfluid state.

In general, the physical picture is that in the presence of an attractive interaction fermions will form pairs and condense at different temperatures. The BCS case is a special limit in which these two temperatures agree. The more general case is that fermions pair at some temperature T^*, forming bosonic degrees freedom which are subsequently driven to condense at $T_c < T^*$, just as in Bose-Einstein condensation. Because of this distinction between the pairing and condensation temperatures, there is also necessarily a distinction between the order parameter $\Delta_{\rm sc}$ and the excitation gap Δ for breaking pairs. The existence of a normal state gap in the pseudogap phase has led to some conjecture that this is the origin of the normal state gap present in high-T_c superconductors [Chen et al., 1999]. One principle supporting this argument being that the total gap in the superconducting phase smoothly evolves into the normal state pseudogap present in the normal phase [Chen et al., 2005]. However, theories of the cuprate pseudogap are still contentious. For a recent review discussing the interpretation of the pseudogap see Ref. [Fradkin et al., 2015].

In this thesis we apply BCS-BEC crossover theory to exciting problems including spin-orbit coupled Fermi gases and the cuprates. Although there are several alternative approaches, of interest is a particular t-matrix theory [Chen et al., 2005, Kosztin et al., 2000] chosen because it is associated with the usual mean-field ground state. This is now briefly summarized; additional technical details can be found in appendix (A). The physical picture considered is that in the normal state preformed pairs form at a mean-field transition temperature T^*. This gap reflects pairing in the absence of phase coherence and corresponds to finite momentum pairs that are not condensed. At lower temperatures, the superfluid transition temperature T_c denotes the temperature at which zero momentum pairs condense, with the finite momentum pairs still persisting in this ordered phase. Finally, at zero temperature all the pairs are condensed. The total gap in this scheme can be expressed as $\Delta^2(T) = \Delta_{\rm sc}^2(T) + \Delta_{\rm pg}^2(T)$. Here $\Delta_{\rm sc}$ represents the order parameter, which satisfies $\Delta_{\rm sc}(T_c) = 0$, while $\Delta_{\rm pg}$ represents the "pseudogap", which satisfies $\Delta_{\rm pg}(T = 0) = 0$ and $\Delta_{\rm pg}(T^*) = 0$, with $T^* > T_c > 0$.

The t-matrix theory under consideration is a natural extension of the BCS ground state based on the work of Refs. [Kadanoff & Martin, 1961, Patton, 1971] and summarized in Refs. [Chen et al., 2005, Kosztin et al., 2000]. One considers an infinite sequence of ladder diagrams, which arise from a truncation of the equations of motion, that give rise to an effective bosonic propagator $t_{\rm pg}(q) = \left[g^{-1} + \chi(q)\right]^{-1}$, where $g > 0$ is a pairing interaction constant and $\chi(q)$ is known as the pair susceptibility. Alternative BCS-BEC crossover theories lead to differing results for $\chi(q)$, depending on whether the desired theory is "phi-derivable" [Baym, 1962], conserving [Baym & Kadanoff, 1961], or consistent with the ground state BCS theory (see Ref. [Loktev et al., 2001] for a good discussion of these different approaches, and also Ref. [Serene, 1989]). Here the latter choice is favored, which leads to the t-matrix theory discussed in more depth in chapters (2-3) and in the appendices (A-B).

One central challenge has been deriving gauge-invariant response functions, with the inclusion of the collective modes, in the ordered phase. Early work attempting to tackle this problem was done in Refs. [Guo et al., 2010, Kosztin et al., 2000] and more recently Ref. [He & Guo, 2015]

solved this problem for a full t-matrix theory, without any assumptions being made. In chapter (5) we study gauge invariance for a very general model which includes the work of Ref. [He & Guo, 2015] and also includes a simple model known as the pseudogap pairing approximation. We will derive exact gauge-invariant response functions, with the inclusion of the collective mode terms.

1.4 BCS-BEC in spin-orbit coupled topological superfluids

The excitement surrounding BCS-BEC crossover physics in ultra cold Fermi superfluids has overlapped with another exciting area of condensed matter physics, namely that of topological superfluids. Interest in non-abelian topological states [Nayak et al., 2008] arises for numerous reasons from quantum computing to fractional quantum Hall states. One exciting proposal for a topological superfluid is the chiral $p_x + ip_y$ superfluid [Read & Green, 2000]. In cold atom systems, the BCS-BEC crossover is important because it is believed [Fu & Kane, 2008, Gong et al., 2011, Sato et al., 2009, Zhang et al., 2008] that in s-wave Fermi superfluids some combination of spin-orbit coupling (SOC) and a magnetic field may yield chiral p-wave physics. [4]

Incorporating SOC in BCS-BEC crossover physics leads to many interesting new phenomena, in both the single-particle and many-particle physics. In Ref. [Vyasanakere & Shenoy, 2011], the two-body bound states of spin-$\frac{1}{2}$ fermions interacting via a contact interaction in the presence of a uniform non-abelian gauge field were studied. The gauge field is denoted by $A_i^\mu = \lambda_i \delta_i^\mu$, where λ_i denotes the SOC momentum strength and $\mu, i = \{x, y, z\}$. The single-particle Hamiltonian for this system is then: $\mathcal{H} = k^2/2m - \boldsymbol{\sigma} \cdot \mathbf{s}(\mathbf{k})$, where $\mathbf{s}(\mathbf{k}) = (\lambda_x k_x, \lambda_y k_y, \lambda_z k_z)$. Three types of gauge-field configurations investigated were: (1) $\lambda_x = \lambda_y = 0$, and $\lambda_z = \lambda$ [extreme prolate (EP)], (2) $\lambda_x = \lambda_y = \lambda$, and $\lambda_z = 0$ [extreme oblate (EO)], and (3) $\lambda_x = \lambda_y = \lambda_z$ [spherical (S)]. The EO SOC case is physically equivalent to the Rashba SOC studied in chapters (2-3) of this thesis.

In the absence of SOC, there is no two-body bound state on the BCS side of resonance. However, Ref. [Vyasanakere & Shenoy, 2011] found that, for any sign of $1/k_F a$, in the presence of

4. Note that, for an intrinsic p-wave superfluid time-reversal symmetry is spontaneously broken, however, a magnetic field explicitly breaks this symmetry.

SOC there is a two-body bound state solution. This was explained as being due to an enhanced density of states at low energies promoting bound-state formation. The same result is also true when a magnetic field is present, provided the magnetic field obeys $b_z < m\lambda^2/\hbar^2$; that is, provided the Rashba ring exists as the lowest single-particle state [Jiang et al., 2011].

Following the studies in Ref. [Vyasanakere & Shenoy, 2011], Ref. [Vyasanakere et al., 2011] investigated the many-body effects on the ground state of the same system within the context of mean-field theory. It was found that, for fixed interaction strength (scattering length), however small and negative, by increasing the SOC strength a crossover from a BCS superfluid to a BEC ground state of bosons is produced. For large values of SOC (gauge couplings), the properties of the BEC that forms are determined solely by the Rashba gauge field. The features of these bosons are quite different from that of non-interacting bosons, which has led to them being called "rashbons". Quite generally, the results of Ref. [Vyasanakere et al., 2011] indicate that another route to obtaining a BCS-BEC crossover is through tuning the SOC strength. A systematic study of the BCS-BEC crossover physics at finite temperature was performed in Ref. [He et al., 2013] using the same formalism applied in this thesis. There it was found that with strong Rashba SOC the pseudogap regime in the normal phase is significantly enhanced.

As mentioned previously, one of the primary motivations behind studying Fermi superfluids with SOC is to study topological Fermi superfluids. In the presence of intrinsic pairing, SOC, and a magnetic field, these three-dimensional (3D) Fermi superfluids can be in either a trivial phase, or one of two topological phases. The topological phases have either four nodes (4-Weyl points) or two nodes (2-Weyl points) [Gong et al., 2011], and the Hamiltonian in both cases are described by a Weyl Hamiltonian. These 3D topological Fermi superfluids do not have Majorana fermions due to the existence of Weyl points, which is in contrast to 2D fully gapped topological Fermi superfluids which do have Majorana fermions [Gong et al., 2011, Nayak et al., 2008]. Signatures of these topological phase transitions can be found in single-particle properties [Gong et al., 2011] or the many-particle electromagnetic response [Ojanen & Kitagawa, 2013].

In chapter (2) we study Rashba SOC using a particular t-matrix theory, discussed briefly in the previous section and in more detail in appendix (A). In agreement with previous studies, it is found that SOC enhances pairing leading to a larger pseudogap regime. We also study the electromagnetic response in both the density and spin channels. In chapter (3) signatures of the topological phase transition are found in both these response functions.

1.5 Fulde-Ferrell and pair-density-wave superfluids

In conventional BCS superconductors electrons pair with equal and opposite momenta to give a zero momentum condensate. However, in certain situations, the formation of a condensate with non-zero momentum can be energetically favorable. This type of condensate occurs for systems with an imbalance in the number of electrons of opposite spin, such as in a weak ferromagnet in the presence of an exchange field. A non-zero spin imbalance frustrates conventional BCS pairing, but if the separation of the Fermi surface for each spin is of the order of the gap, then the formation of pairs of electrons is favored. In this case pairs are formed in which the particles are located part of the time close to their own Fermi surfaces and have momenta of different magnitude. This type of superconductor was first studied, in the context of solid state physics, by Larkin and Ovchinnikov [Larkin & Ovchinnikov, 1965] and Fulde and Ferrell [Fulde & Ferrell, 1964]. These superconductors are now known as LOFF (or FFLO) superconductors.

In general, a LOFF superfluid represents a Fermi superfluid with finite center-of-mass momentum pairing. The FF state is characterized by a complex order parameter given by

$$\Delta_{\mathrm{FF}}(x) = \Delta_{Q_0} e^{i\mathbf{Q}_0\cdot\mathbf{r}+i\phi}. \tag{1.18}$$

The plane wave momentum $\mathbf{Q}_0$ corresponds to the pair-condensation momentum. For comparison, a BCS superfluid has $\mathbf{Q}_0 = 0$. The order parameter in Eq. (1.18) has a single Goldstone mode ϕ, which corresponds to the local superconducting phase. The FF state has a non-zero and spontaneously directed supercurrent which breaks time-reversal symmetry, rotational symmetry (chosen

spontaneously along $\mathbf{Q}_0$), as well as the global $\mathrm{U}(1)$ symmetry. Under a translation by an arbitrary vector $\mathbf{a}$, the order parameter transforms as $\Delta_{\mathrm{FF}} \to \Delta_{\mathrm{FF}} e^{i\mathbf{Q}_0\cdot\mathbf{a}}$, which in itself is not invariant. However, if one first performs an arbitrary spatial translation, followed by a gauge transformation $\phi \to \phi - \mathbf{Q}_0\cdot\mathbf{a}$, then the order parameter is invariant. Therefore, in the FF phase all gauge-invariant observables are translationally invariant [Radzihovsky, 2011].

The LO phase is characterized by a complex order parameter given by

$$\Delta_{\mathrm{LO}}(x) = 2\Delta_{Q_0} e^{i\phi} \cos\left(\mathbf{Q}_0 \cdot \mathbf{r} + \theta\right). \tag{1.19}$$

This order parameter represents a product of a superfluid and a unidirectional density-wave order parameter, characterized by two (independent) Goldstone modes ϕ and θ. The phase mode θ represents the phase of the pair-density wave, while the phase mode ϕ represents the superfluid phase mode. Under a translation by an arbitrary vector $\mathbf{a}$, this order parameter is not invariant. Unlike the FF phase, no gauge transformation can restore translational invariance. Thus, the LO state spontaneously breaks translational symmetry.

In summary, the FF (LO) superfluid spontaneously breaks both a continuous rotational and a global $\mathrm{U}(1)$ symmetry and also breaks (preserves) discrete time-reversal symmetry; in addition the LO superfluid spontaneously breaks translational symmetry. The LO state is therefore a periodically paired superfluid, analogous to a supersolid, and is thus appropriately called a pair-density wave [Radzihovsky, 2011]. The distinction between the LO state and a supersolid being that the former has the absence of a zero-momentum condensate. Moreover, a conventional supersolid spontaneously breaks translational and global $\mathrm{U}(1)$ symmetry due to multiple distinct order parameters, whereas the LO state is governed by only a single order parameter. Thus the LO state is more appropriately called a "pair-density wave".

Another context where superfluids analogous to FF or LO states arise is in the study of nematic and smectic phases of matter [Fradkin, 2012, Fradkin et al., 2010, Soto-Garrido & Fradkin, 2014, Sun et al., 2008]. Quite generally, an electron nematic denotes an electron fluid that spontaneously

breaks a symmetry of the underlying Hamiltonian which interchanges two axes of the system. In its pure form, a nematic phase does not spontaneously break inversion symmetry, time-reversal symmetry, or translational symmetry. Both the nematic and FF phases of matter spontaneously break rotational symmetry, however, they are distinguished by their behavior under time-reversal symmetry: in the FF phase time-reversal symmetry is spontaneously broken, whereas a nematic pair-density wave preserves time-reversal symmetry. The LO phase is also time-reversal invariant. These phases of matter are defined concretely in Refs. [Fradkin, 2012, Kivelson et al., 1998] as follows

- *Crystalline phases*: phases that break all continuous translation symmetries and rotational invariance.
- *Smectic ("stripe") phases*: phases that break one translation symmetry and rotational invariance.
- *Nematic and hexactic phases*: uniform (liquid) phases that break rotational invariance.
- *Isotropic phases*: uniform and isotropic phases.

There are two different mechanisms for producing a nematic phase: The gentle melting of a stripe phase can restore long-range translational symmetry while preserving orientational order. Alternatively, a nematic Fermi fluid can arise through a distortion of the Fermi surface via a Pomeranchuk instability [Fradkin et al., 2010, Pomeranchuk, 1958, Wu et al., 2007]. In general, a sequence of quantum phase transitions from either the weak coupling or strong coupling perspective can be considered. From a weak coupling perspective, a sequence of symmetry breaking phase transitions beginning from the isotropic phase is: Fermi liquid $\rightarrow$ electron nematic $\rightarrow$ electron smectic $\rightarrow$ insulating electron crystal. In this case, one begins with a system well described by the Landau theory of a Fermi liquid, with well defined low energy quasi-particles and a Fermi surface. Possible instabilities then evolve the system into a nematic phase, as well as phase transitions into various striped (or charge-density-wave) phases. From a strong correlation perspective,

a sequence of quantum phase transitions, representing the progressive restoration of symmetry, would be: electron crystal $\rightarrow$ smectic (stripe) $\rightarrow$ nematic $\rightarrow$ isotropic fluid.

An interesting property of the FF superfluid concerns its superfluid density in the directions transverse to the vector $\mathbf{Q}_0$. Under an infinitesimal rotation of the FF pairing vector axis $\mathbf{Q}_0 \rightarrow \mathbf{Q}_0 + \delta\mathbf{Q}_0 \cdot \mathbf{r}$, the order parameter transforms as $\Delta_{\rm FF} \rightarrow \Delta_{\rm FF} e^{i\delta\mathbf{Q}_0\cdot\mathbf{r}} = \Delta_{Q_0} e^{i\mathbf{Q}_0\cdot\mathbf{r} + i[\phi + \delta\mathbf{Q}_0\cdot\mathbf{r}]}$. Thus the phase transforms as $\phi \rightarrow \phi + \delta\mathbf{Q}_0 \cdot \mathbf{r}$. Due to the underlying rotational invariance of the FF state, the Hamiltonian for the Goldstone mode ϕ must be invariant under such phase transformations. For an infinitesimal rotation, this corresponds to phase shifts that are linear in $\mathbf{r}$ and transverse to $\mathbf{Q}_0$. Thus, the Hamiltonian for the Goldstone mode cannot have a $(\nabla_\perp \phi)^2$ term, where $\perp$ denotes axes transverse to the $\mathbf{Q}_0$ axis. A generic form [Radzihovsky, 2011] for the Goldstone-mode Hamiltonian is thus $\mathcal{H}^0_{\rm FF} = \frac{1}{2}K\left(\nabla^2_\perp \phi\right)^2 + \frac{1}{2}n^{\parallel}_{s,\rm FF}\left(\hat{\mathbf{Q}}_0 \cdot \nabla\phi\right)^2$. Therefore the superfluid density in the transverse $(\perp)$ directions must vanish: $n^{\perp}_{s,\rm FF} = 0$. This is a reflection of the underlying rotational symmetry which is spontaneously broken. The longitudinal superfluid density $n^{\parallel}_{s,\rm FF}$, however, can be non-zero.

For the LO superfluid, however, the behavior of the transverse superfluid density is very different. Under an infinitesimal rotation of the $\mathbf{Q}_0$ axis, $\mathbf{Q}_0 \rightarrow \mathbf{Q}_0 + \delta\mathbf{Q}_0 \cdot \mathbf{r}$, the phase of the LO order parameter transforms as $\theta \rightarrow \theta + \delta\mathbf{Q}_0 \cdot \mathbf{r}$. Therefore, due to the underlying rotational invariance of the LO state, the LO Goldstone-mode Hamiltonian must be invariant under this symmetry. As discussed above, this precludes a term of the form $(\nabla_\perp \theta)^2$ in the Hamiltonian. The LO Goldstone-mode Hamiltonian thus has the form $\mathcal{H}^0_{\rm LO} = \frac{1}{2}K\left(\nabla^2_\perp u\right)^2 + \frac{1}{2}B\left(\nabla_\parallel u\right)^2 + \frac{1}{2}n^{\perp}_{s,\rm LO}\left(\nabla_\perp\phi\right)^2 + \frac{1}{2}n^{\parallel}_{s,\rm LO}\left(\nabla_\parallel\phi\right)^2$, where $u = -\theta/Q_0$ is the smectic phonon [Radzihovsky, 2011]. The LO state, in contrast to the FF state, therefore has finite and non-zero transverse superfluid density, and moreover unequal parallel and perpendicular superfluid densities: $n^{\parallel}_{s,\rm LO} \neq n^{\perp}_{s,\rm LO} \neq 0$.

In chapter (7) an exact calculation of the longitudinal superfluid density, in the context of mean-field theory, is presented for the FF superfluid. The collective mode contribution is incorporated and found to be very significant; it causes the superfluid to become unstable at temperatures much lower than the mean-field transition temperature.

1.6 Thesis outline

This thesis broadly studies diagrammatic and functional methods of obtaining gauge-invariant response for strongly correlated (neutral) Fermi systems, in both the normal phase with pairing and the superfluid phase. Chapters (2-4) consider response in the normal phase, where collective-mode effects are absent, whereas chapters (5-7) focus on response in the superfluid phase, where the challenging collective mode effects are addressed.

In particular, in chapters (2-3) we study intrinsic Rashba spin-orbit coupled superfluids in three dimensions in the absence and presence of a magnetic field, respectively. Density and current response functions are derived by solving the Ward-Takahashi identity. To address spin response, new spin f-sum rules are derived, valid even in the absence of a spin-conservation law. Spin correlation functions obeying these sum rules are also derived. Topological order is observed in the density channel via Van Hove singularity effects in the density response functions, whereas in the spin channel it is observed through the merging of distinct peaks in the spin response functions. Chapter (4) studies three models of the cuprate pseudogap phase, focusing on a recent pairing theory known as Amperean pairing. Using the Ward-Takahashi identity, exact gauge-invariant response functions are obtained, and distinguishing features between the models are identified. For applications of response in the superfluid phase, in chapter (5) we study a general model that incorporates models of both BCS-BEC crossover theories and high-T_c superconductor theories. We utilize our diagrammatic method to derive the full electromagnetic vertex and then use this to set up a self-consistent equation for the collective modes. This leads to exact expressions for the collective mode vertices and results in exact gauge-invariant response functions.

In chapter (6), the path integral technique of obtaining exact gauge-invariant response functions is presented. It is proved the current method in the literature of implementing gauge invariance is inconsistent because it leads to a violation of the compressibility sum rule. Since the path integral method allows both electrodynamics and thermodynamics to be derived simultaneously, this presents a serious flaw in the usual approach. A reformulation of the path integral method for Fermi superfluids is derived, which is both manifestly gauge invariant and compatible with the

compressibility sum rule. Our method of restoring gauge invariance in the path integral involves performing the saddle point condition in the presence of a non-zero vector potential. This leads to collective modes that restore gauge invariance and are compatible with the compressibility sum rule. At any level this approach leads to a gauge-invariant and compressibility sum rule consistent treatment of electrodynamics and thermodynamics.

In chapter (7) Fulde-Ferrell superfluids, which have pairing at finite center-of-mass momentum, are studied. We provide the first complete calculation of the gauge-invariant response, including collective modes and with no assumptions made about the magnitude of the order parameter. In particular, we show that the generally omitted collective mode term has a non-negligible contribution to the superfluid density, and moreover it is the amplitude ("Higgs") mode of the order parameter which contributes. Our analysis shows that this mode causes the superfluid to become unstable at temperatures much lower than the mean-field transition temperature.

CHAPTER 2

SIGNATURES OF PAIRING AND SPIN-ORBIT COUPLING IN CORRELATION FUNCTIONS OF FERMI GASES

This chapter derives exact density-density and spin-spin correlation functions in the (greatly enhanced) pseudogap phase of spin-orbit coupled Fermi gases. Density-density correlation functions are found to be relatively insensitive to the presence of these Rashba spin-orbit effects. To arrive at spin-spin correlation functions we derive new f-sum rules, valid even in the absence of a spin conservation law. Our spin-spin correlation functions are shown to be fully consistent with these f-sum rules. Importantly, they provide clear signatures of both the Rashba band structure and the presence of a pseudogap. The work in this chapter is published in Ref. [Wu et al., 2015].

2.1 Introduction

Spin-orbit coupling (SOC) in superconductors and superfluids is a topic of great current interest [Hasan & Kane, 2010, Sato et al., 2009, Zhang et al., 2008]. This is in large part because there is some hope that (particularly in the presence of a magnetic field) they may relate to the much sought after spinless $p_x + ip_y$ superfluid [Read & Green, 2000]. Two communities have united around these issues: those working on ultra cold Fermi superfluids with intrinsic Rashba SOC [Goldman et al., 2014, Zhai, 2015] and those studying superconductivity that is proximity induced in a spin-orbit coupled material [Fu & Kane, 2008]. To achieve this ultimate goal it is important to establish that a given candidate for the $p_x + ip_y$ superfluid simultaneously exhibits signatures of *both* pairing and spin-orbit coupling. This would provide minimal evidence for a properly engineered ultra cold Fermi superfluid. One therefore needs experimental signatures of these simultaneous effects and this provides a central goal for the present chapter.

In this chapter we address the signatures of this anomalous spin-orbit coupled superfluid as reflected in density-density and spin-spin correlation functions. Our work builds on the observation [Gong et al., 2011, Han & Sá de Melo, 2012, Hu et al., 2011, Vyasanakere & Shenoy, 2011,

Vyasanakere et al., 2011, Yu & Zhai, 2011] that in the presence of Rashba SOC, pairing (in the form of pseudogap effects [Chen et al., 2005, Stajic et al., 2004]) is significantly enhanced. For this reason (and because the correlation functions are free of the complications of collective mode effects) we focus here on the normal phase with pairing. We show how, even without condensation, the frequency dependent spin response exhibits features which relate to both the Rashba ring band structure and the presence of a pairing gap. In contrast, the density response is relatively unaffected by SOC. Previous work has focused on identifying SOC without [Cheuk et al., 2012, Wang et al., 2012] or with pairing [Fu et al., 2013] via the one-body spectral function. As compared with Ref. [Fu et al., 2013], we find prominent features in the two-particle response. At the very least the spin-spin correlation functions provide complementary and accessible (via neutrons or two photon Bragg scattering [Veeravalli et al., 2008]) information.

Validating any theory of correlation functions requires satisfying important constraints [Boyack et al., 2014]. Indeed, the absence of conservation laws complicates all spin transport in spin-orbit coupled materials. Thus, it is extremely important to find underlying principles for establishing self consistency. To address this issue, here we use the Heisenberg equations of motion to derive f-sum rules for the spin-spin correlation functions, which also provide important constraints on our numerical calculations. In order to avoid technical complexity in this chapter, we ignore the complication of a magnetic field (which is necessary for arriving at topological order). The next chapter does, however, incorporate the magnetic field. Our formalism leading to the phase diagram and response functions can be extended to include arbitrary SOC and Zeeman fields. However, we expect the Rashba case to be representative of a large class of spin-orbit coupled Hamiltonians. We note there is a substantial literature investigating correlation functions in the superfluid phase (without pseudogap effects) which we cite here [Chung & Roy, 2014, Lutchyn et al., 2008, Ojanen & Kitagawa, 2013, Roy & Kallin, 2008].

In this chapter we present two main results. The first is a consistent derivation of spin-spin correlation functions in spin-orbit coupled Fermi gases. The second establishes qualitative experimental signatures reflecting separately the presence of a pairing gap and of SOC.

2.2 Background theory

We consider a gas of fermions whose single particle Hamiltonian is $H^0(\mathbf{k}) = k^2/2m - \mu + \lambda\boldsymbol{\sigma}\cdot\mathbf{k}_\perp/m$ for a particle of mass m, spin-orbit coupling momentum λ, momentum $\mathbf{k} = (k_x, k_y, k_z)$, in-plane momentum $\mathbf{k}_\perp = (k_x, k_y, 0)$, and vector of Pauli matrices $\boldsymbol{\sigma} = (\sigma_x, \sigma_y, \sigma_z)$. Throughout this chapter we set $\hbar = k_B = c = 1$. To describe this spin-orbit coupled Fermi gas with pairing, we use a 4×4 inverse Nambu Green's function

$$\mathcal{G}^{-1}(K) = \begin{pmatrix} G_0^{-1}(K) & \Delta \\ \Delta & \widetilde{G}_0^{-1}(K) \end{pmatrix}, \tag{2.1}$$

which acts on the spinor $\Psi_{\mathbf{k}}^{\mathsf{T}} = \left(c_{\mathbf{k}\uparrow}, c_{\mathbf{k}\downarrow}, -c_{-\mathbf{k}\downarrow}^{\dagger}, c_{-\mathbf{k}\uparrow}^{\dagger}\right)$ for a fermion annihilation (creation) operator $c_{\mathbf{k}s}(c_{\mathbf{k}s}^{\dagger})$ of spin $s = \uparrow, \downarrow$ and momentum $\mathbf{k}$. In the Green's function, Δ is a pairing gap, the four-vector $K = (i\omega_n, \mathbf{k})$ with fermionic Matsubara frequency $i\omega_n$, and the non-interacting inverse particle Green's function is $G_0^{-1}(K) = i\omega_n - H^0(\mathbf{k})$ and inverse hole Green's function is $\widetilde{G}_0^{-1}(K) = i\sigma_y[G_0^{-1}(-K)]^T i\sigma_y = i\omega_n + H^0(\mathbf{k})$.

This superfluid can be studied at the mean-field level [Gong et al., 2011, Han & Sá de Melo, 2012, Hu et al., 2011, Vyasanakere & Shenoy, 2011, Vyasanakere et al., 2011, Yu & Zhai, 2011], where one has the usual gap equation:

$$1 = \frac{g}{2}\sum_K \mathrm{Tr}\left[G(K)\widetilde{G}_0(K)\right], \tag{2.2}$$

where $\sum_K = T\sum_{i\omega_n}\sum_{\mathbf{k}}$ is a sum over momentum and Matsubara frequencies at temperature T. The many-body Green's function $G(K)$ is found from the inverse of Eq. (2.1):

$$G^{-1}(K) - G_0^{-1}(K) = -\Sigma(K) = -\Delta^2\widetilde{G}_0(K). \tag{2.3}$$

Except for the matrix structure in the above equations, these are the usual definitions of the fermionic Green's function and self energy associated with BCS theory. As in the cold atoms literature, we regularize the gap equation by replacing the interaction strength g with the scattering length a through $1/g = m/4\pi a - \sum_{\mathbf{k}} m/\mathbf{k}^2$.

The goal now is to include pair fluctuations, or pseudogap (pg) effects, in a fashion fully consistent with both the ground state and the mean-field equations. The latter have been extensively studied in previous work [Gong et al., 2011, Han & Sá de Melo, 2012, Hu et al., 2011, Vyasanakere & Shenoy, 2011, Vyasanakere et al., 2011, Yu & Zhai, 2011]. The approach we outline below was introduced in the context of high temperature superconductors [Chen et al., 1999, 2005], but it has been applied also to spin-orbit coupled Fermi superfluids [He et al., 2013].

Pair fluctuations lower the phase transition temperature T_c relative to its mean-field value denoted by T^*. The latter is the temperature at which the pairing gap, determined by Eq. (2.2), first becomes non zero. (Note that T^* does not reflect a broken symmetry state and is not a true phase transition). As a result, a central component of the present theory is that the usual Thouless condition (on the t-matrix) for the instability of the normal phase [Schrieffer, 1964] must be modified to include a well developed excitation gap. Imposing consistency with mean-field theory for the pairing gap $\Delta(T)$, obtained from Eq. (2.2), leads to a modified Thouless condition for the instability temperature:

$$t_{\rm pg}(Q) \equiv \frac{g}{1 + g\chi(Q)} \to \infty, \text{ as } Q \to 0, \tag{2.4}$$

where $\chi(Q) \equiv -\frac{1}{2}\sum_K \mathrm{Tr}\left[G(K)\widetilde{G}_0(K-Q)\right]$. This ensures T_c lies on the mean-field Δ versus T curve. Establishing the specific value of T_c, however, requires that we find an additional constraint associated with the existence of a condensate. As reviewed in appendix (A.1), and discussed in detail elsewhere [Chen et al., 2005], precisely at T_c we have the equation $\Delta^2 = -\sum_{Q\neq 0} t_{\rm pg}(Q)$. The transition temperature T_c is thus determined as the temperature at which this function constraining $\Delta(T)$ intersects with the mean-field gap equation value.

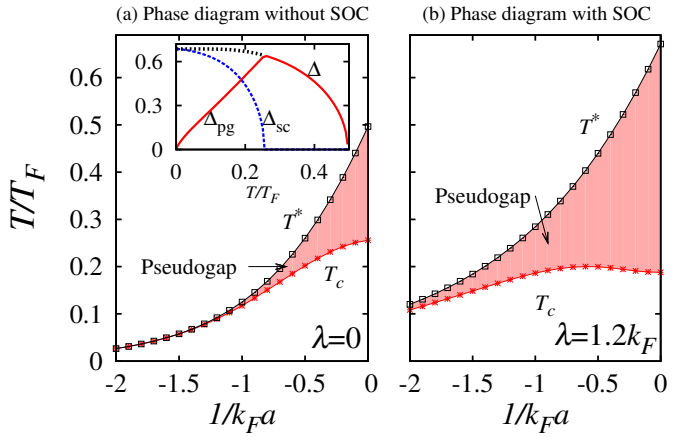

Figure 2.1: Phase diagrams for a degenerate Fermi gas without (a) and with (b) SOC. Plotted is T^* as a function of inverse scattering length, $1/k_F a$, indicating where pairing first sets in, while T_c marks the onset of condensation to the superfluid phase. The plot shows the weakly interacting regime with $1/k_F a < 0$. As spin-orbit coupling is turned on, pairing is enhanced leading to a larger pseudogap region. The inset in (a) indicates the temperature dependence of the component gap parameters (defined in the text) at unitarity, $1/k_F a = 0$.

As discussed in appendix (A.1), away from $T = T_c$ the excitation gap contains the sum of condensed (sc) and non-condensed (pg) contributions: $\Delta^2 = \Delta_{\rm sc}^2 + \Delta_{\rm pg}^2$, where below T_c we have proved $\Delta_{\rm pg}^2 = -\sum_{Q\neq 0} t_{\rm pg}(Q)$. Importantly, we can interpret this last equation as suggesting that $t_{\rm pg}$ is a propagator for a thermal gas of composite (non-condensed) bosons.

Above T_c we take $\Delta_{\rm pg}^2$ to be the mean-field value, although this assumption is unnecessary. [1] The inset of Fig. 2.1(a) plots the temperature dependence for $\Delta_{\rm sc}$, $\Delta_{\rm pg}$, and the total excitation gap Δ. We emphasize that a central distinguishing feature of the present approach is T_c is determined in the presence of a well developed gap at T_c. This contrasts with the scheme of Nozières and Schmitt-Rink (NSR) [Nozières & Schmitt-Rink, 1985]. In the NSR scheme the pair susceptibility $\chi(Q)$ is given by two bare Green's functions, which do not connect to the mean-field gap equation in Eq. (2.2). This approach is similarly different from path integral-collective mode schemes [He & Huang, 2013]. The latter introduce Goldstone bosons, but importantly these do not renormalize the mean-field transition temperature which remains at T^*.

1. It is possible to consider more precise t-matrix based numerical [Maly et al., 1999] and analytic [He et al., 2007b] schemes. As as long as the pseudogap vanishes at the mean field T^*, there is no relevant qualitative difference.

Figure 2.1 shows the calculated phase diagram, plotting T_c and T^*, in the absence (a) and presence (b) of Rashba SOC. The latter is in reasonable agreement with the results of Ref. [He et al., 2013]. We restrict these plots to the weak pairing side of resonance. Here we observe a greatly enhanced pseudogap regime denoted by an enhancement of T^*, without significant enhancement of T_c. The behavior of T^* has been attributed to the enhancement of the pairing attraction [Gong et al., 2011, Han & Sá de Melo, 2012, Hu et al., 2011, Vyasanakere & Shenoy, 2011, Vyasanakere et al., 2011, Yu & Zhai, 2011], due to an increased density of states near the minimum of the Rashba ring. Since T_c is obtained in the presence of a gap at T_c, stronger pairing (reflected in T^*) is offset by an increasingly gapped density of states. This leads to a relatively constant T_c as a function of interaction strength.

2.3 Density/current response and f-sum rules

To characterize the normal phase with pairing and the superfluid phase in more detail, we investigate both the density/current-density/current and spin-spin correlation functions, considering the former first. For systems with a global $\mathrm{U}(1)$ symmetry, the Ward-Takahashi identity (WTI) provides an important constraint on the full vertex, $\Gamma^{\mu}(\widetilde{K}, K)$, which enters into the correlation functions. Given a mean-field-like self energy, it is possible to analytically solve the WTI and obtain the full vertex function and the full correlation function [Boyack et al., 2014, Ryder, 1996]. We define the generalized correlation function

$$P^{\mu\nu}(Q) = \sum_{K} \mathrm{Tr}\left[G(\widetilde{K})\Gamma^{\mu}(\widetilde{K}, K)G(K)\gamma^{\nu}(K, \widetilde{K})\right], \tag{2.5}$$

where $\widetilde{K} \equiv K + Q$ and $\gamma^{\mu}(\widetilde{K}, K)$ is the bare vertex. From this we have the density-density, $\chi_{\rho\rho}(Q) \equiv P^{00}(Q)$, and current-current, $\chi_{JJ}(Q) \equiv P^{ij}(Q), i, j \in \{1, 2, 3\}$, correlation functions.

The bare and full vertices satisfy, respectively

$$q_\mu \gamma^\mu(\widetilde{K}, K) = G_0^{-1}(\widetilde{K}) - G_0^{-1}(K), \tag{2.6}$$

$$q_\mu \Gamma^\mu(\widetilde{K}, K) = G^{-1}(\widetilde{K}) - G^{-1}(K), \tag{2.7}$$

with the latter a consequence of the WTI. We now specialize to systems with the self energy as in Eq. (2.3). Using the WTI above T_c, we have [see appendix (A.3.1)]:

$$\Gamma^\mu(\widetilde{K}, K) = \gamma^\mu(\widetilde{K}, K) + \Delta^2 \widetilde{G}_0(\widetilde{K}) \widetilde{\gamma}^\mu(\widetilde{K}, K) \widetilde{G}_0(K), \tag{2.8}$$

where $\widetilde{\gamma}^\mu(\widetilde{K}, K) = \sigma_y \gamma^\mu(-\widetilde{K}, -K)^T \sigma_y$ is a time-reversed vertex. Inserting the full vertex into Eq. (2.5) then gives the correlation functions above T_c.

One can incorporate superconducting (or equivalently superfluid) terms within this formalism building on Eq. (2.8) and, for example, address the superfluid density [Chen et al., 1999, He & Huang, 2012, Zhou & Zhang, 2012], as outlined in appendix (A.5). One considers the transverse response, $P_T^{\mu\nu}(Q)$, which contains no collective modes:

$$\begin{aligned} P_T^{\mu\nu}(Q) = \sum_K \mathrm{Tr} \Big\{ \Big[& G(\widetilde{K}) \gamma^\mu(\widetilde{K}, K) G(K) + F_{\mathrm{pg}}(\widetilde{K}) \widetilde{\gamma}^\mu(\widetilde{K}, K) \widetilde{F}_{\mathrm{pg}}(K) \\ & - F_{\mathrm{sc}}(\widetilde{K}) \widetilde{\gamma}^\mu(\widetilde{K}, K) \widetilde{F}_{\mathrm{sc}}(K) \Big] \gamma^\nu(K, \widetilde{K}) \Big\}, \end{aligned} \tag{2.9}$$

where $F_\kappa(K) = \Delta_\kappa \widetilde{G}_0(K) G(K) = \widetilde{F}_\kappa(K)$ for $\kappa \in \{\mathrm{sc}, \mathrm{pg}\}$. Note that F_{pg} does not represent an anomalous Green's function, but rather reflects a vertex correction to the correlation functions [Boyack et al., 2014].

As shown in appendix (A.3.2), when one integrates over the entire frequency range, a consequence of the WTI is that the f-sum rule is satisfied:

$$\int \frac{d\omega}{\pi} \left(-\omega \chi''_{\rho\rho}(\omega, \mathbf{q}) \right) = \frac{nq^2}{m}, \tag{2.10}$$

where $\chi''_{\rho\rho}$ is the imaginary part of the density response function. This f-sum rule depends on the total particle number n and the bare mass m. Since λ does not enter, the presence of spin-orbit coupling does not modify the weight of the f-sum rule.

2.4 Spin response and f-sum rules

In the spin channel, there is no global $\mathrm{U}(1)$ symmetry to justify the use of the WTI. Nevertheless, we are able to provide an *a posteriori* check on any proposed correlation function via a sum rule which we now derive. We define $\chi_{S_iS_j}(i\omega,\mathbf{q}) \equiv \int d\tau\, e^{i\omega\tau}\left\langle T_\tau S_{\mathbf{q}i}(\tau)\, S_{-\mathbf{q}j}(0)\right\rangle$ where T_τ is the time ordering operator and $S_{\mathbf{q}i} = \sum_{\mathbf{k},s,s'} c^\dagger_{\mathbf{k}s}(\sigma_i)_{ss'} c_{\mathbf{k}+\mathbf{q}s'}$ is the many-body spin density operator. Using the Heisenberg equations of motion and the properties of Fourier transforms, the sum rule for the spin-spin correlation function $\chi''_{S_iS_j}$ can be shown [Förster, 1975] to be

$$\int \frac{d\omega}{\pi}\left(-\omega\chi''_{S_iS_j}(\omega,\mathbf{q})\right) = \left\langle\left[\left[\mathcal{H}_0, S_{\mathbf{q}i}\right], S_{-\mathbf{q}j}\right]\right\rangle, \tag{2.11}$$

where $\mathcal{H}_0 = \sum_{\mathbf{k},s,s'} c^\dagger_{\mathbf{k}s} H^0_{ss'}(\mathbf{k})\, c_{\mathbf{k}s'}$ and $\chi''_{S_iS_j}$ is the singular part of $\chi_{S_iS_j}$ [Henrici, 1986], found by analytically continuing $i\omega \to \omega + i\delta$ and then taking the $\delta \to 0^+$ limit. A similar analysis relating sum rules to the equation of motion was presented for Bose gases in Ref. [Yu, 2014].

Here we give the explicit result, for two example cases of interest, and present further details in appendix (A.4):

$$\int \frac{d\omega}{\pi}\left(-\omega\chi''_{S_iS_i}(\omega,\mathbf{q})\right) = \frac{nq^2}{m} - \frac{4\lambda}{m}\sum_{\mathbf{k},\alpha}\alpha f_{ii} n_{\mathbf{k}\alpha}. \tag{2.12}$$

where $i \in \{x,z\}$, $f_{zz} = k_\perp$, $f_{xx} = k_x^2/k_\perp$ and $n_{\mathbf{k}\alpha} = T\sum_{i\omega} G^\alpha_H(K)$, with $G^\alpha_H(K)$ a helicity Green's function to be defined in the next section.

2.5 Correlation functions in the helicity basis

In the absence of a magnetic field, helicity is a good quantum number and the correlation functions are most easily expressed in terms of the helicity Green's functions [He et al., 2013]:

$$G_H^\alpha(K) \equiv \frac{u_{\mathbf{k}\alpha}^2}{i\omega - E_{\mathbf{k}\alpha}} + \frac{v_{\mathbf{k}\alpha}^2}{i\omega + E_{\mathbf{k}\alpha}}, \tag{2.13}$$

$$F_H^\alpha(K) \equiv u_{\mathbf{k}\alpha} v_{\mathbf{k}\alpha} \left(\frac{1}{i\omega + E_{\mathbf{k}\alpha}} - \frac{1}{i\omega - E_{\mathbf{k}\alpha}} \right), \tag{2.14}$$

where $E_{\mathbf{k}\alpha} = \sqrt{\xi_{\mathbf{k}\alpha}^2 + \Delta^2}$, $\xi_{\mathbf{k}\alpha} = k^2/2m - \mu + \alpha\lambda k_\perp/m$ is an eigenvalue of $H^0(\mathbf{k})$, and $F_H^\alpha(K)$ represents the pseudogap, or equivalently vertex, contribution. Here $\alpha = \pm$ denotes the helicity index and the coherence factors satisfy $u_{\mathbf{k}\alpha}^2 = \frac{1}{2}(1 + \xi_{\mathbf{k}\alpha}/E_{\mathbf{k}\alpha})$, $u_{\mathbf{k}\alpha}^2 + v_{\mathbf{k}\alpha}^2 = 1$.

It follows from the vertex function in Eq. (2.8) that the explicit form for the f-sum rule consistent [Boyack et al., 2014] density-density correlation function is

$$\chi_{\rho\rho}(\omega, \mathbf{q}) = \frac{1}{2} \sum_{K,\alpha,\alpha'} \left(1 + \alpha\alpha' \cos\left(\phi_{\mathbf{k}+\mathbf{q}} - \phi_{\mathbf{k}}\right)\right) \left[G_H^\alpha(K) G_H^{\alpha'}(\widetilde{K}) + F_H^\alpha(K) F_H^{\alpha'}(\widetilde{K}) \right]. \tag{2.15}$$

The angle $\exp(i\phi_{\mathbf{k}}) = (k_x + ik_y)/k_\perp$, so that $\exp(i\phi_{-\mathbf{k}}) = -\exp(i\phi_{\mathbf{k}})$.

The spin-spin correlation functions are constructed using their form below T_c (deduced using the path integral [Ojanen & Kitagawa, 2013]) appropriately modified in the pseudogap state relative to the condensed phase. These modifications are essential for satisfying sum rules.

As can be shown, in the normal phase the following expression for the spin-spin correlation functions are fully compatible with the spin f-sum rules given in Eq. (2.12):

$$\chi_{S_iS_i}(\omega, \mathbf{q}) = \frac{1}{2} \sum_{K,\alpha,\alpha'} \left(1 \pm \alpha\alpha' \cos\left(\phi_{\mathbf{k}+\mathbf{q}} \pm \phi_{\mathbf{k}}\right)\right) \left[G_H^\alpha(K) G_H^{\alpha'}(\widetilde{K}) + F_H^\alpha(K) F_H^{\alpha'}(\widetilde{K}) \right], \tag{2.16}$$

where the $+, -$signs are for $\chi_{S_xS_x}, \chi_{S_zS_z}$ respectively.

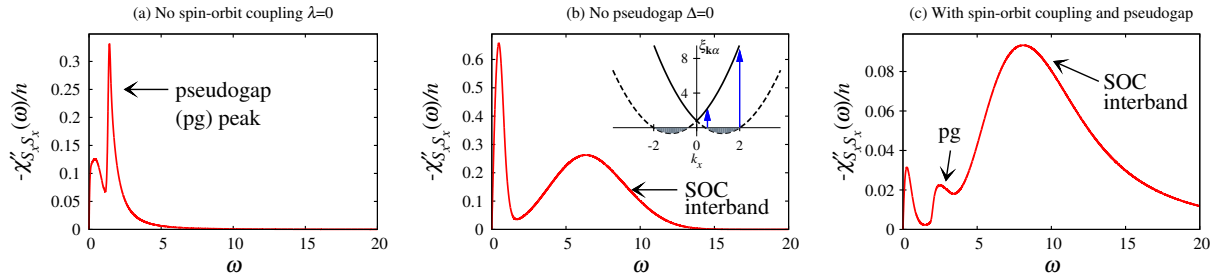

Figure 2.2: The spin-spin response function as a function of frequency. Figure 2.2(a) corresponds to a pseudogap phase without SOC. The peak at lower ω reflects thermally excited fermions while the second peak is at ω comparable to the pseudogap energy scale, where pairs are now broken. Since $\lambda = 0$, the spin-spin and density-density correlation functions are the same. In Fig. 2.2(b) the pseudogap is set to zero with fixed $\lambda = 1.2k_F$. The lower energy intra-helicity band peak is enhanced and one observes an SOC-related peak. As shown in the inset, the low-energy threshold reflects the onset of inter-helicity band transitions, while the high-energy endpoint occurs when these transitions are no longer possible. In Fig. 2.2(c), in the presence of both a pseudogap and SOC, one sees a combination of the effects in the previous two panels. Spectral weight is transferred to yield a larger SOC peak, reflecting the gapping of the low energy contributions. All quantities are measured relative to the Fermi energy, E_F, or Fermi momentum k_F.

2.6 Numerical results

We now look for qualitative new physics in the spin-spin response functions. We numerically calculate the response function $\chi''_{S_xS_x}(\mathbf{q},\omega)$ at fixed $\mathbf{q} = (0.5, 0, 0)k_F$ as a function of ω, [2] and for definiteness consider $T = 0.28T_F > T_c$ and unitary scattering, $1/k_Fa = 0$. The results are plotted in Fig. (2.2). In order to illustrate the physics, in Fig. 2.2(a) and Fig. 2.2(b), Rashba SOC or pseudogap effects were set to zero respectively, while Fig. 2.2(c) shows their combined effects. The f-sum rules derived above are important for constraining numerical results of the spin-spin and density-density correlation functions. Comparison between our numerical calculations and the exact f-sum rules agreed to within a few percent.

In Fig. 2.2(a) we set $\lambda = 0$. In this case, above T_c the spin-spin and density-density correlation functions are equal ($\chi''_{S_xS_x} = \chi''_{\rho\rho}$) and this function is plotted in the figure. Two low energy peaks are observable, as found in earlier work [Guo et al., 2010]. The lower frequency peak reflects

2. We introduce a finite life time $\Gamma = 0.05$ in the self energy, both to distinguish this term from the condensate and for numerical stability.

contributions from thermally excited fermions, while the higher frequency peak is associated with the contribution from broken pairs which appears at a threshold associated with the pseudogap.

In Fig. 2.2(b) we set $\Delta_{\rm pg} = 0$ and plot $\chi''_{S_xS_x}$ for a pure SOC system with $\lambda = 1.2k_F$. (We do not show $\chi''_{\rho\rho}$ since there is still no qualitative signature of $\lambda \neq 0$.) The response $\chi''_{S_xS_x}$ shows two peaks, but one is at a considerably higher energy compared to Fig. 2.2(a). The lower frequency peak reflects intra-helicity band contributions, while the larger frequency peak is due to inter-helicity effects.

Importantly, this figure shows how the physics of the Rashba ring band-structure can be directly probed by the spin-spin response functions. To illustrate this, in the inset we plot the dispersion relation of two helicity bands. The horizontal line denotes the self-consistently determined chemical potential, chosen so that occupied fermions mostly reside in the Rashba ring. The onset of the inter-helicity band transition energy is given by the energy difference between two bands positioned on the inner circle of the ring, while the endpoint frequency for this peak is determined by the outer circle. These energy differences roughly match the width observed in the high frequency peak in the main plot. (The smearing of the width is because we have a non-zero momentum $\mathbf{q}$ and $T \neq 0$.)

Finally, in Fig. 2.2(c) we plot $\chi''_{S_xS_x}$ for the case where both pseudogap and Rashba SOC are present. Here we observe three distinct peaks. The first is associated with thermally excited fermions within the lowest helicity band, the second with the breaking of the preformed (pg) pairs and the third mainly with the inter-helicity transitions discussed in the previous panel. We also observe some inter-play between pairing and the high frequency SOC peak, as this inter-helicity band peak is pushed toward slightly higher energies.

As far as whether or not these effects are experimentally observable, we note the overall small size of the pg-labeled pseudogap peak in Fig. 2.2(c). What is most important is not the small size of this specific feature, but rather the reduction in the overall low frequency weight [for example, relative to Fig. 2.2(b)] associated with the presence of a pseudogap. Such a reduction then shows up as an enhancement of the response at higher frequencies.

2.7 Conclusions

A major finding of this chapter is that spin-spin correlation functions provide a clear signature of the simultaneous presence of Rashba modified band structure and of a pairing gap. Signatures of both are a necessary (but clearly not sufficient) condition for ultimately obtaining a topological superfluid. This should complement observations that are based on the single-particle response functions in different experiments either in ultra cold Fermi gases [Cheuk et al., 2012, Fu et al., 2013, Wang et al., 2012] or in condensed matter. To establish consistency we derived f-sum rules for spin-spin correlation functions and showed that our spin response functions satisfy these sum rules. These sum rules provide important constraints on the spin response, which is complicated by the fact that spin conservation laws are absent in spin-orbit coupled systems.

CHAPTER 3

TOPOLOGICAL EFFECTS ON TRANSITION TEMPERATURES AND RESPONSE FUNCTIONS IN THREE-DIMENSIONAL FERMI SUPERFLUIDS

This chapter builds upon the work done in the previous chapter for spin-orbit coupled Fermi gases in the absence of a magnetic field. In particular, here we investigate the effects of topological order on the transition temperature, T_c, and response functions in three-dimensional spin-orbit coupled Fermi superfluids, now with the inclusion of a transverse magnetic field. Our calculations include fluctuation effects beyond mean-field theory and are compatible with f-sum rules. In the topological phase we find that T_c can be as large as 10% of the Fermi temperature, which should be experimentally accessible in cold gas experiments. At higher temperatures, above T_c, the spin and density response functions provide signatures of topological phases via the recombination or amplification of frequency dependent peaks. The work in this chapter is published in Ref. [Anderson et al., 2015].

3.1 Introduction

The excitement surrounding topological superfluids [Alicea, 2012, Hasan & Kane, 2010, Qi & Zhang, 2011, Read & Green, 2000] derives from both their scientific as well as technological potential. Inspired by the canonical topological superfluid, a spinless $p_x + ip_y$ superfluid [Read & Green, 2000], it has been argued [Fu & Kane, 2008, Sato et al., 2009, Zhang et al., 2008] that some combination of spin-orbit coupling (SOC), magnetic field, as well as superfluid pairing can artificially produce such a state. This was explored via the proximity effect in solid state systems [Fu & Kane, 2008] and using intrinsic pairing in ultra cold Fermi gases [Iskin & Subaşı, 2011, Yi & Guo, 2011, Zhai, 2015, Zhang et al., 2008, Zhou et al., 2011].

In this chapter we study this second case of intrinsic pairing. A central goal is to determine how a transition from a trivial to a topological phase is reflected in the superfluid transition temperature T_c and in response functions. This is particularly important since cold gas experiments have now implemented spin-orbit coupling [Cheuk et al., 2012, Huang et al., 2016, Wang et al., 2012] and, if T_c is sufficiently large, will be able to address topological phases. Calculations of T_c in a topological phase, which necessarily go beyond previous [Gong et al., 2011, Han & Sá de Melo, 2012, Hu et al., 2011, Jiang et al., 2011, Seo et al., 2013, Vyasanakere & Shenoy, 2015, Vyasanakere et al., 2011, Yu & Zhai, 2011] mean-field approaches, are not available. Indeed, topological order at the transition is only a meaningful concept if T_c, itself, is computed in the presence of a pairing gap. Thus, here we emphasize the importance of fluctuations. In a topological phase we find that T_c can be as large as 10% of the Fermi temperature (T_F) which should be quite accessible experimentally. However, we find that these superfluids self-consistently adjust to stabilize topological phases in the lower T_c, BCS regime. (Note that, a recent complementary paper considers fluctuation effects in spin-orbit coupled Fermi superfluids with fixed relative population density using a closely related formalism [Wang & He, 2015].)

In addition to T_c, it is important to establish signatures of topological order as reflected in the band structure. While there have been a number of proposals in the literature [Gong et al., 2011, Ojanen & Kitagawa, 2013, Seo et al., 2012, 2013, Zheng et al., 2014] we approach this challenge via studies of the finite temperature density-density and spin-spin correlation functions, which should be accessible [Veeravalli et al., 2008] in future experiments. We find that the position or threshold of peaks in these responses reflects the topological nature of the band structure. Importantly, these response functions are tightly constrained by sum rules. Our theoretical framework satisfies all sum rules, which serves as a check on our calculations and also implies these signatures of topological order in response functions are unambiguous. In the topological phase we find that a peak in the density response is significantly amplified due to a saddle point Van Hove singularity, often seen in correlated superfluids [James et al., 2012a, Kao et al., 2000]. In the trivial phase the spin response exhibits two distinct peaks, which merge into a single peak in the topological phase.

3.2 Topological superfluids

The concept of topological order is based on the Bogoliubov or fermionic quasi-particle dispersion associated with a mean-field approximation. Therefore we begin with the Bogoliubov-de Gennes (BdG) Hamiltonian for a spin-orbit coupled Fermi superfluid:

$$\mathcal{H}_{\mathrm{BdG}} = \begin{pmatrix} H_0(\mathbf{k}) & \Delta \\ \Delta^* & -\widetilde{H}_0(\mathbf{k}) \end{pmatrix}, \tag{3.1}$$

where Δ is a pairing gap and $\widetilde{H}_0(\mathbf{k}) = \sigma_y \left[H_0^*(-\mathbf{k})\right] \sigma_y$ is the time-reversed single-particle (hole) Hamiltonian. Here the single particle Hamiltonian $H_0(\mathbf{k}) = \xi_{\mathbf{k}} + \mathbf{h}(\mathbf{k}) \cdot \boldsymbol{\sigma}$, where $\xi_{\mathbf{k}} = k^2/2m - \mu$ describes a free particle of momentum $\mathbf{k} = (k_x, k_y, k_z)$, mass m, and chemical potential μ; throughout we set $\hbar = k_B = c = 1$. The spin-orbit coupling enters through the vector $\mathbf{h}(\mathbf{k}) = \mathbf{h}_\perp(\mathbf{k}) + \mathbf{h}_\parallel(\mathbf{k})$, which couples the spin-$\frac{1}{2}$ operator $\boldsymbol{\sigma} = (\sigma_x, \sigma_y, \sigma_z)$ to a magnetic field $\mathbf{h}_\parallel(\mathbf{k}) = b_z \hat{z}$ and an in-plane SOC field $\mathbf{h}_\perp(\mathbf{k}) = \lambda \mathbf{k}_\perp / m$, with SOC strength λ.

Of significant theoretical interest has been isotropic (Rashba) SOC, described by $\mathbf{k}_\perp = (k_x, k_y, 0)$ with an out-of-plane momentum $\mathbf{k}_\parallel = \mathbf{k} - \mathbf{k}_\perp = (0, 0, k_z)$. While we consider the Rashba case in this chapter, we note that most experimental success [Cheuk et al., 2012, Wang et al., 2012] has related to the crossed-Raman configuration [Higbie & Stamper-Kurn, 2004, Lin et al., 2011] where $\mathbf{k}_\perp = (k_x, 0, 0)$ and $\mathbf{k}_\parallel = (0, k_y, k_z)$. For the crossed-Raman case we found similar results.

There are four branches in the BdG eigenvalue spectrum, $\eta E_{\alpha\mathbf{k}}$ for $\alpha, \eta = \pm 1$ with the positive energy dispersion

$$E_{\alpha\mathbf{k}} = \sqrt{\xi_{\mathbf{k}}^2 + |\mathbf{h}|^2 + \Delta^2 + 2\alpha\sqrt{\xi_{\mathbf{k}}^2 |\mathbf{h}|^2 + \Delta^2 b_z^2}}. \tag{3.2}$$

For the three-dimensional case, this leads to three distinct topological phases. The topological phase diagram is specified by inequalities derived from solving $E_-(\mathbf{k}_\parallel, \mathbf{k}_\perp = 0) = 0$. No nodes appear when $b_z < \Delta$, corresponding to a non-topological or "trivial" superfluid. If $\mu > 0$ and $(\mu^2 + \Delta^2) > b_z^2 > \Delta^2$, the topological superfluid has four nodes (4-Weyl points) which emerge

at $k_\parallel^2/2m = \mu \pm \sqrt{b_z^2 - \Delta^2}$. Finally, for arbitrary μ, the system is a topological superfluid with two nodes (2-Weyl points) when $b_z^2 > (\mu^2 + \Delta^2)$ [Jiang et al., 2011, Seo et al., 2012, 2013]. For Rashba SOC, the dispersion around the nodes is linear in momentum, and is described by a Weyl Hamiltonian with topologically protected nodes.

Along with the usual number equation determining μ, central to mean-field theory is the self-consistent condition or gap equation [Jiang et al., 2011, Seo et al., 2012, 2013], which determines Δ. We rewrite this suggestively as

$$\Gamma^{-1}(0,T) = \frac{1}{2}\sum_{\mathbf{k}}\sum_{\eta\alpha\alpha'} \frac{\delta_{\eta,+1} - (\eta f(E_{\alpha\mathbf{k}}) + f(\xi_{\alpha'\mathbf{k}}))}{\eta E_{\alpha\mathbf{k}} + \xi_{\alpha'\mathbf{k}}} v_{\eta\alpha\alpha'}(\mathbf{k},\mathbf{k}) + g^{-1} = 0, \tag{3.3}$$

where $f(x)$ is the Fermi distribution and $g > 0$ is an attractive interaction. Where relevant, we regularize integrals by introducing a scattering length defined through $g^{-1} = m/4\pi a - \sum_{\mathbf{k}} m/\mathbf{k}^2$ [Ketterle & Zwierlein, 2008]. The coherence factor $v_{\eta\alpha\alpha'}(\mathbf{k},\mathbf{k})$ [and its generalization, $v_{\eta\alpha\alpha'}(\mathbf{k},\mathbf{k}-\mathbf{q})$] is presented in appendix (B.1). Their specific form is irrelevant for the present discussion.

3.3 Fluctuation formalism

The transition temperature, T_c, necessarily contains fluctuation effects [Chen et al., 2005, Wu et al., 2015] which serve to distinguish it from the lowest temperature, denoted T^*, at which the mean-field gap equation satisfies $\Delta(T^*) = 0$. The fluctuations in question are non-condensed pairs [Chen et al., 1999, 2005]. We choose these pairs in a specific manner [Chen et al., 2005] to satisfy the Hugenholtz-Pines constraint, making use of Eq. (3.3). Requiring that these pair excitations are gapless in the ordered phase, we extend Eq. (3.3) to finite $Q \equiv (i\omega, \mathbf{q})$ (where $i\omega$ is a Bosonic Matsubara frequency) which leads to:

$$\Gamma^{-1}(Q,T) = \frac{1}{2}\sum_{\mathbf{k}}\sum_{\eta\alpha\alpha'} \frac{\delta_{\eta,+1} - \left(\eta f(E_{\alpha\mathbf{k}}) + f\left(\xi_{\alpha'\mathbf{k}-\mathbf{q}}\right)\right)}{\left(\eta E_{\alpha\mathbf{k}} + \xi_{\alpha'\mathbf{k}-\mathbf{q}}\right) - i\omega} v_{\eta\alpha\alpha'}(\mathbf{k},\mathbf{k}-\mathbf{q}) + g^{-1}. \tag{3.4}$$

From the structure of Eq. (3.3) it is apparent that $\Gamma\left(0,T\right)$ depends on both the full energy spectrum $E_{\alpha\mathbf{k}}$ as well as the bare energy $\xi_{\alpha\mathbf{k}}$. Thus, one might expect [as implemented in Eq. (3.4)], that the fluctuation propagator $\Gamma(Q,T)$ should depend on an asymmetric combination of bare and dressed Green's functions. [1]

We next consider the propagator in Eq. (3.4) expanded at small momenta, where [using Eq. (3.3)] $\Gamma\left(Q,T\right) \approx a_0^{-1}(i\omega-\omega_{\mathbf{q}})^{-1}$. Here both $a_0 = \partial_{i\omega}\Gamma^{-1}\left(Q,T\right)\big|_{Q=0}$ and the pair dispersion $\omega_{\mathbf{q}} = -a_0^{-1}\left[\Gamma^{-1}\left(\mathbf{q},T\right)-\Gamma^{-1}\left(0,T\right)\right] \approx q_\perp^2/2M_\perp + q_\parallel^2/2M_\parallel$ depend implicitly on T. We identify $M_\perp$ ($M_\parallel$) as the effective pair mass for the component of momentum parallel (perpendicular) to the SOC vector. While it is sometimes possible to calculate the effective pair masses $M_\perp$, $M_\parallel$ analytically, in general this is not necessary. Rather, it suffices to calculate numerically the second-order derivative at small $\mathbf{q}$. [2]

Notice that the small-Q form of $\Gamma\left(Q,T\right)$ reflects, up to a constant, the non-interacting Green's function of a thermal Bose gas with pair dispersion $\omega_{\mathbf{q}}$, at or below the condensation temperature $[\Gamma^{-1}\left(0,T\leq T_c\right)=0]$. This implies $n_B \equiv -a_0\sum_Q \Gamma\left(Q,T\right)$ can be interpreted as a Bose occupation number. At $T=T_c$, the form of the fermionic self-energy forces

$$-\sum_Q \Gamma\left(Q,T_c\right) = \Delta^2. \tag{3.5}$$

This equation constrains $\Gamma\left(Q,T_c\right)$, and characterizes the excitation gap in the limit in which all pairs are non-condensed. The condition for T_c is then simply obtained [Chen et al., 1999, 2005, Wu et al., 2015] by equating the constraint on $\Delta(T_c)$ via Eq. (3.5) with that obtained from the mean-field gap equation in Eq. (3.3).

1. However, within the widely used saddle-point approximation, the effective vertex obtained via the path integral can include Green's functions only in a symmetric manner.

2. Since $\Gamma\left(0,\mathbf{q}\right)$ will be symmetric in $\mathbf{q}$ for inversion-symmetric systems, the first and third order terms in $\mathbf{q}$ will vanish, and the lowest order correction will come in at fourth order.

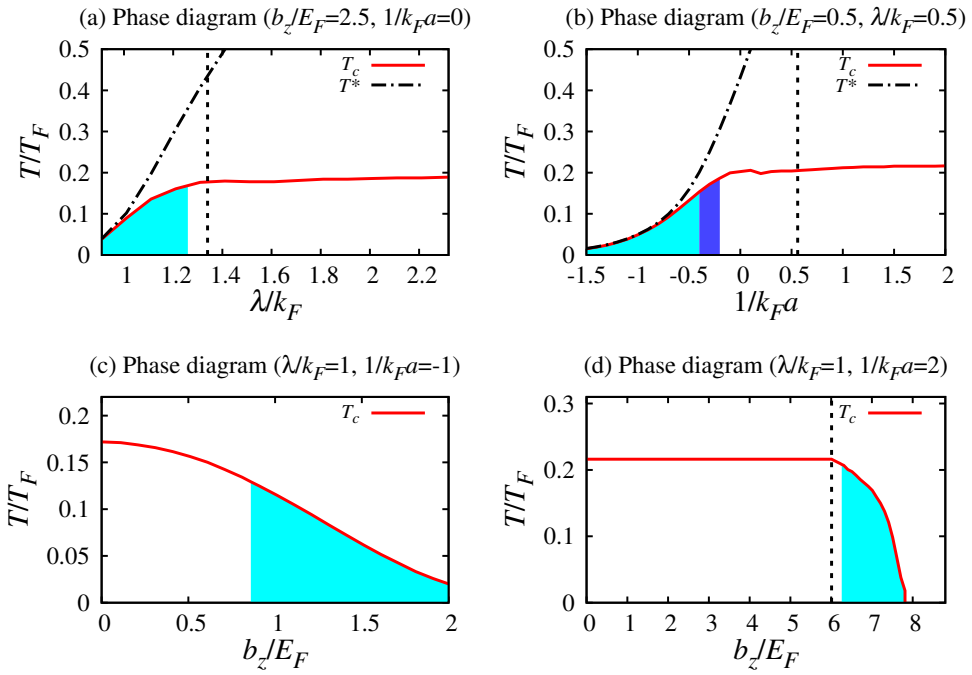

Figure 3.1: Phase diagrams for the superfluid temperature T_c and (where shown) the mean-field transition temperature T^*. The $T = 0$ topological phases are indicated by shaded regions in light (dark) blue color with 2 (4)-Weyl points. The top two panels show the dependence on either SOC strength λ (left) or scattering length $1/k_Fa$ (right), with other parameters fixed. The lower panels show T_c versus b_z with $\lambda/k_F = 1$ for both panels, $1/k_Fa = -1$ on the left and $1/k_Fa = 2$ on the right. Dotted lines indicate $\delta\mu = 0$. Once a topological phase is entered the system becomes more BCS-like.

Importantly, this approach, which can be generalized to *any* BCS-BEC mean-field theory, explicitly avoids the non-physical first order transition found in all other BCS-BEC theories [Fukushima et al., 2007, Haussmann et al., 2007, Hu et al., 2007, Pieri et al., 2004]. Interpreting Eq. (3.3) and Eq. (3.5), we observe that Eq. (3.3) is equivalent to setting the bosonic chemical potential to zero below T_c and Eq. (3.5) guarantees that the number of non-condensed bosons reaches a maximum at T_c (which is determined by the fermionic pairing gap). We will assume throughout that, above T_c, the mean-field gap represents a reasonable (but not essential) approximation for the normal state Δ. [3]

3. One can improve upon this approach. However, the added complexity does not affect T_c or lead to qualitatively new physics [He et al., 2007b, Maly et al., 1999].

3.4 Phase diagram

To understand the effects of SOC and the magnetic field on condensation and pairing, we numerically compute T^* and T_c, varying $1/k_F a$, b_z, and λ. Where relevant, we measure quantities in terms of the Fermi momentum (k_F), energy (E_F), or temperature (T_F) as defined with respect to the $\lambda = b_z = 0$ limit. It is convenient to define a shifted chemical potential, $\delta\mu = \mu - \mu_0$, where $\mu_0 = -E_{\rm so}(1 + b_z^2/E_{\rm so}^2)/2$ if $E_{\rm so} \geq b_z$ and $\mu_0 = -b_z$ if $E_{\rm so} < b_z$; here the SOC energy is $E_{\rm so} = \lambda^2/m$. A necessary (but not sufficient) condition for a topological phase is then $\delta\mu > 0$.

Figure (3.1) plots T_c and (in some cases) the pairing onset temperature T^* as a function of either λ, b_z, or $1/k_F a$. Dotted lines indicate where $\delta\mu = 0$. Where relevant, these plots are consistent with earlier work [Zheng et al., 2014]. A close analogy between varying λ and varying $1/k_F a$ is seen in Fig. 3.1(a) and Fig. 3.1(b). We define "weak" or "enhanced" pairing relative to $b_z = 0$. The former is associated with small λ or negative $1/k_F a$ while the latter corresponds to either large λ or large positive $1/k_F a$. Thus, Fig. 3.1(c) is characteristic of the generic weak pairing regime while Fig. 3.1(d) is characteristic of the strong pairing case produced by either large $1/k_F a$ or large λ.

We analyze the top two figures by focusing on a decreasing abscissa which effects a transition from a trivial to topological phase (shown as shaded). In Fig. 3.1(a), corresponding to $1/k_F a = 0$ and $b_z = 2.5E_F$, this transition is driven by varying the SOC strength λ. In Fig. 3.1(b) it is driven by varying the scattering length $1/k_F a$; somewhat after the point $\delta\mu > 0$ is crossed, a further *decrease* in $1/k_F a$ (towards the BCS limit) allows the system to reach a topological phase. Here we observe a series of two transitions from topologically trivial to 4-Weyl and then to 2-Weyl superfluids. While there is some initial decline in T_c with diminishing $1/k_F a$, the most significant decrease in T_c occurs in the 2-Weyl case. The next two panels contrast the regime of weak pairing [Fig. 3.1(c)] with that of enhanced pairing [Fig. 3.1(d)]. In Fig. 3.1(c), the system is BCS-like everywhere. Increasing b_z gradually suppresses T_c and there is no clear signature in T_c of the change from a trivial to a topological phase (shown as shaded in the figure). In Fig. 3.1(d), when the pairing is enhanced, T_c becomes insensitive to variations in the magnetic field until $\delta\mu = 0$.

Shortly thereafter, the topological phase transition is crossed and T_c rapidly declines.

From the last figure, in particular, we observe that the satisfaction of the topological inequality and the $\delta\mu = 0$ condition importantly define a transition [often quite sharp, as in Fig. 3.1(d)] between a superfluid, characterized by a larger gap, and larger pair mass, $M_\perp \sim 2m$ (i.e., more "BEC-like"), and a superfluid with a small gap, $\Delta/E_F \ll 1$, and a small pair mass $M_\perp \ll m$ which is "BCS-like". The resulting behavior of T_c in the topological phase arises because there is a competition between the effects of a decreasing pair mass and a decreasing mean-field pairing gap as b_z increases. The net effect is a lowering of T_c in the topological phase. This can, in turn, be viewed as a form of BEC-BCS transition.

One can inquire as to why the topological transition becomes more apparent (as reflected in T_c) in the strong pairing limit [Fig. 3.1(d)], whereas it is less evident (from the perspective of T_c) in the weak pairing limit [Fig. 3.1(c)]. These differences are reflected in the evolution of the band structure, via a Van Hove singularity, as the topological transition is crossed. To address this, Fig. (3.2) presents a constant energy contour plot for the band $+E_{-1,\mathbf{k}}$. The two axes correspond to the in-plane ($k_\perp$) and out-of-plane ($k_\parallel$) momenta. For definiteness, we have chosen $1/k_F a = 0$ and $\mu(T)$, $\Delta(T)$ are determined for a temperature just above T_c. Local extrema in this figure reflect Van Hove singularities, either at isolated points or extended in a ring-like structure. Each of the three panels in a given row corresponds to increasing values of b_z with only the left-most figures in the trivial phase. The top three figures are in the weak pairing regime whereas the bottom three figures are in the regime of enhanced pairing.

A key observation from these figures is that in the weak pairing limit there is a smooth evolution from a trivial to topological phase, whereas for enhanced pairing the band-structure evolves rather dramatically from a trivial and BEC-like phase to a topological and BCS-like phase. Indeed, the topological transition in the lower panel is roughly correlated with the appearance of additional Van Hove singularities (as indicated). This is in contrast to the upper panel where Van Hove singularities of the trivial and topological phases are relatively unchanged. These figures help interpret the behavior observed in Fig. 3.1(c) and Fig. 3.1(d).

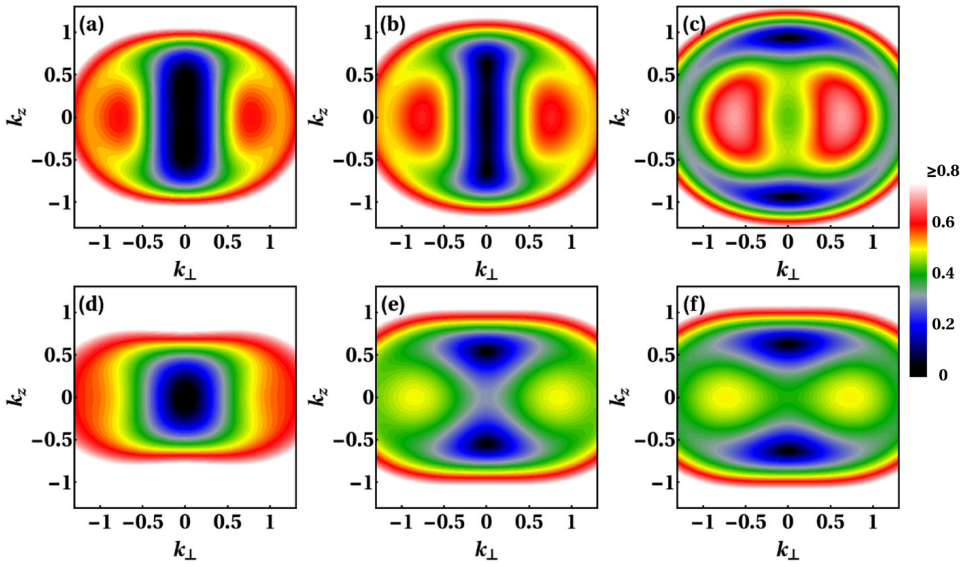

Figure 3.2: Evolution of the dispersion as the topological transition is crossed by tuning b_z. In the weak pairing limit (top panel), the system smoothly evolves across the transition, whereas for enhanced pairing (bottom panel) there is a more abrupt change in band-structure. In all plots we show constant energy contours $+E_{-1,\mathbf{k}}/E_F$ at unitarity, with $k_\perp$ and $k_{||}$ in units of k_F. For panels (a)-(c) we set $\lambda/k_F = 0.5$ and the magnetic field $b_z/E_F = 0.4, 0.6, 0.8$, whereas for panels (d)-(f) we set $\lambda/k_F = 1$ and $b_z/E_F = 1.2, 1.7, 1.8$ respectively. Only the left-most figures are in a trivial phase.

3.5 Frequency dependent spin and density response functions

It is important to establish tightly constrained experimental signatures of topological order. There are proposals in the literature suggesting the topological phase might be observed in atomic Fermi gases through the compressibility κ [Seo et al., 2013, Zheng et al., 2014] or via radio frequency (RF) based probes [Gong et al., 2011]. However, changes in κ appear to reflect topology only in the limit of small SOC [Seo et al., 2013, Zheng et al., 2014]. RF experiments in principle measure the electronic dispersion, but resolution and finite temperature broadening effects are not yet [Stewart et al., 2008] well controlled. Our approach is to study density and spin responses, and their associated sum rules [Wu et al., 2015].

Here, as in the previous chapter, we consider the correlation functions (above T_c) given by

$$\chi_{S_iS_j}(i\omega, \mathbf{q}) = \sum_{\mathbf{k}} \sum_{\alpha\alpha',\eta\eta'} \left(\frac{f(\eta E_{\alpha\mathbf{k}}) - f(\eta' E_{\alpha'\mathbf{k}+\mathbf{q}})}{\eta E_{\alpha\mathbf{k}} - \eta' E_{\alpha'\mathbf{k}+\mathbf{q}} + i\omega} \right) w_{\alpha\alpha',\eta\eta'}(\mathbf{k}, \mathbf{k}+\mathbf{q}). \tag{3.6}$$

The density-density correlation function $\chi_{\rho\rho}(i\omega, \mathbf{q})$ corresponds to $i = j = 0$, with $\sigma_0 = \mathbb{1}_2$, whereas $i, j \in \{x, y, z\}$ gives the corresponding spin-spin correlation function. The differences between the density or spin responses are the coherence factors $w_{\alpha\alpha',\eta\eta'}(\mathbf{k}, \mathbf{k}+\mathbf{q})$, which are presented in appendix (B.2). As a numerical check on these calculations, the f-sum rule for the density response and related sum rules for the spin responses hold for all $\mathbf{q}$ [Wu et al., 2015].

Quite generally, the correlation functions for a normal phase with pairing can be decomposed into two parts; one involving the difference: $E^{(2,-)}(\mathbf{k}, \mathbf{q}) = |E_{-1,\mathbf{k}} - E_{\pm 1,\mathbf{k}+\mathbf{q}}|$ which enters as a thermal contribution (at $T \neq 0$), and the other involving the sum: $E^{(2,+)}(\mathbf{k}, \mathbf{q}) = |E_{-1,\mathbf{k}} + E_{\pm 1,\mathbf{k}+\mathbf{q}}|$, which we call the multiparticle contribution. We address the $\mathbf{q} = 0$ spin response, $\chi_{S_iS_j}(\omega, 0)$, (where i, j are x or y, and we henceforth analytically continue $i\omega \to \omega + i0^+$) so that inter-band terms dominate. Thus, for the ± 1 subscript in the density response, the -1 band label yields the main contribution, whereas in the spin response the $+1$ band label is most important.

Figure 3.3(a) shows $\chi_{S_xS_y}(\omega, 0)$ for both the trivial and topological phases. In the trivial phase there are two clearly resolvable peaks; the first peak is associated with the thermal contribution and the second with the multiparticle contribution. By contrast, there is only one peak in the topological phase. A related signature for the Hall conductivity (in 2D) at $T = 0$, rather than, as here, above T_c, was suggested earlier [Ojanen & Kitagawa, 2013]. Importantly, this provides a means of distinguishing between the trivial and topological phases. We can analytically identify the position of the maximum in the first (thermal) peak, which is due to a flat band in $E^{(2,-)}(\mathbf{k}, 0)$, and appears precisely at $2b_z$. The threshold for the second peak is $\omega_1 \equiv \min_{\mathbf{k}} E^{(2,+)}(\mathbf{k}, 0)$. In the trivial phase we find that, if $\mu > 0$, $\omega_1 = 2\Delta$, whereas if $\mu < 0$, $\omega_1 = 2(\Delta^2 + \mu^2)^{1/2}$. Hence ω_1 is strictly greater than the frequency of the first peak ($2b_z$), thus yielding two distinct peaks in the response function. In the topological phase, $\omega_1 = 2b_z$ so that the two peaks merge.

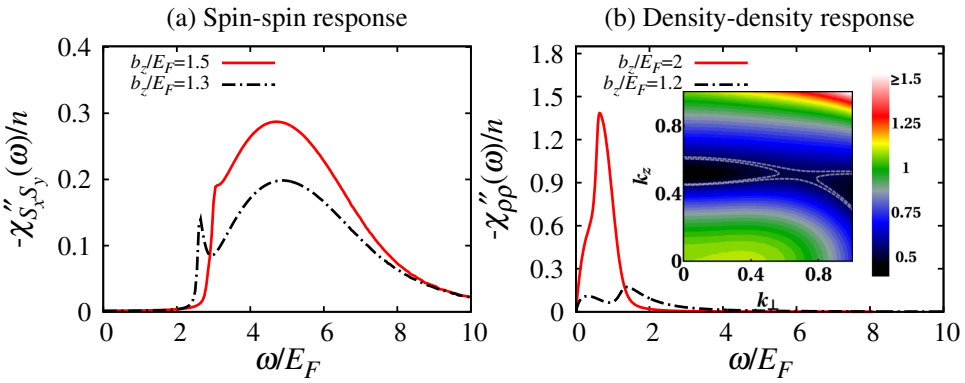

Figure 3.3: Contrast between topological (solid, red) and trivial (dashed, black) phases of the frequency dependent spin-spin [panel (a)] and density-density [panel (b)] correlation functions. Both response functions are calculated at $1/k_F a = 0$ and $\lambda/k_F = 1$, with respective wave-vectors of $\mathbf{q} = 0$ and $\mathbf{q} = 0.5k_F\hat{z}$ for the spin and charge responses. The inset in panel (b) shows the energy contours of $E^{(2,+)}(\mathbf{k},\mathbf{q})/E_F$ in the topological phase, with $k_\perp$ and $k_{||}$ in units of k_F. The dashed lines highlight the saddle point Van Hove singularity whose magnitude determines the frequency location of the peak response in panel (b).

We now focus on the density-density correlation function, $\chi_{\rho\rho}(\omega,\mathbf{q})$, which is only non-zero when $\mathbf{q} \neq 0$. This is shown in Fig. 3.3(b) for the case of unitarity: $1/k_F a = 0$, and we can again compare the trivial and topological phases. Here $\lambda/k_F = 1$ and we plot the imaginary part of the response function, $\chi''_{\rho\rho}(\omega,\mathbf{q})$ [Wu et al., 2015], deep in the topological phase ($b_z/E_F = 2$) and in the trivial phase ($b_z/E_F = 1.2$) at $\mathbf{q} = 0.5k_F\hat{z}$ and $T = 0.21T_F$ (just above T_c).

In the trivial phase there are two peaks, one associated with thermal contributions involving $E^{(2,-)}(\mathbf{k},\mathbf{q})$ and the second with the multiparticle component involving $E^{(2,+)}(\mathbf{k},\mathbf{q})$. In the topological phase, there is a large peak at $\omega/E_F = 0.6$, which arises from a (2D) saddle point Van Hove singularity contribution in $E^{(2,+)}(\mathbf{k},\mathbf{q})$. This is associated with $\nabla_{\mathbf{k}}E^{(2,+)}(\mathbf{k},\mathbf{q}) = 0$, which (via the density of states) enters as a denominator in the the response functions. These saddle point Van Hove singularity effects are well known [James et al., 2012a, Kao et al., 2000] and are illustrated in the inset on the right. Importantly, here we observe that as the system enters the topological phase they amplify the peaks in the density-density correlation function, thus helping to distinguish between the trivial and topological phases.

3.6 Conclusions

This chapter addresses how an intrinsically produced condensation temperature varies across a topological transition, induced by varying SOC, magnetic field coupling, or the scattering length. Importantly, the introduction of fluctuations necessarily introduces a feedback of the topological band structure into T_c. The passage from the trivial to the topological phase is accompanied by a transition in which the system is driven towards a low T_c, more BCS-like phase, with smaller pair mass and smaller gap. Nevertheless, there is a range of b_z in the topological phase where $T_c \sim 0.1 T_F$, which is experimentally accessible [Ketterle & Zwierlein, 2008].

We presented methods of detecting the topological band-structure above T_c, exploiting frequency dependent peaks in the density and spin responses. The topological transition appears in the spin response as a recombination of two peaks, which are separate in the trivial phase. In the topological superfluid, the dynamical density response exhibits a greatly amplified peak associated with a (2D) saddle point Van Hove singularity.

CHAPTER 4

EXACT CORRELATION FUNCTIONS IN THE CUPRATE PSEUDOGAP PHASE: COMBINED EFFECTS OF CHARGE ORDER AND PAIRING

There are a multiplicity of charge-ordered, pairing-based or pair-density-wave theories of the cuprate pseudogap, albeit arising from different microscopic mechanisms. For mean-field schemes (of which there are many) we demonstrate they have important implications for two-body physics in the same way they are able to address the one-body physics of photoemission spectroscopy. This is because the full vertex can be obtained exactly from the Ward-Takahashi identity. As an illustration we present the spin response functions, finding that a recently proposed pair-density-wave (Amperean-pairing) scheme is readily distinguishable from other related scenarios. The work in this chapter is published in Ref. [Boyack et al., 2014, 2017b].

4.1 Introduction

Numerous theories associated with the cuprate pseudogap phase have recently been suggested, based on now widely observed charge order [Comin et al., 2014, Ghiringhelli et al., 2012, Hinkov et al., 2007, Wise et al., 2008]. While the underlying physics may be different, what emerges rather generally are BCS-based pairing theories of the normal state with band-structure reconstruction [Chen et al., 2004, Lee, 2014, Yang et al., 2006]. Distinguishing between theories has mostly been based on angle resolved photoemission spectroscopy (ARPES) [Loeser et al., 1996]. However, the majority of data available for the cuprates involves two-particle properties: for example, the optical absorption [Corson et al., 1999], diamagnetism [Li et al., 2010], quasi-particle interference in scanning tunneling microscope (STM) studies [Pan et al., 2000], neutron [Dai et al., 1999, Hinkov et al., 2007, Stock et al., 2004] and inelastic x-ray scattering in the charge [Comin et al., 2014] and spin [Le Tacon et al., 2011] sectors.

In this chapter we use the Ward-Takahashi identity (WTI) [Ryder, 1996, Schrieffer, 1964] to derive exact two-body response functions for these pairing-based pseudogap theories. Such exact

response functions make it possible to address two-particle cuprate experiments, including the list above, from the perspective of many different theories. As an illustration, we compute the spin-spin correlation functions relevant to neutron scattering in three pseudogap scenarios. Since the response functions analytically (and numerically) satisfy the f-sum rule, this provides confidence there are no missing Feynman diagrams or significant numerical inaccuracies.

By comparing the Amperean-pairing scheme [Lee, 2014], and that of Yang, Rice, and Zhang [Yang et al., 2006] with a simple d-wave pseudogap scenario, we find that the Amperean theory leads to a relatively featureless neutron cross section in contrast to the peaks (at and near the anti-ferromagnetic wave vector), found for the other two theories.

In this Amperean-pairing scheme [Lee, 2014] the mean-field self energy is

$$\begin{aligned}\Sigma_{pg}(K) = & \frac{\Delta_1^2}{\omega + \xi_{\mathbf{k}-\mathbf{p}} - \frac{\Delta_2^2}{\omega - \xi_{\mathbf{k}-2\mathbf{p}}}} + \frac{\Delta_2^2}{\omega + \xi_{\mathbf{k}+\mathbf{p}} - \frac{\Delta_1^2}{\omega - \xi_{\mathbf{k}+2\mathbf{p}}}} \\ & + \frac{C_1^2}{\omega - \xi_{\mathbf{k}+2\mathbf{p}} - \frac{\Delta_1^2}{\omega + \xi_{\mathbf{k}+\mathbf{p}}}} + \frac{C_2^2}{\omega - \xi_{\mathbf{k}-2\mathbf{p}} - \frac{\Delta_2^2}{\omega + \xi_{\mathbf{k}-\mathbf{p}}}} \\ & + \frac{2\Delta_1\Delta_2 C_1}{\left(\omega + \xi_{\mathbf{k}+\mathbf{p}}\right)\left(\omega - \xi_{\mathbf{k}+\mathbf{2p}}\right) - \Delta_1^2} + \frac{2\Delta_1\Delta_2 C_2}{\left(\omega + \xi_{\mathbf{k}-\mathbf{p}}\right)\left(\omega - \xi_{\mathbf{k}-\mathbf{2p}}\right) - \Delta_2^2}. \end{aligned} \tag{4.1}$$

We single this particular theory out as an example which is complex and therefore somewhat more inclusive. In Eq. (4.1), $\Sigma_{pg}(K)$ is expressed in terms of two different finite momentum ($\mathbf{p}$) pseudogaps, $\Delta_1 \equiv \Delta_{\mathbf{p}}$ and $\Delta_2 \equiv \Delta_{-\mathbf{p}}$. In addition we have introduced charge-density-wave (CDW) amplitudes $C_1 \equiv C_{2\mathbf{p}}$ and $C_2 \equiv C_{-2\mathbf{p}}$. From the self energy, the full (inverse) Green's function can be deduced: $G^{-1}(K) \equiv G_0^{-1}(K) - \Sigma_{pg}(K) = \omega - \xi_{\mathbf{k}} - \Sigma_{pg}(K)$. This then determines the renormalized band structure, which can be compared with ARPES experiments.

It is observed from Eq. (4.1) that in the Amperean-pairing case a BCS-like self energy appears in a continued fraction form within the self energy itself. There are analogies with the approach of Yang, Rice, and Zhang (YRZ) [Yang et al., 2006] in the limit that only one gap term is present, say Δ_1, and when the CDW ordering is absent. Importantly, this single-gap self energy involves two types of dispersion relations, so that the pairing term leads to pockets or a reconstruction

of the band structure. For a simpler d-wave pseudogap, with a single-gap model, both of these dispersion relations are taken to be the same, as was studied microscopically [Chen et al., 2005] and phenomenologically [Norman et al., 1998]. A central contribution of this chapter is to show how, via two-particle properties, important distinctions between these three different pseudogap theories can be established.

While it is argued to be appropriate for the pseudogap phase [Lee, 2014], the self energy of Eq. (4.1) is indistinguishable from that of a superconducting state. It is important, then, to ensure that this form for Σ_{pg} does not correspond to an ordered phase. Phase fluctuations have been phenomenologically invoked [Chen et al., 2004, Lee, 2014] to destroy order. Regardless of this phenomenology there is a quantitative constraint to be satisfied: the absence of a Meissner effect above T_c implies that the zero frequency and zero momentum current-current correlation function satisfies $-\overleftrightarrow{P}(0) = \left(\frac{\overleftrightarrow{n}}{m}\right)_{\rm dia} \equiv 2\sum_K \frac{\partial^2 \xi_{\mathbf{k}}}{\partial \mathbf{k}\partial \mathbf{k}} G(K)$, so that there is a precise cancellation between the diamagnetic and paramagnetic current-current correlation functions in the normal state.

Performing integration by parts [1] and using the identity $\partial G(K)/\partial \mathbf{k} = -G^2(K)\partial G^{-1}(K)/\partial \mathbf{k}$ then yields the following expression for $\overleftrightarrow{P}(0)$:

$$\overleftrightarrow{P}(0) = 2\sum_K G^2(K)\left\{ \frac{\partial \xi_{\mathbf{k}}}{\partial \mathbf{k}} + \frac{\partial \Sigma_{pg}(K)}{\partial \mathbf{k}} \right\} \frac{\partial \xi_{\mathbf{k}}}{\partial \mathbf{k}}. \tag{4.2}$$

Here $K = (\omega, \mathbf{k})$. Given the self energy from Eq. (4.1), it is then straightforward to arrive at the quantity $\overleftrightarrow{P}(0)$:

$$\begin{aligned}\overleftrightarrow{P}(0) = 2\sum_K G^2(K)\Big\{ &\frac{\partial \xi_{\mathbf{k}}}{\partial \mathbf{k}} - \Delta_1^2 G_{1,1}^2(-K)\frac{\partial \xi_{\mathbf{k},2}}{\partial \mathbf{k}} + \Delta_1^2\Delta_2^2 G_{1,1}^2(-K)G_{0,4}^2(K)\frac{\partial \xi_{\mathbf{k},4}}{\partial \mathbf{k}} \\ &- \Delta_2^2 G_{1,2}^2(-K)\frac{\partial \xi_{\mathbf{k},1}}{\partial \mathbf{k}} + \Delta_2^2\Delta_1^2 G_{1,2}^2(-K)G_{0,3}^2(K)\frac{\partial \xi_{\mathbf{k},3}}{\partial \mathbf{k}} \Big\} \frac{\partial \xi_{\mathbf{k}}}{\partial \mathbf{k}}. \end{aligned} \tag{4.3}$$

1. For simplicity, we ignore terms arising from the wave-vector dependence of the d-wave gap function. In general this is a small effect. We can observe via the sum rule accuracy the importance of including the full wave-vector dependence of the d-wave gap. When the wave-vector dependence of the gap is ignored, the sum rule accuracy is still very good, but now of the order of $2-3\%$.

For simplicity, throughout the chapter we set $C_1 = C_2 = 0$ and present the complete expressions in appendix (C.1). Here we have defined the following four bare (inverse) Green's functions $G_{0,i}^{-1}(K) = (\omega - \xi_{\mathbf{k},i}), \quad i \in \{1,2,3,4\}$, where $\xi_{\mathbf{k},1} = \xi_{\mathbf{k}+\mathbf{p}}$, $\xi_{\mathbf{k},2} = \xi_{\mathbf{k}-\mathbf{p}}$, $\xi_{\mathbf{k},3} = \xi_{\mathbf{k}+2\mathbf{p}}$, $\xi_{\mathbf{k},4} = \xi_{\mathbf{k}-2\mathbf{p}}$ are four dispersion relations. [The usual bare inverse Green's function is denoted by $G_0^{-1}(K) = \omega - \xi_{\mathbf{k}} = \omega - \epsilon_{\mathbf{k}} + \mu$.] The partially-dressed Green's functions (which are neither bare nor full) associated with Eq. (4.1) are

$$G_{1,1}^{-1}(K) = \omega - \xi_{\mathbf{k},1} - \frac{\Delta_2^2}{\omega + \xi_{-\mathbf{k},4}}, \tag{4.4}$$

$$G_{1,2}^{-1}(K) = \omega - \xi_{\mathbf{k},2} - \frac{\Delta_1^2}{\omega + \xi_{-\mathbf{k},3}}. \tag{4.5}$$

In terms of these partially-dressed Green's functions, the self energy in Eq. (4.1) for the case where $C_1 = C_2 = 0$ has the compact form $\Sigma_{pg}(K) = -\Delta_1^2 G_{1,1}(-K) - \Delta_2^2 G_{1,2}(-K)$. The quantity $\overleftrightarrow{P}(0)$ in Eq. (4.3) provides a template for the form of the Feynman diagrams that we will find in $\overleftrightarrow{P}(Q)$.

4.2 Full vertex and Ward-Takahashi identity

The exact expression for the current-current correlation function, $\overleftrightarrow{P}(Q)$, is contained in the response functions written as

$$P^{\mu\nu}(Q) = 2\sum_K G(\widetilde{K})\Gamma^\mu(\widetilde{K}, K)G(K)\gamma^\nu(K, \widetilde{K}), \tag{4.6}$$

where we define $\widetilde{K} \equiv K + Q$. The full electromagnetic vertex in four-vector notation is given by $\Gamma^\mu(\widetilde{K}, K) = (\Gamma^0(\widetilde{K}, K), \mathbf{\Gamma}(\widetilde{K}, K))$, where the first (second) argument denotes the incoming (outgoing) momentum. Here the quantity $\gamma^\nu(K, \widetilde{K})$ represents the bare vertex.

The full response kernel is $K^{\mu\nu}(Q) \equiv P^{\mu\nu}(Q) + \left(\frac{n}{m}\right)_{\rm dia}^{\mu\nu}(1 - \delta_{0,\nu}\delta_{\mu,\nu})$, where there is no summation over indices in the second term. The Ward-Takahashi identity in quantum field theory is an identity that imposes a symmetry between response functions. The particular symmetry

of interest is the global $\mathrm{U}(1)$ symmetry [Ryder, 1996]. As we will show, satisfying the WTI also leads to manifestly sum rule consistent response functions. Charge conservation is an exact relation between the current-current and density-density response functions which follows from this global $\mathrm{U}(1)$ symmetry. The WTI reflects this charge conservation, which imposes the constraint: $\Omega K^{0\nu} + i\mathrm{div}_{\mathbf{q}} K^{j\nu} = 0$. The WTI, for the vertex $\Gamma^{\mu}(\widetilde{K}, K)$, on a lattice is

$$\begin{aligned}\Omega\Gamma^{0}(\widetilde{K}, K) + i\mathrm{div}_{\mathbf{q}}\mathbf{\Gamma}(\widetilde{K}, K) &= G^{-1}(\widetilde{K}) - G^{-1}(K), \\ &= \Omega + i\mathrm{div}_{\mathbf{q}}\boldsymbol{\gamma}(\widetilde{K}, K) + \Sigma_{pg}(K) - \Sigma_{pg}(\widetilde{K}). \end{aligned} \tag{4.7}$$

The WTI for the bare vertex, $\gamma^{\mu}(\widetilde{K}, K)$, is $\Omega + i\mathrm{div}_{\mathbf{q}}\boldsymbol{\gamma} = G_0^{-1}(\widetilde{K}) - G_0^{-1}(K) = \Omega - \xi_{\mathbf{k}+\mathbf{q}} + \xi_{\mathbf{k}}$. Similarly, we introduce bare vertices $\gamma_i^{\mu}(\widetilde{K}, K)$ which are associated with the dispersion relations $\xi_{\mathbf{k},i}$. Here $\mathrm{div}_{\mathbf{q}}\mathbf{\Gamma}(\widetilde{K}, K)$, complicated due to lattice effects, is the Fourier transform of the divergence of $\mathbf{\Gamma}$.

In the limit $Q \to 0$, the Ward-Takahashi identity reduces to the Ward identity: $\delta\Gamma^{\mu}(K, K) \equiv \Gamma^{\mu}(K, K) - \gamma^{\mu}(K, K) = -\partial\Sigma_{pg}(K)/\partial k_{\mu}$. This is fully consistent with the arguments leading up to the no-Meissner constraint in Eq. (4.2). In the continuum limit ($q \to 0$) the WTI and charge conservation have familiar forms: $q_{\mu}\Gamma^{\mu}(\widetilde{K}, K) = G^{-1}(\widetilde{K}) - G^{-1}(K)$ and $q_{\mu}K^{\mu\nu}(Q) = 0$.

We emphasize that, given an arbitrary self energy, solving the WTI analytically for the full vertex $\Gamma^{\mu}(\widetilde{K}, K)$ is generally not possible. However, there is a well-defined procedure to determine this vertex in principle. One inserts the bare vertex in all possible locations in the self-energy diagram and sums the resulting series of diagrams. For the class of theories considered in this chapter, Σ itself does not depend on the full Green's function $G(\Sigma)$, but rather depends on the bare Green's functions G_0 and their simple extensions; this is associated with generalized mean-field theories. For example, in strict BCS theory $\Sigma(K) = -\Delta^2 G_0(-K)$.

Importantly, it follows that in the BCS-like theories of interest here, the full vertex, $\Gamma^{\mu}(\widetilde{K}, K)$, can be deduced from the equivalent WTI by considering only finitely many loop diagrams. We illustrate this procedure specifically for the first term in the Amperean self energy in Eq. (4.1).

Using the form of the self energy, along with the bare WTI, we have:

$$\begin{aligned}\Sigma_1(K) - \Sigma_1(\widetilde{K}) &= \Delta_1^2 G_{1,1}(-K) G_{1,1}(-\widetilde{K})\{[\Omega + \xi_{\mathbf{k}+\mathbf{q}-\mathbf{p}} - \xi_{\mathbf{k}-\mathbf{p}}] \\ &\quad + \Delta_2^2 G_{0,4}(K) G_{0,4}(\widetilde{K})[\Omega - \xi_{\mathbf{k}+\mathbf{q}-2\mathbf{p}} + \xi_{\mathbf{k}-2\mathbf{p}}]\}, \\ &= \Delta_1^2 G_{1,1}(-K) G_{1,1}(-\widetilde{K})\{[\Omega + i\mathrm{div}_{\mathbf{q}}\boldsymbol{\gamma}_1(-K, -\widetilde{K})] \\ &\quad + \Delta_2^2 G_{0,4}(K) G_{0,4}(\widetilde{K})[\Omega + i\mathrm{div}_{\mathbf{q}}\boldsymbol{\gamma}_4(\widetilde{K}, K)]\}. \end{aligned} \tag{4.8}$$

From the full WTI, we then obtain

$$\begin{aligned}\Omega\Gamma^0(\widetilde{K}, K) + i\mathrm{div}_{\mathbf{q}}\boldsymbol{\Gamma} = \Omega + i\mathrm{div}_{\mathbf{q}}\boldsymbol{\gamma} + \Delta_1^2 G_{1,1}(-K) G_{1,1}(-\widetilde{K})\{[\Omega + i\mathrm{div}_{\mathbf{q}}\boldsymbol{\gamma}_1(-K, -\widetilde{K})] \\ + G_{0,4}(K) G_{0,4}(\widetilde{K})[\Omega + i\mathrm{div}_{\mathbf{q}}\boldsymbol{\gamma}_4(\widetilde{K}, K)]\}. \end{aligned} \tag{4.9}$$

In this form we can then solve for the exact full vertex:

$$\begin{aligned}\Gamma^\mu(\widetilde{K}, K) &= \gamma^\mu(\widetilde{K}, K) \\ &\quad + \Delta_1^2 G_{1,1}(-K) G_{1,1}(-\widetilde{K})[\gamma_1^\mu(-K, -\widetilde{K}) + \Delta_2^2 G_{0,4}(K) G_{0,4}(\widetilde{K})\gamma_4^\mu(\widetilde{K}, K)] \\ &\quad + \Delta_2^2 G_{1,2}(-K) G_{1,2}(-\widetilde{K})[\gamma_2^\mu(-K, -\widetilde{K}) + \Delta_1^2 G_{0,3}(K) G_{0,3}(\widetilde{K})\gamma_3^\mu(\widetilde{K}, K)]. \end{aligned} \tag{4.10}$$

Here we have now included the second term from $\Sigma_{pg}(K)$ in Eq. (4.1).

We emphasize this is not an expansion in the bare vertices. Rather, the WTI is used to obtain the exact full vertex. The crucial step is that the self energy does not depend on the full Green's function. If it did, then the full vertex would appear on both sides of the equation, reducing the problem to a Bethe-Salpeter equation [Schrieffer, 1964].

Using the full vertex, the exact response function can then be determined via Eq. (4.6). The Amperean-pairing response functions have twenty one associated Feynman diagrams if one considers the charge-density wave: one of one-loop order (two Green's functions), four of two-loop order (four Green's functions), and four of three-loop order (six Green's functions), plus another

twelve diagrams with an odd number of Green's functions. The twenty one Feynman diagrams contributing to the response functions are presented in appendix (C.1).

The bare vertices for the density component are given by $\gamma^0(\widetilde{K},K) = \gamma_i^0(\widetilde{K},K) = 1$. This then allows the exact density-density response function $P_{\rho\rho}(Q)$ to be computed for all Q. More complicated, for an arbitrary band structure, are the bare vertices that enter into the current-current correlation function. However, in the limit $q \to 0$ these can be determined from Eq. (4.3). The same reasoning which is used to determine $P_{\rho\rho}(Q)$ for all Q is applicable to the spin (density) response, as measured in neutron experiments.

The full spin response function, $P_S^{\mu\nu}(Q)$, is defined by

$$P_S^{\mu\nu}(Q) = \sum_K \sum_\sigma G(\widetilde{K})\Gamma^\mu_{S_\sigma}(\widetilde{K},K)G(K)\gamma^\nu_{S_\sigma}(K,\widetilde{K}). \tag{4.11}$$

Here the bare spin vertex is denoted by $\gamma^\mu_{S_\sigma}(\widetilde{K},K)$, where $S_\sigma = \pm 1$ and $S_{\bar{\sigma}} = -S_\sigma$. The bare WTI for the spin vertex is $\Omega + i\mathrm{div}_{\mathbf{q}}\boldsymbol{\gamma}_{S_\sigma} = S_\sigma[G_0^{-1}(\widetilde{K}) - G_0^{-1}(K)] = S_\sigma(\Omega - \xi_{\mathbf{k}+\mathbf{q}} + \xi_{\mathbf{k}})$. Similarly the full WTI for the full spin vertex $\Gamma^\mu_{S_\sigma}(\widetilde{K},K)$ is:

$$\Omega\Gamma^0_{S_\sigma} + i\mathrm{div}_{\mathbf{q}}\boldsymbol{\Gamma}_{S_\sigma} = S_\sigma[G^{-1}(\widetilde{K}) - G^{-1}(K)]. \tag{4.12}$$

We can then read off the spin-spin correlation function directly using Eq. (4.10).

From the established constraints on the bare and full vertices one can directly derive [Bergeron et al., 2011] the f-sum rule for the density-density and spin-density response functions:

$$\int \frac{d\omega}{\pi}(-\omega \mathrm{Im}P^{00}(Q)) = 2\sum_{\mathbf{k}} n_{\mathbf{k}}[\xi_{\mathbf{k}+\mathbf{q}} + \xi_{\mathbf{k}-\mathbf{q}} - 2\xi_{\mathbf{k}}], \tag{4.13}$$

where $n_{\mathbf{k}} = T\sum_{i\omega} G(K)$. Importantly, this sum rule (and counterparts for the current-current correlation function) are satisfied exactly providing the response functions are consistent with the WTI. This is discussed in more detail in appendix (C.2).

4.3 Behavior of the neutron cross section: comparison between pseudogap theories

For illustrative purposes we focus on the spin-density response function, conventionally called $\chi_0(Q)$. Importantly, ensuring Eq. (4.13) is satisfied provides tight control over numerical calculations of this correlation function. When no simplifications are introduced, our numerical calculations agree with the sum rule to an accuracy of the order of $0.1 - 0.2\%$ in all three models. [2] The quantity $\mathrm{Im}\chi_0(Q) \equiv -\mathrm{Im}P^{00}(Q)$ is the theoretical basis for neutron scattering experiments. [Note we adopt the sign convention $P_{\rho\rho}(Q) = P^{00}(Q)$ for spin and charge correlations.]

For simple d-wave pairing models, a reasonable comparison between theory and neutron data has been reported at high temperatures (where one sees a reflection of the fermiology [Si et al., 1993, Zha et al., 1993b]) and below T_c (where one sees both commensurate (π, π) [Liu et al., 1995] and slightly incommensurate frequency dependent "hourglass" structure [Kao et al., 2000, Zha et al., 1993a]). This approach to neutron scattering presents a (rather successful) rival scheme to stripe approaches; many different theories, built on different microscopics, have arrived at similar behavior [Brinckmann & Lee, 1999, James et al., 2012b, Norman, 2000, Stemmann et al., 1994]. In the pseudogap phase (which has received less attention theoretically), there are peaks at and near (π, π) [Dai et al., 1999, Hinkov et al., 2007, Stock et al., 2004] which have been recently argued [Hinkov et al., 2007] to reflect some degree of broken orientation symmetry.

Here we compare the results for $\chi_0(Q)$ using three different theories of the pseudogap: a simple d-wave pseudogap, the theory of Yang, Rice, and Zhang, and that of Amperean pairing. For the Amperean case we follow Ref. [Lee, 2014] and consider the simpler 3×3 reduced Hamiltonian. In this 3×3 form, $C_1 = C_2 = 0$ and terms involving $\xi_{\mathbf{k}\pm 2\mathbf{p}}$ are dropped.

2. When the wave-vector dependence of the gap is ignored, the sum rule accuracy is still very good, but now of the order of $2 - 3\%$.

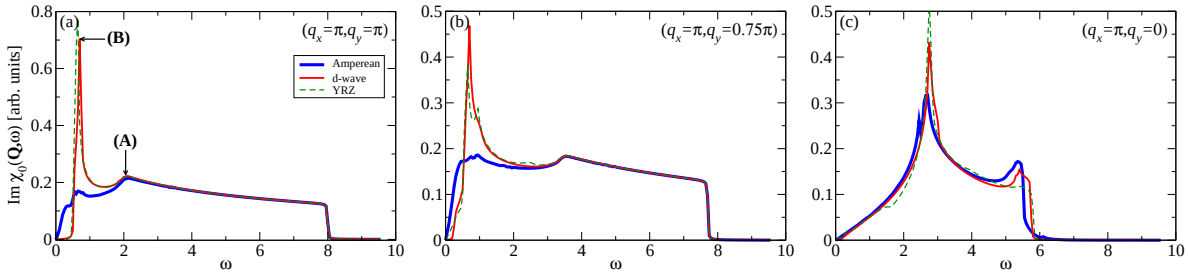

Figure 4.1: Comparison of the spin-density correlation function $\mathrm{Im}\chi_0(Q) = -\mathrm{Im}P_S^{00}(\mathbf{q},\omega)$ for three different values of $\mathbf{q}$ in Amperean, d-wave, and YRZ pseudogap theories. In (a) we have labeled the Van Hove peaks appearing in the d-wave theory, which appear as saddle points in the contour plot of Fig. (4.2). Here we use the band structure given in Ref. [Comin et al., 2014] with $T = 0.01$ and a broadening of $\Gamma = 0.01$. The doping $p = 0.12$ and the chemical potential μ is fixed by the Luttinger sum rule. The band structure and frequency are all normalized by t, and the gap function has an amplitude of $\Delta_0 = 0.15$. For the Amperean theory we use a k_x, k_y-symmetrized Gaussian [Lee, 2014] gap function.

We do not include the effects of the widely used RPA enhanced denominator introduced in Ref. [Si et al., 1992]. In the RPA enhanced form $\chi(Q) = \chi_0(Q)/[1 + J(Q)\chi_0(Q)]$, where $J(Q)$ is an effective exchange. Even though $\chi_0(Q)$ is exact, introducing this ratio will lead to a violation of the f-sum rule; this effect is not central to distinguishing between theories, as is our goal here.

Figure (4.1) presents a plot of $\mathrm{Im}\chi_0(Q)$, for three fixed $\mathbf{q}$ corresponding to (π, π) in (a), $(\pi, 0.75\pi)$ in (b) and $(\pi, 0)$ in (c) as functions of ω. The normal state (above T^*) band structure is taken to be the same, as is the pseudogap amplitude. The behavior in the low ω regime is principally, but not exclusively, dominated by the effects of the gap, while at very high ω the behavior is band-structure dominated. Importantly, all theories essentially converge once ω is much larger than the gap. This means that interesting effects associated with high energy scales [Le Tacon et al., 2011], such as observed in recent experiments, would not be specific to a given theory.

Figure (4.1) shows that there is little difference in the spin dynamics between the approach of YRZ [Yang et al., 2006] and that of a d-wave pseudogap, emphasized earlier in a different context [Scherpelz et al., 2014] and helps to explain the literature claims of successful reconciliation with the data that surround both scenarios [James et al., 2012b, Kao et al., 2000, Zha et al., 1993a].

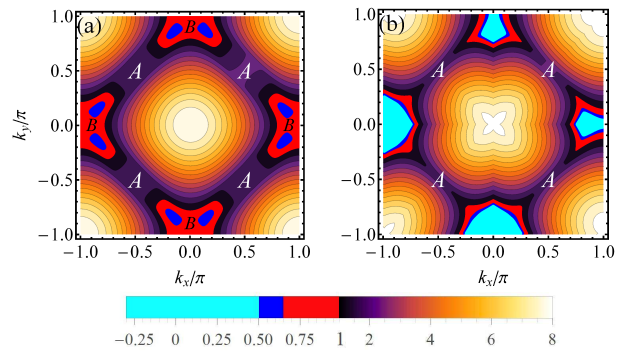

Figure 4.2: The equal energy contours $E_2(\mathbf{k}) \equiv E_{\mathbf{k}} + E_{\mathbf{k}+\mathbf{q}}$, which appear as the integrand in $\mathrm{Im}\chi_0(\mathbf{q},\omega)$, for both (a) d-wave and (b) the Amperean pseudogap schemes. Here $\mathbf{q} = (\pi,\pi)$. Note there are several energy scales as indicated by the legend. The labels A and B indicate the location of the saddle points of $\mathrm{Im}\chi_0(\mathbf{q},\omega)$.

What appears most distinctive is the Amperean-pairing response function, particularly away from $\mathbf{q} = (\pi, 0)$. Notable here is the absence of the sharp Van Hove peak [marked by B in Fig. (4.1)] which appears in both other theories and which is ultimately responsible for commensurate peaks or neutron resonance effects [Liu et al., 1995]. Also missing from the Amperean scenario is the so-called spin-gap, apparent at (π,π) in both the other two theories. Rather, for Amperean pairing there are multiple low energy processes which contribute to the spin density correlation function.

To understand these processes better, in Fig. (4.2) we probe the dominant component of the integrand in $\mathrm{Im}\chi_0(Q)$ near $\mathbf{q} = (\pi,\pi)$ for both the Amperean (right) and d-wave pseudogap (left) scenarios. We show the equal energy contours for the sum of the quasi-particle dispersions: $E_2(\mathbf{k}) \equiv E_{\mathbf{k}} + E_{\mathbf{k}+\mathbf{q}}$ versus k_x and k_y in the pseudogap state. [3] Indicated on the figure are the Van Hove singularities A and B (saddle points in the contour plot), as labeled in Fig. (4.1a). The lower energy Van Hove point (point B) is clearly suppressed in the Amperean-pairing case, while it is very pronounced and found to be important [Kao et al., 2000] for the d-wave case. Also evident from the cyan region in Fig. (3.2) is the absence of a low ω minimum (spin gap) in $E_2(\mathbf{k})$, as found in both the other two theories, as well as in the integrated response function.

3. For the 3×3 Amperean theory, we chose the top band for both $E_{\mathbf{k}}$ and $E_{\mathbf{k}+\mathbf{q}}$.

4.4 Conclusions

The central contribution of this chapter has been to establish an analytically and numerically controlled methodology for addressing the long list of two particle cuprate measurements. Given a mean-field-like self energy, the exploitation of the Ward Takahashi identity (and related sum rules) allows one to evaluate two-particle properties, and in this way achieve the same level of accuracy in these comparisons, as in, say, ARPES. To demonstrate the utility of this method, we address the spin density response functions of neutron scattering and have singled out signatures of the recently proposed Amperean-pairing theory [Lee, 2014]. We cannot firmly establish that this pair-density-wave theory is inconsistent with experiments (without digressing from our goals and including the sum-rule-inconsistent RPA enhancement denominator [Si et al., 1992]), but it does lead to a rather featureless neutron cross section. [4] We report two distinctive observations: the absence of spin gap effects and the absence of the sharp low energy Van Hove peak near (π, π).

4. In addition to the Gaussian gap model of Ref. [Lee, 2014], we have found similar featureless results for a simple d-wave gap shape as well.

CHAPTER 5

GAUGE INVARIANT THEORIES OF LINEAR RESPONSE FOR STRONGLY CORRELATED SUPERFLUIDS

This chapter presents a diagrammatic theory for determining consistent electromagnetic response functions in strongly correlated Fermi superfluids. While a gauge-invariant electromagnetic response is well understood at the BCS level, a treatment of correlations beyond BCS theory requires extending this theoretical formalism. The challenge in such systems is to maintain gauge invariance, while simultaneously incorporating additional self energy terms arising from strong correlation effects. Central to our approach is the application of the Ward-Takahashi identity, which introduces collective mode contributions in the response functions and guarantees the f-sum rule is satisfied. We outline a powerful method which determines these collective modes in the presence of correlation effects and in a manner compatible with gauge invariance. Since this method is based on fundamental aspects of quantum field theory, the underlying principles are broadly applicable to strongly correlated superfluids. As an illustration of the technique, we apply it to a simple class of theoretical models containing a frequency independent order parameter. These models include BCS-BEC crossover theories of the ultra cold Fermi gases, along with models specifically associated with the high-T_c cuprates. Finally, as an alternative approach, we contrast with the path integral formalism. In this case the calculation of gauge-invariant response appears more straightforward. However, the collective modes introduced are those of strict BCS theory, without any modification from additional correlations. As the path integral simultaneously addresses electrodynamics and thermodynamics, we emphasize that it should be subjected to a consistency test beyond gauge invariance, namely that of the compressibility sum rule. We show how this sum rule fails in the conventional path integral approach. The next chapter provides a reformulation of the path integral method for fermionic superfluids, which is consistent with both gauge invariance and the compressibility sum rule. The work in this chapter is published in Ref. [Boyack et al., 2016]

5.1 Introduction

There has been great interest recently in strongly correlated superconductors and superfluids. This interest has arisen in two different contexts, via ultra cold Fermi gases [Diener et al., 2008, Taylor et al., 2006] and via high-T_c superconductors [Chen et al., 2005, Lee, 2014, Norman et al., 1998, Yang et al., 2006]. A major challenge in studying these two different systems is to arrive at exact expressions for the electromagnetic (EM) properties, such as the superfluid density and the density-density correlation function, which characterize superconductors and superfluids.

In strict BCS theory there are two different conventional techniques for addressing electromagnetic response while ensuring gauge invariance: the path integral [Altland & Simons, 2010, Lutchyn et al., 2008, Ojanen & Kitagawa, 2013] and the Ward-Takahashi identity [Nambu, 1960]. The first of these methods depends on the derivation of a generating functional while the second depends on the form of the diagrammatic self energy. This body of work has enabled a complete understanding of the gauge-invariant electromagnetic response at the BCS level. It does not, however, answer the important questions about how to incorporate stronger correlation effects.

Studies of high-T_c superconductors, which necessarily require a beyond-BCS formalism, are better suited to the Ward-Takahashi based approach. These studies focus on different models for the self energy associated with a normal state that includes pairing, known as the pseudogap phase [Chen et al., 2005, Lee, 2014, Norman et al., 1998, Yang et al., 2006]. This correlation contribution to the self energy has been extensively characterized [Loeser et al., 1996] above the transition temperature T_c. In the superfluid phase, presumably one adds to this normal state self energy [Chen et al., 2005, Yang et al., 2006] an additional BCS self energy contribution. The challenge in studying strongly correlated superfluids, however, is ensuring gauge invariance. This means that the self-consistent collective modes, compatible with gauge invariance, must be properly included. In this chapter we show that a diagrammatic self energy and the gap equation provide all the ingredients required to unambiguously establish the exact electromagnetic response at all temperatures. The main goals are: (1) To show how to arrive at the exact gauge-invariant electromagnetic response of strongly correlated superfluids. This is based upon an implementation of the

Ward-Takahashi identity given an arbitrary diagrammatic scalar self energy. (2) To provide a powerful method for obtaining the collective modes in a gauge-invariant manner for strongly correlated Fermi superfluids. This is based on the gap equation, and the vertex derived above in (1).

The electrodynamics of superconductors is also widely addressed via the path integral approach [Altland & Simons, 2010, Lutchyn et al., 2008, Ojanen & Kitagawa, 2013] which requires the introduction of Gaussian-level (beyond saddle-point) fluctuations. Incorporating gauge invariance is relatively straightforward, which is in large part due to the fact that the collective modes entering at this level and beyond are those of strict BCS theory [Anderson et al., 2016]. We shall revisit this conventional calculation of response functions at the strict BCS level, while simultaneously considering thermodynamics. We find there is a serious shortcoming that has not previously been identified in the literature. This arises from an inconsistency between electrodynamics and thermodynamics, which is manifested as a failure of the compressibility sum rule. Our emphasis here is not on a critique of previous work since, quite generally, in the literature the focus has been on either thermodynamics [Diener et al., 2008] or electrodynamics [Altland & Simons, 2010, Lutchyn et al., 2008, Ojanen & Kitagawa, 2013], but not on both simultaneously. Nevertheless, the violation of the compressibility sum rule is a serious shortcoming. The source of this sum rule violation comes from the fact that the BCS-level electrodynamics is derived by incorporating beyond-BCS Gaussian fluctuations. This would seem to require we also include Gaussian fluctuations in the number equation. However, this in fact leads to the failure of the compressibility sum rule. A detailed discussion of how to implement consistency between electrodynamics and thermodynamics is presented in the next chapter [Anderson et al., 2016].

It is crucial when studying transport phenomena to ensure that all conservation laws, such as energy, momentum, and charge, are satisfied [Baym, 1962, Baym & Kadanoff, 1961]. In particular, ensuring gauge invariance, and thus charge conservation, in a superconductor has long been a problem of great importance [Anderson, 1958, Guo et al., 2013a, Kadanoff & Martin, 1961, Kulik et al., 1981, Nambu, 1960]. The crucial insight in preserving gauge invariance, even in the presence of a Meissner effect, was the necessity of long-wavelength collective excitations [Anderson, 1958,

Rickayzen, 1959]. Following this initial insight, Nambu [Nambu, 1960] developed a diagrammatic approach to maintain gauge invariance, similar to the establishment of gauge invariance in quantum electrodynamics. Nambu's method of establishing a gauge-invariant electromagnetic response was to set up a gauge-invariant vertex at the same level of approximation as the self energy. He then showed that this produces a vertex which satisfies the Ward-Takahashi identity (WTI), a condition equivalent to gauge invariance [Ryder, 1996, Sterman, 1993].

A modern understanding of the role of gauge invariance in a superconductor is best understood from this field theoretic point of view: collective modes are excitations which restore gauge invariance. In the language of quantum field theory, they can be interpreted as the Nambu-Goldstone bosons arising from spontaneous symmetry breaking in the condensed phase. Strictly speaking, in a superconductor or superfluid local gauge invariance is never broken [Greiter, 2005]. Quite generally, the impossibility of breaking local gauge invariance without explicit gauge fixing, at least for abelian gauge fields, was proved early on by Elitzur [Elitzur, 1975]. Rather, due to the presence of a condensate, global phase invariance is spontaneously broken. In the case of a neutral order parameter the excitation spectrum contains a gapless mode, which corresponds to the collective mode discussed throughout this chapter. For a charged superfluid the Goldstone mode couples to the longitudinal degrees of freedom of the gauge field, and is gapped out. A diagrammatic framework of establishing gauge invariance in BCS superconductors, at all temperatures, and with the inclusion of the Coulomb potential, can be found in Ref. [Arseev et al., 2006].

In going beyond the BCS theory of superconductivity it is essential that charge conservation is maintained in any approximation scheme. We note that the Kadanoff-Baym approach [Baym, 1962, Baym & Kadanoff, 1961], extended below T_c, provides a sufficient, but not necessary, condition for a theory to satisfy macroscopic conservation laws. It is inapplicable to the strongly-correlated theories considered in this chapter, where the self energy is not derivable from a Luttinger-Ward functional of the full Green's function. Nonetheless, the exact gauge-invariant EM response can be obtained using the diagrammatic formalism based on points (1) - the WTI and (2) - self-consistent collective modes.

In particular, Refs. [Boyack et al., 2014, Scherpelz et al., 2014] implemented the WTI for a number of different exotic normal phases, above the transition temperature, which led to a consistent framework for computing all vertex corrections. The challenge in the present chapter then is to extend this body of work and formulate a gauge-invariant theory below the transition temperature. In this context, Ref. [He & Guo, 2015] used the WTI to formulate a gauge-invariant response for a specific BCS-BEC theory valid at all temperatures. This theory accounts for non-condensed fermionic pairs by adding a t-matrix self energy to the standard BCS self energy. Inspired by this work, in this chapter we will use the WTI to study a broader class of theories, addressed in the context of high-T_c superconductors and atomic Fermi superfluids, which are based on an extension of a BCS-based self energy.

Within these approaches we go beyond the pioneering work of Nambu and show by extending the method of Ref. [He & Guo, 2015], that both the full vertex and the collective modes can be explicitly derived for a class of strongly correlated superfluids. In particular we derive closed form expressions for the response functions. Theories which belong to this class include the work of Refs. [Boyack et al., 2014, Scherpelz et al., 2014] along with additional theories such as that proposed in Ref. [Yang et al., 2006], Ref. [Lee, 2014], and Refs. [Andrenacci et al., 2003, Perali et al., 2004, Pieri et al., 2004].

5.2 Correlation effects beyond BCS theory: Ward-Takahashi identity

5.2.1 Kubo formulae

The goal of this section of the chapter is to incorporate correlations which go beyond the mean-field BCS theory and, making use of Kubo formulae, arrive at properly gauge-invariant linear response functions. We begin by summarizing the Kubo formalism for a many-body theory of interacting fermions. In what follows we shall primarily be concerned with neutral superfluids. Incorporating Coulomb effects can be done through the random phase approximation (RPA) formalism [Lutchyn et al., 2008], once the exact response functions are obtained for the neutral system.

In the presence of a weak and externally applied EM field, with four-vector potential $A^\mu = (\phi, \mathbf{A})$, the four-current density $J^\mu = (\rho, \mathbf{J})$ is given by

$$J^\mu(q) = K^{\mu\nu}(q) A_\nu(q), \tag{5.1}$$

where $q^\mu = (i\Omega_m, \mathbf{q})$ is a four-momentum, with a bosonic Matsubara frequency $i\Omega_m$. The quantity $K^{\mu\nu}$ is the EM response kernel, which is of principal interest here. Charge (in the neutral case, particle number) conservation ($q_\mu J^\mu = 0$) implies that the response kernel $K^{\mu\nu}$ must satisfy the condition $q_\mu K^{\mu\nu} = 0$. The satisfaction of this condition is what we will mean by a gauge-invariant many-body theory. We emphasize that A^μ is a non-dynamical external field, incorporated here, even for a neutral superfluid, merely to derive the EM response kernel in the context of linear response theory. Once the EM response is obtained, A^μ is set to zero. For further details see Ref. [Lutchyn et al., 2008].

The response kernel $K^{\mu\nu}$ can be written in a general form as [Schrieffer, 1964]

$$K^{\mu\nu}(q) = 2\sum_k G(k_+)\Gamma^\mu(k_+, k_-)G(k_-)\gamma^\nu(k_-, k_+) + \frac{n}{m}\delta^{\mu\nu}(1 - \delta_{0\mu}), \tag{5.2}$$

where the full and bare vertices are $\Gamma^\mu(k_+, k_-)$, $\gamma^\nu(k_+, k_-)$ respectively, and $k_\pm \equiv k \pm q/2$ is the incoming (+) or outgoing $(-)$ momenta of a vertex. The four-vector summation is defined by $\sum_k \equiv (\beta)^{-1}\sum_{i\omega_n}\sum_{\mathbf{k}}$, where $\beta = 1/k_B T$ and T is the temperature. The particle number is n and m denotes the fermion mass. The full Green's function is denoted by $G(k)$, which we define in terms of the bare Green's function, $G_0^{-1}(k) = i\omega - \xi_{\mathbf{k}}$, in Eq. (5.4). Here the single particle dispersion is $\xi_{\mathbf{k}} = k^2/2m - \mu$, where μ is the chemical potential. We set $\hbar = c = 1$. We now introduce a framework that encapsulates both BCS theory and stronger correlations beyond BCS theory. The general principles we outline (in the next two sections) should be applicable to more complicated theories such as Eliashberg theory [Eliashberg, 1960], where, because of the dynamics of the order parameter, the establishment of a gauge-invariant EM response may be prohibitively difficult to implement.

To understand what is meant by these correlation effects, here we consider a scalar correlated self energy $\Sigma_{\rm corr}(k)$. In order to simultaneously describe a wide variety of theories, we define the partially-dressed Green's function

$$(G_0^\alpha)^{-1}(k) = G_0^{-1}(k) - \alpha\Sigma_{\rm corr}(k). \tag{5.3}$$

This depends on the strong correlation contribution to the self energy $\Sigma_{\rm corr}$ for $\alpha = 1$, and does not include strong correlation effects for $\alpha = 0$. The fermionic Green's function is then given by Dyson's equation

$$G^{-1}(k) = G_0^{-1}(k) - \Sigma(k), \tag{5.4}$$

where the self energy consists of two terms:

$$\Sigma(k) = \Sigma_{\rm corr}(k) - |\Delta_{\rm sc}|^2 G_0^\alpha(-k), \tag{5.5}$$

for a superconducting order parameter $\Delta_{\rm sc}$. (In Nambu space $\Delta_{\rm sc}$ is the anomalous, off-diagonal, self-energy component.) For convenience we assume that $\Delta_{\rm sc}$ is momentum independent, in contrast with Eliashberg theory. However, the more general case could also be considered. Equivalently, $\Sigma(k) = \Sigma_{\rm corr}(k) + \Sigma_{\rm sc}(k)$, where $\Sigma_{\rm sc}(k) = -|\Delta_{\rm sc}|^2 G_0^\alpha(-k)$ is the superconducting self energy contribution.[1]

Note that, when $\alpha = 0$ the partially-dressed Green's function $G_0^\alpha(k)$ reduces to the bare Green's function $G_0(k)$, so that there are no correlation effects incorporated in the superconducting self energy term $\Sigma_{\rm sc}(k)$. However, for $\alpha = 1$ the partially-dressed Green's function $G_0^\alpha(k)$ does depend on the strong correlations, via Eq. (5.3), and thus gives rise to correlation effects present in the superconducting self energy $\Sigma_{\rm sc}(k)$. The gap equation can be written [Chen et al., 2005, Yang et al., 2006] as $1 - g\sum_k G_0^\alpha(-k)G(k) = 0$. Multiplying both sides of this equation by $\Delta_{\rm sc}$, and

1. For comparison to other notation in the literature, we note that the Green's function is occasionally [Sakai et al., 2016] written as $G^{-1}(k) = G_0^{-1}(k) - \Sigma^{\rm nor}(k) - W(k)$, where $W(k) = -\Sigma^{\rm ano}(k)^2[G_0^{-1}(-k) - \Sigma^{\rm nor}(-k)]^{-1}$. In our notation this corresponds to $\Sigma^{\rm ano}(k) \equiv \Delta_{\rm sc}$, $\Sigma^{\rm nor}(k) \equiv \Sigma_{\rm corr}(k)$, $W(k) \equiv \Sigma_{\rm sc}(k)$, $G_0^{-1}(-k) - \Sigma^{\rm nor}(-k) \equiv G_0^\alpha(-k)(\alpha = 1)$.

then rearranging, we obtain

$$\Delta_{\rm sc}/g = \sum_k \Delta_{\rm sc} G_0^\alpha(-k) G(k) \equiv \sum_k F_{\rm sc}(k). \tag{5.6}$$

In this expression the Gorkov Green's function $F_{\rm sc}(k)$ has dependence on $\Sigma_{\rm corr}(k)$ via $G_0^\alpha(k)$ and $G(k)$, and there is also implicit dependence on α through $G_0^\alpha(k)$.

This represents a fairly generic class of strongly correlated superfluid systems. When $\Sigma_{\rm corr} = 0$ the system reverts to conventional BCS theory. Thus, the challenge is to include the correlation effects associated with the self energy $\Sigma_{\rm corr}$. Models of this sort are associated with the work of Yang, Rice, and Zhang [Yang et al., 2006], and also with the work of Refs. [Andrenacci et al., 2003, Perali et al., 2004, Pieri et al., 2004], who address BCS-BEC crossover effects via a t-matrix theory. Also belonging to this class is an alternate t-matrix theory of BCS-BEC crossover [Chen et al., 2005, He & Guo, 2015], which, in contrast to the work of Ref. [Perali et al., 2004], is more directly associated with a BCS-based ground state.

5.2.2 Full vertex and Ward-Takahashi identity

In order to derive the gauge-invariant EM response, we now apply the Ward-Takahashi identity (WTI). For a quantum field theory with a global $\mathrm{U}(1)$ symmetry the WTI is an exact relation between the many-body vertex function appearing in correlation functions and the self energy entering in the Green's function. Moreover, as shown in appendix (D.4), given a full vertex satisfying the WTI, the f-sum rule is satisfied and thus charge is conserved.

Given the bare Green's function $G_0(k)$, and the full Green's function $G(k)$, the WTI constrains the full vertex $\Gamma^\mu(k_+, k_-)$ to satisfy [Ryder, 1996]

$$\begin{aligned} q_\mu \Gamma^\mu(k_+, k_-) &= G^{-1}(k_+) - G^{-1}(k_-), \\ &= q_\mu \gamma^\mu(k_+, k_-) + \Sigma(k_-) - \Sigma(k_+). \end{aligned} \tag{5.7}$$

The bare WTI, $q_\mu \gamma^\mu(k_+, k_-) = G_0^{-1}(k_+) - G_0^{-1}(k_-)$, is satisfied by the bare vertex $\gamma^\mu(k_+, k_-) = (1, \mathbf{k}/m)$. Therefore, given a self energy $\Sigma(k)$, the above equation provides a constraint that can be used to determine the full vertex.

The WTI is equivalent to self-consistent perturbation theory, and allows one to compute the exact n-loop full vertex, given any n-loop self energy. If the self energy depends on the full Green's function, then applying the WTI leads to an integral equation for the full vertex of the Bethe-Salpeter form [Nozières, 1964]. However, if the self energy depends on only a finite number of bare or partially-dressed Green's functions, then this integral equation terminates, and the full vertex can be obtained exactly. This is the situation with regard to the strong correlation approaches we consider in section (5.2.4).

We now turn to the superconducting case. For a superconductor, where gauge invariance is "spontaneously broken", the presence of a condensate below the transition temperature leads to a more complicated formulation of the WTI. Imposing gauge invariance in the presence of a condensate requires excitations known as collective modes. The explicit form of the collective modes, however, must be derived from the gap equation [He & Guo, 2015].

The Ward-Takahashi identity is equivalent to requiring the full vertex be obtained by performing all possible vertex insertions in the self energy [Nambu, 1960]. Below the transition temperature, however, we must account for the effect of an external (non-dynamical) vector potential A_μ on the self-consistency condition [Eq. (5.6)]. This necessitates the introduction of collective mode vertices $\Pi^\mu(q)$, $\bar{\Pi}^\mu(q)$ in the full vertex, which are inserted in every location of the condensate terms Δ_{sc}, Δ_{sc}^*, respectively. The next section discusses these collective mode vertices in greater detail. As shown in appendix (D.1), performing all vertex insertions in the self energy of Eq. (5.5), and using Eq. (5.7), then gives the full vertex:

$$\begin{aligned}\Gamma^\mu(k_+, k_-) = \gamma^\mu(k_+, k_-) + \Lambda^\mu(k_+, k_-) - \Delta_{\text{sc}}^* \Pi^\mu(q) G_0^\alpha(-k_-) - \Delta_{\text{sc}} \bar{\Pi}^\mu(q) G_0^\alpha(-k_+) \\ - |\Delta_{\text{sc}}|^2 G_0^\alpha(-k_-)[\gamma^\mu(-k_-, -k_+) + \alpha \Lambda^\mu(-k_-, -k_+)] G_0^\alpha(-k_+). \qquad (5.8)\end{aligned}$$

Here we have introduced the vertex correction $\Lambda^\mu(k_+, k_-)$, which relates to the correlated self energy contribution and satisfies $q_\mu \Lambda^\mu(k_+, k_-) = \Sigma_{\rm corr}(k_-) - \Sigma_{\rm corr}(k_+)$. The collective mode vertices in this expression are (as yet) unknowns which satisfy $q_\mu \Pi^\mu(q) = 2\Delta_{\rm sc}$, $q_\mu \bar{\Pi}^\mu(q) = -2\Delta^*_{\rm sc}$. However, by ensuring these collective mode vertices are consistent with the gap equation, a unique expression for them can be obtained [He & Guo, 2015]. This will be outlined in the next section. Using these relations, along with the bare WTI, one can check explicitly that this full vertex satisfies the full WTI in Eq. (5.7).

By way of comparison, we note that the full vertex in Eq. (5.8) is analogous to the BCS full vertex, but with the mapping $\gamma^\mu \to \gamma^\mu + \alpha\Lambda^\mu, G_0 \to G_0^\alpha$. The many-body effect of the correlation term $\Sigma_{\rm corr}$ (in the partially-dressed Green function G_0^α) is therefore to modify both the bare vertex and the single particle Green's function appearing in the superconducting part of the full vertex. The expression in Eq. (5.8) is completely general, given a self energy of the form in Eq. (5.5). In what follows we will illustrate how to compute the full vertex, and corresponding response kernel, for some examples of strongly correlated superfluids.

Two important limiting cases of the full vertex in Eq. (5.8) can be checked against known results. When $\Sigma_{\rm corr} = 0$, then $\Lambda^\mu = 0$, and the full vertex reduces to the known strict BCS case [Guo et al., 2013a]. If we set $\Delta_{\rm sc} = 0$, then the full vertex reduces to the form of the full vertex for the normal phase with pairing [Boyack et al., 2014, Scherpelz et al., 2014].

5.2.3 Collective mode vertices

A general challenge in studying strongly correlated Fermi superfluids, at temperatures below the transition temperature, is to treat the collective modes in a manner compatible with gauge invariance. In this section we implement a powerful method of obtaining the expressions for the collective mode vertices $\Pi^\mu(q)$, $\bar{\Pi}^\mu(q)$. Gauge invariance alone requires $q_\mu \Pi^\mu(q) = 2\Delta_{\rm sc}$, $q_\mu \bar{\Pi}^\mu(q) = -2\Delta^*_{\rm sc}$. The gap equation imposes a self-consistency condition on both vertices, which we will use in order to determine the explicit form of these vertices. This gap equation is written in Eq. (5.6) and in what follows we also consider the conjugate gap equation.

In Fig. (5.1) the gap equation is expressed as a Feynman diagram.

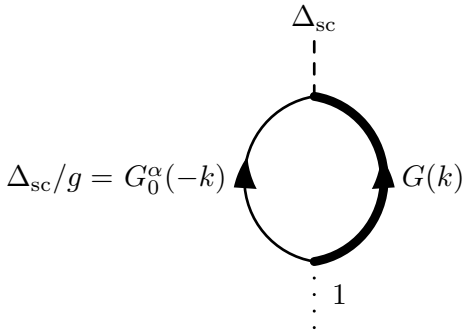

Figure 5.1: Feynman diagram for the gap equation $\Delta_{\rm sc}/g = \Delta_{\rm sc}\sum_k G_0^\alpha(-k)G(k)$.

Diagrammatically, the collective mode vertices are obtained by performing all possible vertex insertions in the gap equation. In Fig. (5.1) there are three possible vertex insertions: (1) at the $\Delta_{\rm sc}$ location one can insert $\Pi^\mu(q)$, (2) at the full Green function $G(k)$ location one can insert the full vertex $\Gamma^\mu(k_+,k_-)$, (3) at the partially-dressed Green function $G_0^\alpha(-k)$ location one can insert the partially-dressed vertex $\gamma^\mu(-k_-,-k_+)+\alpha\Lambda^\mu(-k_-,-k_+)$. After performing these vertex insertions we obtain the equation in Fig. (5.2) expressed in terms of Feynman diagrams.

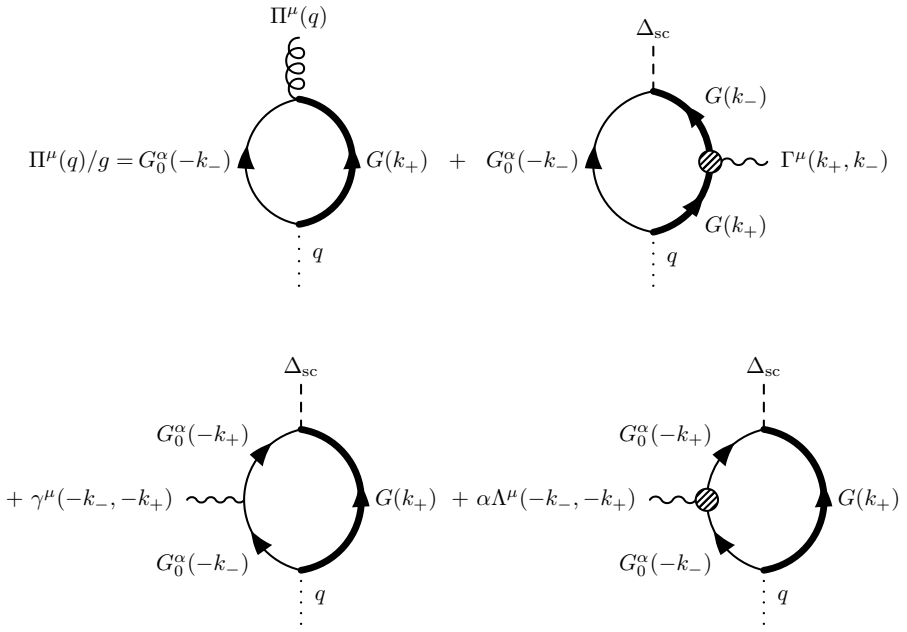

Figure 5.2: Self-consistent equation for the collective modes after performing all possible vertex insertions in the gap equation of Eq. (5.6).

Mathematically, Fig. (5.2) implies the collective mode vertices satisfy the following equation

$$\begin{aligned}\Pi^{\mu}(q)/g = \Pi^{\mu}(q) \sum_{k} G_0^{\alpha}(-k_-)G(k_+) \\ + \Delta_{\rm sc} \sum_{k} G_0^{\alpha}(-k_-)G(k_+)\Gamma^{\mu}(k_+,k_-)G(k_-) \\ + \Delta_{\rm sc} \sum_{k} G_0^{\alpha}(-k_-)\left[\gamma^{\mu}(-k_-,-k_+) + \alpha\Lambda^{\mu}(-k_-,-k_+)\right] G_0^{\alpha}(-k_+)G(k_+). \quad (5.9)\end{aligned}$$

Notice that the full vertex $\Gamma^{\mu}(k_+,k_-)$ appears in this expression. The full vertex was already determined in Eq. (5.8) using the Ward-Takahashi identity. Therefore if we insert the expression for the full vertex, which contains the collective mode vertices, into Eq. (5.9) (and its conjugate), then Eq. (5.9) (and its conjugate) becomes a self-consistent set of equations for the collective mode vertices Π^{μ} and $\bar{\Pi}^{\mu}$. The solution to this self-consistent set of linear equations will uniquely determine the collective mode vertices.

Inserting the full vertex into Eq. (5.9), and doing the same analysis for the conjugate gap equation, then gives the following two self-consistent equations for the collective mode vertices

$$\begin{aligned}\Pi^{\mu}(q)/g = \Pi^{\mu}(q) \sum_{k} G(k_+)G_0^{\alpha}(-k_-)\left[1-\Delta_{\rm sc}^{*}F_{\rm sc}(k_-)\right] - \bar{\Pi}^{\mu}(q)\sum_{k} F_{\rm sc}(k_+)F_{\rm sc}(k_-) \\ + \sum_{k}\left[\gamma^{\mu}(-k_-,-k_+) + \alpha\Lambda^{\mu}(-k_-,-k_+)\right] F_{\rm sc}(k_+)G_0^{\alpha}(-k_-)\left[1-\Delta_{\rm sc}^{*}F_{\rm sc}(k_-)\right] \\ + \sum_{k}\left[\gamma^{\mu}(k_+,k_-) + \Lambda^{\mu}(k_+,k_-)\right] G(k_+)F_{\rm sc}(k_-), \quad (5.10)\end{aligned}$$

$$\begin{aligned}\bar{\Pi}^{\mu}(q)/g = \bar{\Pi}^{\mu}(q) \sum_{k} G(k_-)G_0^{\alpha}(-k_+)\left[1-\Delta_{\rm sc}F_{\rm sc}^{*}(k_+)\right] - \Pi^{\mu}(q)\sum_{k} F_{\rm sc}^{*}(k_+)F_{\rm sc}^{*}(k_-) \\ + \sum_{k}\left[\gamma^{\mu}(-k_-,-k_+) + \alpha\Lambda^{\mu}(-k_-,-k_+)\right] G_0^{\alpha}(-k_+)F_{\rm sc}^{*}(k_-)\left[1-\Delta_{\rm sc}F_{\rm sc}^{*}(k_+)\right] \\ + \sum_{k}\left[\gamma^{\mu}(k_+,k_-) + \Lambda^{\mu}(k_+,k_-)\right] F_{\rm sc}^{*}(k_+)G(k_-). \quad (5.11)\end{aligned}$$

This can be expressed as a matrix equation if we define the two-point correlation functions

$$Q_{+-}(q) = 1/g - \sum_k G(k_+)G_0^{\alpha}(-k_-)\left[1 - \Delta_{\rm sc}^* F_{\rm sc}(k_-)\right], \tag{5.12}$$

$$Q_{-+}(q) = 1/g - \sum_k G(k_-)G_0^{\alpha}(-k_+)\left[1 - \Delta_{\rm sc} F_{\rm sc}^*(k_+)\right], \tag{5.13}$$

$$\begin{aligned} Q_{++}(q) &= \sum_k F_{\rm sc}(k_+)F_{\rm sc}(k_-) = Q_{--}^*(q), \\ P_+^{\mu}(q) &= \sum_k \left[\gamma^{\mu}(k_+,k_-) + \Lambda^{\mu}(k_+,k_-)\right] G(k_+)F_{\rm sc}(k_-) \\ &\quad + \sum_k \left[\gamma^{\mu}(-k_-,-k_+) + \alpha\Lambda^{\mu}(-k_-,-k_+)\right] F_{\rm sc}(k_+)G_0^{\alpha}(-k_-)\left[1 - \Delta_{\rm sc}^* F_{\rm sc}(k_-)\right], \end{aligned} \tag{5.14}$$

$$\begin{aligned} P_-^{\mu}(q) &= \sum_k \left[\gamma^{\mu}(k_+,k_-) + \Lambda^{\mu}(k_+,k_-)\right] F_{\rm sc}^*(k_+)G(k_-) \\ &\quad + \sum_k \left[\gamma^{\mu}(-k_-,-k_+) + \alpha\Lambda^{\mu}(-k_-,-k_+)\right] G_0^{\alpha}(-k_+)F_{\rm sc}^*(k_-)\left[1 - \Delta_{\rm sc} F_{\rm sc}^*(k_+)\right]. \end{aligned} \tag{5.15}$$

Note that, $Q_{-+}(q) = Q_{+-}^*(q)$, $Q_{--}(q) = Q_{++}^*(q)$, $\Delta_{\rm sc}^* P_+^{\mu}(q) = \Delta_{\rm sc} P_-^{\mu}(-q)$. To connect to the literature, we define an alternative set of of two-point correlation functions Q_{ab} and $Q^{a\mu}$, where $a, b = 1, 2$ through, $Q_{11} = Q_{+-} + Q_{-+} + Q_{++} + Q_{--}$, $Q_{22} = Q_{+-} + Q_{-+} - Q_{++} - Q_{--}$, $Q_{12} = i(Q_{+-} - Q_{-+} + Q_{--} - Q_{++})$, $Q_{21} = -i(Q_{+-} - Q_{-+} + Q_{++} - Q_{--})$, and $Q^{1\mu} = -\left(P_+^{\mu} + P_-^{\mu}\right)$, $Q^{2\mu} = -i(P_-^{\mu} - P_+^{\mu})$. Similarly, we define the collective mode vertices $\Pi_{1,2}^{\mu}(q)$ through $\Pi^{\mu}(q) = \Pi_1^{\mu}(q) + i\Pi_2^{\mu}(q)$, $\bar{\Pi}^{\mu}(q) = \Pi_1^{\mu}(q) - i\Pi_2^{\mu}(q)$. This amounts to a change of basis from a complex to a real and imaginary parameterization. From Eq. (5.10) and Eq. (5.11), these vertices satisfy the relation

$$\begin{pmatrix} \Pi_1^{\mu} \\ \Pi_2^{\mu} \end{pmatrix} = -\begin{pmatrix} Q_{11} & Q_{12} \\ Q_{21} & Q_{22} \end{pmatrix}^{-1} \begin{pmatrix} Q^{1\mu} \\ Q^{2\mu} \end{pmatrix}. \tag{5.16}$$

The form of these collective mode vertices is structurally similar to the BCS case [Guo et al., 2013a, He & Guo, 2015], and in the strict BCS limit they agree with the literature [Guo et al., 2013a]. The matrix Q_{ab} can be interpreted as a propagator for bosonic degrees of freedom. However, the explicit response functions entering on the right hand side of Eq. (5.16) are modified due to the presence of the self energy $\Sigma_{\rm corr}$.

In appendix (D.2) we verify the collective mode vertices $\Pi^\mu(q)$ and $\bar{\Pi}^\mu(q)$ satisfy the conditions $q_\mu \Pi^\mu(q) = 2\Delta_{\rm sc}$, $q_\mu \bar{\Pi}^\mu(q) = -2\Delta^*_{\rm sc}$, which was assumed in their definitions and required for gauge invariance.

5.2.4 Λ^μ vertex correction

We can now summarize the central results of this chapter and repeat key equations. The full electromagnetic response kernel can generically be written as

$$K^{\mu\nu}(q) = 2\sum_k G(k_+)\Gamma^\mu(k_+,k_-)G(k_-)\gamma^\nu(k_-,k_+) + \frac{n}{m}\delta^{\mu\nu}(1-\delta_{0\mu}), \tag{5.2}$$

where the full vertex

$$\begin{aligned}\Gamma^\mu(k_+,k_-) = \gamma^\mu(k_+,k_-) + \Lambda^\mu(k_+,k_-) - \Delta^*_{\rm sc}\Pi^\mu(q)G_0^\alpha(-k_-) - \Delta_{\rm sc}\bar{\Pi}^\mu(q)G_0^\alpha(-k_+) \\ - |\Delta_{\rm sc}|^2 G_0^\alpha(-k_-)[\gamma^\mu(-k_-,-k_+) + \alpha\Lambda^\mu(-k_-,-k_+)]G_0^\alpha(-k_+),\end{aligned} \tag{5.8}$$

contains contributions due to both the collective mode vertices Π^μ and $\bar{\Pi}^\mu$ [computed in Eq. (5.16)] and the vertex contribution Λ^μ arising from the self energy $\Sigma_{\rm corr}$.

The techniques described above are sufficient to calculate the gauge-invariant response function for a large class of theories. All that is required to derive the full gauge-invariant electromagnetic response is to arrive at a form of Λ^μ. This vertex depends on the details of the correlation self energy, $\Sigma_{\rm corr}$, so we must consider it on a case by case basis. We now consider three relevant examples from the literature.

Pairing pseudogap approximation

The first type of strongly correlated system we study is proposed in Ref. [Norman et al., 1998] at a phenomenological level and in Ref. [Chen et al., 2005] from a more microscopic perspective. In Ref. [Kosztin et al., 2000] an early attempt to address how collective modes are affected by these pseudogap effects was performed. This model is based on a BCS-like self energy but with a normal state gap $\Delta_{\rm pg}$. For this model, which we call the "pairing pseudogap approximation", $\alpha = 0$ in Eq. (5.3), and the correlated self energy in Eq. (5.5) is given by

$$\Sigma_{\rm corr}(k) = -\Delta_{\rm pg}^2 G_0(-k). \tag{5.17}$$

The pairing gap $\Delta_{\rm pg}$ is non-zero in the range of temperatures $T^* > T > 0$, where T^* is the mean-field transition temperature [$\Delta_{\rm pg}(T^*) = 0$]. At a microscopic level [Chen et al., 2005] $\Delta_{\rm pg}$ is to be associated with non-condensed (finite momentum) pairs and is distinct from the superconducting order parameter $\Delta_{\rm sc}$, which corresponds to a condensate of pairs at zero net momentum.

Unlike the order parameter $\Delta_{\rm sc}$, the gap $\Delta_{\rm pg}$ does not fluctuate in the presence of A_μ. Nevertheless, its inclusion in the self energy will lead to a vertex correction. Using this form of $\Sigma_{\rm corr}(k)$, along with the definition $q_\mu \Lambda^\mu(k_+, k_-) = \Sigma_{\rm corr}(k_-) - \Sigma_{\rm corr}(k_+)$, we obtain

$$\Lambda^\mu(k_+, k_-) = \Delta_{\rm pg}^2 G_0(-k_-)\gamma^\mu(-k_-, -k_+)G_0(-k_+). \tag{5.18}$$

Inserting this expression into Eq. (5.8), along with $\alpha = 0$, then gives the full superconducting vertex in the pairing pseudogap approximation. The pseudogap self energy is an approximation of a theory with $\alpha = 0$ and $\Sigma_{\rm corr}(k) = \sum_l t_{\rm pg}(l) G_0(l - k)$, where $t_{\rm pg}(l)$ is a t-matrix. This theory was studied in Ref. [He & Guo, 2015], and the vertex Λ^μ was calculated exactly. The exact $t_{\rm pg}$ depends on the full Green's function, so the exact Λ^μ will itself depend on the full vertex Γ^μ, and thus a self-consistent integral equation will arise for Γ^μ. In the pairing pseudogap approximation, since $\Delta_{\rm pg}$ does not fluctuate with A_μ, no vertex insertions in the gap are possible in Λ^μ.

YRZ model

As a second model we consider a phenomenological self energy developed for the high-T_c superconductors and associated with Yang, Rice, and Zhang [Yang et al., 2006]. This is known as the YRZ model. For the YRZ model, in Eq. (5.3) and Eq. (5.5) one sets $\alpha = 1$ and

$$\Sigma_{\rm corr}(k) = -\Delta_{\rm pg}^2 G_0(-k). \tag{5.19}$$

Since $\Sigma_{\rm corr}(k)$ is the same as in the pairing pseudogap approximation, the YRZ model also has

$$\Lambda^\mu(k_+, k_-) = \Delta_{\rm pg}^2 G_0(-k_-)\gamma^\mu(-k_-, -k_+)G_0(-k_+). \tag{5.20}$$

Inserting this vertex correction into Eq. (5.8), along with $\alpha = 1$, then gives the full superconducting vertex in the YRZ model. In the normal state, this full vertex, along with the response kernel in Eq. (5.2), is in agreement with the results obtained in Ref. [Scherpelz et al., 2014]. Here we have extended this work to the superconducting case.

Particle-only t-matrix

A third and final model was introduced by Strinati and collaborators using a generalized t-matrix [Andrenacci et al., 2003, Perali et al., 2004, Pieri et al., 2004]. In this model the self energy is obtained from Eq. (5.3) and Eq. (5.5) by setting $\alpha = 1$ and

$$\Sigma_{\rm corr}(k) = \sum_l t(l)G(l-k). \tag{5.21}$$

Here G is the full Green's function, $t(l)$ is a t-matrix, the details of which are presented in appendix (D.3.3). In Ref. [Andrenacci et al., 2003], the authors propose "good candidates" for the response function Feynman diagrams. We emphasize the WTI provides a direct procedure to determine not just good candidates but the exact gauge-invariant full vertex [Eq. (5.8)].

The challenge here is in determining the exact vertex correction $\Lambda^{\mu}(k_+, k_-)$. This is more complicated than in the previous two cases. Nevertheless, following the procedure outlined above, the vertex correction due to this self energy can be obtained by performing all possible vertex insertions in all internal lines. That is, by inserting all possible vertices into both the Green's function and the t-matrix. In appendix (D.3.3) we explicitly derive the vertex correction Λ^{μ} for the self energy appearing in Eq. (5.21). We should note that the authors of this body of work do not presume a self-consistent gap equation, such as that appearing in Eq. (5.6), and such as we have assumed in arriving at Eq. (5.16). Rather, they fix the order parameter to be the same as in BCS theory, and add additional correlations to the number equation only.

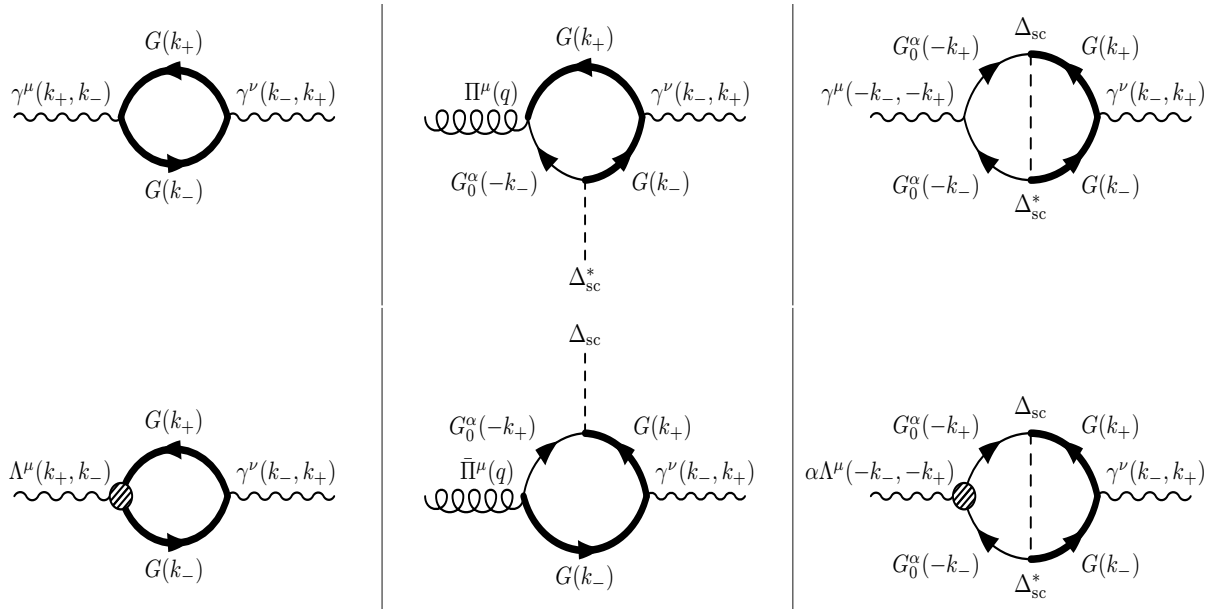

Figure 5.3: Feynman diagrams for the two particle response function $P^{\mu\nu}(q)$, given a self energy of the form in Eq. (5.5). The order of appearance of the diagrams, from top to bottom and left to right, corresponds directly to the order of appearance of terms in Eq. (5.8). The pseudogap approximation corresponds to $\alpha = 0, \Sigma_{\rm corr}(k) = -\Delta_{\rm pg}^2 G_0(-k)$, for the YRZ model $\alpha = 1, \Sigma_{\rm corr}(k) = -\Delta_{\rm pg}^2 G_0(-k)$, and for the t-matrix model $\alpha = 1, \Sigma_{\rm corr}(k) = \sum_l t(l) G(l-k)$.

In summary, this section showed how to derive the gauge-invariant full vertex for a generic self energy of the form in Eq. (5.5). Using the Ward-Takahashi identity there is an exact procedure to determine the full vertex. Moreover there is an analogous procedure to determine the collective modes and thus maintain gauge invariance. The resulting Feynman diagrams, shown in Fig. (5.3), are then completely determined.

5.3 Alternative approach to Ward-Takahashi: Path integral

5.3.1 Gauge-invariant electrodynamics

A large class of theories in the literature derive the gauge-invariant electromagnetic response using a path integral approach [Altland & Simons, 2010, Lutchyn et al., 2008, Ojanen & Kitagawa, 2013]. We now connect, where possible, the above results using the Ward-Takahashi identity to the EM response as calculated in the path integral literature. Here we will include both amplitude and phase fluctuations of the order parameter [Diener et al., 2008, Taylor et al., 2006]. This is in contrast to previous studies [Altland & Simons, 2010, Lutchyn et al., 2008, Ojanen & Kitagawa, 2013] which incorporate only phase fluctuations. We introduce these amplitude fluctuations in order to address the compressibility sum rule.

The inverse Nambu Green's function is $\mathcal{G}^{-1} = \mathcal{G}_0^{-1} - \Sigma$, where $\mathcal{G}_0^{-1} = i\omega - \xi_{\mathbf{k}}\tau_3$ and the self energy is $\Sigma = -\Delta(x)\tau_+ - \Delta^*(x)\tau_-$. The Nambu Pauli matrices are $\tau_{1,2,3}$, which define the raising and lowering operators $\tau_\pm = \frac{1}{2}(\tau_1 \pm i\tau_2)$. We begin with the action functional in terms of the Hubbard-Stratonovich field Δ [Taylor et al., 2006]:

$$S[\Delta^*, \Delta, A^\mu] = -\mathrm{Tr}\,\ln\left[-\beta\mathcal{G}^{-1}\right] + \int dx\, \frac{|\Delta(x)|^2}{g}, \tag{5.22}$$

and following convention, the trace Tr represents a trace over both Nambu and position indices. As in section (5.2), here we consider only neutral superfluids. In Eq. (5.22) we have introduced a non-dynamical external field A^μ through minimal-coupling to obtain the EM response; at the end

of the calculation $A^\mu \to 0$. (Note that, the minimal-coupling here is through the electron charge, not the charge of the neutral superfluid.) We now follow the literature and perform the saddle-point expansion. To lowest order the effective action is $S_{\rm eff}[\Delta^*, \Delta, A^\mu] = S_{\rm mf}[\Delta^*_{\rm mf}, \Delta_{\rm mf}]$, where the mean-field (mf) action is

$$S_{\rm mf}[\Delta^*_{\rm mf}, \Delta_{\rm mf}] = -{\rm Tr}\,\ln\left[-\beta\mathcal{G}^{-1}_{\rm mf}\right] + \int dx\,\frac{|\Delta_{\rm mf}|^2}{g}, \tag{5.23}$$

and the inverse mean-field Nambu Green's function is $\mathcal{G}^{-1}_{\rm mf} = \mathcal{G}^{-1}_0 - \Sigma[\Delta(x) \to \Delta_{\rm mf}]$. The BCS gap equation then follows upon setting $\delta S_{\rm mf}[\Delta^*_{\rm mf}, \Delta_{\rm mf}]/\delta\Delta^*_{\rm mf} = 0$. It is straightforward to show the resulting response kernel is not gauge invariant.

We now calculate the gauge-invariant EM response kernel $K^{\mu\nu}$. In order to implement gauge invariance, the conventional literature introduces fluctuations $\eta(x)$ about the mean-field value of the order parameter $\Delta_{\rm mf}$, expressing $\Delta(x) = \Delta_{\rm mf} + \eta(x)$. [In section (5.2), $\Delta_{\rm sc} \equiv \Delta_{\rm mf}$ for strict BCS theory.] Expanding the action functional to second order in $\eta(x)$ gives $S[\Delta^*, \Delta, A^\mu] \approx S_{\rm mf}[\Delta^*_{\rm mf}, \Delta_{\rm mf}] + S^{(2)}[\eta^*, \eta, A^\mu]$. To calculate $S^{(2)}[\eta^*, \eta, A^\mu]$, we first consider fluctuations of the Green's function about the mean-field solution:

$$\mathcal{G}^{-1} - \mathcal{G}^{-1}_{\rm mf} = -\delta\Gamma - \Sigma_\eta, \tag{5.24}$$

where $\delta\Gamma = \Gamma_1 + \Gamma_2$, with $\Gamma_1 = \hat{\gamma}_\mu A^\mu$, $\Gamma_2 = (\mathbf{A}^2/2m)\tau_3$, is a vector potential fluctuation and $\Sigma_\eta = \Sigma[\Delta(x) \to \eta(x)]$ is a gap fluctuation. Expanding to second order in η and A_μ, the second order action functional is

$$\begin{aligned} S^{(2)}[\eta^*, \eta, A^\mu] = \frac{1}{2}\sum_q \Big[A_\mu(q) K^{\mu\nu}_{0,{\rm mf}}(q) A_\nu(-q) + \eta_a(q) Q^{ab}_{\rm mf}(q)\eta_b(-q)\Big] \\ - \frac{1}{2}\sum_q \Big[A_\mu(q) Q^{\mu b}_{\rm mf}(q)\eta_b(-q) + \eta_a(q) Q^{a\nu}_{\rm mf}(q) A_\nu(-q)\Big]. \end{aligned}$$

In this expression we write $\eta(x) = \eta_1(x) - i\eta_2(x)$ with $\eta_1(x), \eta_2(x) \in \mathbb{R}$. This decomposes the fluctuations into their (Cartesian) real and imaginary parts, which amounts to an amplitude and phase decomposition. Since we keep the saddle-point condition at the mean-field level, an explicit amplitude and phase decomposition, in polar coordinates, will lead to the same electromagnetic response. (If one uses a different saddle-point condition, not relevant to this work, then issues associated with the use of either a Cartesian or polar decomposition may arise [Diener et al., 2008].) Even within this framework, we shall point out an inconsistency within the conventional path integral formalism in failing to satisfy the compressibility sum rule.

To complete the calculation, we transform to momentum space, $k = (i\omega_n, \mathbf{k})$ and $q = (i\Omega_m, \mathbf{q})$, where $i\omega_n$ ($i\Omega_m$) is a fermionic (bosonic) Matsubara frequency. The Nambu-space bare vertex in momentum space is defined by $\hat{\gamma}^\mu(k_+, k_-) = (\tau_3, \mathbf{k}/m)$. If we denote the trace over Nambu indices by tr, then the "bubble" response kernel is $K^{\mu\nu}_{0,\mathrm{mf}}(q) = \mathrm{tr}\sum_k \mathcal{G}_{\mathrm{mf}}(k_+)\hat{\gamma}^\mu(k_+, k_-)\mathcal{G}_{\mathrm{mf}}(k_-)\hat{\gamma}^\nu(k_-, k_+) + \frac{n}{m}\delta^{\mu\nu}(1-\delta_{\mu 0})$ and the two-point response function $Q^{ab}_{\mathrm{mf}}(q) = \frac{2}{g}\delta_{ab} + \mathrm{tr}\sum_k \mathcal{G}_{\mathrm{mf}}(k_+)\tau_a\mathcal{G}_{\mathrm{mf}}(k_-)\tau_b$ can be viewed as a bosonic propagator. We also have $Q^{\mu a}_{\mathrm{mf}}(q) = \mathrm{tr}\sum_k \mathcal{G}_{\mathrm{mf}}(k_+)\hat{\gamma}^\mu(k_+, k_-)\mathcal{G}_{\mathrm{mf}}(k_-)\tau_a$, and $Q^{b\nu}_{\mathrm{mf}}(q)$ has $(\mu, a) \leftrightarrow (b, \nu)$. These mean-field response functions are equivalent to previous results in the literature [Guo et al., 2013a]. They are also equivalent to the response functions which appear in Eq. (5.16) for a theory with only a strict BCS self energy.

After integrating out the η field, the beyond-mean-field effective action contribution is

$$S_{\mathrm{eff}} - S_{\mathrm{mf}} = \sum_q A_\mu(q) K^{\mu\nu}_{\mathrm{mf}}(q) A_\nu(-q) + \frac{1}{2}\mathrm{Tr}\,\ln\left[Q^{ab}_{\mathrm{mf}}(q)\right]. \tag{5.25}$$

Thus the fluctuation action decomposes into two separate terms. The second term in the fluctuation action provides a contribution to thermodynamics arising from Gaussian fluctuations. This form of the Gaussian fluctuation part of the action is equivalent to the standard results in the literature [Diener et al., 2008]. The first term is the gauge-invariant EM response kernel, with both amplitude and phase fluctuations of the order parameter included, defined by

$K^{\mu\nu}_{\rm mf}(q) = K^{\mu\nu}_{0,{\rm mf}}(q) - \sum_{a,b} Q^{\mu a}_{\rm mf}(q) \left[Q^{ab}_{\rm mf}(q)\right]^{-1} Q^{b\nu}_{\rm mf}(-q)$. If we expand the response kernel appearing in Eq. (5.25), then we obtain [Guo et al., 2013a, Kulik et al., 1981]:

$$K^{\mu\nu}_{\rm mf} = K^{\mu\nu}_{0,{\rm mf}} - \frac{Q_{11}Q^{\mu 2}_{\rm mf}Q^{2\nu}_{\rm mf} + Q_{22}Q^{\mu 1}_{\rm mf}Q^{1\nu}_{\rm mf} - Q_{12}Q^{\mu 1}_{\rm mf}Q^{2\nu}_{\rm mf} - Q_{21}Q^{\mu 2}_{\rm mf}Q^{1\nu}_{\rm mf}}{Q_{11}Q_{22} - Q_{12}Q_{21}}. \tag{5.26}$$

In Ref. [Guo et al., 2013a] it is proved that the response kernel in Eq. (5.26) is both gauge invariant $q_\mu K^{\mu\nu}_{\rm mf}(q) = 0$, and charge conserving $K^{\mu\nu}_{\rm mf}(q)q_\nu = 0$. References [Guo et al., 2013a, Kulik et al., 1981] used a matrix linear response formalism known as "consistent fluctuation of the order parameter". Our derivation, however, is based on the path integral.

5.3.2 Inconsistency with the compressibility sum rule

We now turn to the implications of the two contributions to the action in Eq. (5.25). Here we focus on the compressibility sum rule, which provides an important consistency check on the path integral approach. The explicit form of the compressibility sum rule is [Pines & Nozières, 1966]:

$$\lim_{\mathbf{q}\to 0}\left[K^{00}(\omega = 0, \mathbf{q})\right] = -\frac{\partial n}{\partial \mu}. \tag{5.27}$$

Here the real frequency ω is the analytic continuation of the Matsubara frequency $i\Omega_m$, defined by $i\Omega_m = \omega + i\gamma$ with $\gamma \to 0^+$. This sum rule shows how to associate the electromagnetic contributions to the action with their counterpart contributions to the thermodynamic response. The compressibility, $\kappa = n^{-2}(\partial n/\partial \mu)$, is then related to the density response via Eq. (5.27).

In relation to section (5.2), we note that satisfying the WTI does not imply the compressibility sum rule is satisfied [Guo et al., 2013a,b]. In the appropriate limits, the WTI gives a constraint on the vector component of the full vertex: $\lim_{\mathbf{q}\to 0}\left[\mathbf{q}\cdot\mathbf{\Gamma}(k_+, k_-)|_{\omega=0}\right] = -\lim_{\mathbf{q}\to 0}\left[\left(G^{-1}(k_+) - G^{-1}(k_-)\right)|_{\omega=0}\right]$, whereas the compressibility sum rule is $\lim_{\mathbf{q}\to 0}\left[\Gamma^0(k_+, k_-)|_{\omega=0}\right] = 1 - \partial\Sigma(k)/\partial\mu$, which is a constraint on the time component of the full vertex. We emphasize that the order of limits is crucial: first the frequency

ω is set to zero, and then the momentum $\mathbf{q} \to 0$. Thus the WTI is not a sufficient condition to ensure satisfaction of the compressibility sum rule. In the path integral formalism, however, both the electrodynamics and thermodynamics arise from the same action, and so Eq. (5.27) is an important constraint relating the two responses.

The relationship in Eq. (5.27) is also particularly useful in characterizing various orders of approximation within the path integral scheme. This is because at the heart of the path integral is a close connection between electrodynamics and thermodynamics. With the inclusion of amplitude fluctuations, which are essential for this sum rule, we can now test the compressibility sum rule within the standard path integral formalism in the literature.

Note that, this sum rule depends on the number equation. Consistency would seem to require that we include Gaussian fluctuations $n_{\rm fl} = -\beta^{-1}\partial S_{\rm fl}[\Delta^*_{\rm mf}, \Delta_{\rm mf}]/\partial\mu$ to the number equation coming from the second line in Eq. (5.25). This is, in fact, incorrect and points to an underlying inconsistency. Instead, we will show the proper calculation level for thermodynamics is that of pure mean-field, giving a mean-field particle number

$$n_{\rm mf} = -\frac{1}{\beta}\frac{\partial S_{\rm mf}[\Delta^*_{\rm mf}, \Delta_{\rm mf}]}{\partial\mu} = 2\sum_k G(k). \tag{5.28}$$

Taking the derivative of the mean-field number equation with respect to μ gives

$$\frac{\partial n_{\rm mf}}{\partial\mu} = -2\sum_k \left[G^2(k) - F^2(k) + 2G(k)F(k)\frac{\partial\Delta_{\rm mf}}{\partial\mu}\right], \tag{5.29}$$

where we henceforth take $\Delta_{\rm mf} = \Delta^*_{\rm mf}$ for convenience. Here we define the single particle Green's function in terms of the Nambu Green's function by $G(k) = [\mathcal{G}_{\rm mf}(k)]_{11} = -[\mathcal{G}_{\rm mf}(-k)]_{22}$, and the Gorkov Green's function is similarly $F(k) = \Delta_{\rm mf}G(k)G_0(-k) = [\mathcal{G}_{\rm mf}(k)]_{12} = [\mathcal{G}^*_{\rm mf}(k)]_{21}$.

The fluctuation of the mean-field gap with respect to the chemical potential, $\partial\Delta_{\rm mf}/\partial\mu$, can be found using the BCS gap equation

$$\mathrm{GAP}[\Delta_{\rm mf},\mu] := \frac{\Delta_{\rm mf}}{g} - \sum_k \mathrm{Tr}[\mathcal{G}(k)\tau_-] = 0. \tag{5.30}$$

Since $\Delta_{\rm mf}$ depends on μ, by taking the total derivative with respect to μ we arrive at the condition

$$\frac{\partial\Delta_{\rm mf}}{\partial\mu} = -\frac{\partial\mathrm{GAP}/\partial\mu}{\partial\mathrm{GAP}/\partial\Delta_{\rm mf}}. \tag{5.31}$$

To prove the compressibility sum rule is satisfied, notice that $\partial\mathrm{GAP}/\partial\mu = 2\sum_k G(k)F(k)$ and $\partial\mathrm{GAP}/\partial\Delta = 2\sum_k F(k)F(k)$. Therefore, the last term in Eq. (5.29) can be expressed as $2\frac{(\partial\mathrm{GAP}/\partial\mu)^2}{\partial\mathrm{GAP}/\partial\Delta_{\rm mf}}$. Now, in the limit that $\omega = 0, \mathbf{q} \to 0$, the following identifications can be made: $Q^{10}_{\rm mf} = 2\partial\mathrm{GAP}/\partial\mu$, and $Q^{11}_{\rm mf} = 2\partial\mathrm{GAP}/\partial\Delta_{\rm mf}$. By computing the summation over Matsubara frequencies, one also obtains $2\sum_k \left[G^2(k) - F^2(k)\right] = K^{00}_{0,\rm mf}$. Therefore, using Eq. (5.26), Eq. (5.29) now becomes

$$-\frac{\partial n_{\rm mf}}{\partial\mu} = K^{00}_{0,\rm mf} - \frac{Q^{10}_{\rm mf}Q^{01}_{\rm mf}}{Q_{11}} = K^{00}(0,\mathbf{q}\to 0). \tag{5.32}$$

This demonstrates the expected consistency between $-(\partial n_{\rm mf}/\partial\mu)$ and $K^{00}(0,\mathbf{q}\to 0)$ and proves the compressibility sum rule at the BCS level [Guo et al., 2013a].

The reason for the need to include amplitude fluctuations in the density response can be seen from Eq. (5.29). This equation shows that fluctuations in the gap ($\partial\Delta_{\rm mf}/\partial\mu$) must be included, and therefore amplitude fluctuations in the gap are necessary in order to satisfy the compressibility sum rule. If only phase fluctuations are retained, the compressibility sum rule is violated. For a different context where amplitude fluctuations are important see Ref. [Salasnich et al., 2013].

The compressibility sum rule has been satisfied only by ignoring the Gaussian fluctuations in the number equation. Had these been included, we would obtain $-\partial n/\partial\mu = -\partial n_{\rm mf}/\partial\mu - \partial n_{\rm fl}/\partial\mu \neq K^{00}(0, \mathbf{q}\to 0)$, which violates the compressibility sum rule. [2]

In summary, the path integral formalism, as currently applied in the literature, treats electrodynamics and thermodynamics inconsistently. In this derivation of gauge-invariant electrodynamics at the BCS level, beyond-BCS fluctuations are necessarily incorporated in thermodynamics. However, these thermodynamic fluctuations should not appear in the number equation if the compressibility sum rule is to be satisfied. The discussion in section (5.2) provides insights into the resolution to this inconsistency: there gauge invariance is established by determining the collective modes via performing all possible vertex insertions in the gap equation. This suggests that, within the path integral formalism, one should consider a new saddle-point condition in the presence of a non-zero vector potential. More details on this resolution are presented in the next chapter and in Ref. [Anderson et al., 2016].

5.4 Conclusions

The goal of this chapter was to show how to arrive at a proper gauge-invariant description of the electromagnetic response in strongly correlated Fermi superfluids. In this chapter correlation effects are represented by "correlated self energy" contributions which appear in addition to the usual superconducting self energy of the condensate. The theoretical approach is sufficiently general to apply to a theory that has (1) a scalar diagrammatic self energy and (2) a frequency independent self-consistent gap equation. Using (1) the Ward-Takahashi identity and (2) insertions on the self-consistent gap equation, the exact gauge-invariant electromagnetic response can then, in prin-

2. We note that the failure to satisfy the compressibility sum rule is not a consequence of an inconsistency between the number equation and the Green's function [Serene, 1989]. Indeed, the number equation is $n = n_{\rm mf} + n_{\rm fl}$, where $n_{\rm mf} = -\partial\Omega_{\rm mf}/\partial\mu = {\rm Tr}\mathcal{G}_{\rm mf}$ and a fluctuation term $n_{\rm fl} = -\partial\Omega_{\rm fl}/\partial\mu$. If one calculates $\mathcal{G} = \mathcal{G}_{\rm mf}+\mathcal{G}_{\rm fl}$ at the fluctuation level, then $n = n_{\rm mf} + n_{\rm fl} = {\rm Tr}(\mathcal{G}_{\rm mf} + \mathcal{G}_{\rm fl})$ is obtained. Taking two derivatives of $n = n_{\rm mf} + n_{\rm fl}$, with respect to μ, the result is $-\partial n/\partial\mu = \partial^2\Omega_{\rm mf}/\partial\mu^2 + \partial^2\Omega_{\rm fl}/\partial\mu^2 = K_{00}(\omega = 0, \mathbf{q}\to 0) + \partial^2\Omega_{\rm fl}/\partial\mu^2 \neq K_{00}(\omega = 0, \mathbf{q}\to 0)$. As stated in the main text, gauge invariance (equivalently charge conservation) is not a sufficient condition to ensure that the compressibility sum rule is satisfied.

ciple, be calculated for any theory satisfying these conditions. Adopting a rather generic class of strongly correlated models (widely used for the high transition temperature superconductors and ultra cold Fermi gases) we were able to give exact expressions for the electromagnetic response. This method, which obtains expressions for all vertex corrections and collective modes in a manner compatible with the f-sum rule, is an important tool for studying strongly correlated superfluids and superconductors.

For comparison we also discussed an alternative tool which builds on the path integral approach. With few exceptions this method has been used to address the BCS-level response, i.e., in the absence of stronger correlations. In contrast to approaches that build on the Ward-Takahashi identity, here gauge invariance and the f-sum rule are relatively straightforward to ensure. What is more complicated is to arrive at consistency with the compressibility sum rule. This sum rule relates electrodynamics and thermodynamics and provides a natural test of the path integral approach, since the two are simultaneously calculated. We showed the conventional path integral treatment in the literature for the gauge-invariant electrodynamics at the BCS level violates the compressibility sum rule.

CHAPTER 6

GOING BEYOND THE BCS LEVEL IN THE SUPERFLUID PATH INTEGRAL: A CONSISTENT TREATMENT OF ELECTRODYNAMICS AND THERMODYNAMICS

In this chapter we derive the full gauge-invariant electromagnetic response beyond the BCS level using the fermionic superfluid path integral. In the process we identify and redress a failure to satisfy the compressibility sum rule; this shortcoming is associated with the conventional path-integral formulation of BCS-level electrodynamics. The approach in this chapter builds on an alternative saddle-point scheme. At the mean-field level, this leads to the well known gauge-invariant electrodynamics of BCS theory and to the satisfaction of the compressibility sum rule. Moreover, this scheme can be readily extended to address arbitrary higher order fluctuation theories, for example at the Gaussian level. At all levels this approach leads to a gauge-invariant and compressibility sum rule consistent treatment of electrodynamics and thermodynamics. The work in this chapter is published in Ref. [Anderson et al., 2016].

6.1 Introduction

Understanding superfluids [Drummond et al., 2009, Giorgini et al., 2008, Hu, 2012, Zwerger, 2011] and superconductors [Chen et al., 2005, Hur & Maurice Rice, 2009] with strong correlations beyond BCS is important to many diverse physics communities. These strong correlations are present in both high temperature superconductors and ultra cold Fermi superfluids. At the heart of probes of superfluidity are electrodynamic and thermodynamic responses. Therefore, it is important to have a consistent theory for addressing both of these. One consistency requirement is that of gauge invariance. This affects only the electrodynamics, and importantly introduces collective modes of the order parameter. Another consistency requirement involves the inter-connection between electrodynamics and thermodynamics. This is encapsulated in the compressibility sum rule [Pines & Nozières, 1966].

The path integral approach is particularly well suited to consistency checks related to this interconnection because it *simultaneously* derives electrodynamics and thermodynamics. As shown in section (5.3.2), however, this standard approach in the literature is not compatible with the compressibility sum rule [Boyack et al., 2016]. This inconsistency shows up at the widely applied [Altland & Simons, 2010, Goryo & Ishikawa, 1999, Lutchyn et al., 2008, Ojanen & Kitagawa, 2013] saddle-point plus Gaussian fluctuation level of approximation. This is the approximation level that is argued to be essential for obtaining the gauge-invariant electrodynamics of BCS theory.

In this chapter we present an alternative to this standard literature path integral approach [Altland & Simons, 2010, Goryo & Ishikawa, 1999, Lutchyn et al., 2008, Ojanen & Kitagawa, 2013]. The main goals are: (1) To obtain a fully gauge-invariant theory of electrodynamics *beyond* BCS theory. (2) To ensure the electrodynamics and thermodynamics are consistent with the compressibility sum rule. (3) To establish the physically observable consequence that if the electrodynamics are described by strict BCS theory then, *the thermodynamics should not include collective mode contributions*. There seems to be no consensus about whether these non-BCS terms should or should not be considered in thermodynamics [Vollhardt & Wolfle, 2013, Yu et al., 2009]. In our path integral re-formulation, for both the lowest order mean-field, and Gaussian fluctuation levels, we will derive theories fully consistent with gauge invariance and the compressibility sum rule. Indeed, this consistency can in principle be achieved at all orders of approximation.

We begin by addressing the compressibility sum rule. Define $\Omega = \Omega_{\rm mf} + \Omega_{\rm fl}$ as the thermodynamic potential resulting from a calculation that uses Gaussian fluctuations ($\rm fl$) around mean-field theory ($\rm mf$) to establish a BCS-level gauge-invariant electromagnetic response. We consider n particles having chemical potential μ. Within this formulation, which we call the gauge restoring Gaussian fluctuation (GRGF) theory, the number of particles $n = -\partial\Omega/\partial\mu$ has a leading order mean-field term $n_{\rm mf}$ and a fluctuation contribution $n_{\rm fl}$. Similarly the electromagnetic kernel which derives from Ω contains the counterpart mean-field and fluctuation terms, both of which combined lead to a proper gauge-invariant BCS density-density correlation function $K^{00}(\omega, \mathbf{q})$.

One can show that [see section (5.3.2)]

$$K^{00}(\omega = 0, \mathbf{q} \to 0) = -\frac{\partial n_{\rm mf}}{\partial \mu} \neq -\frac{\partial n}{\partial \mu}, \tag{6.1}$$

where $n = n_{\rm mf} + n_{\rm fl}$. This demonstrates an explicit violation [Boyack et al., 2016] of the compressibility sum rule, which should read $K^{00}(\omega = 0, \mathbf{q} \to 0) = -\partial n/\partial \mu$. It also demonstrates (at least at an empirically suggestive level) what assumptions need to be made to satisfy the compressibility sum rule within BCS theory.

In the GRGF approach leading to Eq. (6.1) and presented in a fairly extensive literature [Altland & Simons, 2010, Goryo & Ishikawa, 1999, Lutchyn et al., 2008, Ojanen & Kitagawa, 2013], fluctuations of the mean-field phase ϕ were used to restore gauge invariance. These fluctuations enter as a "dressed" vector potential $\widetilde{A}_\mu = A_\mu + \partial_\mu \phi$, which is then expanded to quadratic order. Integration of the fluctuations ϕ resulted in the standard electromagnetic response kernel of strict BCS theory. We emphasize here that the focus was on electrodynamics, while the thermodynamic implications were of no concern. In contrast, understanding thermodynamics associated with Gaussian fluctuation theories (beyond the BCS level) was the focus of work by a different community studying ultra cold Fermi superfluids [Diener et al., 2008, Engelbrecht et al., 1997, He et al., 2015, Hu et al., 2006, Loktev et al., 2001, Taylor et al., 2007]. In these neutral superfluids, soft bosonic collective modes arising from fluctuations were shown to provide new thermodynamic contributions in addition to those of the fermionic quasi-particles of BCS theory.

Yet another series of studies incorporated these Gaussian-level (beyond-BCS) fluctuations to revisit electrodynamics in a higher level theory. By introducing a small phase twist in the thermodynamic potential, it was argued that one could determine the superfluid density ρ_s [Fukushima et al., 2007, Taylor et al., 2006]. This leads to bosonic contributions not present in BCS theory. These were somewhat similar (but not equivalent) to contributions found within a very different diagrammatic formalism [Andrenacci et al., 2003]. In contrast to the present work, these electromagnetic calculations did not establish consistency with gauge invariance.

All this previous literature relating to Gaussian fluctuations can be summarized by noting that there have been separate path integral studies of superfluid electrodynamics and of thermodynamics. What is missing is an analysis of the constraints relating the two. This chapter addresses this shortcoming.

6.2 Path integral and mean-field formalism

Here we consider a fermionic partition function for a neutral, attractive, Fermi superfluid with s-wave pairing. The techniques presented here can be readily extended to higher order pairing, and Coulomb interactions can be included at the RPA level [Lutchyn et al., 2008]. The partition function is calculated using the Hubbard-Stratonovich (HS) path integral

$$\mathcal{Z}[A] = \int \mathcal{D}[\mathbf{\Delta}]\, e^{-S_{\mathrm{HS}}[\mathbf{\Delta},A]}, \tag{6.2}$$

where the HS action takes the usual form $S_{\mathrm{HS}}[\mathbf{\Delta},A] = \int dx \frac{|\Delta|^2}{g} - \mathrm{Tr}\ln\left[-\mathcal{G}^{-1}[\mathbf{\Delta},A]\right]$ [Altland & Simons, 2010, Fradkin, 2013], $g > 0$ is an interaction constant, and $\mathrm{Tr}[\cdot]$ includes a trace over both position and Nambu indices; throughout we set $\hbar = k_B = c = 1$. The inverse Nambu Green's function $\mathcal{G}^{-1}[\mathbf{\Delta},A] = \mathcal{G}_0^{-1}[A] - \Sigma[\mathbf{\Delta}]$ is constructed from a single particle Green's function $\mathcal{G}_0[A]$ and a self-energy $\Sigma = -\mathbf{\Delta}\cdot\boldsymbol{\tau}$, with $\boldsymbol{\tau} = (\tau_1,\tau_2)$ a vector of Nambu Pauli matrices. Throughout we use the notation $\mathbf{\Delta} = (\Delta_1,\Delta_2)$ to represent two real HS fields $\Delta_a(x)$, with $a = 1,2$, consistent with previous literature.[1] The single particle Green's function $\mathcal{G}_0[A]$ is kept general, but we note that an electromagnetic vector potential A_μ has been explicitly included.

We now calculate $\mathcal{Z}[A]$ at the mean-field level using the saddle-point approximation

$$\delta S_{\mathrm{HS}}[\mathbf{\Delta},A]/\delta\Delta_a = 0, \tag{6.3}$$

1. This notation is equivalent to that in Refs. [Boyack et al., 2016, Guo et al., 2013a, Kosztin et al., 2000, Kulik et al., 1981]. The reality condition is expressed in position space; a momentum-space parameterization has a different condition [Guo et al., 2013a]. The conventional BCS self energy $\Sigma[\mathbf{\Delta}] = -(\Delta\tau_+ + \Delta^*\tau_-)$ suggests an equivalent complex parameterization $\Delta_\pm = \Delta_1 \pm i\Delta_2$ where the BCS gap is identified through $\Delta \equiv \Delta_-$. See appendix (E) for further details.

in the presence of $A_\mu \neq 0$. This is to be contrasted with previous work (belonging to the GRGF scheme) [Altland & Simons, 2010, Goryo & Ishikawa, 1999, Lutchyn et al., 2008, Ojanen & Kitagawa, 2013] where the saddle-point condition assumed $A_\mu = 0$. Here, explicit calculation produces the standard BCS gap equation, $0 = 2\Delta_a [A]/g - \mathrm{Tr}[\mathcal{G}[\mathbf{\Delta}[A], A]\tau_a]$, *in the presence of a non-zero vector potential* A_μ. The solution to this gap equation is defined as $\mathbf{\Delta}^{\mathrm{mf}}[A]$, which depends on A_μ. We note that other communities have also exploited the advantages of considering alternative saddle-point schemes [Ercolessi et al., 2000, Kamenev & Andreev, 1999].

At the present mean-field (saddle-point) level, we can write $\mathcal{Z}_{\mathrm{mf}}\left[\mathbf{\Delta}^{\mathrm{mf}}[A], A\right] = e^{-S_{\mathrm{mf}}}$, where the mean-field action $S_{\mathrm{mf}} = S_{\mathrm{HS}}\left[\mathbf{\Delta}^{\mathrm{mf}}[A], A\right]$ is the HS action evaluated at the solution to the saddle-point equations. In general we cannot explicitly calculate the solution to the gap equation for $A_\mu \neq 0$. Instead, we will first use the self-consistent gap equation to find the variation of $\mathbf{\Delta}^{\mathrm{mf}}[A]$ with respect to a variation in A_μ. We then take the $A_\mu \to 0$ limit, after which all quantities are calculated using $\mathbf{\Delta}^{\mathrm{mf}} \equiv \mathbf{\Delta}^{\mathrm{mf}}[0]$. Thus, no additional computational difficulties arise when using this self-consistency condition compared to the GRGF formalism.

6.3 Response functions at saddle-point level

Given an arbitrary "effective action" $S_{\mathrm{eff}}[A] = -\ln \mathcal{Z}[A]$ in the presence of a weak perturbation A_μ, the response kernel comes from the second functional derivative of the action in the $A_\mu \to 0$ limit. Thus, we can expand $S_{\mathrm{eff}}[A] \approx S_{\mathrm{eff}}[0] + \frac{1}{2}\int dx \int dx' A_\mu(x) K^{\mu\nu}(x, x') A_\nu(x')$ to second order in the vector potential A_μ, where

$$K^{\mu\nu}(x, x') = \left.\frac{\delta^2 S_{\mathrm{eff}}[A]}{\delta A_\mu(x)\, \delta A_\nu(x')}\right|_{A\to 0} \tag{6.4}$$

is the response kernel for an arbitrary effective action $S_{\mathrm{eff}}[A]$ [Fradkin, 2013]. We now calculate the mean-field response using the definition in Eq. (6.4) by including a non-zero vector potential in the saddle-point condition, i.e., replace $S_{\mathrm{eff}}[A]$ by $S_{\mathrm{mf}} = S_{\mathrm{mf}}\left[\mathbf{\Delta}^{\mathrm{mf}}[A], A\right]$. When taking a functional derivative with respect to A_μ, new terms arise from a "functional chain rule" [Altland

& Simons, 2010] applied to the self-consistent gap $\mathbf{\Delta}^{\mathrm{mf}}[A]$. These terms, which do not emerge for a gap calculated around $A_\mu = 0$ as in GRGF, are crucial for maintaining gauge invariance. The full response kernel then takes the form:

$$\begin{aligned} K^{\mu\nu}_{\mathrm{mf}}(x,x') = & \left.\frac{\delta^2 S_{\mathrm{mf}}}{\delta A^x_\mu \delta A^{x'}_\nu}\right|_{\mathbf{\Delta}^{\mathrm{mf}}} + \left.\frac{\delta \Delta^y_a}{\delta A^x_\mu}\,\frac{\delta^2 S_{\mathrm{mf}}}{\delta \Delta^y_a \delta \Delta^{y'}_b}\right|_{\mathbf{\Delta}^{\mathrm{mf}}} \frac{\delta \Delta^{y'}_b}{\delta A^{x'}_\nu} \\ & + \left.\frac{\delta \Delta^y_a}{\delta A^x_\mu}\,\frac{\delta^2 S_{\mathrm{mf}}}{\delta \Delta^y_a \delta A^{x'}_\nu}\right|_{\mathbf{\Delta}^{\mathrm{mf}}} + \left.\frac{\delta^2 S_{\mathrm{mf}}}{\delta A^x_\mu \delta \Delta^y_a}\right|_{\mathbf{\Delta}^{\mathrm{mf}}} \frac{\delta \Delta^y_a}{\delta A^{x'}_\nu} \\ & + \left.\frac{\delta S_{\mathrm{mf}}}{\delta \Delta^y_a}\right|_{\mathbf{\Delta}^{\mathrm{mf}}} \frac{\delta^2 \Delta^y_a}{\delta A^x_\mu \delta A^{x'}_\nu}, \end{aligned} \tag{6.5}$$

where the $A_\mu \to 0$ limit is applied after taking all derivatives. In this equation we have introduced the notation $\Delta^x_a \equiv \Delta_a(x)$ and $A^x_\mu \equiv A_\mu(x)$; repeated subscript (superscript) indices a, b (y, y') should be interpreted as an implied Einstein summation (integration.)

To express Eq. (6.5) in a more suggestive form, we define the set of two-point response functions [Boyack et al., 2016, Guo et al., 2013a, Kosztin et al., 2000, Kulik et al., 1981]:

$$\mathcal{Q}^{\alpha\beta}_{\mathrm{mf}}(x,x') \equiv \left.\frac{\delta^2 S_{\mathrm{mf}}\left[\mathbf{\Delta}^{\mathrm{mf}}, A\right]}{\delta \mathcal{A}_\alpha(x)\,\delta \mathcal{A}_\beta(x')}\right|_{A\to 0}, \tag{6.6}$$

where $\mathcal{A}_\alpha = \left(\Delta^{\mathrm{mf}}_1, \Delta^{\mathrm{mf}}_2, A_\mu\right)$ parameterizes both gap and vector potential response. The kernel $K^{\mu\nu}_{0,\mathrm{mf}} \equiv \mathcal{Q}^{\mu\nu}_{\mathrm{mf}}$ is the standard (non-gauge-invariant) response as calculated with a gap $\mathbf{\Delta}^{\mathrm{mf}}$; the functions $Q^{a\mu}_{\mathrm{mf}} = \mathcal{Q}^{a\mu}_{\mathrm{mf}}$ and $Q^{ab}_{\mathrm{mf}} = \mathcal{Q}^{ab}_{\mathrm{mf}}$ come from "partial" derivatives in the functional chain rule. We note that the propagator Q^{ab}_{mf} is equivalent to a "GG" t-matrix for a BCS self-energy, and therefore can be interpreted as an emergent bosonic propagator [Chen et al., 2005, Pieri & Strinati, 2005]. Using these definitions, the mean-field level gauge-invariant response is compactly written

$$K^{\mu\nu}_{\mathrm{mf}} = K^{\mu\nu}_{0,\mathrm{mf}} + \Pi^\mu_a Q^{a\nu}_{\mathrm{mf}} + Q^{\mu a}_{\mathrm{mf}} \Pi^\nu_a + \Pi^\mu_a Q^{ab}_{\mathrm{mf}} \Pi^\nu_b, \tag{6.7}$$

where we include an implicit integration over y, y' for every Einstein summation over a, b.

In Eq. (6.7) we have introduced the collective mode terms

$$\Pi_a^\mu\left(x,x'\right) \equiv \delta\Delta_a^{\mathrm{mf}}\left[A\right]\left(x'\right)/\delta A_\mu\left(x\right)\Big|_{A\to 0}. \tag{6.8}$$

These terms explicitly restore gauge invariance beyond the "bubble" response kernel $K_{0,\mathrm{mf}}^{\mu\nu}$ [Boyack et al., 2016, Guo et al., 2013a, Kosztin et al., 2000, Kulik et al., 1981]. In the saddle-point response, the third line in Eq. (6.5) vanishes.

Using the revised saddle-point condition, along with the above definitions, the collective modes are $\Pi_a^\mu = -\left[Q_{\mathrm{mf}}^{ab}\right]^{-1} Q_{\mathrm{mf}}^{b\mu}$ where the inverse $\left[Q_{\mathrm{mf}}^{ab}\right]^{-1}$ is taken over both position and Nambu indices [see appendix (E.2)]. We emphasize these collective modes are associated with the mean-field level of approximation. After taking the $A_\mu \to 0$ limit, the momentum space response is

$$K_{\mathrm{mf}}^{\mu\nu}\left(q\right) = K_{0,\mathrm{mf}}^{\mu\nu}\left(q\right) - Q_{\mathrm{mf}}^{\mu a}\left(-q\right)\left[Q_{\mathrm{mf}}^{ab}\left(q\right)\right]^{-1} Q_{\mathrm{mf}}^{b\nu}\left(q\right). \tag{6.9}$$

This is the usual gauge-invariant response kernel in BCS theory [Kulik et al., 1981], which includes both amplitude and phase collective modes.

Importantly, the explicitly gauge-invariant response kernel $K_{\mathrm{mf}}^{\mu\nu}$ was obtained without including Gaussian fluctuations, which are usually invoked in the GRGF literature. In this way, *the self-consistent treatment of the gap in the presence of a vector potential restores gauge invariance at the mean-field level.* Because there are no accompanying bosonic degrees of freedom in the thermodynamics, the compressibility sum rule will be shown to be exactly satisfied using this method, in contrast to the more conventional path integral methodology.

6.4 Beyond saddle point

Often it is desirable to calculate the path integral beyond the saddle-point approximation. In order to do this, one changes variables from the HS field $\boldsymbol{\Delta}$ to a fluctuation $\boldsymbol{\eta} = (\eta_1, \eta_2)$ around the saddle-point solution defined through $\boldsymbol{\Delta} = \boldsymbol{\Delta}^{\mathrm{mf}}\left[A\right] + \boldsymbol{\eta}$. Note that, since $\boldsymbol{\eta}$ is a dynamical

variable, it does not have any dependence on A_μ. The full action is then expressed exactly as $S_{\rm HS}\left[\boldsymbol{\Delta}, A\right] = S_{\rm mf} + S_\eta$, where the action $S_\eta \equiv S_\eta\left[\boldsymbol{\Delta}^{\rm mf}\left[A\right], A, \boldsymbol{\eta}\right] = S_{\rm HS}\left[\boldsymbol{\Delta}^{\rm mf}\left[A\right] + \boldsymbol{\eta}, A\right] - S_{\rm HS}\left[\boldsymbol{\Delta}^{\rm mf}\left[A\right], A\right]$ is $\mathcal{O}\left(\eta^2\right)$ or higher, since any term linear in $\boldsymbol{\eta}$ vanishes by the saddle-point condition. This definition allows for the exact factorization of the partition function $\mathcal{Z}\left[A\right] = \mathcal{Z}_{\rm mf}\left[\boldsymbol{\Delta}^{\rm mf}\left[A\right], A\right]\mathcal{Z}_{\rm fl}\left[\boldsymbol{\Delta}^{\rm mf}\left[A\right], A\right]$, where

$$\mathcal{Z}_{\rm fl}\left[\boldsymbol{\Delta}^{\rm mf}\left[A\right], A\right] = \int \mathcal{D}\left[\boldsymbol{\eta}\right] e^{-S_\eta\left[\boldsymbol{\Delta}^{\rm mf}[A], A, \boldsymbol{\eta}\right]} \tag{6.10}$$

is the contribution due to fluctuations beyond mean field.

In calculations of response beyond saddle point, one uses Eq. (6.4) with an effective action $S_{\rm eff}\left[A\right] = -\ln \mathcal{Z}\left[A\right] = S_{\rm mf} + S_{\rm fl}$, and the fluctuation action $S_{\rm fl} = -\ln \mathcal{Z}_{\rm fl}\left[\boldsymbol{\Delta}^{\rm mf}\left[A\right], A\right]$ also depends on the self-consistent gap $\boldsymbol{\Delta}^{\rm mf}\left[A\right]$. The response kernel is linear in the action, so that $K^{\mu\nu} = K^{\mu\nu}_{\rm mf} + K^{\mu\nu}_{\rm fl}$, where the mean-field response is given in Eq. (6.9). The new contribution to the response, $K^{\mu\nu}_{\rm fl}$, has a form identical to Eq. (6.5), only with $S_{\rm mf}$ replaced by $S_{\rm fl}$. Note, however, that the collective mode terms Π^μ_a still arise from the mean-field self-consistent gap condition; these collective modes are always constructed from the $Q_{\rm mf}$ propagators, and not from an analogous $Q_{\rm fl}$.

This higher order fluctuation response again contains a "bubble" term, $K^{\mu\nu}_{0,{\rm fl}}$, which arises from bosonic fluctuations. On its own, $K^{\mu\nu}_{0,{\rm fl}}$ is not gauge invariant. Analogous to the saddle-point response, the collective modes Π^μ_a, along with the corresponding $Q_{\rm fl}$ response functions, are necessary to restore gauge invariance. To show that this arbitrary fluctuation theory is fully gauge invariant, one can verify that $\partial_\mu K^{\mu\nu}_{\rm fl} = 0$ is satisfied [see appendix (E.3)]. In this way, gauge invariance holds term by term in the expansion of the action beyond mean field. This method of calculating gauge-invariant response beyond BCS is a completely general and sum rule consistent method and is a central result of this chapter.

6.5 Compressibility sum rule

Thermodynamic quantities can be calculated from derivatives of the thermodynamic potential, $\Omega = -T \ln \mathcal{Z} = T S_{\text{eff}}$, which is the effective action up to the prefactor T. Since electromagnetic response functions also come from derivatives of the effective action, it is clear that there should be an intimate connection between the two. An important requirement for consistency between electrodynamics and thermodynamics is contained in the compressibility sum rule: $\partial n / \partial \mu = -K^{00}(0, \mathbf{q} \to 0)$ [Pines & Nozières, 1966].

A formal derivation of this sum rule, for the exact action, arises from twice invoking the identity $\int dx\, \delta \mathcal{G}_0^{-1} / \delta A_0(x) = -\partial \mathcal{G}_0^{-1} / \partial \mu$ on the partition function in Eq. (6.2). A more intuitive derivation of this sum rule follows from the fermionic path integral, before applying the HS transformation. The atom number is $n \equiv \left\langle \int dx\, \hat{n}(x) \right\rangle = -\partial \Omega / \partial \mu$, where $\hat{n}(x) = \sum_{s=\uparrow,\downarrow} \psi_s^\dagger(x) \psi_s(x)$ is the local fermion density operator. A second derivative gives $\partial n / \partial \mu = -\partial^2 \Omega / \partial \mu^2 = -\left\langle \left(\int dx\, \hat{n}(x) \right)^2 \right\rangle$. On the other hand, the small momentum limit of the density-density correlation function is $K^{00}(0, \mathbf{q} \to 0) = \int dx \int dx' K^{00}(x, x')$, where $K^{00}(x, x') = \left\langle \hat{n}(x)\, \hat{n}(x') \right\rangle$ follows from Eq. (6.4). It is straightforward to see this response function is just $K^{00}(0, \mathbf{q} \to 0) = -\partial n / \partial \mu$ as defined above. Therefore, *provided no approximations are made*, the compressibility sum rule is an exact consequence of the path integral approach.

When considering *only* thermodynamics, it is not necessary to keep track of the vector potential in the self-consistent solution, and S_{eff} can be calculated for $A_\mu = 0$ and $\mathbf{\Delta}^{\text{mf}}[0]$. When simultaneously considering electrodynamics and thermodynamics, however, it is important to calculate $S_{\text{eff}}[A]$ to the same level of approximation for both quantities. Due to the linear dependence of both electrodynamic and thermodynamic quantities on the effective action, any theory studying both quantities, which considers a *consistent* approximation scheme, will also satisfy the compressibility sum rule.

6.6 Gaussian fluctuations

An exact calculation of $\mathcal{Z}_{\rm fl}$ is difficult in general, and frequently it is treated at the Gaussian level in the literature. We similarly consider response at this level: fluctuations $\boldsymbol{\eta}$ about the saddle-point solution are assumed small and the fluctuation action is expanded to quadratic order: $S_\eta\left[\boldsymbol{\Delta}^{\rm mf}\left[A\right],A\right] \approx \frac{1}{2}\eta_a \widetilde{Q}^{ab}_{\rm mf}\eta_b$. The path integral can then be solved exactly; integration of the fluctuation field $\boldsymbol{\eta}$ gives an effective action $S^{(2)}_{\rm fl} = \frac{1}{2}{\rm Tr}\ln\left[\widetilde{Q}^{ab}_{\rm mf}\right]$ at the Gaussian level. We emphasize that in the calculation of the fluctuation response kernel, $K^{\mu\nu}_{\rm fl}$, the propagator $\widetilde{Q}^{ab}_{\rm mf} = \widetilde{Q}^{ab}_{\rm mf}\left[\boldsymbol{\Delta}^{\rm mf}\left[A\right],A\right]$ includes dependence on A_μ both explicitly, and through the mean-field solution. This is in contrast to previous literature which used the fluctuation propagator $Q^{ab}_{\rm mf}$.

It is clear that setting $A_\mu = 0$ will reproduce beyond-BCS thermodynamics found in the literature [Diener et al., 2008, Engelbrecht et al., 1997, He et al., 2015, Hu et al., 2006, Loktev et al., 2001, Taylor et al., 2007]. Our formalism can also recover the bosonic contributions to the superfluid density $\rho_s \sim K^{ii}\left(0,\mathbf{q}\to 0\right)$ found in Refs. [Fukushima et al., 2007, Taylor et al., 2006]. This calculation introduced a phase twist $\mathbf{Q}\to 0$, which is equivalent to our counterpart calculation after the replacement $A_\mu \to \mathbf{Q}$. Since ρ_s is a purely transverse quantity, this prior work did not need to include collective mode contributions emphasized in the present formalism. Our results thus reproduce and extend previous explorations of Gaussian fluctuations, now establishing consistency with the compressibility sum rule.

6.7 Amplitude and phase fluctuations

While not explicitly discussed, amplitude fluctuations of the gap were implicitly included in the compressibility sum rule arguments presented in this chapter. These are often ignored, although they have been introduced in the literature via an alternative parameterization of the gap, by writing $\Delta = \rho e^{i2\phi}$, where $\rho = |\Delta|$ and $2\phi = \arg\Delta$ are respectively the amplitude and phase of the order parameter. Including amplitude fluctuations by setting $\rho = \rho_0 + \delta\rho$ and integrating out both $\partial_\mu\phi$ and $\delta\rho$ fluctuations results in a different gauge-invariant formulation, but one which is

equivalent to the η fluctuation used above. It should be noted that while amplitude fluctuations result in a contribution to electrodynamic (and thermodynamic) response, phase fluctuations alone are sufficient to restore gauge invariance at both the mean-field and fluctuation levels. We note, however, that by neglecting amplitude fluctuations, the compressibility sum rule will be violated and this violation is apparent even at the mean-field level of strict BCS theory.

6.8 Conclusions

In this chapter we have presented a path integral formulation for superfluids and superconductors which: (1) allows for a consistent calculation of (gauge-invariant) electrodynamic and thermodynamic response at any desired level of approximation, and (2) gives the full gauge-invariant response kernel for beyond-mean-field physics. The consistency of our formulation is apparent in the compressibility sum rule which relates electrodynamics and thermodynamics. This sum rule is not satisfied at the BCS level in the path integral formalism if Gaussian fluctuations are invoked as in GRGF. A consistent treatment involves finding the saddle-point solution in the presence of a vector potential. Our way of introducing collective mode effects is closer in spirit to earlier self-consistency approaches [Ambegaokar & Kadanoff, 1961, Parks, 1969, Rickayzen, 1965] derived using strict BCS theory.

We emphasize an important physical implication of the current approach. Within the conventional path integral approach, Gaussian fluctuations are needed to arrive at gauge-invariant electrodynamics. One might posit that there ought to be fluctuation contributions to thermodynamics. Specifically, in a neutral superfluid these collective modes would seem to require power law contributions, say in the specific heat. We argue here, despite some controversy in the literature [Vollhardt & Wolfle, 2013, Yu et al., 2009], including these correction terms in strict BCS theory is unphysical, as they are inconsistent with the compressibility sum rule.

Within the present formalism the next level of approximation, involving Gaussian fluctuations, then emerges as a true beyond-BCS theory in which there are inter-related (by the compressibility sum rule) contributions to both thermodynamics and the electromagnetic response. This beyond-

BCS level of approximation provides a starting point for studying strongly correlated superfluids. It should be viewed as an alternative to the approach in the previous chapter which was based on a correlation self energy and the Ward-Takahashi identity [Boyack et al., 2016].

This approach provides a promising new route to bench marking beyond-BCS calculations derived from the path integral. There are indications from the superfluid density at the Gaussian level that possibly unphysical non-monotonic behavior arises [Fukushima et al., 2007]. These may also be present when comparing with density correlation functions measured in Bragg scattering experiments. Nevertheless it will be interesting to look at these higher level (Gaussian) corrections in a variety of physical contexts, including, for example, their role in topological [Goryo & Ishikawa, 1999, Lutchyn et al., 2008, Ojanen & Kitagawa, 2013] or disordered [Kamenev & Andreev, 1999] superfluids. Indeed, Ref. [He, 2016] recently considered electromagnetic response (in the density and spin channels) at the Gaussian level. Our more general framework includes these results at the Gaussian fluctuation level, where $S_{\rm fl}^{(2)} = \frac{1}{2}\mathrm{Tr}\ln\left[\widetilde{Q}_{\rm mf}^{ab}\right]$ presented above. Quite generally, the work in this chapter should be viewed as providing a new paradigm for exploring beyond-BCS physics using path integral techniques.

CHAPTER 7

COLLECTIVE MODE CONTRIBUTIONS TO THE MEISSNER EFFECT: FULDE-FERRELL AND PAIR-DENSITY WAVE SUPERFLUIDS

In this chapter we demonstrate the necessity of including the generally omitted collective mode contributions in calculations of the Meissner effect for non-uniform superconductors. We consider superconducting pairing with non-zero center-of-mass momentum, as is possibly relevant to high transition temperature cuprates, cold atoms, and color superconductors in quantum chromodynamics. For the concrete example of the Fulde-Ferrell phase we present a quantitative calculation of the superfluid density, showing the collective mode contributions are not only appreciable but that they derive from the amplitude mode of the order parameter. This latter mode is generally viewed as being invisible in conventional superconductors. However, our analysis shows that it is extremely important in pair-density-wave-type superconductors, where it destroys stable superfluidity well before the mean-field order parameter vanishes. The work in this chapter is published in Ref. [Boyack et al., 2017a].

7.1 Introduction

There is a large amount of interest in amplitude modes of superconductors, in large part stimulated by the excitement surrounding the discovery of the Higgs boson [Lykken & Spiropulu, 2013]. Nevertheless, there is a widespread belief that observing these modes, directly or indirectly, is particularly challenging [Parks, 1969, Pekker & Varma, 2015]. As a result they only infrequently appear in condensed matter physics [Anderson et al., 2016, Browne & Levin, 1983, Endres et al., 2012, Littlewood & Varma, 1981, Matsunaga et al., 2013, Pollet & Prokof'ev, 2012, Sherman et al., 2015]. In this chapter we show that in a class of very topical superconductors, collective mode effects associated with the amplitude of the order parameter play an essential role in the most fundamental quantity, the superfluid density tensor n_s^{ij}. The superconductors in question are those which have a "pair-density wave" order parameter. These are a large class of theoretical models

(awaiting firm experimental confirmation) associated with pairing of electrons at non-zero center-of-mass momentum $\mathbf{Q}$. Much attention has focused on these systems from the perspective of high temperature superconductivity (in condensed matter physics [Fradkin et al., 2015, Hamidian et al., 2016]) and color superconductors (in particle physics [Casalbuoni & Nardulli, 2004]).

For this class of superfluids, the collective mode contribution to the superfluid density has been largely ignored in previous literature [Samokhin, 2010, Yin et al., 2014], with the exception of the original calculation of the electromagnetic current by Larkin and Ovchinnikov [Larkin & Ovchinnikov, 1965]. Discussion of this effect can also be found in Ref. [Millis, 1987] for a different situation involving non s-wave superconductors. [1] In both cases, however, the sizes of the collective mode contributions were not accessible.

We provide two different, but related, derivations of the superfluid density for the tractable case of the Fulde-Ferrell (FF) superfluid [Fulde & Ferrell, 1964]. Importantly, this enables us to compute numerical values for the sizeable collective mode effects in n_s^{ij}. The first method is based on using the Ward-Takahashi identity in the Kubo formalism, while the second method is based on studying the equilibrium current. In both approaches particle number is manifestly conserved and gauge invariance is maintained. Through these approaches we find that amplitude collective modes drive the superfluid density (along the direction parallel to $\mathbf{Q}$) to zero at temperatures lower than those associated with the vanishing of the mean-field order parameter.

Before giving these more complete calculations, here we provide a general argument for the necessity of including collective mode effects in non-uniform superconductors. The origin of collective mode contributions to the Meissner effect [Larkin & Ovchinnikov, 1965, Millis, 1987] is due to the fact that, in the presence of a vector potential A^μ, the order parameter Δ will depend on A^μ through the gap (saddle-point) equation [Abrikosov et al., 1975, Anderson et al., 2016].

1. In Ref. [Millis, 1987] non s-wave superconductors with finite *relative* momentum pairing were studied, in contrast to the finite *center-of-mass* momentum pairing of interest in this chapter. For that particular case, Ref. [Millis, 1987] rigidly pinned the order parameter so that the phase mode was the only relevant collective mode. For the FF superfluid under discussion, it is the amplitude mode and not the phase mode which contributes to the superfluid density.

A series expansion of $\Delta[A]$, in powers of A^μ, is thus

$$\Delta[A] = \Delta^{(0)}[A=0] + \Delta^{(1)}[A] + \mathcal{O}(A^2). \tag{7.1}$$

Here $\Delta^{(0)}$ is the order parameter in the absence of A^μ and $\Delta^{(1)}$ is a correction linear in A^μ. It is this term which gives rise to the rarely discussed collective mode contributions to the superfluid density. Since $\Delta^{(1)}$ is a scalar quantity, it can depend on only scalar, linear functionals of A^μ. Therefore, in a uniform superfluid $\Delta^{(1)}$ is a functional of only $\nabla \cdot \mathbf{A}$. [2] Thus, if one chooses the ("transverse") gauge such that $\nabla \cdot \mathbf{A} = 0$, the collective mode contribution $\Delta^{(1)}$ vanishes identically [Abrikosov et al., 1975].

However, for a non-uniform system there are other scalar, linear functionals of A^μ. In particular, for a pair-density-wave superfluid with pairing vector $\mathbf{Q}$, $\Delta^{(1)}$ can depend on other scalar, linear quantities such as $\mathbf{A} \cdot \mathbf{Q}$. Hence, for this non-uniform superfluid, even in the gauge where $\nabla \cdot \mathbf{A} = 0$, $\Delta^{(1)}$ may still be non-zero. In principle, this allows for a collective mode contribution to the superfluid density. [For future use in the discussion below, we define $\Delta^{(1)} = \int dq\, \Pi^\mu(q) A_\mu(q)$ and $\Pi^\mu(q) = \left(\delta\Delta[A]/\delta A_\mu(q)\right)\big|_{A=0}$.] This argument emphasizes that, for any non-uniform superfluid with a pairing vector present, one must consider collective mode contributions. In particular, it also applies to a system where $\mathbf{Q}$ is *a priori* fixed, such as in a crystalline superconductor, where the rotational symmetry is explicitly broken. Due to the presence of a finite $\mathbf{Q}$ vector, here one would still need to consider the collective mode contributions to the superfluid density .

For concreteness we will illustrate these collective mode effects in the FF superfluid, where pairing at finite $\mathbf{Q}$ arises due to a spin (or mass) imbalance causing a Fermi surface mismatch between up and down spins. For simplicity we take the FF pairing vector to be $\mathbf{Q} = Q\hat{z}$. In the FF phase specifically, both a continuous rotational and global $\mathrm{U}(1)$ symmetry are spontaneously broken. Similarly discrete time-reversal symmetry is also spontaneously broken. However, gauge-invariant observables are translationally invariant [Radzihovsky, 2011]. Due to the underlying

2. In general, for a uniform superfluid $\Delta^{(1)}$ will be a functional of $\partial_\mu A^\mu$. For the superfluid density, however, only the vector component of A^μ is of interest.

rotational symmetry of the FF state, the superfluid density vanishes along the directions transverse to $\mathbf{Q}$. Hence $n_s^{xx} = n_s^{yy} = 0$, and thus only n_s^{zz} needs to be considered [Radzihovsky, 2011].

As has been posited [Fulde & Ferrell, 1964], and will be shown in more detail below, the superfluid density for the FF superfluid can be written as

$$\left.\frac{\partial j^z}{\partial Q}\right|_{\mu,h} = \frac{1}{2}\left(\frac{n_s^{zz}}{m}\right), \tag{7.2}$$

where $j^z(Q)$ is the equilibrium current. It is useful to express Eq. (7.2) in terms of the mean-field thermodynamic potential Ω, where $j^z(Q) = 2\left(\partial\Omega/\partial Q\right)|_{\mu,h,|\Delta|}$. The saddle-point condition determining the mean-field value of Q is then $j^z(Q) = 0$. Similarly, the saddle-point condition determining the mean-field value of Δ is $\left(\partial\Omega/\partial\Delta^*\right)|_{\mu,h,Q} = 0$. In terms of Ω, Eq. (7.2) becomes

$$\left.\frac{\partial j^z}{\partial Q}\right|_{\mu,h} = 2\left[\left.\frac{\partial^2\Omega}{\partial Q^2}\right|_{\mu,h,|\Delta|} - \left(\frac{\partial^2\Omega}{\partial|\Delta|\partial Q}\right)^2 \Big/ \left.\frac{\partial^2\Omega}{\partial|\Delta|^2}\right|_{\mu,h,Q}\right], \tag{7.3}$$

where the two saddle-point equations and the equality of mixed partial derivatives have been used.

Equation (7.3) indicates there are two contributions to the superfluid density. The first is the conventional "bubble" term (which is usually assumed to be sufficient) and the second represents the collective mode contribution required for gauge invariance. Importantly, a stability inequality for the FF superfluid based on the thermodynamic potential curvature [Chien et al., 2006, He et al., 2007a, Wang et al., 2017] is equivalent to requiring that both n_s^{zz}, as derived above, and $\left(\partial^2\Omega/\partial|\Delta|^2\right)\big|_{\mu,h,Q}$ are positive. It follows from the latter condition that for a stable FF superfluid the collective mode contribution always acts to reduce the overall size of the superfluid density. These arguments, however, still do not indicate how large the magnitude of this effect is.

In this chapter the collective mode contribution will be found to be appreciable; this underlines the inadequacy of including only the so-called bubble term [Samokhin, 2010, Yin et al., 2014]. Equally important is the nature of these collective mode corrections. For the FF superfluid we will show they arise from the *amplitude* mode of the order parameter. This mode is thought to be rather invisible in conventional superconductors [Parks, 1969, Pekker & Varma, 2015]. Nevertheless, we

include the amplitude collective mode in our derivation of the full gauge-invariant electromagnetic (EM) response, and we also show that it has a significant contribution to the superfluid density.

7.2 Theoretical formalism

7.2.1 Mean-field formalism

The FF mean-field Hamiltonian, in the $\psi_{\mathbf{k}}^{\mathsf{T}} = (c_{\mathbf{k},\uparrow}, c_{-\mathbf{k}+\mathbf{Q},\downarrow}^{\dagger})$ basis, is $H_{\mathrm{FF}} = \sum_{\mathbf{k}} \psi_{\mathbf{k}}^{\dagger} \mathcal{H}_{\mathrm{FF}} \psi_{\mathbf{k}}$, where [Chen et al., 2007]

$$\mathcal{H}_{\mathrm{FF}} = \begin{pmatrix} \xi_{\mathbf{k},\uparrow} & -\Delta \\ -\Delta^{*} & -\xi_{\mathbf{k}-\mathbf{Q},\downarrow} \end{pmatrix}. \tag{7.4}$$

Here an irrelevant constant $-\sum_{\mathbf{k}} \xi_{\mathbf{k}-\mathbf{Q},\downarrow}$ has been ignored. The notation is as follows: the dispersion relation is defined by $\xi_{\mathbf{k},\sigma} = \mathbf{k}^2/2m - \mu_\sigma$, where μ_σ is the fermionic chemical potential for a species with spin $\sigma =\uparrow,\downarrow$, m is the fermion mass, and Δ denotes an s-wave pairing gap. It is useful to define $\mu = \frac{1}{2}\left(\mu_\uparrow + \mu_\downarrow\right)$ and $h = \frac{1}{2}\left(\mu_\uparrow - \mu_\downarrow\right)$. The dispersion relations are then written compactly as $\xi_{\mathbf{kQ}} = (1/2m)[\mathbf{k}^2 + (\mathbf{Q}/2)^2] - \mu$, $E_{\mathbf{kQ}}^2 = \xi_{\mathbf{kQ}}^2 + |\Delta|^2$, $h_{\mathbf{kQ}} = h - \mathbf{k}\cdot\mathbf{Q}/2m$. Throughout this chapter $\hbar = k_B = c = 1$.

The inverse Nambu Green's function is then $\mathcal{G}^{-1} = i\omega_n - \mathcal{H}_{\mathrm{FF}}$, where $i\omega_n$ is a fermionic Matsubara frequency. The inverse bare Green's function is defined by $G_{0,\sigma}^{-1}(k) = i\omega_n - \xi_{\mathbf{k}}$. Thus, the off-diagonal Gorkov function is $\mathcal{G}_{12}(k) = \Delta G_{0,\downarrow}(-k+Q)G_\uparrow(k)$, where the (spin-up) Green's function is $G_\uparrow(k) = \mathcal{G}_{11}(k)$. Note that Greek indices denote spacetime coordinates: $x^\mu = (t,x,y,z)$; whereas Roman indices denote spatial coordinates: $x^i = (x,y,z)$. Here $Q^\mu = (0,\mathbf{Q})$. Explicit calculation then gives the full Green's function which has appeared in the literature [Chen et al., 2007, Yin et al., 2014]. Indeed, from Dyson's equation, $G_\sigma^{-1}(k) = G_{0,\sigma}^{-1}(k) - \Sigma_\sigma(k)$, the self energy is $\Sigma_\sigma(k) = -|\Delta|^2 G_{0,\bar{\sigma}}(-k+Q)$. [For convenience later, we define $\widetilde{k}_{\pm}^{\mu} \equiv k^\mu \pm Q^\mu/2$.]

7.2.2 *Electromagnetic response and Ward-Takahashi identity*

We now study the EM response of the FF superfluid and consider the superfluid density for the case of a neutral superfluid. Our observation that collective modes are necessary to ensure a gauge-invariant calculation of the superfluid density should apply to a charged system as well, but we avoid here the complexities associated with the Coulomb interaction. We apply linear response theory, where a fictitious vector potential A^μ is applied to the system. The resulting EM current is $j^\mu(q) = K^{\mu\nu}(q)A_\nu(q)$, where $K^{\mu\nu}(q)$ is the EM response kernel. The response kernel can also be expressed as $K^{\mu\nu}(q) = P^{\mu\nu}(q) + (n/m)\delta^{\mu\nu}(1-\delta_{\mu 0})$ (with μ and ν not summed over) where the EM response functions are denoted by $P^{\mu\nu}(q)$. In the Kubo formalism the EM response functions for a superfluid are

$$P^{\mu\nu}(q) = \sum_\sigma \sum_k G_\sigma(k_+)\Gamma^\mu_\sigma(k_+,k_-)G_\sigma(k_-)\gamma^\nu_\sigma(k_-,k_+), \tag{7.5}$$

where $q^\mu = (i\Omega_m, \mathbf{q})$, with $i\Omega_m$ a bosonic Matsubara frequency.

The important quantity $\Gamma^\mu(k_+,k_-)$ denotes the full EM vertex, where the incoming (outgoing) momentum is k_+ (k_-), with $k^\mu_\pm \equiv k^\mu \pm q^\mu/2$. To determine the full vertex $\Gamma^\mu(k_+,k_-)$, we apply the Ward-Takahashi identity (WTI) [Ryder, 1996]:

$$\begin{aligned} q_\mu\Gamma^\mu_\sigma(k_+,k_-) &= G^{-1}_\sigma(k_+) - G^{-1}_\sigma(k_-), \\ &= q_\mu\gamma^\mu_\sigma(k_+,k_-) + \Sigma_\sigma(k_-) - \Sigma_\sigma(k_+). \end{aligned} \tag{7.6}$$

This is an exact relation in quantum field theory relating the single particle Green's function to the full vertex. It is a gauge-invariant statement and here it reflects the underlying global $\mathrm{U}(1)$ symmetry. Similarly, the bare WTI, $q_\mu\gamma^\mu_\sigma(k_+,k_-) = G^{-1}_{0,\sigma}(k_+) - G^{-1}_{0,\sigma}(k_-)$, is satisfied by the bare vertex $\gamma^\mu_\sigma(k_+,k_-) = (1, \mathbf{k}/m)$.

Satisfying the WTI ensures conservation of particle number (or charge in the charged superfluid case). The particle number can be written in terms of the single particle Green's function as $n = \sum_\sigma \sum_k G_\sigma(k)$, where $\sum_k \equiv \beta^{-1} \sum_{i\omega_n} \sum_{\mathbf{k}}$ with β being inverse temperature. In the limit $q^\mu \to 0$, the WTI reduces to the Ward identity: $\Gamma^\mu_\sigma(k,k) = \gamma^\mu_\sigma(k,k) - [\partial\Sigma_\sigma(k)/\partial k_\mu]$. The second term in this equation diagrammatically represents a vertex insertion in the self energy. This relation then importantly shows the full vertex can be obtained by performing all possible vertex insertions in the full Green's function [Nambu, 1960, Ryder, 1996].

For the FF self energy given in section (7.2.1), there are three possible positions where the bare vertex can be inserted: the bare Green's function and the two gaps Δ and Δ^*. Inserting the bare vertex in the location of the two gaps leads to the collective mode vertices, discussed in more detail in the next section, which are of crucial importance to ensure gauge invariance.

7.2.3 Collective mode vertices

This section discusses the properties of the collective mode vertices and how they contribute to the superfluid density. By inserting the bare vertex in the two gaps (Δ, Δ^*) one obtains the collective mode vertices $\Pi^\mu(q)$ and $\bar{\Pi}^\mu(q)$, respectively. Appendix (F.3) presents details showing how $\Pi^\mu(q)$ and $\bar{\Pi}^\mu(q)$ are obtained by performing these vertex insertions in the gap equation, which can be written as $\Delta/g \ = \Delta \sum_\sigma \sum_k G_{0,\downarrow}(-k+Q) G_\uparrow(k) = \sum_\sigma \sum_k \mathcal{G}_{12}(\widetilde{k})$ [Chen et al., 2007].

Due to the spontaneously broken global $\mathrm{U}(1)$ symmetry, the gaps Δ, Δ^* are themselves not gauge invariant. There are, however, two natural gauge-invariant combinations of the collective mode vertices; these appear as $\left(\Delta^*\Pi^\mu - \Delta\bar{\Pi}^\mu\right)$ and $\left(\Delta^*\Pi^\mu + \Delta\bar{\Pi}^\mu\right)$. In order to associate these combinations with the appropriate phase or amplitude modes of the order parameter, we contract these quantities with q_μ. In appendix (F.3) it is proved that, for $q_\mu \neq 0$, the collective mode vertices obey $q_\mu \Pi^\mu(q) = 2\Delta, q_\mu \bar{\Pi}^\mu(q) = -2\Delta^*$. These relations then lead to

$$q_\mu \left(\Delta^*\Pi^\mu - \Delta\bar{\Pi}^\mu\right) = 4\left|\Delta\right|^2, \tag{7.7}$$

$$q_\mu \left(\Delta^*\Pi^\mu + \Delta\bar{\Pi}^\mu\right) = 0. \tag{7.8}$$

The right hand sides of these expressions are gauge-invariant quantities, and thus so too are the expressions in parentheses, as claimed.

The limit $q_\mu \to 0$ of these contractions is of particular interest. For Eq. (7.7) the right hand side is finite, non-zero, and independent of q_μ; this applies to the left hand side as well. As $q_\mu \to 0$, it follows that the quantity in parentheses must become singular in this limit. This indicates it has a zero momentum pole; we can conclude that this is to be associated with the Nambu-Goldstone boson which restores the global $\mathrm{U}(1)$ symmetry. Since the phase mode of the order parameter is responsible for restoring gauge invariance, it follows that $\left(\Delta^* \Pi^\mu - \Delta \bar{\Pi}^\mu\right)$ corresponds to the phase mode of the order parameter.

On the other hand, for Eq. (7.8) the right hand side is zero and independent of q_μ; this applies to the left hand side as well. As $q_\mu \to 0$, it follows that the quantity in parentheses must be non-singular in this limit. This indicates the quantity in parentheses does not have a zero momentum pole. It follows that $\left(\Delta^* \Pi^\mu + \Delta \bar{\Pi}^\mu\right)$ corresponds to the amplitude mode of the order parameter.

The next section studies the superfluid density where we find that $\left(\Delta^* \Pi^z + \Delta \bar{\Pi}^z\right)$ and not $\left(\Delta^* \Pi^z - \Delta \bar{\Pi}^z\right)$ contributes. Thus the phase mode, while contained within the individual Π^μ and $\bar{\Pi}^\mu$ expressions, does not directly contribute to the superfluid density. [3]

We end by noting that Δ is a function of the FF pairing vector Q, and by differentiating the gap equation with respect to Q (at fixed μ and h) one can obtain $\left(\partial |\Delta|^2 / \partial Q\right)\big|_{\mu,h}$. An explicit calculation then gives the following important identity, for $\Delta \neq 0$, which relates in a more transparent way to the amplitude mode:

$$\Delta^* \Pi^z(0) + \Delta \bar{\Pi}^z(0) = P_0^z / M_0 = 2 \left(\partial |\Delta|^2 / \partial Q\right)\Big|_{\mu,h} . \tag{7.9}$$

3. It is important to note that, while phase fluctuations alone are sufficient to restore gauge invariance they are not necessary [Anderson et al., 2016]. Amplitude fluctuations must also be considered to derive the full gauge-invariant response. The $\Pi^\mu, \bar{\Pi}^\mu$ collective mode vertices contain both phase and amplitude fluctuations of the order parameters Δ, Δ^*; however, it is found that for the FF superfluid density only the gauge-invariant combination $\Delta^* \Pi^z(0) + \Delta \bar{\Pi}^z(0)$ contributes. The superfluid density is a zero momentum response and thus the gapped nature of the amplitude modes is not of crucial importance. In particular, for the FF superfluid, Q/k_F is an important scale for the size of the contribution of the amplitude modes to the superfluid density. In section (7.4) it is found that this effect can be appreciable.

The order of limits in which frequency and momentum are taken to zero is important; frequency $i\Omega_m$ and q^z are set to zero, and then $q^x, q^y \to 0$. In the following section this will be clarified. The quantities P_0^z and M_0 are generalized three-particle and four-particle Green's functions, respectively, which are defined in the next section. The generalized Green's functions in Eq. (7.9) also appear in a similar form in the work of Larkin and Ovchinnikov [Larkin & Ovchinnikov, 1965] and Millis [Millis, 1987]. Finally, note that when $Q = 0$, $P_0^z = 0$, and thus this collective mode term does not contribute for a uniform superfluid. The size of the amplitude mode contribution is thus set (in part) by Q/k_F. In principle this allows for a significant collective mode contribution, as will be discussed further in section (7.4).

7.3 Superfluid density

7.3.1 Superfluid density derivation via Kubo formula

In this section we use the Kubo formula and Eq. (7.5) to derive the superfluid density tensor:

$$(n_s^{ij}/m) = (n/m)\delta^{ij} + P^{ij}(\omega = 0, \mathbf{q} \to 0). \tag{7.10}$$

Note that, the order of limits in the above expression is crucial. To compute n_s^{ij}, first set $\omega = q^i = q^j = 0$, then take $q^k \to 0$, where $k \neq i, j$. Collective modes are contained within the second term.

Evaluating this expression we find

$$\left(\frac{n_s^{ij}}{m}\right) = \sum_{\mathbf{k}} \frac{|\Delta|^2}{E_{\mathbf{kQ}}^2}\left(\frac{X_{\mathbf{k}}}{E_{\mathbf{kQ}}} - \beta Y_{\mathbf{k}}\right)(\widetilde{k}_-^i/m)(\widetilde{k}_+^j/m) - \delta^{iz}\delta^{jz}(P_0^z)^2/M_0, \tag{7.11}$$

where we define $X_{\mathbf{k}} \equiv D^{-1}\sinh(\beta E_{\mathbf{kQ}})$, and $Y_{\mathbf{k}} \equiv D^{-2}\left[1 + \cosh(\beta E_{\mathbf{kQ}})\cosh(\beta h_{\mathbf{kQ}})\right]$ with $D \equiv \cosh(\beta E_{\mathbf{kQ}}) + \cosh(\beta h_{\mathbf{kQ}})$.

The first term in Eq. (7.11) represents the usual [Samokhin, 2010, Yin et al., 2014] "bubble" contribution, due to bubble terms in both $(n/m)\delta^{ij}$ and $P^{ij}(0)$. The second term represents the collective mode contribution arising solely from $P^{ij}(0)$. As an important check, we

note that Eq. (7.11) is identical to the superfluid density obtained from Eq. (7.2) and Eq. (7.3). Explicit calculation shows that the bubble term is $4\left(\partial^2\Omega/\partial Q^2\right)\big|_{\mu,h,|\Delta|}$ and $(\partial^2\Omega/\partial|\Delta|\partial Q) = -|\Delta|P_0^z$, $(\partial^2\Omega/\partial|\Delta|^2)\big|_{\mu,h,Q} = 4|\Delta|^2 M_0$, where the mean-field thermodynamic potential [Wang et al., 2017, Yin et al., 2014] is

$$\Omega = |\Delta|^2/g - \beta^{-1}\sum_{\mathbf{k}}\left\{\log[2\cosh(\beta E_{\mathbf{kQ}}) + 2\cosh(\beta h_{\mathbf{kQ}})] - \beta\xi_{\mathbf{kQ}}\right\}. \tag{7.12}$$

Note that the collective mode contribution is only along the direction of the FF pairing vector, in agreement with the general arguments presented earlier. Direct calculation shows that n_s^{ij} is diagonal, with $n_s^{xx} = n_s^{yy} = 0$, as required by symmetry.

7.3.2 Superfluid density derivation via equilibrium current

A verification of this Kubo analysis and the collective mode contributions can be made in a slightly simpler fashion. Here we derive the superfluid density in the direction along the FF pairing vector using only the equilibrium current and its partial derivative with respect to Q. The equilibrium current in the z-direction is $j^z(Q) = \sum_\sigma \sum_k (\widetilde{k}_+^z/m) G_\sigma(\widetilde{k})$. This expression follows from $j^z = 2\left(\partial\Omega/\partial Q\right)|_{\mu,h,|\Delta|}$. By symmetry the mean-field currents in the other directions vanish: $j^x = j^y = 0$.

In what follows it will be important to fix μ and h to their mean-field values, and to consider the Q-dependence of only the gap: $\Delta(Q)$. The following lemma, whose proof is given in appendix (F.5.1), will also be required: $\left(\partial G_\sigma^{-1}(\widetilde{k}_+)/\partial Q\right)\Big|_{\mu,h} = -(1/2)\Gamma_\sigma^z(\widetilde{k}_+, \widetilde{k}_+)$. The partial derivative of j^z can now be computed. Using the number equation $n = \sum_\sigma \sum_k G_\sigma(k)$, along with the aforementioned lemma, the partial derivative of j^z is then $(\partial j^z/\partial Q)|_{\mu,h} = (n/2m) - \sum_\sigma \sum_k (\widetilde{k}_+^z/m) G_\sigma^2(\widetilde{k})\left(\partial G_\sigma^{-1}(\widetilde{k}_+)/\partial Q\right)\Big|_{\mu,h} = (n_s^{zz}/2m)$. Note that the above expression, which reproduces Eq. (7.2) and Eq. (7.11), includes collective mode contributions arising through $\Gamma^z(\widetilde{k}_+, \widetilde{k}_+)$.

7.4 Numerical results

We now illustrate numerically the regime of stability of the FF phase. First, we require that the superfluid density n_s^{zz} as computed in the theory outlined above is positive, and secondly, that the state of interest is a minimum of the thermodynamic potential. These conditions correspond to: $n_s^{zz} > 0$ and $(\partial^2\Omega/\partial|\Delta|^2)\big|_{\mu,h,Q} > 0$. Although derived differently, these criteria coincide with results in the recent literature [Wang et al., 2017]. Importantly, they are a useful way to characterize the various temperature regimes in mean-field FF superfluid systems. We associate the critical temperature T_c^{FF} with the point at which either one of these stability conditions fails. Additionally, we associate the temperature T_Q as the temperature at which the FF pairing vector Q vanishes. Finally, T_Δ represents the temperature at which the mean-field pairing gap vanishes.

For the specific region of the phase diagram studied, our numerical calculations show that there are three temperature regimes of interest: (i) $0 \leq T < T_c^{FF}$ is the regime where a stable FF phase exists: both $n_s^{zz} > 0$ and $(\partial^2\Omega/\partial|\Delta|^2)\big|_{\mu,h,Q} > 0$. (ii) $T_c^{FF} \leq T < T_Q$ is the regime where an unstable FF phase exists. Either one or the other (or both) of the stability conditions fails; that is $n_s^{zz} < 0$ or $(\partial^2\Omega/\partial|\Delta|^2)\big|_{\mu,h,Q} < 0$. (iii) $T_Q < T < T_\Delta$ is the regime where $\Delta \neq 0$, but $Q = 0$. This corresponds to the Sarma phase. Since $Q = 0$ in this regime, there is no collective mode contribution to the superfluid density, and moreover $n_s^{zz} = n_s^{xx} = n_s^{yy} > 0$.

Figure (7.1) encapsulates the important point that collective modes of the order parameter substantially reduce the region where there is a stable FF phase. In Fig. 7.1(a) we plot the superfluid density with collective mode effects (blue curve) as a function of temperature for the case where polarization $p = 0.75$ and interaction strength (in terms of the scattering amplitude) $1/k_F a = 0$. Similarly, Fig. 7.1(b) plots the superfluid density with collective mode effects (blue curve) for a more BCS-like case with $p = 0.4$ and $1/k_F a = -0.5$. The red curves in Fig. (7.1) denote the bubble contribution to the superfluid density which is historically [Samokhin, 2010, Yin et al., 2014] all that is considered. The green curves plot the transverse superfluid density. As required by symmetry, $n_s^{xx} = 0$ for all $T < T_Q$ for which the FF pairing vector Q persists.

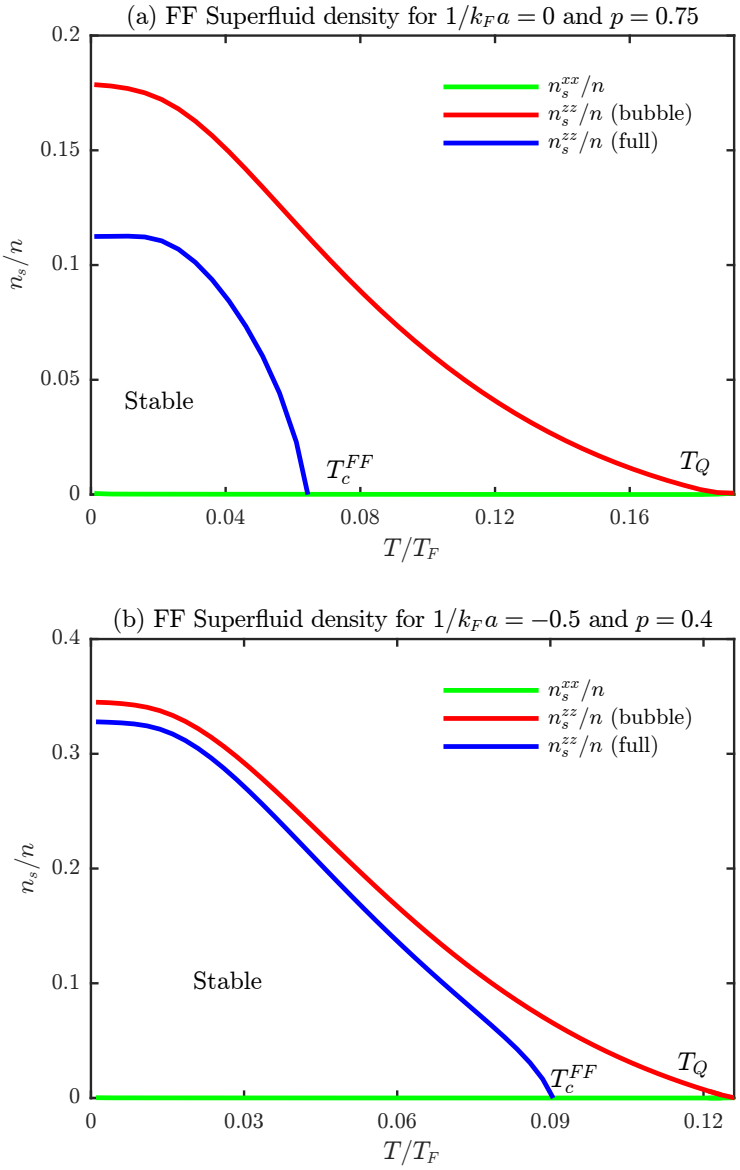

Figure 7.1: Superfluid density as a function of temperature for the FF phase (a) at unitarity $(1/k_Fa = 0)$ and with polarization $p = (n_\uparrow - n_\downarrow)/n$ set to $p = 0.75$, (b) in the near-BCS regime $(1/k_Fa = -0.5)$ with polarization $p = 0.4$. The blue curves plot the full expression for n_s^{zz}/n, given in Eq. (7.11), while the red curves plot the bubble contribution alone, given in the first term of Eq. (7.11). The green curves plot n_s^{xx}/n; in this case there are no collective modes and so the bubble and full expressions are equivalent. In agreement with symmetry considerations, for all $T < T_Q$, $n_s^{xx}/n = 0$.

In Fig. 7.1(a) we identify $T_c^{FF}/T_F \sim 0.06 - 0.065$, in rough agreement with Ref. [Wang et al., 2017]. Additionally, $T_Q \sim 0.2T_F$, and $T_\Delta \sim 0.24T_F$ [not shown in Fig. 7.1(a)]. Even though this plot is in the strong interaction regime, for quantitative purposes, strict mean-field parameters are used in this plot. It should be noted that the effects of the collective modes are quite appreciable in this plot. This follows because the bubble term is proportional to $(\Delta/E_F)^2$, whereas the collective mode term is proportional to $(Q/k_F)^2$. (Note though the integrands in both expressions are somewhat different.) Near zero temperature, with $p = 0.75$ and $1/k_F a = 0$, $\Delta/E_F \sim 0.16$ whereas $Q/k_F \sim 0.71$. Thus qualitatively the collective mode contribution is expected to be an important contribution in this regime.

One can determine from Fig. 7.1(b) that the highest temperature for which the FF superfluid is stable is given by $T_c^{FF}/T_F \sim 0.09 - 0.095$, (in rough agreement with Ref. [He et al., 2007a]). The other temperature scales of interest are roughly found to be $T_Q \sim 0.13T_F$, and $T_\Delta \sim 0.17T_F$. In this plot the effects of the collective modes are not as appreciable. Near zero temperature, with $p = 0.4$ and $1/k_F a = -0.5$, we find $\Delta/E_F \sim 0.13$ whereas $Q/k_F \sim 0.38$, so that the collective mode contribution is still expected to be appreciable, albeit not as large as exhibited in Fig. 7.1(a).

For numerical checks on our results we have verified that, in the stable regime, our mean-field solutions are global minima of the thermodynamic potential [Radzihovsky & Sheehy, 2010] and the blue curve computed via Eq. (7.11) is numerically equivalent to that computed via the equilibrium current using Eq. (7.2).

7.5 Conclusions

In this chapter we have computed the superfluid density tensor n_s^{ij} for the FF superfluid phase. Importantly, we have shown (using multiple, distinct theoretical frameworks) that widely neglected collective (amplitude) mode contributions cannot be ignored. In general they will affect n_s^{ij} for the broad class of $\mathbf{Q} \neq 0$ pair-density wave superconductors. Indeed, while Fig. (7.1) was obtained using the specific microscopic approach of Fulde and Ferrell, we believe its qualitative features (except for the behavior of the transverse superfluid density) are more generic.

In the original paper by Larkin and Ovchinnikov [Larkin & Ovchinnikov, 1965] the authors addressed the superfluid density of pair-density-wave phases; however, they used a small Δ expansion, necessarily valid near T_Δ. Note that our numerical results show this may be well removed from the stable FF regime.

Given the intense interest in condensed matter observations of a Higgs mode, one can inquire about the relation between the amplitude mode evident in pair-density wave superconductors and the Higgs mode in condensed matter [Anderson et al., 2016, Browne & Levin, 1983, Endres et al., 2012, Littlewood & Varma, 1981, Matsunaga et al., 2013, Sherman et al., 2015, Soto-Garrido et al., 2017]. The Higgs mechanism is associated with a charged system, where the Nambu-Goldstone mode is gapped out due to the Englert-Brout-Higgs-Guralnik-Hagen-Kibble mechanism. In the present theory we argue that the general observation of amplitude modes affecting the superfluid density applies, even though we have implemented the calculations for the neutral case. Moreover, in the present theory we incorporate the effects of the amplitude mode only at zero frequency and zero wave number so that the amplitude mode is not observed as a collective resonance.

Recently, the "Higgs" mode in FF and other pair-density-wave superfluids was addressed in Ref. [Soto-Garrido et al., 2017]. However, as in the present work, the authors focused on neutral systems. Their work addresses the finite frequency behavior of the amplitude mode in these systems. In our formalism, this mode can be obtained from the finite frequency branch cut in $\Pi^\mu, \bar{\Pi}^\mu$, which can be found from the analytic expressions given for these quantities in appendix (F.3). In summary, in this chapter we have ascertained that the existence of collective modes has important consequences for readily accessible physical quantities in FF superfluids, and more generally in pair-density-wave superconductors.

CHAPTER 8

CONCLUSIONS

Exotic superfluids and superconductors have numerous experimental and theoretical applications within condensed matter physics. In order to gain better understanding of these systems, both experiments and theory play an equally important role. Many experimental studies, however, focus on single-particle properties. On the other hand, it is the electromagnetic response which is at the heart of superfluidity. The distinction between pairing in the normal phase and superfluidity in the ordered phase is an inherent feature of many two-particle properties of superfluids. This is because the ordered phase introduces collective excitations, which often have a non-trivial contribution to the response. The fundamental questions addressed throughout this thesis are then: (1) For strongly correlated Fermi superfluids, how does one compute the superfluid response in a manner respecting all the necessary consistency requirements? (2) What are the quantitative implications of these response functions and how can they be experimentally probed?

This thesis focuses on studying exact electromagnetic response in strongly correlated Fermi superfluids, in both the non-condensed and condensed phases. A central challenge involved in studying electromagnetic response is to ensure that all the appropriate sum rules are satisfied. In particular, ensuring gauge invariance in superfluids and superconductors has been of crucial importance, right from the early days of BCS theory. In this thesis a diagrammatic method has been utilized to derive gauge-invariant response in Fermi superfluids, and thus answer question (1) posed at the beginning of this chapter. In each system considered important experimental signatures have been obtained, answering question (2) above. We discuss these in more detail individually.

The diagrammatic method was based on satisfying the Ward-Takahashi identity. This identity is well known in quantum electrodynamics, and satisfying it ensures gauge-invariant response. It is an exact relation, holds to all orders of perturbation theory, and provides an important connection between the many-body Green's function and the full electromagnetic vertex. This connection then relates single-particle response (quantities dependent on the Green's function) and two-particle response (quantities dependent on the full vertex). In general, this identity leads to a complicated

integral equation for the full vertex which is not amenable to an exact solution. What made the use of this identity tractable is the fact that all the self energies considered in this thesis are of the mean-field form. That is, the self energy contains only bare or partially-dressed Green's functions, and not the full Green's function itself. From the given form of the self energy, there is then a well-defined procedure to obtain the full vertex and thus the gauge-invariant many-body response. We applied this identity to several strongly correlated Fermi superfluids of interest.

A second method, based on the fermionic path integral, was also investigated. This method, however, is of very restricted utility in that only mean-field or Gaussian fluctuations are analytically tractable. In this approach one starts with the Hubbard-Stratonovich action for a Fermi superfluid. The mean-field equations are then derived by imposing the saddle-point condition on the action. What is crucial in this method is that when one considers the electromagnetic response, one must perform the saddle-point approximation in the presence of the non-zero vector potential. This gives rise to collective modes which restore gauge invariance. A crucial aspect to this approach is that, in contrast to other approaches in the literature, it obeys the compressibility sum rule. Hence, both electrodynamics and thermodynamics can be treated on an equal footing and respect all sum rules.

In chapters (2-3) Rashba spin-orbit coupled Fermi superfluids with intrinsic pairing were studied in the normal phase, in the absence and presence of a magnetic field, respectively. It was found that the Ward-Takahashi identity can be applied to derive the density and current response functions. However, the density response is largely unaffected by spin-orbit coupling due to the weight of the f-sum rule being independent of the spin-orbit coupling strength. We also derived spin correlation functions in the presence of spin-orbit coupling. For this case the Ward-Takahashi identity is not applicable, due to spin no longer being conserved. However, by studying the Heisenberg equations of motion, we were able to derive exact spin sum rules. We proved analytically that our spin correlation functions satisfy these sum rules, verifying their validity. From these spin correlation functions we found experimental signatures of observing the topological phase transition in these systems. The topological transition appears in the spin response as a recombination of two peaks, which are separate in the trivial phase

In chapter (4) several different models of the cuprate pseudogap phase were studied. Our primary focus was on a recent Amperean-pairing theory, which includes both charge ordering and pairing. The self-energies considered are of the mean-field form, and in the particular case of Amperean pairing the self energy is a complicated continued fraction. These mean-field-like self energies allowed the Ward-Takahashi identity to be utilized to derive the gauge-invariant response. The exact gauge-invariant density response was obtained, and several distinguishing features between Amperean-pairing versus d-wave and YRZ theories were established. The absence of a spin gap in the Amperean-pairing scenario is an experimentally verifiable prediction distinguishing it from these other theories.

In chapter (5) a diagrammatic formalism for studying the exact response functions, in both the condensed and non-condensed phases, of a (neutral) Fermi superfluid was outlined. This formalism was based on a self-consistent gap equation and a mean-field-like self energy which included strong correlation effects. By utilizing both the Ward-Takahashi identity and the diagrammatic form of the gap equation, a gauge-invariant framework for deriving the collective modes was established. The method involved performing all possible vertex insertions in both the self energy and the gap. This led to self-consistent equations for the collective modes, which ensures the Ward-Takahashi identity is satisfied. In particular, it was possible to simultaneously study several different theories of strongly correlated Fermi superfluids, from the YRZ theory to models of BCS-BEC crossover.

In chapter (6) an alternative approach to studying Fermi superfluids based on the path integral was studied. This approach is of restricted applicability due to the inability to compute the functional integral in all but the simplest (mean-field and Gaussian) cases. It was shown in chapter (5) that the conventional method of applying the path integral violates the compressibility sum-rule. Chapter (6) provides a reformulation of the path integral method, which is both gauge invariant and satisfies the compressibility sum rule. The key insight was to apply the saddle-point condition in the presence of a non-zero vector potential. In this way, collective modes arise due to the functional dependence of the gap on the vector potential. At all levels of approximation, the path integral was shown to be both gauge invariant and consistent with the compressibility sum rule.

Finally, in chapter (7) the electrodynamics of the Fulde-Ferrell (FF) superfluid was investigated. We utilized our diagrammatic method of obtaining gauge-invariant response from chapter (5) to study the more complicated FF system, which involves pairing at finite center-of-mass momentum. This diagrammatic approach enabled the collective modes to be obtained, and the full gauge-invariant response was determined also. Of particular interest is the fact that the amplitude collective mode contributes to the superfluid density (along the direction of pairing) and acts to reduce the superfluid density before the mean-field order parameter vanishes. Two distinct derivations of the superfluid density were provided, one based on the Kubo formula and the other based on the equilibrium current. It was found that recent stability criteria for FF superfluids can be interpreted in terms of the positivity of both the superfluid density and another thermodynamic potential derivative. Our calculation provides the first gauge-invariant calculation of the FF superfluid density, without any approximations on the size of the order parameter.

In summary, we showed how to implement exact diagrammatic identities to the study of strongly correlated Fermi superfluids. We have implemented this diagrammatic method in several systems: spin-orbit coupled Fermi superfluids, strongly correlated superfluids, and Fulde-Ferrell superfluids. Given that one of the central challenges in superfluids and superconductors is ensuring gauge invariance, while simultaneously incorporating the appropriate collective modes, this diagrammatic framework represents a central achievement of this thesis. We also showed how to apply the path integral method in a manner respecting gauge invariance and the compressibility sum rule. The crucial aspect being that gauge invariance is restored due to the functional dependence of the gap on the vector potential. These diagrammatic and functional integral methods represent very general and modern methods of studying Fermi superfluids, and there application in this thesis provides a framework for extending these methods to other (and possibly more complicated) systems of interest.

APPENDIX A

SIGNATURES OF PAIRING AND SPIN-ORBIT COUPLING IN CORRELATION FUNCTIONS OF FERMI GASES

A.1 Overview of present pseudogap formalism

In this section we give an overview of the present pseudogap formalism. This formalism is based on an underlying consistency with the usual mean-field theory. For example, the gap equation in the presence of spin orbit coupling is of the general form

$$0 = 1 + g\sum_{\mathbf{k},\alpha}\left[\frac{1-f(E_{\mathbf{k}\alpha})-f(\xi_{\mathbf{k}-\mathbf{q}\alpha})}{E_{\mathbf{k}\alpha}+\xi_{\mathbf{k}-\mathbf{q}\alpha}-\Omega-i0^{+}}u^{2}_{\mathbf{k}\alpha}-\frac{f(E_{\mathbf{k}\alpha})-f(\xi_{\mathbf{k}-\mathbf{q}\alpha})}{E_{\mathbf{k}\alpha}-\xi_{\mathbf{k}-\mathbf{q}\alpha}+\Omega+i0^{+}}v^{2}_{\mathbf{k}\alpha}\right], \tag{A.1}$$

where we have analytically continued $i\omega \to \Omega + i0^{+}$. Here $u^{2}_{\mathbf{k}\alpha}, v^{2}_{\mathbf{k}\alpha} = \frac{1}{2}(1 \pm \xi_{\mathbf{k}\alpha}/E_{\mathbf{k}\alpha})$ are the usual coherence factors, and $f(x)$ is the Fermi distribution function. This mean-field gap equation can be thought of as a BEC condition, allowing us to interpret

$$t_{\mathrm{pg}}(Q) \equiv \frac{g}{1+g\chi(Q)}, \qquad Q \neq 0\,, \tag{A.2}$$

with

$$\begin{aligned}\chi(Q) = \sum_{\mathbf{k},\alpha,\alpha'}&\left[\frac{1-f(E_{\mathbf{k}\alpha})-f(\xi_{\mathbf{k}-\mathbf{q}\alpha'})}{E_{\mathbf{k}\alpha}+\xi_{\mathbf{k}-\mathbf{q}\alpha'}-\Omega-i0^{+}}u^{2}_{\mathbf{k}\alpha}-\frac{f(E_{\mathbf{k}\alpha})-f(\xi_{\mathbf{k}-\mathbf{q}\alpha'})}{E_{\mathbf{k}\alpha}-\xi_{\mathbf{k}-\mathbf{q}\alpha'}+\Omega+i0^{+}}v^{2}_{\mathbf{k}\alpha}\right]\\ &\times\left(\frac{1+\alpha\alpha'\cos\left(\phi_{\mathbf{k}}-\phi_{\mathbf{k}-\mathbf{q}}\right)}{2}\right),\end{aligned} \tag{A.3}$$

as an effective bosonic propagator. This t-matrix is consistent with a susceptibility of the form

$$\chi(Q) = -\frac{1}{2}\sum_{K}\mathrm{Tr}\left[G(K)\widetilde{G}_{0}(K-Q)\right], \tag{A.4}$$

as defined in Ref. [He et al., 2013].

Using this t-matrix, the BEC condition (or equivalently the Thouless criteria): $t_{\rm pg}\left(0\right) = \infty$, $[t_{\rm pg}^{-1}\left(0\right) = 0]$, reproduces the gap equation, even at finite Δ. This particular t-matrix scheme, which is necessary to reproduce the standard mean-field theory, introduces the combination of one bare and one dressed Green's function. That is, from Eq. (A.1) the gap equation contains both the bare energy and the dressed energy dispersions.

Next we use this t-matrix scheme to separate the contributions from condensed and non-condensed pairs. Below the condensation transition temperature, denoted by T_c, the t-matrix can be split into two contributions:

$$t(Q) = t_{\rm pg}(Q) + t_{\rm sc}(Q), \tag{A.5}$$

$$t_{\rm sc}(Q) = -\frac{\Delta_{\rm sc}^2}{T}\delta(Q), \tag{A.6}$$

which correspond to non-condensed ($\rm pg$) and condensed ($\rm sc$) pairs. This implies that the fermion self energy can be similarly split up:

$$\Sigma(K) = \Sigma_{\rm pg}(K) + \Sigma_{\rm sc}(K) = -\sum_Q t(Q)\widetilde{G}_0(K-Q), \tag{A.7}$$

where $\widetilde{G}_0(K)$ is the "hole" Green's function as defined in section (2.2). It follows that

$$\Sigma_{\rm sc}(K) = -\sum_Q t_{\rm sc}(Q)\widetilde{G}_0(K-Q) = \Delta_{\rm sc}^2\widetilde{G}_0(K). \tag{A.8}$$

A BEC condition (or vanishing pair chemical potential) means that $t_{\rm pg}(Q)$ diverges at $Q = 0$ when $T \leq T_c$. Thus, we approximate Eq. (A.7) to yield

$$\Sigma(K) \approx \Delta^2\widetilde{G}_0(K), \tag{A.9}$$

where

$$\Delta^2(T) \equiv \Delta_{\rm sc}^2(T) + \Delta_{\rm pg}^2(T)\,, \tag{A.10}$$

is the total gap found from Eq. (A.1). Importantly, we are led to identify the quantity

$$\Delta_{\rm pg}^2 \equiv -\sum_{Q\neq 0} t_{\rm pg}(Q) \tag{A.11}$$

as the total magnitude of the finite-momentum non-condensed pairs.

We now have a closed set of equations for addressing the ordered phase. The propagator for non-condensed pairs can now be quantified, using the self-consistently determined pair susceptibility. At small four-vector Q, we may expand the inverse of $t_{\rm pg}$:

$$t_{\rm pg}^{-1}(Q) \approx Z\left(\Omega - \Omega_{\mathbf{q}}\right), \tag{A.12}$$

where we associate

$$\Omega_{\mathbf{q}} \approx \frac{q_i q_j}{2M_{ij}} \tag{A.13}$$

with a quadratic pair dispersion, and define an effective pair mass tensor, M_{ij}, for $i,j = x,y,z$. This can be calculated via a small Q expansion of $\chi(Q)$:

$$Z = \left.\frac{\partial\chi}{\partial\Omega}\right|_{\Omega=0,\mathbf{q}=0}, \qquad \frac{1}{2M_{ij}} = -\left.\frac{1}{2Z}\frac{\partial^2\chi}{\partial q_i \partial q_j}\right|_{\Omega=0,\mathbf{q}=0}. \tag{A.14}$$

Since $\chi(0,-\mathbf{q}) = \chi(0,\mathbf{q})$ (the t-matrix is inversion symmetric), the off diagonal elements of $1/M_{ij}$ vanish. Furthermore, rotational symmetry implies that $M_{xx} = M_{yy} \equiv M_\perp$.

Finally, one can rewrite Eq. (A.11) as

$$\Delta_{\rm pg}^2(T) = Z^{-1}\sum_{\mathbf{q}} b(\Omega_{\mathbf{q}}), \tag{A.15}$$

where $b(x)$ is the Bose distribution function. The central consequence of this formalism is a natural way to compute T_c within a scheme that builds on the usual mean-field theory. The superfluid transition temperature T_c is determined as the temperature at which $\Delta_{\rm pg}^2$, as defined through Eq. (A.11), intersects the mean-field value of Δ^2.

A.2 Green's functions and self energy in the helicity basis

In evaluating the correlation functions, it is convenient to have the Green's functions written in the helicity basis. For notational clarity, we consider only Rashba spin-orbit coupling. We emphasize that such a basis decomposition can be made for arbitrary spin-orbit coupling, provided there is no magnetic field present.

Here we present a brief discussion of the simple expressions used in section (2.5):

$$G_H^{\alpha}(K) \equiv \frac{u_{\mathbf{k}\alpha}^2}{i\omega - E_{\mathbf{k}\alpha}} + \frac{v_{\mathbf{k}\alpha}^2}{i\omega + E_{\mathbf{k}\alpha}}, \tag{A.16}$$

$$F_H^{\alpha}(K) \equiv u_{\mathbf{k}\alpha} v_{\mathbf{k}\alpha} \left(\frac{1}{i\omega + E_{\mathbf{k}\alpha}} - \frac{1}{i\omega - E_{\mathbf{k}\alpha}} \right), \tag{A.17}$$

where the Bogoliubov spectrum $E_{\mathbf{k}\alpha} = \sqrt{\xi_{\mathbf{k}\alpha}^2 + \Delta^2}$ with corresponding coherence factors satisfying $u_{\mathbf{k}\alpha}^2 = \frac{1}{2}(1 + \xi_{\mathbf{k}\alpha}/E_{\mathbf{k}\alpha})$, $u_{\mathbf{k}\alpha}^2 + v_{\mathbf{k}\alpha}^2 = 1$. Note that the helicity Green's functions have the standard form, aside from the index α.

We define the Nambu spinor $\Psi_{\mathbf{k}}^{\mathsf{T}} = \left(c_{\mathbf{k}\uparrow}, c_{\mathbf{k}\downarrow}, -c_{-\mathbf{k}\downarrow}^{\dagger}, c_{-\mathbf{k}\uparrow}^{\dagger} \right)$ of annihilation and creation operators. The many-body Nambu Green's function is then defined as

$$\mathcal{G}(K) = -\int_0^{\beta} d\tau e^{i\omega\tau} \left\langle T_\tau \Psi_{\mathbf{k}}(\tau) \Psi_{\mathbf{k}}^{\dagger}(0) \right\rangle = \begin{pmatrix} G(K) & F(K) \\ \widetilde{F}(K) & \widetilde{G}(K) \end{pmatrix}, \tag{A.18}$$

where $\beta = 1/T$ is the inverse temperature. The Green's function $G(K)$, time-reversed Green's function $\widetilde{G}(K) = i\sigma_y [G(-K)]^T i\sigma_y$, and the anomalous Green's functions $F(K)$ and $\widetilde{F}(K)$ are now in general 2×2 matrices.

Using the equations of motion for the Nambu Green's function in the pairing approximation, we have

$$\mathcal{G}^{-1}(K) = \begin{pmatrix} G_0^{-1}(K) & \Delta \\ \Delta^* & \widetilde{G}_0^{-1}(K) \end{pmatrix}. \tag{A.19}$$

For the remainder of this appendix, as well as in chapter (2), we choose Δ to be real. The non-interacting Green's function of the particle sector is $G_0^{-1}(K) \equiv i\omega - H^0(\mathbf{k})$, and the hole Green's function is defined through $\widetilde{G}_0^{-1}(K) = i\sigma_y[G_0^{-1}(-K)]^T i\sigma_y = i\omega + H^0(\mathbf{k})$. This non-interacting Green's function depends on the single particle Hamiltonian through $H^0(\mathbf{k}) = k^2/2m - \mu + \lambda \mathbf{k}_\perp \cdot \boldsymbol{\sigma}/m$ where $\boldsymbol{\sigma} = (\sigma_x, \sigma_y, \sigma_z)$ is a vector of Pauli matrices in spin space. We consider 2D Rashba SOC, so that $\boldsymbol{\sigma}$ is coupled only to the in plane momentum $\mathbf{k}_\perp = (k_x, k_y, 0)$. Taking the block matrix inverse gives the following 2×2 matrix Green's functions:

$$G(K) = \left[G_0^{-1}(K) - \Delta^2 \widetilde{G}_0(K)\right]^{-1}, \tag{A.20}$$

$$F(K) = \Delta G_0(K) \widetilde{G}(K). \tag{A.21}$$

In the pairing approximation, the structure of the block matrix inverse forces $\widetilde{F}(K) = (\Delta^*/\Delta)\, F(K) = F(K)$. For pure SOC, i.e., no magnetic field, the system is time-reversal invariant and helicity is a good quantum number. Therefore, the hole Green's function and the particle Green's function can be diagonalized simultaneously with the same unitary transformation: $U_\mathbf{k} = \exp\left[-i\phi_\mathbf{k}\pi/4 \left(\widehat{\mathbf{k}}_\perp \times \hat{z}\right) \cdot \boldsymbol{\sigma}\right]$, with $\widehat{\mathbf{k}}_\perp = \mathbf{k}_\perp/k_\perp$ and $e^{i\phi_\mathbf{k}} = (k_x + ik_y)/k_\perp$. This unitary transformation will then diagonalize the non-interacting Green's function $G_0(K)$, and leads to the identity:

$$G_0(K) = \sum_\alpha \frac{1}{i\omega - \xi_{\mathbf{k}\alpha}} P_{\mathbf{k}\alpha}, \tag{A.22}$$

where $P_{\mathbf{k}\alpha} = U_\mathbf{k}(1 + \alpha\sigma_z)U_\mathbf{k}^\dagger/2 = (1 + \alpha \mathbf{k}_\perp \cdot \boldsymbol{\sigma}/k_\perp)/2$ is a projector into the helicity state $\alpha = \pm 1$. We can now express $G(K)$ and $F(K)$ in terms of the projector $P_{\mathbf{k}\alpha}$ and the helicity Green's functions in Eq. (A.16) and Eq. (A.17) through:

$$G(K) = \sum_\alpha G_H^\alpha(K) P_{\mathbf{k}\alpha}, \tag{A.23}$$

$$F(K) = \sum_\alpha F_H^\alpha(K) P_{\mathbf{k}\alpha}. \tag{A.24}$$

A.3 Full vertex and Ward-Takahashi identity

A.3.1 Deriving the full electromagnetic vertex

The Ward-Takahashi identity (WTI) in quantum field theory is an exact identity that imposes a symmetry between response functions. The particular symmetry we are interested in is the abelian global $\mathrm{U}(1)$ symmetry, which is present in the density/current channel. Since the pseudogap phase self energy is of the mean-field form, the WTI provides a powerful tool in deriving the full vertex appearing in correlation functions. This is because the WTI can be used to explicitly solve for the full vertex function, and thereby obtain the exact correlation functions. We confine our attention here to the normal phase, where there are no collective mode effects.

The WTI for the full vertex $\Gamma^{\mu}(\widetilde{K}, K)$ is [Ryder, 1996]

$$q_{\mu}\Gamma^{\mu}(\widetilde{K}, K) = G^{-1}(\widetilde{K}) - G^{-1}(K). \tag{A.25}$$

Similarly the WTI for the bare vertex, $\gamma^{\mu}(\widetilde{K}, K)$, is $q_{\mu}\gamma^{\mu}(\widetilde{K}, K) = G_0^{-1}(\widetilde{K}) - G_0^{-1}(K)$ and we also define $q_{\mu}\widetilde{\gamma}^{\mu}(\widetilde{K}, K) = \widetilde{G}_0^{-1}(\widetilde{K}) - \widetilde{G}_0^{-1}(K)$. Here $\widetilde{K} \equiv K + Q$. In the pseudogap phase the mean-field self energy is $\Sigma(K) = \Delta^2 \widetilde{G}_0(K)$. Using this self energy, the WTI becomes

$$\begin{aligned}
q_{\mu}\Gamma^{\mu}(\widetilde{K}, K) &= G_0^{-1}(\widetilde{K}) - G_0^{-1}(K) - \Sigma(\widetilde{K}) + \Sigma(K), \\
&= G_0^{-1}(\widetilde{K}) - G_0^{-1}(K) - \Delta^2 \left[\widetilde{G}_0(\widetilde{K}) - \widetilde{G}_0(K)\right], \\
&= q_{\mu}\gamma^{\mu}(\widetilde{K}, K) - \Delta^2 \widetilde{G}_0(\widetilde{K}) \left[\widetilde{G}_0^{-1}(K) - \widetilde{G}_0^{-1}(\widetilde{K})\right] \widetilde{G}_0(K), \\
&= q_{\mu}\gamma^{\mu}(\widetilde{K}, K) - \Delta^2 \widetilde{G}_0(\widetilde{K}) \left[-q_{\mu}\widetilde{\gamma}^{\mu}(\widetilde{K}, K)\right] \widetilde{G}_0(K).
\end{aligned} \tag{A.26}$$

It follows that the full vertex is then

$$\Gamma^{\mu}(\widetilde{K}, K) = \gamma^{\mu}(\widetilde{K}, K) + \Delta^2 \widetilde{G}_0(\widetilde{K}) \widetilde{\gamma}^{\mu}(\widetilde{K}, K) \widetilde{G}_0(K). \tag{A.27}$$

It is important to note that this expression is exact and is not a perturbation expansion in terms of bare vertices.

A.3.2 f-sum rule and longitudinal sum rule

We now show that, given the exact correlation functions obtained by using the WTI, the f-sum rule is explicitly satisfied. This ensures the correlation functions are consistent with particle number conservation. The correlation functions are given by

$$P^{\mu\nu}(Q) = \sum_K \mathrm{Tr}\left[G(\widetilde{K})\Gamma^{\mu}(\widetilde{K},K)G(K)\gamma^{\nu}(K,\widetilde{K})\right]. \tag{A.28}$$

Inserting the full vertex from Eq. (A.27) gives the correlation functions above T_c as:

$$P^{\mu\nu}(Q) = \sum_K \mathrm{Tr}\Big\{[G(\widetilde{K})\gamma^{\mu}(\widetilde{K},K)G(K) + F_{\mathrm{pg}}(\widetilde{K})\widetilde{\gamma}^{\mu}(\widetilde{K},K)\widetilde{F}_{\mathrm{pg}}(K)]\gamma^{\nu}(K,\widetilde{K})\Big\}. \tag{A.29}$$

where $F_{\mathrm{pg}}(K) = \Delta_{\mathrm{pg}}G_0(K)\widetilde{G}(K)$, $\widetilde{F}_{\mathrm{pg}}(K) = \Delta_{\mathrm{pg}}\widetilde{G}_0(K)G(K) = F_{\mathrm{pg}}(K)$.

Applying the WTI to $P^{\mu\nu}(Q)$, and using the cyclic property of the trace, then gives

$$\Omega P^{0\nu}(Q) - \mathbf{q}\cdot P^{i\nu}(Q) = \sum_K \mathrm{Tr}\Big\{G(K)[\gamma^{\nu}(K,K+Q) - \gamma^{\nu}(K-Q,K)]\Big\}. \tag{A.30}$$

Here, and in what follows, the left (right) spatial dot products of $\mathbf{q}$ with $P^{\mu\nu}$ are with respect to the first (second) spatial index of $P^{\mu\nu}$. For the SOC system the bare vertex is $\gamma^{\mu}(\widetilde{K},K) = \left(1, \frac{\mathbf{k}+\mathbf{q}/2}{m} + \frac{\lambda}{m}\boldsymbol{\sigma}_{\perp}\right)$. Using this yields

$$\Omega P^{0\nu}(Q) - \mathbf{q}\cdot P^{i\nu}(Q) = \frac{q^{\nu}}{m}(1-\delta_{0,\nu})\sum_K \mathrm{Tr}\left\{G(K)\right\} = \frac{nq^{\nu}}{m}(1-\delta_{0,\nu}). \tag{A.31}$$

Here we have used $n = \sum_K \mathrm{Tr}\left\{G(K)\right\}$.

In terms of components, this equation becomes

$$\omega P^{00}(\omega, \mathbf{q}) - \mathbf{q} \cdot \mathbf{P}^{i0}(\omega, \mathbf{q}) = 0, \tag{A.32}$$

$$\omega \mathbf{P}^{0j}(\omega, \mathbf{q}) - \mathbf{q} \cdot \overleftrightarrow{P}^{ij}(\omega, \mathbf{q}) = \frac{n}{m}\mathbf{q}. \tag{A.33}$$

Setting $\omega = 0$ in the second equation and then taking the dot product with $\mathbf{q}$ gives

$$\mathbf{q} \cdot \overleftrightarrow{P}^{ij}(0, \mathbf{q}) \cdot \mathbf{q} = -\frac{nq^2}{m}. \tag{A.34}$$

Now use the identity $\mathrm{Im}P^{i0}(\omega, \mathbf{q}) = -\mathrm{Im}P^{0i}(-\omega, -\mathbf{q})$ and solve for $\mathrm{Im}P^{00}$ in terms of $\mathrm{Im}\overleftrightarrow{P}^{ij}$. Applying the Kramers-Kronig relations and Eq. (A.34) then gives

$$\begin{aligned}
\int \frac{d\omega}{\pi}(-\omega \mathrm{Im}P^{00}(\omega, \mathbf{q})) &= \int \frac{d\omega}{\pi}\left(-\frac{\mathbf{q} \cdot \mathrm{Im}\overleftrightarrow{P}^{ij}(\omega, \mathbf{q}) \cdot \mathbf{q}}{\omega}\right) \\
&= -\mathbf{q} \cdot \mathrm{Re}\overleftrightarrow{P}^{ij}(\mathbf{q}, 0) \cdot \mathbf{q} \\
&= \frac{nq^2}{m}.
\end{aligned} \tag{A.35}$$

Defining $\chi_{\rho\rho}(Q) \equiv P^{00}(Q)$, $\overleftrightarrow{\chi}_{JJ}(Q) \equiv P^{ij}(Q), i, j \in \{1, 2, 3\}$, the f-sum rule is thus

$$\int \frac{d\omega}{\pi}\left(-\omega \chi''_{\rho\rho}(\omega, \mathbf{q})\right) = \frac{nq^2}{m}. \tag{A.36}$$

This identity holds for all $\mathbf{q}$. Here the singular part of the correlation function, $\chi''_{\rho\rho}(\omega, \mathbf{q})$, is equal to $\mathrm{Im}\chi_{\rho\rho}(\omega, \mathbf{q})$, which is true only in the density/current channel. The next section on the spin-spin correlation functions elaborates further on this point. Similarly the longitudinal sum rule, which holds for all $\mathbf{q}$ in this continuum case, above T_c, is thus

$$\int \frac{d\omega}{\pi}\left(-\frac{\mathbf{q} \cdot \overleftrightarrow{\chi}''_{JJ}(\omega, \mathbf{q}) \cdot \mathbf{q}}{\omega}\right) = \frac{nq^2}{m}. \tag{A.37}$$

A.4 Spin-spin correlation functions and sum rules

A.4.1 General sum rules for spin density-spin density correlation functions

Here we investigate both the spin-spin correlation functions and sum rules. In the presence of SOC, spin is no longer conserved. The WTI is therefore inapplicable to deduce the form of the spin-spin correlation functions. However, the Heisenberg equations of motion can be utilized to derive a sum rule for spin density-spin density correlation functions.

The definition of the spin-spin correlation function, as given in section (2.4), is $\chi_{S_iS_j}(i\omega,\mathbf{q}) \equiv \int d\tau\, e^{i\omega\tau}\left\langle T_\tau S_{\mathbf{q}i}(\tau)\, S_{-\mathbf{q}j}(0)\right\rangle$, for a many-body spin operator $S_{\mathbf{q}i} = \sum_{s,s',\mathbf{k}} c^\dagger_{\mathbf{k}s}(\sigma_i)_{ss'}\, c_{\mathbf{k}+\mathbf{q}s'}$. We consider a general many-body Hamiltonian $\mathcal{H} = \mathcal{H}_0 + \mathcal{H}_I$, where the contribution $\mathcal{H}_0 = \sum_{s,s',\mathbf{k}} c^\dagger_{\mathbf{k}s} H^0_{ss'}(\mathbf{k})\, c_{\mathbf{k}s'}$ is constructed from an arbitrary single-particle Hamiltonian $H^0_{ss'}(\mathbf{k})$. It is assumed also that the interaction Hamiltonian commutes with the spin-operator, $\left[\mathcal{H}_I, S_{\mathbf{q}i}\right] = 0$.

In order to constrain the spin-spin correlation function, we investigate the analogous sum rule for $\chi''_{S_iS_j}(\omega,\mathbf{q})$ that is derived in the previous section for the density/current response. To do this, we first analytically continue $\chi_{S_iS_j}(i\omega,\mathbf{q})$ to real frequency by setting $i\omega = \omega + i\delta$, then letting $\delta \to 0$, and finally invoking the Sokhotski–Plemelj theorem [Henrici, 1986]. This is expressed mathematically as

$$\begin{aligned}\chi_{S_iS_j}(\omega,\mathbf{q}) &\equiv \lim_{\delta\to 0}\chi_{S_iS_j}(i\omega,\mathbf{q})\Big|_{i\omega=\omega+i\delta},\\ &= \chi'_{S_iS_j}(\omega,\mathbf{q}) + i\chi''_{S_iS_j}(\omega,\mathbf{q}),\\ &= \mathcal{P}\int \frac{dz}{\pi}\frac{\chi''_{S_iS_j}(z,\mathbf{q})}{z-\omega} + i\chi''_{S_iS_j}(\omega,\mathbf{q}).\end{aligned} \tag{A.38}$$

Here $\mathcal{P}$ denotes the Cauchy principal value. Note that, for $i \neq j$, $\chi''_{S_iS_j}(\omega,\mathbf{q})$ need not necessarily be real [Förster, 1975]. Returning to the time domain, the singular response function is $\chi''_{S_iS_j}(t,\mathbf{q}) = \frac{1}{2}\left\langle\left[S_{\mathbf{q}i}(t), S_{-\mathbf{q}j}(0)\right]\right\rangle$.

We now can derive the sum rule. Using the properties of Fourier transforms, we have

$$\begin{aligned}\int \frac{d\omega}{\pi}\left(-\omega\chi''_{S_iS_j}(\omega,\mathbf{q})\right) &= -2i\partial_t\,\chi''_{S_iS_j}(t,\mathbf{q})\Big|_{t=0}, \\ &= -\left\langle\left[i\partial_t S_{\mathbf{q}i}(t), S_{-\mathbf{q}j}(0)\right]\right\rangle\Big|_{t=0}, \\ &= \left\langle\left[\left[\mathcal{H}, S_{\mathbf{q}i}\right], S_{-\mathbf{q}j}\right]\right\rangle, \end{aligned} \tag{A.39}$$

where we have used the Heisenberg equations of motion $i\partial_t S_{\mathbf{q}i}(t) = -\left[\mathcal{H}, S_{\mathbf{q}i}(t)\right]$ and the commutators on the last line are taken at equal time. The problem thus reduces to calculating the equal-time commutator $\left\langle\left[\left[\mathcal{H}_0, S_{\mathbf{q}i}\right], S_{-\mathbf{q}j}\right]\right\rangle$.

The commutator in Eq. (A.39) is tedious but straightforward to calculate. After much algebra we arrive at the f-sum rule, or analogue thereof, for spin density-spin density response:

$$\begin{aligned}&\int \frac{d\omega}{\pi}\left(-\omega\chi''_{S_iS_j}(\omega,\mathbf{q})\right) \\ &= \frac{1}{2}\sum_{s,s',\mathbf{k}}\Bigg(\left\{\sigma_i, H^0(\mathbf{k}) - H^0(\mathbf{k}+\mathbf{q})\right\}\sigma_j - \sigma_j\left\{\sigma_i, H^0(\mathbf{k}-\mathbf{q}) - H^0(\mathbf{k})\right\} \\ &\quad + \left[H^0(\mathbf{k}) + H^0(\mathbf{k}+\mathbf{q}), \sigma_i\right]\sigma_j - \sigma_j\left[H^0(\mathbf{k}-\mathbf{q}) + H^0(\mathbf{k}), \sigma_i\right]\Bigg)_{ss'}\left\langle c^\dagger_{\mathbf{k}s}c_{\mathbf{k}s'}\right\rangle. \end{aligned} \tag{A.40}$$

This expression can be further simplified as follows. The Hamiltonian can be expressed as $H^0(\mathbf{k}) = h_\mu(\mathbf{k})\,\sigma^\mu$ where $h_\mu(\mathbf{k}) = \frac{1}{2}\mathrm{Tr}\left[\sigma_\mu H^0(\mathbf{k})\right]$ and $\sigma^\mu = (1, \boldsymbol{\sigma})$. After using the commutation and anti-commutation rules for Pauli matrices, the sum rule becomes

$$\begin{aligned}&\int \frac{d\omega}{\pi}\left(-\omega\chi''_{S_iS_j}(\omega,\mathbf{q})\right) \\ &= \sum_{\mathbf{k}}\Bigg\{\mathrm{Tr}\left[\left(H^0(\mathbf{k}+\mathbf{q}) + H^0(\mathbf{k}-\mathbf{q}) - 2H^0(\mathbf{k})\right)g_{\mathbf{k}}\right]\delta_{ij} \\ &\quad - 2\left[\left(\mathbf{h}(\mathbf{k}+\mathbf{q}) + \mathbf{h}(\mathbf{k}-\mathbf{q})\right)\cdot\mathbf{s}_{\mathbf{k}}\delta_{ij} - \left(h_i(\mathbf{k}+\mathbf{q}) + h_i(\mathbf{k}-\mathbf{q})\right)s_{\mathbf{k}j}\right] \\ &\quad - i\left[\left(h_k(\mathbf{k}+\mathbf{q}) - h_k(\mathbf{k}-\mathbf{q})\right)n_{\mathbf{k}} - \left(h_0(\mathbf{k}+\mathbf{q}) - h_0(\mathbf{k}-\mathbf{q})\right)s_{\mathbf{k}k}\right]\epsilon_{ijk}\Bigg\}, \end{aligned} \tag{A.41}$$

where we have defined $g_{\mathbf{k}} = T\sum_{i\omega} G(i\omega, \mathbf{k})$, $n_{\mathbf{k}} = \mathrm{Tr}\left[g_{\mathbf{k}}\right]$ and $s_{\mathbf{k}i} = \mathrm{Tr}\left[\sigma_i g_{\mathbf{k}}\right]$.

The first line, appearing only for $i = j$, can be seen to be equal to the density f-sum rule contribution. The second line can give diagonal contributions, resulting in a deviation of the spin-density response from the density response, in the presence of SOC. The third line vanishes for $i = j$. It is of note that this line is purely imaginary, and can give an imaginary f-sum rule contribution. This is only possible for correlation functions of two distinct operators, as was noted in the literature [Förster, 1975]. This implies that $\chi''_{S_iS_j} \neq \mathrm{Im}\chi_{S_iS_j}$ for $i \neq j$. Finally, the first and third lines of Eq. (A.41) are symmetric under interchange of $i \leftrightarrow j$ and $\mathbf{q} \leftrightarrow -\mathbf{q}$, while the second line is not. This can be explained by observing that Eq. (A.39) is not fully symmetric under the the exchange of $i \leftrightarrow j$ and $\mathbf{q} \leftrightarrow -\mathbf{q}$.

A.4.2 Explicit spin-spin correlation functions and sum rules for Rashba SOC

We now present simplified expressions for the correlation functions and sum rules for the case of Rashba SOC. Due to symmetry in the x-y plane, there are only four unique correlation functions of interest. The remaining spin density correlation functions can be found through exchanging $x \to y$ where relevant. The explicit spin-spin correlation functions are

$$\chi_{S_xS_x}(\omega, \mathbf{q}) = \frac{1}{2}\sum_{K,\alpha,\alpha'} \left(1 + \alpha\alpha' \cos\left(\phi_{\mathbf{k}+\mathbf{q}} + \phi_{\mathbf{k}}\right)\right)\left[G_H^{\alpha}(K)G_H^{\alpha'}(\widetilde{K}) + F_H^{\alpha}(K)F_H^{\alpha'}(\widetilde{K})\right], \tag{A.42}$$

$$\chi_{S_xS_z}(\omega, \mathbf{q}) = \frac{i}{2}\sum_{K,\alpha,\alpha'} \left(\alpha' \sin\left(\phi_{\mathbf{k}+\mathbf{q}}\right) - \alpha\sin(\phi_{\mathbf{k}})\right)\left[G_H^{\alpha}(K)G_H^{\alpha'}(\widetilde{K}) + F_H^{\alpha}(K)F_H^{\alpha'}(\widetilde{K})\right], \tag{A.43}$$

$$\chi_{S_zS_z}(\omega, \mathbf{q}) = \frac{1}{2}\sum_{K,\alpha,\alpha'} \left(1 - \alpha\alpha' \cos\left(\phi_{\mathbf{k}+\mathbf{q}} - \phi_{\mathbf{k}}\right)\right)\left[G_H^{\alpha}(K)G_H^{\alpha'}(\widetilde{K}) + F_H^{\alpha}(K)F_H^{\alpha'}(\widetilde{K})\right], \tag{A.44}$$

$$\chi_{S_xS_y}(\omega, \mathbf{q}) = 0. \tag{A.45}$$

Note that the response $\chi_{S_xS_y}$ vanishes identically, as it must due to in-plane rotational symmetry.

For each of the above correlation functions, we have explicitly integrated the left hand side of the sum rule, Eq. (A.41), and found:

$$\int \frac{d\omega}{\pi}\left(-\omega\chi''_{S_xS_x}(\omega,\mathbf{q})\right) = \frac{nq^2}{m} - \frac{4\lambda}{m}\sum_{\mathbf{k}\alpha}\alpha\frac{k_x^2}{k_\perp}n_{\mathbf{k}\alpha}, \tag{A.46}$$

$$\int \frac{d\omega}{\pi}\left(-\omega\chi''_{S_xS_z}(\omega,\mathbf{q})\right) = -i\frac{q_y}{m}\sum_{\mathbf{k}\alpha}\left(\alpha\frac{k_y^2}{k_\perp} - \lambda\right)n_{\mathbf{k}\alpha}, \tag{A.47}$$

$$\int \frac{d\omega}{\pi}\left(-\omega\chi''_{S_zS_z}(\omega,\mathbf{q})\right) = \frac{nq^2}{m} - \frac{4\lambda}{m}\sum_{\mathbf{k}\alpha}\alpha k_\perp n_{\mathbf{k}\alpha}, \tag{A.48}$$

where $n_{\mathbf{k}\alpha} = T\sum_{i\omega} G_H^\alpha(K)$. These results are consistent with the form using the right hand side of Eq. (A.41). Note further that the sum rule for $\chi_{S_xS_z}$ is purely imaginary. This is not surprising, as mentioned above [Förster, 1975].

A.5 Superfluid density

The formalism underlying this work is capable of addressing the superfluid phase. However, many response functions in this phase require the inclusion of collective mode effects. The superfluid density, which can be obtained using a transverse response, does not require collective modes. The superfluid density $\left(\frac{\overleftrightarrow{n_s}}{m}\right)$ is defined by

$$\left(\frac{\overleftrightarrow{n_s}}{m}\right) \equiv \left(\frac{\overleftrightarrow{n}}{m}\right)_{\text{dia}} + \overleftrightarrow{\chi}^T_{JJ}(0), \tag{A.49}$$

where $\overleftrightarrow{\chi}^T_{JJ}(Q)$ is the transverse part of the current-current correlation function.

This contains two contributions from: (i) quasi-particles which are reflected in the current-current correlation function and (ii) the diamagnetic current which above T_c must precisely cancel the quasi-particle term. Below T_c the current-current correlation function acquires an additional contribution which depends on the anomalous Green's function F_{sc}. Note that the diamagnetic current is dependent on the total pairing gap. The current-current correlation function depends on

the function $F_{\rm pg}$ as defined above, and arises from vertex corrections.

Using Eq. (2.9) from section (2.3), the current-current correlation function and diamagnetic response tensors are

$$\overleftrightarrow{\chi}_{JJ}(Q) = \sum_K \mathrm{Tr}\Big[\mathbf{J}(\mathbf{k},\mathbf{q})G(\widetilde{K})\mathbf{J}(\mathbf{k},\mathbf{q})G(K) - \mathbf{J}(\mathbf{k},\mathbf{q})F_{\rm pg}(\widetilde{K})\mathbf{J}(\mathbf{k},\mathbf{q})\widetilde{F}_{\rm pg}(K) + \mathbf{J}(\mathbf{k},\mathbf{q})F_{\rm sc}(\widetilde{K})\mathbf{J}(\mathbf{k},\mathbf{q})\widetilde{F}_{\rm sc}(K)\Big], \tag{A.50}$$

$$\left(\frac{\overleftrightarrow{n}}{m}\right)_{\rm dia} = \sum_K \mathrm{Tr}\Big[-\mathbf{J}(\mathbf{k},0)G(K)\mathbf{J}(\mathbf{k},0)G(K) + \mathbf{J}(\mathbf{k},0)F_{\rm pg}(K)\mathbf{J}(\mathbf{k},0)\widetilde{F}_{\rm pg}(K) + \mathbf{J}(\mathbf{k},0)F_{\rm sc}(K)\mathbf{J}(\mathbf{k},0)\widetilde{F}_{\rm sc}(K)\Big], \tag{A.51}$$

where $\mathbf{J}(\mathbf{k},\mathbf{q}) = \left(\frac{\mathbf{k}+\mathbf{q}/2}{m} + \frac{\lambda}{m}\boldsymbol{\sigma}_\perp\right)$ is the current operator. Notice that the relative sign between the $F_{\rm sc}$ and $F_{\rm pg}$ contributions is different in $\overleftrightarrow{\chi}^T_{JJ}(Q)$ and in the diamagnetic current. The superfluid density tensor is thus

$$\left(\frac{n_s^{ij}}{m}\right) = 2\sum_K \mathrm{Tr}\left[J_i(\mathbf{k},0)F_{\rm sc}(K)J_j(\mathbf{k},0)\widetilde{F}_{\rm sc}(K)\right]. \tag{A.52}$$

Due to symmetry, the off-diagonal ($i \neq j$) elements vanish. Furthermore, the SOC leads to different in-plane ($i = j = x, y$) and out-of-plane ($i = j = z$) response. Despite a significantly different form, we can show this expression for the superfluid density is consistent with that derived by adding a phase twist to the order parameter [He & Huang, 2012, 2013, Zhou & Zhang, 2012].

APPENDIX B

TOPOLOGICAL EFFECTS ON TRANSITION TEMPERATURES AND RESPONSE FUNCTIONS IN THREE-DIMENSIONAL FERMI SUPERFLUIDS

B.1 Derivations of the vertex function $\Gamma(Q,T)$ and coherence factors

Here we present derivations of the vertex function $\Gamma(Q,T)$, where $Q \equiv (i\omega, \mathbf{q})$, along with the coherence factors $v_{\eta\alpha\alpha'}(\mathbf{k}, \mathbf{k}-\mathbf{q})$ and $w_{\alpha\alpha',\eta\eta'}(\mathbf{k}, \mathbf{k}+\mathbf{q})$, which appear in Eq. (3.3) and Eq. (3.6) of chapter (3). The non-interacting Green's function can be written in terms of projectors as follows

$$G_0(K) = \sum_{\alpha} \frac{P^0_{\alpha}(\mathbf{k})}{i\nu - \xi_{\alpha\mathbf{k}}}, \tag{B.1}$$

where $K \equiv (i\nu, \mathbf{k})$ and $P^0_{\alpha}(\mathbf{k}) = \frac{1}{2} U_{\mathbf{k}} (1 + \alpha\sigma_z) U^{\dagger}_{\mathbf{k}}$ is a projector into the band $\alpha = \pm 1$. The unitary matrix $U_{\mathbf{k}}$ is the unitary operator which diagonalizes $H_0(\mathbf{k})$ to produce the single particle dispersion $\xi_{\alpha\mathbf{k}} = \xi_{\mathbf{k}} + \alpha|\mathbf{h}|$.

The Nambu Green's function $\mathcal{G}(K)$ for a superfluid can be written in terms of projectors as

$$\begin{aligned} \mathcal{G}(K) &= [i\nu - \mathcal{H}_{\mathrm{BdG}}(\mathbf{k})]^{-1}, \\ &= \begin{pmatrix} G(K) & F(K) \\ \widetilde{F}(K) & \widetilde{G}(K) \end{pmatrix}, \\ &= \sum_{\alpha\eta} \frac{\mathcal{P}_{\eta\alpha}}{i\nu - \eta E_{\alpha\mathbf{k}}}, \end{aligned} \tag{B.2}$$

where we have used the inverse of the BdG Hamiltonian, $\mathcal{H}_{\mathrm{BdG}}$, to define the normal and anomalous Green's functions $G(K)$ and $F(K)$, along with their time-reversed counterparts $\widetilde{G}(K) = i\sigma_y [G(-K)]^T i\sigma_y$ and $\widetilde{F}(K) = i\sigma_y [F(-K)]^T i\sigma_y$.

The projectors $\mathcal{P}_{\eta\alpha} = \psi_{\eta\alpha}\psi_{\eta\alpha}^{\dagger}$ are constructed from the BdG eigenvectors

$$\psi_{\eta\alpha} = \mathcal{U}_{\mathbf{k}} \begin{pmatrix} \alpha\sqrt{\frac{1}{2}\left(1+\alpha\frac{\xi_{\mathbf{k}}}{E_{0\mathbf{k}}}\right)}\sqrt{\frac{1}{2}\left(1+\alpha\eta\frac{\zeta_{\alpha\mathbf{k}}}{E_{\alpha\mathbf{k}}}\right)} \\ \eta\sqrt{\frac{1}{2}\left(1-\alpha\frac{\xi_{\mathbf{k}}}{E_{0\mathbf{k}}}\right)}\sqrt{\frac{1}{2}\left(1-\alpha\eta\frac{\zeta_{\alpha\mathbf{k}}}{E_{\alpha\mathbf{k}}}\right)} \\ \alpha\eta\sqrt{\frac{1}{2}\left(1+\alpha\frac{\xi_{\mathbf{k}}}{E_{0\mathbf{k}}}\right)}\sqrt{\frac{1}{2}\left(1-\alpha\eta\frac{\zeta_{\alpha\mathbf{k}}}{E_{\alpha\mathbf{k}}}\right)} \\ \sqrt{\frac{1}{2}\left(1-\alpha\frac{\xi_{\mathbf{k}}}{E_{0\mathbf{k}}}\right)}\sqrt{\frac{1}{2}\left(1+\alpha\eta\frac{\zeta_{\alpha\mathbf{k}}}{E_{\alpha\mathbf{k}}}\right)} \end{pmatrix}, \tag{B.3}$$

where $\mathcal{U}_{\mathbf{k}} = \mathrm{diag}\left\{U_{\mathbf{k}}, V_{\mathbf{k}}\right\}$ rotates the particle (hole) sector to the spin-orbit basis with a unitary matrix $U_{\mathbf{k}}$ ($V_{\mathbf{k}}$), and we have defined $\theta = \cos^{-1}(b_z/|\mathbf{h}|)$, $E_{0\mathbf{k}} = \sqrt{\xi_{\mathbf{k}}^2 + \Delta^2\cos^2\theta}$, and $\zeta_{\alpha\mathbf{k}} = E_{0\mathbf{k}} + \alpha|\mathbf{h}|$. Note that $\zeta_{\alpha\mathbf{k}}$ limits to $\xi_{\alpha\mathbf{k}}$ as $\Delta \to 0$ or $b_z \to 0$, and to $\sqrt{\xi_{\mathbf{k}}^2 + \Delta^2} + \alpha b_z$ as $\lambda \to 0$.

For convenience, the 4×4 projector matrices can be expressed as four 2×2 sub-matrices as

$$\mathcal{P}_{\eta\alpha}(\mathbf{k}) \equiv \begin{pmatrix} P_{\eta\alpha}(\mathbf{k}) & Q_{\eta\alpha}(\mathbf{k}) \\ R_{\eta\alpha}(\mathbf{k}) & S_{\eta\alpha}(\mathbf{k}) \end{pmatrix}. \tag{B.4}$$

The Green's function $G\left(K\right)$ is found from the appropriate 2×2 sub-matrix with the corresponding projector

$$P_{\eta\alpha}(\mathbf{k}) = \frac{1}{4E_{0\mathbf{k}}E_{\alpha\mathbf{k}}} U_{\mathbf{k}} \begin{pmatrix} \left(E_{0\mathbf{k}} + \alpha\xi_{\mathbf{k}}\right)\left(E_{\alpha\mathbf{k}} + \alpha\eta\zeta_{\alpha\mathbf{k}}\right) & \alpha\Delta^2\sin\theta\cos\theta \\ \alpha\Delta^2\sin\theta\cos\theta & \left(E_{0\mathbf{k}} - \alpha\xi_{\mathbf{k}}\right)\left(E_{\alpha\mathbf{k}} - \alpha\eta\zeta_{\alpha\mathbf{k}}\right) \end{pmatrix} U_{\mathbf{k}}^{\dagger}. \tag{B.5}$$

We now define the quantity $\chi\left(Q\right)$, known as the pair susceptibility, which appears in $\Gamma\left(Q,T\right)$ and is a natural extension of $\chi\left(0\right)$:

$$\chi\left(Q\right) \equiv -\frac{1}{2}\mathrm{Tr}\left[\sum_{K} G\left(K\right)\widetilde{G}_0\left(K-Q\right)\right], \tag{B.6}$$

where $\widetilde{G}_0\left(K\right) = i\sigma_y\left[G_0\left(-K\right)\right]^T i\sigma_y$ is the time-reversed, or hole, Green's function. [Note that we have not explicitly labeled the T dependence in $\chi\left(Q\right)$.]

Substituting the above definitions then gives

$$\chi(Q) = -\frac{1}{2}\mathrm{Tr}\left[\sum_{K}\sum_{\eta\alpha}\frac{P_{\eta\alpha}(\mathbf{k})}{i\nu-\eta E_{\alpha\mathbf{k}}}\sum_{\alpha'}\frac{P^{0}_{\alpha'}(\mathbf{k}-\mathbf{q})}{i\nu-i\omega+\xi_{\alpha'\mathbf{k}-\mathbf{q}}}\right],$$
$$= -\frac{1}{2}\sum_{\mathbf{k}}\sum_{\eta\alpha\alpha'}\left(\sum_{i\nu}\frac{1}{i\nu-\eta E_{\alpha\mathbf{k}}}\frac{1}{i\nu-\left(i\omega-\xi_{\alpha'\mathbf{k}-\mathbf{q}}\right)}\right)\mathrm{Tr}\left[P_{\eta\alpha}(\mathbf{k})\,P^{0}_{\alpha'}(\mathbf{k}-\mathbf{q})\right]. \tag{B.7}$$

Performing the summation over Matsubara frequencies reduces this expression to

$$\chi(Q) = \frac{1}{2}\sum_{\mathbf{k}}\sum_{\eta\alpha\alpha'}\left(\frac{f(\eta E_{\alpha\mathbf{k}})-f\left(-\xi_{\alpha'\mathbf{k}-\mathbf{q}}\right)}{i\omega-\left(\eta E_{\alpha\mathbf{k}}+\xi_{\alpha'\mathbf{k}-\mathbf{q}}\right)}\right)v_{\eta\alpha\alpha'}(\mathbf{k},\mathbf{k}-\mathbf{q}). \tag{B.8}$$

Here the coherence factor discussed in Eq. (3.3) and Eq. (3.4) of chapter (3) is

$$v_{\eta\alpha\alpha'}(\mathbf{k},\mathbf{k}-\mathbf{q}) = \mathrm{Tr}\left[P_{\eta\alpha}(\mathbf{k})\,P^{0}_{\alpha'}(\mathbf{k}-\mathbf{q})\right]. \tag{B.9}$$

The vertex function can now be defined by $\Gamma(Q,T) \equiv \left[\chi(Q)+g^{-1}\right]^{-1}$. Using the expression for the susceptibility in Eq. (B.8), we obtain the vertex function $\Gamma(Q,T)$ as given in Eq. (3.4) of section (3.3). The familiar gap equation can then also be obtained from the Thouless criteria: $\chi(0)+g^{-1}=0$.

B.2 Density and spin correlation functions

We now derive the density and spin correlation functions for the normal phase ($T > T_c$) in the presence of SOC and a Zeeman field. In the normal phase there are no collective-mode contributions. The density-density or spin-spin correlation functions can be written as $\chi_{S_iS_j}(i\omega,\mathbf{q}) \equiv \int d\tau\, e^{i\omega\tau}\left\langle T_\tau S_{\mathbf{q}i}(\tau)\,S_{-\mathbf{q}j}(0)\right\rangle$, for a many-body density or spin operator $S_{\mathbf{q}i} = \sum_{s,s',\mathbf{k}} c^{\dagger}_{\mathbf{k}s}(\sigma_i)_{ss'}\,c_{\mathbf{k}+\mathbf{q}s'}$. Here $i=j=0$, with $\sigma_0=\mathbb{1}_2$, corresponds to the density-density correlation function $\chi_{\rho\rho}(i\omega,\mathbf{q})$, and $i,j\in\{x,y,z\}$ gives the corresponding spin-spin correlation function.

We emphasize the normal state has no anomalous Green's function component, but the existence of normal state pairs allows one to write the correlation functions as the sum of two terms

$$\chi_{S_iS_j}(i\omega,\mathbf{q}) = \sum_K \mathrm{Tr}\left[\sigma_i G(K)\sigma_j G(K+Q) + \sigma_i F(K)\sigma_j \widetilde{F}(K+Q)\right]. \tag{B.10}$$

Here we associate $F(K) = (\Delta/\Delta^*)\widetilde{F}(K)$ with a pseudogap vertex contribution, which leads to

$$\chi_{S_iS_j}(i\omega,\mathbf{q}) = \sum_K \sum_{\alpha\alpha',\eta\eta'} \left(\frac{1}{i\nu - \eta E_{\alpha\mathbf{k}}}\frac{1}{i\nu + i\omega - \eta' E_{\alpha'\mathbf{k}+\mathbf{q}}}\right) w_{\alpha\alpha',\eta\eta'}(\mathbf{k},\mathbf{k}+\mathbf{q}), \tag{B.11}$$

where we have introduced the coherence factor

$$w_{\alpha\alpha',\eta\eta'}(\mathbf{k},\mathbf{k}+\mathbf{q}) = \mathrm{Tr}[\sigma_i P_{\eta\alpha}(\mathbf{k})\sigma_j P_{\eta'\alpha'}(\mathbf{k}+\mathbf{q})] + \mathrm{Tr}[\sigma_i Q_{\eta\alpha}(\mathbf{k})\sigma_j R_{\eta'\alpha'}(\mathbf{k}+\mathbf{q})]. \tag{B.12}$$

Upon performing the summation over Matsubara frequencies, we obtain the expression for the density-density or spin-spin correlation function given in Eq. (3.6) of section (3.5).

APPENDIX C

EXACT CORRELATION FUNCTIONS IN THE CUPRATE PSEUDOGAP PHASE: COMBINED EFFECTS OF CHARGE ORDER AND PAIRING

C.1 Inclusion of both charge-density-wave and pair-density-wave effects

Here we extend our results to include the effects of the charge-density waves C_1 and C_2, where $C_1, C_2 \neq 0$. The full self energy, as in Eq. (4.1) of section (4.1), is given by

$$\begin{aligned}\Sigma_{pg}(K) = &\frac{\Delta_1^2}{\omega + \xi_{\mathbf{k}-\mathbf{p}} - \frac{\Delta_2^2}{\omega - \xi_{\mathbf{k}-2\mathbf{p}}}} + \frac{\Delta_2^2}{\omega + \xi_{\mathbf{k}+\mathbf{p}} - \frac{\Delta_1^2}{\omega - \xi_{\mathbf{k}+2\mathbf{p}}}} \\ &+ \frac{C_1^2}{\omega - \xi_{\mathbf{k}+2\mathbf{p}} - \frac{\Delta_1^2}{\omega + \xi_{\mathbf{k}+\mathbf{p}}}} + \frac{C_2^2}{\omega - \xi_{\mathbf{k}-2\mathbf{p}} - \frac{\Delta_2^2}{\omega + \xi_{\mathbf{k}-\mathbf{p}}}} \\ &+ \frac{2\Delta_1\Delta_2 C_1}{\left(\omega - \xi_{\mathbf{k}+\mathbf{2p}}\right)\left(\omega + \xi_{\mathbf{k}+\mathbf{p}}\right) - \Delta_1^2} + \frac{2\Delta_1\Delta_2 C_2}{\left(\omega - \xi_{\mathbf{k}-\mathbf{2p}}\right)\left(\omega + \xi_{\mathbf{k}-\mathbf{p}}\right) - \Delta_2^2}. \end{aligned} \tag{C.1}$$

For convenience we define the following four bare (inverse) Green's functions $G_{0,i}^{-1}(K) = (\omega - \xi_{\mathbf{k},i}), i \in \{1,2,3,4\}$, where $\xi_{\mathbf{k},1} = \xi_{\mathbf{k}+\mathbf{p}}$, $\xi_{\mathbf{k},2} = \xi_{\mathbf{k}-\mathbf{p}}$, $\xi_{\mathbf{k},3} = \xi_{\mathbf{k}+2\mathbf{p}}$, $\xi_{\mathbf{k},4} = \xi_{\mathbf{k}-2\mathbf{p}}$ are four dispersion relations. (The usual bare inverse Green's function is denoted by $G_0^{-1}(K) = \omega - \xi_{\mathbf{k}} = \omega - \epsilon_{\mathbf{k}} + \mu$.) Using these definitions, we can then define the following partially-dressed Green's functions:

$$G_{1,1}^{-1}(K) = \omega - \xi_{\mathbf{k},1} - \frac{\Delta_2^2}{\omega + \xi_{\mathbf{k},3}} = G_{0,1}^{-1}(K) + \Delta_2^2 G_{0,4}(-K), \tag{C.2}$$

$$G_{1,2}^{-1}(K) = \omega - \xi_{\mathbf{k},2} - \frac{\Delta_1^2}{\omega + \xi_{\mathbf{k},4}} = G_{0,2}^{-1}(K) + \Delta_1^2 G_{0,3}(-K), \tag{C.3}$$

$$G_{1,3}^{-1}(K) = \omega - \xi_{\mathbf{k},3} - \frac{\Delta_1^2}{\omega + \xi_{\mathbf{k},1}} = G_{0,3}^{-1}(K) + \Delta_1^2 G_{0,2}(-K), \tag{C.4}$$

$$G_{1,4}^{-1}(K) = \omega - \xi_{\mathbf{k},4} - \frac{\Delta_2^2}{\omega + \xi_{\mathbf{k},2}} = G_{0,4}^{-1}(K) + \Delta_2^2 G_{0,1}(-K). \tag{C.5}$$

The full self energy of the Amperean-pairing theory is then

$$\begin{aligned}\Sigma_{pg}(K) = &- \Delta_1^2 G_{1,1}(-K) - \Delta_2^2 G_{1,2}(-K) + C_1^2 G_{1,3}(K) + C_2^2 G_{1,4}(K) \\ &- \Delta_1\Delta_2 C_1 G_{0,2}(-K) G_{1,3}(K) - \Delta_1\Delta_2 C_1 G_{0,3}(K) G_{1,2}(-K) \\ &- \Delta_1\Delta_2 C_2 G_{0,1}(-K) G_{1,4}(K) - \Delta_1\Delta_2 C_2 G_{0,4}(K) G_{1,1}(-K). \end{aligned} \tag{C.6}$$

Note, $G_{0,4}(K)G_{1,1}(-K) = G_{0,1}(-K)G_{1,4}(K)$ and $G_{0,3}(K)G_{1,2}(-K) = G_{0,2}(-K)G_{1,3}(K)$; thus the two terms on the second and third lines can each be combined into a single expression. However, from here on out we will use the symmetric form of the self energy as given in Eq. (C.6).

In order to derive the full vertex $\Gamma^\mu(\widetilde{K}, K)$, where $\widetilde{K} \equiv K + Q$, associated with the self energy in Eq. (C.1) and Eq. (C.6), we use the Ward-Takahashi identity (WTI). The WTI, for the vertex $\Gamma^\mu = \big(\Gamma^0, \mathbf{\Gamma}\big)$, on a lattice is

$$\begin{aligned}\Omega\Gamma^0(\widetilde{K}, K) + i\mathrm{div}_{\mathbf{q}}\mathbf{\Gamma}(\widetilde{K}, K) &= G^{-1}(\widetilde{K}) - G^{-1}(K), \\ &= \Omega + i\mathrm{div}_{\mathbf{q}}\boldsymbol{\gamma}(\widetilde{K}, K) + \Sigma_{pg}(K) - \Sigma_{pg}(\widetilde{K}). \end{aligned} \tag{C.7}$$

Here we have used Dyson's equation, $G^{-1}(K) = G_0^{-1}(K) - \Sigma_{pg}(K)$, along with the bare WTI: $\Omega\gamma^0(\widetilde{K}, K) + i\mathrm{div}_{\mathbf{q}}\boldsymbol{\gamma}(\widetilde{K}, K) = G_0^{-1}(\widetilde{K}) - G_0^{-1}(K)$. Since the self energy contains only bare and partially-dressed Green's functions, the WTI allows the full vertex $\Gamma^\mu(\widetilde{K}, K)$ to be obtained explicitly. To show this, we need to compute the difference $\Sigma_{pg}(K) - \Sigma_{pg}(\widetilde{K})$ appearing in Eq. (C.7).

Using the self energy in Eq. (C.6), we find that

$$
\begin{aligned}
&\Sigma_{pg}(K) - \Sigma_{pg}(\widetilde{K}) = \\
&\Delta_1^2 G_{1,1}(-K)\left[G_{1,1}^{-1}(-K) - G_{1,1}^{-1}(-\widetilde{K})\right] G_{1,1}(-\widetilde{K}) \\
+&\Delta_2^2 G_{1,2}(-K)\left[G_{1,2}^{-1}(-K) - G_{1,2}^{-1}(-\widetilde{K})\right] G_{1,2}(-\widetilde{K}) \\
+&C_1^2 G_{1,3}(\widetilde{K})\left[G_{1,3}^{-1}(\widetilde{K}) - G_{1,3}^{-1}(K)\right] G_{1,3}(K) \\
+&C_2^2 G_{1,4}(\widetilde{K})\left[G_{1,4}^{-1}(\widetilde{K}) - G_{1,4}^{-1}(K)\right] G_{1,4}(K) \\
+&\Delta_1\Delta_2 C_1 G_{1,3}(K) G_{0,2}(-K)\left[G_{0,2}^{-1}(-K) - G_{0,2}^{-1}(-\widetilde{K})\right] G_{0,2}(-\widetilde{K}) \\
-&\Delta_1\Delta_2 C_1 G_{0,2}(-\widetilde{K}) G_{1,3}(\widetilde{K})\left[G_{1,3}^{-1}(\widetilde{K}) - G_{1,3}^{-1}(K)\right] G_{1,3}(K) \\
+&\Delta_1\Delta_2 C_1 G_{1,2}(-K)\left[G_{1,2}^{-1}(-K) - G_{1,2}^{-1}(-\widetilde{K})\right] G_{1,2}(-\widetilde{K}) G_{0,3}(\widetilde{K}) \\
-&\Delta_1\Delta_2 C_1 G_{0,3}(\widetilde{K})\left[G_{0,3}^{-1}(\widetilde{K}) - G_{0,3}^{-1}(K)\right] G_{0,3}(K) G_{1,2}(-K) \\
+&\Delta_1\Delta_2 C_2 G_{1,4}(K) G_{0,1}(-K)\left[G_{0,1}^{-1}(-K) - G_{0,1}^{-1}(-\widetilde{K})\right] G_{0,1}(-\widetilde{K}) \\
-&\Delta_1\Delta_2 C_2 G_{0,1}(-\widetilde{K}) G_{1,4}(\widetilde{K})\left[G_{1,4}^{-1}(\widetilde{K}) - G_{1,4}^{-1}(K)\right] G_{1,4}(K) \\
+&\Delta_1\Delta_2 C_2 G_{1,1}(-K)\left[G_{1,1}^{-1}(-K) - G_{1,1}^{-1}(-\widetilde{K})\right] G_{1,1}(-\widetilde{K}) G_{0,4}(\widetilde{K}) \\
-&\Delta_1\Delta_2 C_2 G_{0,4}(\widetilde{K})\left[G_{0,4}^{-1}(\widetilde{K}) - G_{0,4}^{-1}(K)\right] G_{0,4}(K) G_{1,1}(-K). \qquad \text{(C.8)}
\end{aligned}
$$

The terms in square brackets can all be expressed as contractions of various bare vertices, by using the bare Ward-Takahashi identities. For example, using Eqs. (C.2-C.5), we can write:

$$
\begin{aligned}
G_{1,1}^{-1}(-K) - G_{1,1}^{-1}(-\widetilde{K}) &= G_{0,1}^{-1}(-K) - G_{0,1}^{-1}(-\widetilde{K}) \\
&\quad + \Delta_2^2 G_{0,4}(K) G_{0,4}(\widetilde{K})\left[G_{0,4}^{-1}(\widetilde{K}) - G_{0,4}^{-1}(K)\right] \\
&= \Omega\gamma_1^0(-K, -\widetilde{K}) + i\mathrm{div}_{\mathbf{q}}\boldsymbol{\gamma}_1(-K, -\widetilde{K}) \\
&\quad + \Delta_2^2 G_{0,4}(\widetilde{K})\left[\Omega\gamma_4^0(\widetilde{K}, K) + i\mathrm{div}_{\mathbf{q}}\boldsymbol{\gamma}_4(\widetilde{K}, K)\right] G_{0,4}(K). \qquad \text{(C.9)}
\end{aligned}
$$

$$
\begin{aligned}
G_{1,2}^{-1}(-K) - G_{1,2}^{-1}(-\widetilde{K}) &= G_{0,2}^{-1}(-K) - G_{0,2}^{-1}(-\widetilde{K}) \\
&\quad + \Delta_1^2 G_{0,3}(K) G_{0,3}(\widetilde{K}) \left[G_{0,3}^{-1}(\widetilde{K}) - G_{0,3}^{-1}(K) \right] \\
&= \Omega \gamma_2^0(-K, -\widetilde{K}) + i \mathrm{div}_{\mathbf{q}} \boldsymbol{\gamma}_2(-K, -\widetilde{K}) \\
&\quad + \Delta_1^2 G_{0,3}(\widetilde{K}) \left[\Omega \gamma_3^0(\widetilde{K}, K) + i \mathrm{div}_{\mathbf{q}} \boldsymbol{\gamma}_3(\widetilde{K}, K) \right] G_{0,3}(K). \qquad \text{(C.10)}
\end{aligned}
$$

$$
\begin{aligned}
G_{1,3}^{-1}(\widetilde{K}) - G_{1,3}^{-1}(K) &= G_{0,3}^{-1}(\widetilde{K}) - G_{0,3}^{-1}(K) \\
&\quad + \Delta_1^2 G_{0,2}(-K) G_{0,2}(-\widetilde{K}) \left[G_{0,2}^{-1}(-K) - G_{0,2}(-\widetilde{K}) \right] \\
&= \Omega \gamma_3^0(\widetilde{K}, K) + i \mathrm{div}_{\mathbf{q}} \boldsymbol{\gamma}_3(\widetilde{K}, K) \\
&\quad + \Delta_1^2 G_{0,2}(-K) \left[\Omega \gamma_2^0(-K, -\widetilde{K}) + i \mathrm{div}_{\mathbf{q}} \boldsymbol{\gamma}_2(-K, -\widetilde{K}) \right] G_{0,2}(-\widetilde{K}).
\end{aligned}
\qquad \text{(C.11)}
$$

$$
\begin{aligned}
G_{1,4}^{-1}(\widetilde{K}) - G_{1,4}^{-1}(K) &= G_{0,4}^{-1}(\widetilde{K}) - G_{0,4}^{-1}(K) \\
&\quad + \Delta_2^2 G_{0,1}(-K) G_{0,1}(-\widetilde{K}) \left[G_{0,1}^{-1}(-K) - G_{0,1}^{-1}(-\widetilde{K}) \right] \\
&= \Omega \gamma_4^0(\widetilde{K}, K) + i \mathrm{div}_{\mathbf{q}} \boldsymbol{\gamma}_4(\widetilde{K}, K) \\
&\quad + \Delta_2^2 G_{0,1}(-K) \left[\Omega \gamma_1^0(-K, -\widetilde{K}) + i \mathrm{div}_{\mathbf{q}} \boldsymbol{\gamma}_1(-K, -\widetilde{K}) \right] G_{0,1}(-\widetilde{K}).
\end{aligned}
\qquad \text{(C.12)}
$$

In the last step in each of these expressions we have used the bare WTI's. This procedure reduces the terms in square brackets in Eq. (C.8) to a contraction of the time component and vector component of a bare vertex. Since the full WTI involves a similar contraction of the time component and vector component of the full vertex, we can assert then that the vertices appearing above are contributions to the full vertex. Performing this procedure for all terms in Eq. (C.8) then allows us to extract the full vertex via Eq. (C.7).

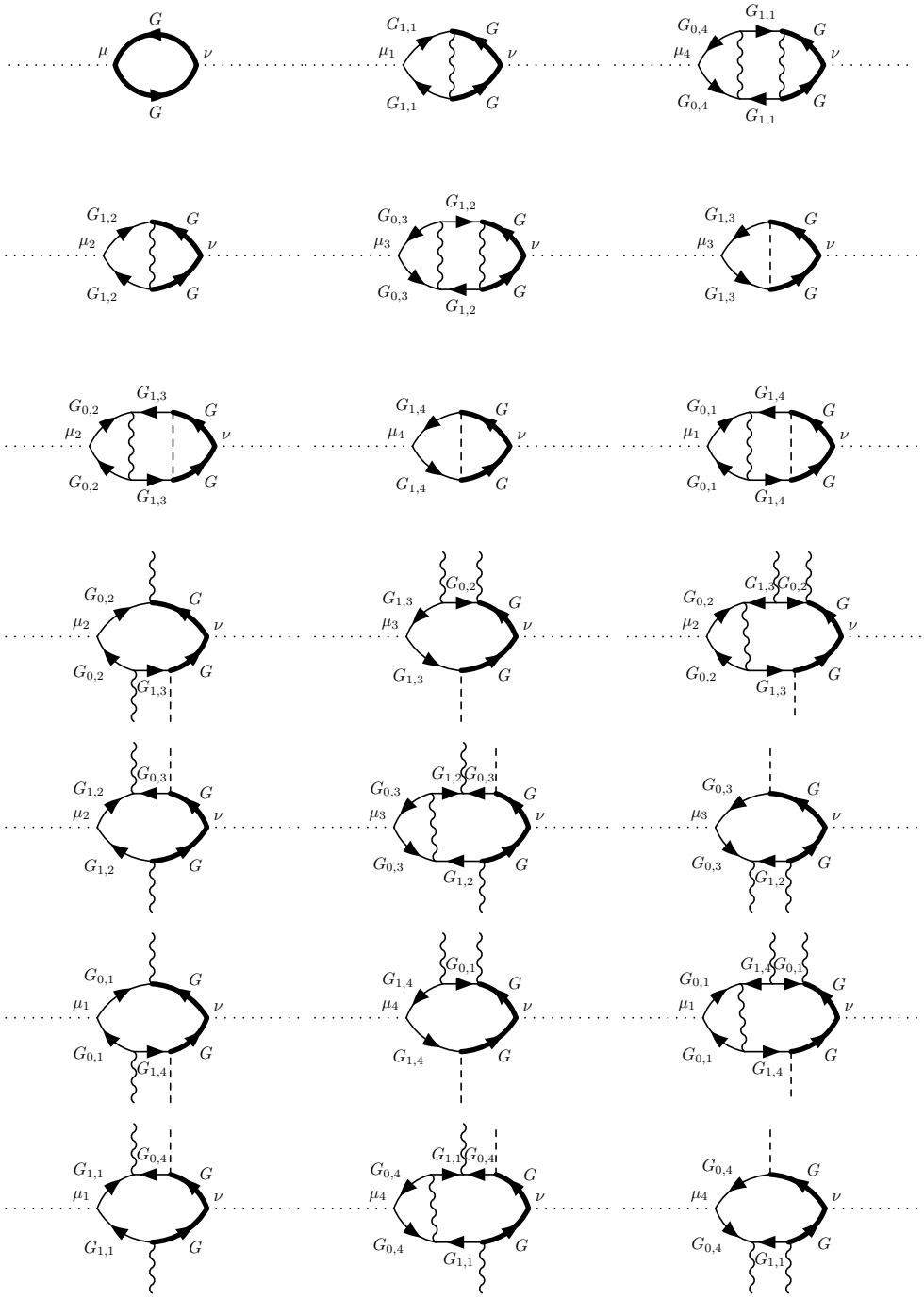

Figure C.1: All twenty one Feynman diagrams which contribute to the response functions $P^{\mu\nu}(Q)$. The wavy lines denote either Δ_1 or Δ_2, whereas the dashed lines denote either C_1 or C_2. The various Green's functions are labeled. The order of the Feynman diagrams, from left to right and top to bottom, corresponds to the terms appearing in Eq. (C.13).

This gives the full vertex as

$$
\begin{aligned}
&\Gamma^{\mu}(\widetilde{K},K)\\
&=\gamma^{\mu}(\widetilde{K},K)\\
&\quad+\Delta_1^2 G_{1,1}(-K)\left[\gamma_1^{\mu}(-K,-\widetilde{K})+\Delta_2^2 G_{0,4}(\widetilde{K})\gamma_4^{\mu}(\widetilde{K},K)G_{0,4}(K)\right]G_{1,1}(-\widetilde{K})\\
&\quad+\Delta_2^2 G_{1,2}(-K)\left[\gamma_2^{\mu}(-K,-\widetilde{K})+\Delta_1^2 G_{0,3}(\widetilde{K})\gamma_3^{\mu}(\widetilde{K},K)G_{0,3}(K)\right]G_{1,2}(-\widetilde{K})\\
&\quad+C_1^2 G_{1,3}(\widetilde{K})\left[\gamma_3^{\mu}(\widetilde{K},K)+\Delta_1^2 G_{0,2}(-K)\gamma_2^{\mu}(-K,-\widetilde{K})G_{0,2}(-\widetilde{K})\right]G_{1,3}(K)\\
&\quad+C_2^2 G_{1,4}(\widetilde{K})\left[\gamma_4^{\mu}(\widetilde{K},K)+\Delta_2^2 G_{0,1}(-K)\gamma_1^{\mu}(-K,-\widetilde{K})G_{0,1}(-\widetilde{K})\right]G_{1,4}(K)\\
&\quad+\Delta_1\Delta_2 C_1 G_{1,3}(K)G_{0,2}(-K)\gamma_2^{\mu}(-K,-\widetilde{K})G_{0,2}(-\widetilde{K})\\
&\quad-\Delta_1\Delta_2 C_1 G_{0,2}(-\widetilde{K})G_{1,3}(\widetilde{K})\left[\gamma_3^{\mu}(\widetilde{K},K)+\Delta_1^2 G_{0,2}(-K)\gamma_2^{\mu}(-K,-\widetilde{K})G_{0,2}(-\widetilde{K})\right]G_{1,3}(K)\\
&\quad+\Delta_1\Delta_2 C_1 G_{1,2}(-K)\left[\gamma_2^{\mu}(-K,-\widetilde{K})+\Delta_1^2 G_{0,3}(\widetilde{K})\gamma_3^{\mu}(\widetilde{K},K)G_{0,3}(K)\right]G_{1,2}(-\widetilde{K})G_{0,3}(\widetilde{K})\\
&\quad-\Delta_1\Delta_2 C_1 G_{0,3}(\widetilde{K})\gamma_3^{\mu}(\widetilde{K},K)G_{0,3}(K)G_{1,2}(-K)\\
&\quad+\Delta_1\Delta_2 C_2 G_{1,4}(K)G_{0,1}(-K)\gamma_1^{\mu}(-K,-\widetilde{K})G_{0,1}(-\widetilde{K})\\
&\quad-\Delta_1\Delta_2 C_2 G_{0,1}(-\widetilde{K})G_{1,4}(\widetilde{K})\left[\gamma_4^{\mu}(\widetilde{K},K)+\Delta_2^2 G_{0,1}(-K)\gamma_1^{\mu}(-K,-\widetilde{K})G_{0,1}(-\widetilde{K})\right]G_{1,4}(K)\\
&\quad+\Delta_1\Delta_2 C_2 G_{1,1}(-K)\left[\gamma_1^{\mu}(-K,-\widetilde{K})+\Delta_2^2 G_{0,4}(\widetilde{K})\gamma_4^{\mu}(\widetilde{K},K)G_{0,4}(K)\right]G_{1,1}(-\widetilde{K})G_{0,4}(\widetilde{K})\\
&\quad-\Delta_1\Delta_2 C_2 G_{0,4}(\widetilde{K})\gamma_4^{\mu}(\widetilde{K},K)G_{0,4}(K)G_{1,1}(-K). \qquad \text{(C.13)}
\end{aligned}
$$

Given the full and bare vertices $\Gamma^{\mu},\gamma^{\nu}$, the full response functions are then

$$P^{\mu\nu}(Q)=2\sum_K G(\widetilde{K})\Gamma^{\mu}(\widetilde{K},K)G(K)\gamma^{\nu}(K,\widetilde{K}). \qquad \text{(C.14)}$$

There are twenty one Feynman diagrams, shown in Figure (C.1), which contribute to the response functions. In the more general case of wave-vector-dependent gaps, there are additional terms involving the derivatives of the gap, which, in the 3×3 reduced Hamiltonian theory give an essentially negligible contribution [see section (4.3)]. The response functions are completely specified once the various bare vertices are given. We have to rely on the semi-classical approximation to

obtain the form of the bare vertices associated with the current. In the limit $\mathbf{q} \to 0$, this approximation becomes rigorously correct.

C.2 Relation between sum rules and the Ward-Takahashi identity

C.2.1 f-sum rule

The exact response functions are determined from Eq. (C.14). (We take the density-density correlation function to be $P_{\rho\rho}(Q) = P^{00}(Q)$ and the current-current correlation function is $\overleftrightarrow{P}(Q) = P^{ij}(Q)$, $i, j \in \{1, 2, 3\}$.) In section (4.2) we assert that, given bare and full vertices that satisfy the associated WTI, the following f-sum rule is satisfied

$$\int \frac{d\omega}{\pi}(-\omega \mathrm{Im} P^{00}(Q)) = 2\sum_{\mathbf{k}} n_{\mathbf{k}}(\xi_{\mathbf{k}+\mathbf{q}} + \xi_{\mathbf{k}-\mathbf{q}} - 2\xi_{\mathbf{k}}), \tag{C.15}$$

where $n_{\mathbf{k}} = T\sum_{i\omega} G(K)$. This sum rule can be established as follows.

The WTI for the full and bare vertices Ryder [1996], $\Gamma^{\mu}(\widetilde{K}, K) = (\Gamma^0(\widetilde{K}, K), \mathbf{\Gamma}(\widetilde{K}, K))$ and $\gamma^{\mu}(\widetilde{K}, K) = (1, \boldsymbol{\gamma}(\widetilde{K}, K))$ are

$$\begin{aligned} \Omega\Gamma^0 + i\mathrm{div}_{\mathbf{q}}\mathbf{\Gamma} &= G^{-1}(\widetilde{K}) - G^{-1}(K), \\ \Omega + i\mathrm{div}_{\mathbf{q}}\boldsymbol{\gamma} &= G_0^{-1}(\widetilde{K}) - G_0^{-1}(K) = \Omega - \xi_{\mathbf{k}+\mathbf{q}} + \xi_{\mathbf{k}}. \end{aligned} \tag{C.16}$$

The response kernel is defined as $K^{\mu\nu}(Q) = P^{\mu\nu}(Q) + \left(\frac{n}{m}\right)^{\mu\nu}_{\mathrm{dia}}(1 - \delta_{0,\nu}\delta_{\mu,\nu})$, where there is no summation over indices in the second term. Applying the WTI to $P^{\mu 0}$ while setting $\nu = 0$ the result is

$$\Omega P^{00} + i\mathrm{div}_{\mathbf{q}} P^{i0} = 2\sum_{K} G(\widetilde{K})G(K)[G^{-1}(\widetilde{K}) - G^{-1}(K)] = 0. \tag{C.17}$$

If we set $\nu = j = \{1, 2, 3\}$ and apply the WTI to $P^{\mu j}$ the result is

$$\Omega P^{0j} + i\mathrm{div}_{\mathbf{q}} P^{ij} = 2\sum_{K} G(K)[\boldsymbol{\gamma}(K, \widetilde{K}) - \boldsymbol{\gamma}(K - Q, K)]. \tag{C.18}$$

Setting $\Omega = 0$ and then operating with $i\mathrm{div}_{\mathbf{q}}$ gives

$$i\mathrm{div}_{\mathbf{q}} i\mathrm{div}_{\mathbf{q}} P^{ij}(\mathbf{q}, 0) = 2\sum_{\mathbf{k}} n_{\mathbf{k}}[2\xi_{\mathbf{k}} - \xi_{\mathbf{k}+\mathbf{q}} - \xi_{\mathbf{k}-\mathbf{q}}]. \tag{C.19}$$

Now use the identity $\mathrm{Im}P^{i0}(\mathbf{q}, \omega) = -\mathrm{Im}P^{0i}(-\mathbf{q}, -\omega)$ and Eq. (C.17), Eq. (C.18) and Eq. (C.19) to solve for $\mathrm{Im}P^{00}$ in terms of $\mathrm{Im}P^{ij}$. By applying the Kramers-Kronig relations we then have the sum rule in Eq. (C.15). Importantly, we have proved the f-sum rule for all values of $\mathbf{q}$. This proof depends on having bare and full vertices $\gamma^{\mu}(\widetilde{K}, K)$ and $\Gamma^{\mu}(\widetilde{K}, K)$ which satisfy the Ward Takahashi identity.

C.2.2 Longitudinal sum rule

By using the relationship between $\mathrm{Im}P^{ij}$ and $\mathrm{Im}P^{00}$, along with the f-sum rule, the longitudinal sum rule is obtained. The abstract form of the longitudinal sum rule is

$$\int \frac{d\omega}{\pi}\left(-\frac{\mathrm{Im}\{i\mathrm{div}_{\mathbf{q}} i\mathrm{div}_{\mathbf{q}} \overleftrightarrow{P}(Q)\}}{\omega}\right) = 2\sum_{\mathbf{k}} n_{\mathbf{k}}(\xi_{\mathbf{k}+\mathbf{q}} + \xi_{\mathbf{k}-\mathbf{q}} - 2\xi_{\mathbf{k}}). \tag{C.20}$$

The WTI for the bare vertices implies that $i\mathrm{div}_{\mathbf{q}}\gamma = \xi_{\mathbf{k}} - \xi_{\mathbf{k}+\mathbf{q}}$. Thus by applying this identity to the vertices that appear in Eq. (C.13), the longitudinal sum rule is manifestly satisfied. While the response functions can be shown to satisfy the longitudinal sum rule based on the WTI, an explicit proof is somewhat more difficult. For free-particle dispersion there is no difficulty. The complication is due to the fact that the bare vertex $\boldsymbol{\gamma}(\widetilde{K}, K)$ can be written down only in the small $\mathbf{q}$ limit in a periodic potential. Here one imposes the semi-classical approximation, appropriate to $\mathbf{q} \to 0$, so that the bare vertices are given by

$$\gamma_i^{\mu}(\widetilde{K}, K) = \left(1, \frac{\partial \xi_{\mathbf{k}+\mathbf{q}/2,i}}{\partial \mathbf{k}}\right). \tag{C.21}$$

For example, in the case where $C_1 = C_2 = 0$, and in the limit that $\mathbf{q} \to 0$, the current-current correlation function becomes

$$\overleftrightarrow{P}(Q) = 2\sum_K G(\widetilde{K})\frac{\partial \xi_{\mathbf{k}+\mathbf{q}/2}}{\partial \mathbf{k}} G(K)\Bigg\{\frac{\partial \xi_{\mathbf{k}+\mathbf{q}/2}}{\partial \mathbf{k}}$$
$$+ \Delta_1^2 G_{1,1}(-K)G_{1,1}(-\widetilde{K})\left[-\frac{\partial \xi_{\mathbf{k}+\mathbf{q}/2,2}}{\partial \mathbf{k}} + \Delta_2^2 G_{0,4}(K)G_{0,4}(\widetilde{K})\frac{\partial \xi_{\mathbf{k}+\mathbf{q}/2,4}}{\partial \mathbf{k}}\right]$$
$$+ \Delta_2^2 G_{1,2}(-K)G_{1,2}(-\widetilde{K})\left[-\frac{\partial \xi_{\mathbf{k}+\mathbf{q}/2,1}}{\partial \mathbf{k}} + \Delta_1^2 G_{0,3}(K)G_{0,3}(\widetilde{K})\frac{\partial \xi_{\mathbf{k}+\mathbf{q}/2,3}}{\partial \mathbf{k}}\right]\Bigg\}, \quad \text{(C.22)}$$

which is in agreement with the form of $\overleftrightarrow{P}(0)$ obtained in Eq. (4.3) of section (4.1) by imposing the absence of a Meissner effect in the normal phase. The longitudinal sum rule in this particular limit reduces to

$$\int \frac{d\omega}{\pi}\left(-\frac{\mathrm{Im}\mathbf{q}\cdot\overleftrightarrow{P}(Q)\cdot\mathbf{q}}{\omega}\right) = 2\sum_{\mathbf{k}} n_{\mathbf{k}}(\xi_{\mathbf{k}+\mathbf{q}} + \xi_{\mathbf{k}-\mathbf{q}} - 2\xi_{\mathbf{k}}), \quad \text{(C.23)}$$

which is in agreement with appendix (A) of Ref. [Bergeron et al., 2011].

C.3 Spin response functions

In this section we extend our results to include spin response functions. Let $\sigma = \uparrow\downarrow$ denote spin indices with $\overline{\sigma}$ the opposite of σ. The density-density and current-current correlation functions are response functions related by the global $\mathrm{U}(1)_{\mathrm{EM}}$ symmetry and the associated Ward-Takahashi identity. The analogous spin response functions are related by the global $\mathrm{U}(1)_{\mathrm{z}}$ symmetry and the associated Ward-Takahashi identity.

The familiar global $\mathrm{U}(1)_{\mathrm{EM}}$ symmetry theory is based on the four-vector potential $A^\mu = (\phi, \mathbf{A})$. For the global $\mathrm{U}(1)_{\mathrm{z}}$ symmetry theory the external vector field is $A^\mu = (B_z, \mathbf{m})$, where $\mathbf{m}$ is the magnetization. The associated Hamiltonian describes a generalized spin-magnetic field interaction, and the Noether current for the global $\mathrm{U}(1)_{\mathrm{z}}$ symmetry is a magnetization current. An important difference between these two symmetries is that below T_c the global $\mathrm{U}(1)_{\mathrm{EM}}$ symme-

try is spontaneously broken. Therefore to restore gauge invariance collective mode effects must be incorporated. On the other hand the global $\mathrm{U}(1)_{\mathrm{z}}$ symmetry is not spontaneously broken and therefore does not require any collective physics. Since we are only considering the response functions above T_c this difference is not central to our discussion.

The bare spin vertex is denoted by $\gamma^{\mu}_{S_\sigma}(\widetilde{K}, K)$, where $S_\sigma = \pm 1$ and $S_{\bar{\sigma}} = -S_\sigma$. The bare and full Ward-Takahashi identities for the spin vertices are discussed in section (4.2) [see Eq. (4.12)]. The full spin response function, $P_S^{\mu\nu}(Q)$, is defined by

$$P_S^{\mu\nu}(Q) = \sum_{\sigma} \sum_{K} G(\widetilde{K}) \Gamma^{\mu}_{S_\sigma}(\widetilde{K}, K) G(K) \gamma^{\nu}_{S_\sigma}(K, \widetilde{K}). \tag{C.24}$$

Following chapter (4), given the form of the self energy the WTI can be used to obtain the full vertex, for both the charge and spin response functions. The procedure is equivalent to that in appendix (C.1), and so here we omit the explicit expression. We note that the spin response full vertex is obtained from the charge response full vertex [Eq. (C.13)], with the mapping $\gamma^{\mu} \to \gamma^{\mu}_{S_\sigma}$, $\gamma^{\mu}_i \to \gamma^{\mu}_{i,S_\sigma}$ etc.

The proof of the f-sum rule in appendix (C.2) can be performed for the spin response function $P_S^{00}(Q)$ in an analogous manner, by using the WTI for the spin vertices. In this case we obtain

$$\int \frac{d\omega}{\pi} (-\omega \mathrm{Im} P_S^{00}(Q)) = 2 \sum_{\mathbf{k}} n_{\mathbf{k}} (\xi_{\mathbf{k}+\mathbf{q}} + \xi_{\mathbf{k}-\mathbf{q}} - 2\xi_{\mathbf{k}}), \tag{C.25}$$

where $n_{\mathbf{k}} = T \sum_{i\omega} G(K)$ and the factor of two arises from summation over pseudo spin indices.

APPENDIX D

GAUGE INVARIANT THEORIES OF LINEAR RESPONSE FOR STRONGLY CORRELATED SUPERFLUIDS

D.1 Deriving the full electromagnetic vertex

Here we show how to apply the Ward-Takahashi identity to obtain the gauge-invariant full vertex for a given self energy. If we define the partially dressed Green's function $G_0^\alpha(k)$ by

$$(G_0^\alpha)^{-1}(k) = G_0^{-1}(k) - \alpha\Sigma_{\rm corr}(k), \tag{D.1}$$

where $\Sigma_{\rm corr}$ is a self energy describing strong correlations, then the class of self-energies considered in chapter (5) are of the form

$$\Sigma(k) = \Sigma_{\rm corr}(k) - |\Delta_{\rm sc}|^2 G_0^\alpha(-k). \tag{D.2}$$

The second term in this expression represents the superconducting self energy $\Sigma_{\rm sc}(k) = -|\Delta_{\rm sc}|^2 G_0^\alpha(-k)$. For convenience we treat $\Delta_{\rm sc}$ and $\Delta_{\rm sc}^*$ as independent degrees of freedom. This will be important in the next section, but for now it is not essential. Writing the self energy in this form shows that the second term is a BCS-like self energy, but with the bare Green's function G_0 replaced by the partially dressed Green's function G_0^α. Strict BCS theory is obtained by setting $\Sigma_{\rm corr} = 0$. The three models we will consider are the pairing pseudogap approximation [Chen et al., 2005, Norman et al., 1998], the Yang, Rice, and Zhang (YRZ) model [Yang et al., 2006], and the t-matrix model of Ref. [Perali et al., 2004]. For the pairing pseudogap approximation, $\alpha = 0, \Sigma_{\rm corr}(k) = -\Delta_{\rm pg}^2 G_0(-k)$, for the YRZ model $\alpha = 1, \Sigma_{\rm corr}(k) = -\Delta_{\rm pg}^2 G_0(-k)$, and for the t-matrix model $\alpha = 1, \Sigma_{\rm corr}(k) = \sum_l t(l) G(l-k)$.

The bare Ward-Takahashi identity is $q_\mu \gamma^\mu(k_+, k_-) = G_0^{-1}(k_+) - G_0^{-1}(k_-)$. Using this, it follows that the Ward-Takahashi identity for the full vertex is [Ryder, 1996]

$$\begin{aligned} q_\mu \Gamma^\mu(k_+, k_-) &= G^{-1}(k_+) - G^{-1}(k_-), \\ &= q_\mu \gamma^\mu(k_+, k_-) + \Sigma(k_-) - \Sigma(k_+). \end{aligned} \tag{D.3}$$

As discussed in chapter (5), both the strong correlation self energy $\Sigma_{\rm corr}$ and the superconducting self energy $\Sigma_{\rm sc}$ give rise to vertex contributions. Hence we write $\Sigma(k) = \Sigma_{\rm corr}(k) + \Sigma_{\rm sc}(k)$ and derive the vertex contributions from both self-energies separately. The strong correlation self energy gives a vertex contribution $\Lambda^\mu(k_+, k_-)$ defined by

$$q_\mu \Lambda^\mu(k_+, k_-) = \Sigma_{\rm corr}(k_-) - \Sigma_{\rm corr}(k_+). \tag{D.4}$$

The general form of this vertex depends on the specific model under consideration. In appendix (D.3) we will derive the explicit form of this vertex for three models of interest in the literature. The superconducting vertex is defined by

$$q_\mu \Gamma^\mu_{\rm sc}(k_+, k_-) = \Sigma_{\rm sc}(k_-) - \Sigma_{\rm sc}(k_+). \tag{D.5}$$

Using these definitions, the full vertex is then

$$\Gamma^\mu(k_+, k_-) = \gamma^\mu(k_+, k_-) + \Lambda^\mu(k_+, k_-) + \Gamma^\mu_{\rm sc}(k_+, k_-), \tag{D.6}$$

which can be found from the full Ward-Takahashi identity in Eq. (D.3).

We now derive the explicit form of $\Gamma^\mu_{\rm sc}$. The superconducting vertex contributions are most easily found by defining the collective mode vertices $\Pi^\mu(q)$ and $\bar{\Pi}^\mu(q)$ such that $q_\mu \Pi^\mu(q) = 2\Delta_{\rm sc}$, $q_\mu \bar{\Pi}^\mu(q) = -2\Delta^*_{\rm sc}$. For now these are left as definitions, but the explicit form of Π^μ, $\bar{\Pi}^\mu$, along with the contraction identities, are derived in section (5.2.3) and appendix (D.2), respectively.

Using the superconducting self energy given in Eq. (D.2), we then have

$$\Sigma_{\rm sc}(k_-) - \Sigma_{\rm sc}(k_+) = -\Delta^*_{\rm sc} q_\mu \Pi^\mu(q) G_0^\alpha(-k_-) - \Delta_{\rm sc} q_\mu \bar{\Pi}^\mu(q) G_0^\alpha(-k_+) \\ - |\Delta_{\rm sc}|^2 \left[G_0^\alpha(-k_+) - G_0^\alpha(-k_-)\right]. \tag{D.7}$$

The difference of the two partially dressed Green's functions is

$$G_0^\alpha(-k_+) - G_0^\alpha(-k_-) = G_0^\alpha(-k_-)\Big[G_0^{-1}(-k_-) - G_0^{-1}(-k_+) \\ + \alpha\left(\Sigma_{\rm corr}(-k_+) - \Sigma_{\rm corr}(-k_-)\right)\Big] G_0^\alpha(-k_+), \\ = G_0^\alpha(-k_-)\left[q_\mu \gamma^\mu(-k_-,-k_+) + \alpha q_\mu \Lambda^\mu(-k_-,-k_+)\right] G_0^\alpha(-k_+). \tag{D.8}$$

In the second line we have used both the bare Ward-Takahashi identity and the definition of the Λ^μ vertex. Substituting Eq. (D.7) and Eq. (D.8) into Eq. (D.5) then gives the superconducting vertex:

$$\Gamma^\mu_{\rm sc}(k_+,k_-) = -\Delta^*_{\rm sc}\Pi^\mu(q) G_0^\alpha(-k_-) - \Delta_{\rm sc}\bar{\Pi}^\mu(q) G_0^\alpha(-k_+) \\ - |\Delta_{\rm sc}|^2 G_0^\alpha(-k_-)\left[\gamma^\mu(-k_-,-k_+) + \alpha\Lambda^\mu(-k_-,-k_+)\right] G_0^\alpha(-k_+). \tag{D.9}$$

This then produces the exact gauge-invariant full vertex given in Eq. (5.8) of section (5.2.2).

$$\Gamma^\mu(k_+,k_-) = \gamma^\mu(k_+,k_-) + \Lambda^\mu(k_+,k_-) - \Delta^*_{\rm sc}\Pi^\mu(q) G_0^\alpha(-k_-) - \Delta_{\rm sc}\bar{\Pi}^\mu(q) G_0^\alpha(-k_+) \\ - |\Delta_{\rm sc}|^2 G_0^\alpha(-k_-)[\gamma^\mu(-k_-,-k_+) + \alpha\Lambda^\mu(-k_-,-k_+)] G_0^\alpha(-k_+). \tag{D.10}$$

From the above expression it is clear that if $\Sigma_{\rm corr} = 0 \Rightarrow \Lambda^\mu = 0$, then the full vertex reduces to the BCS full vertex [Guo et al., 2013a, He & Guo, 2015]. Similarly if $\Delta_{\rm sc} = 0$, then the full vertex reduces to the form of the full vertex for the normal phase with pairing [Boyack et al., 2014, Scherpelz et al., 2014]. In order to uniquely determine the full vertex, the collective mode vertices $\Pi^\mu(q)$, $\bar{\Pi}^\mu(q)$ and the vertex correction $\Lambda^\mu(k_+,k_-)$ must be determined.

D.2 Collective mode vertices

In this section we verify the collective mode vertices $\Pi^\mu(q)$ and $\bar{\Pi}^\mu(q)$ satisfy the following conditions required for gauge invariance: $q_\mu \Pi^\mu(q) = 2\Delta_{\rm sc}$, $q_\mu \bar{\Pi}^\mu(q) = -2\Delta^*_{\rm sc}$, which was assumed in the previous section. These vertices are conveniently expressed as a matrix equation if we define the two-point correlation functions

$$Q_{+-}(q) = 1/g - \sum_k G(k_+) G_0^\alpha(-k_-) \left[1 - \Delta^*_{\rm sc} F_{\rm sc}(k_-)\right], \tag{D.11}$$

$$Q_{-+}(q) = 1/g - \sum_k G(k_-) G_0^\alpha(-k_+) \left[1 - \Delta_{\rm sc} F^*_{\rm sc}(k_+)\right], \tag{D.12}$$

$$Q_{++}(q) = \sum_k F_{\rm sc}(k_+) F_{\rm sc}(k_-) = Q^*_{--}(q), \tag{D.13}$$

$$\begin{aligned} P^\mu_+(q) = &\sum_k \left[\gamma^\mu(k_+, k_-) + \Lambda^\mu(k_+, k_-)\right] G(k_+) F_{\rm sc}(k_-) \\ &+ \sum_k \left[\gamma^\mu(-k_-, -k_+) + \alpha \Lambda^\mu(-k_-, -k_+)\right] F_{\rm sc}(k_+) G_0^\alpha(-k_-) \left[1 - \Delta^*_{\rm sc} F_{\rm sc}(k_-)\right], \end{aligned} \tag{D.14}$$

$$\begin{aligned} P^\mu_-(q) = &\sum_k \left[\gamma^\mu(k_+, k_-) + \Lambda^\mu(k_+, k_-)\right] F^*_{\rm sc}(k_+) G(k_-) \\ &+ \sum_k \left[\gamma^\mu(-k_-, -k_+) + \alpha \Lambda^\mu(-k_-, -k_+)\right] G_0^\alpha(-k_+) F^*_{\rm sc}(k_-) \left[1 - \Delta_{\rm sc} F^*_{\rm sc}(k_+)\right]. \end{aligned} \tag{D.15}$$

From Eqs. (5.10-5.11) of section (5.2.3), the collective mode vertices can then be written as

$$\begin{pmatrix} \Pi^\mu \\ \bar{\Pi}^\mu \end{pmatrix} = \begin{pmatrix} Q_{+-} & Q_{++} \\ Q_{--} & Q_{-+} \end{pmatrix}^{-1} \begin{pmatrix} P^\mu_+ \\ P^\mu_- \end{pmatrix}. \tag{D.16}$$

We now contract each side of Eq. (D.16) with q_μ. In order to calculate the right-hand side, we calculate the contraction $q_\mu P^\mu_\pm(q)$:

$$\begin{aligned} q_\mu P^\mu_+(q) = q_\mu \sum_k \left[\gamma^\mu(k_+,k_-) + \Lambda^\mu(k_+,k_-)\right] G(k_+) F_{\rm sc}(k_-) \\ + q_\mu \sum_k \left[\gamma^\mu(-k_-,-k_+) + \alpha\Lambda^\mu(-k_-,-k_+)\right] F_{\rm sc}(k_+) G_0^\alpha(-k_-)[1-\Delta^*_{\rm sc}F_{\rm sc}(k_-)]. \end{aligned} \tag{D.17}$$

Explicit calculation shows that both lines have the same value, so that

$$\begin{aligned} q_\mu P^\mu_+(q) &= 2\Bigg[\Delta_{\rm sc}\left(1/g - \sum_k G(k_+)G_0^\alpha(-k_-)[1-\Delta^*_{\rm sc}F_{\rm sc}(k_-)]\right) \\ &\quad - \Delta^*_{\rm sc}\sum_k F_{\rm sc}(k_-)F_{\rm sc}(k_+)\Bigg], \\ &= 2\left(\Delta_{\rm sc}Q_{+-} - \Delta^*_{\rm sc}Q_{++}\right). \end{aligned} \tag{D.18}$$

Similarly, since $\Delta^*_{\rm sc}P^\mu_+(q) = \Delta_{\rm sc}P^\mu_-(-q)$, we also find $q_\mu P^\mu_-(q) = -\left(q_\mu P^\mu_+(q)\right)^*$. The contractions of the collective mode vertices are then

$$\begin{pmatrix} q_\mu\Pi^\mu \\ q_\mu\bar\Pi^\mu \end{pmatrix} = \begin{pmatrix} Q_{+-} & Q_{++} \\ Q_{--} & Q_{-+} \end{pmatrix}^{-1} \begin{pmatrix} 2\left(\Delta_{\rm sc}Q_{+-} - \Delta^*_{\rm sc}Q_{++}\right) \\ -2\left(\Delta^*_{\rm sc}Q_{-+} - \Delta_{\rm sc}Q_{--}\right) \end{pmatrix} = \begin{pmatrix} 2\Delta_{\rm sc} \\ -2\Delta^*_{\rm sc} \end{pmatrix}. \tag{D.19}$$

This confirms that, for all $q^\mu \neq 0$, we have the desired relations

$$q_\mu\Pi^\mu(q) = 2\Delta_{\rm sc}, \quad q_\mu\bar\Pi^\mu(q) = -2\Delta^*_{\rm sc}. \tag{D.20}$$

Finally, we now show that at $q = 0$ the gap equation is consistent with the poles of the collective mode vertices. These poles are given by the solution of $\det(Q_{ab}) = Q_{+-}Q_{-+} - Q_{++}Q_{--} = 0$, which arises when taking the matrix inverse of Eq. (D.16). Let $q = 0$, and suppose $\Delta_{\rm sc} = \Delta^*_{\rm sc}$, then the poles occur when $Q_{+-} - Q_{++} = 0$. Using the expressions in Eqs. (D.11-D.13), and the

definition of $F_{\rm sc}(k)$, this reduces to

$$1 - g \sum_k G_0^\alpha(-k) G(k) = 0, \tag{D.21}$$

which is the gap equation.

In summary, we have obtained the collective mode vertices and thus obtained the gauge-invariant full vertex. The next section determines the form of the Λ^μ vertex for three example cases of $\Sigma_{\rm corr}$.

D.3 Specific examples for the Λ^μ vertex correction

D.3.1 Pairing pseudogap approximation

In the pairing pseudogap approximation [Chen et al., 2005, Norman et al., 1998], $\Sigma_{\rm corr}(k) = -\Delta_{\rm pg}^2 G_0(-k)$, which implies that

$$\begin{aligned} q_\mu \Lambda^\mu(k_+, k_-) &= \Sigma_{\rm corr}(k_-) - \Sigma_{\rm corr}(k_+), \\ &= \Delta_{\rm pg}^2 G_0(-k_-) q_\mu \gamma^\mu(-k_-, -k_+) G_0(-k_+). \end{aligned} \tag{D.22}$$

Thus, it follows that

$$\Lambda^\mu(k_+, k_-) = \Delta_{\rm pg}^2 G_0(-k_-) \gamma^\mu(-k_-, -k_+) G_0(-k_+). \tag{D.23}$$

D.3.2 YRZ

In the YRZ model [Yang et al., 2006], $\Sigma_{\rm corr}(k) = -\Delta_{\rm pg}^2 G_0(-k)$. Thus, as in the case for the pairing pseudogap approximation, we obtain

$$\Lambda^\mu(k_+, k_-) = \Delta_{\rm pg}^2 G_0(-k_-) \gamma^\mu(-k_-, -k_+) G_0(-k_+). \tag{D.24}$$

D.3.3 Particle-only t-matrix

In the t-matrix model of Ref. [Perali et al., 2004], $\Sigma_{\rm corr}(k) = \sum_l t(l)G(l-k) = \sum_l t(l+k)G(l)$. (In Ref. [Perali et al., 2004] the gap is fixed to be the BCS gap, arising from a BCS Gorkov Green's function. However, in the number equation additional correlations are added via adding $\Sigma_{\rm corr}$ to the BCS self-energy. In order to implement a consistent framework, based on Ref. [Perali et al., 2004], we take the self energy to be $\Sigma = \Sigma_{\rm corr} + \Sigma_{\rm sc}$, where $\Sigma_{\rm sc} = -|\Delta_{\rm sc}|^2 G_0^\alpha(k)$, and $\alpha = 1$. The gap is thus set to be $\Delta_{\rm sc}$ and the additional correlations are present in the number equation.) Here $G(k)$ is the full Green's function, where we define

$$\begin{aligned} G^{-1}(k) &= G_0^{-1}(k) - \Sigma(k), \\ F(k) &= \Delta_{\rm sc} G_0^\alpha(-k) G(k). \end{aligned} \tag{D.25}$$

The self energy is $\Sigma(k) = \Sigma_{\rm corr}(k) - |\Delta_{\rm sc}|^2 G_0^\alpha(-k)$, where $\Delta_{\rm sc}$ is the superconducting gap and $\alpha = 1$ in $G_0^\alpha(k)$, defined in Eq. (5.3) of section (5.2). The Gorkov Green's function satisfies $F(k) = F(-k)$.

The inverse t-matrix $t^{-1}(l)$ in the formalism of Ref. [Perali et al., 2004] is given by

$$t^{-1}(l) = \chi_{11}(l) - \chi_{22}^{-1}(l)\chi_{12}(l)\chi_{21}(l), \tag{D.26}$$

where the susceptibilities are given by

$$\begin{aligned} \chi_{11}(l) &= \frac{1}{g} - \sum_m G(l+m)G(-m), \\ \chi_{12}(l) &= \sum_m F(l+m)F^*(-m), \end{aligned} \tag{D.27}$$

where g is the standard s-wave interaction [Perali et al., 2004]. Note that $\chi_{22}(l) = \chi_{11}(-l)$, and because $F(m)$ is even, $\chi_{12}(l) = \chi_{21}^*(l) = \chi_{21}(l)$.

The vertex correction Λ^μ for this model is defined by Eq. (D.4). We now proceed to evaluate the right hand side of Eq. (D.4). From the definition of $\Sigma_{\rm corr}$, it follows that

$$\Sigma_{\rm corr}(k_-) - \Sigma_{\rm corr}(k_+) = 2\sum_l G(l)t(l+k_+)t(l+k_-)\left[t^{-1}(l+k_+) - t^{-1}(l+k_-)\right] - \sum_l t(l)G(l-k_+)G(l-k_-)\left[G^{-1}(l-k_+) - G^{-1}(l-k_-)\right]. \tag{D.28}$$

The full Green's function obeys the Ward-Takahashi identity, which defines the full vertex Γ^μ:

$$q_\mu \Gamma^\mu(k_+, k_-) = G^{-1}(k_+) - G^{-1}(k_-). \tag{D.29}$$

Equivalently, Γ^μ is given by Eq. (D.10). Thus, we now have

$$\Sigma_{\rm corr}(k_-) - \Sigma_{\rm corr}(k_+) = 2\sum_l G(l)t(l+k_+)t(l+k_-)\left[t^{-1}(l+k_+) - t^{-1}(l+k_-)\right] + \sum_l t(l)G(l-k_-)q_\mu\Gamma^\mu(l-k_-, l-k_+)G(l-k_+). \tag{D.30}$$

From the t-matrix definition in Eq. (D.26), the difference of the two inverse t-matrices is

$$t^{-1}(l+k_+) - t^{-1}(l+k_-) = \chi_{11}(l+k_+) - \chi_{11}(l+k_-) + \chi_{22}^{-1}(l+k_-)\chi_{12}(l+k_-)\chi_{21}(l+k_-) - \chi_{22}^{-1}(l+k_+)\chi_{12}(l+k_+)\chi_{21}(l+k_+). \tag{D.31}$$

For the first line of this expression we can use the Ward-Takahashi identity in Eq. (D.29) to obtain

$$\chi_{11}(l+k_+) - \chi_{11}(l+k_-) = \sum_m G(-m)G(l+m+k_+)q_\mu\Gamma^\mu(l+m+k_+, l+m+k_-)G(l+m+k_-). \tag{D.32}$$

It remains to compute the additional difference terms in Eq. (D.31). To do this, first note that

$$\begin{aligned}
&\chi_{22}^{-1}(l+k_-)\chi_{12}(l+k_-)\chi_{21}(l+k_-) - \chi_{22}^{-1}(l+k_+)\chi_{12}(l+k_+)\chi_{21}(l+k_+) \\
&= \Big\{ [\chi_{22}(l+k_+) - \chi_{22}(l+k_-)]\chi_{12}(l+k_-)\chi_{21}(l+k_-) \\
&+ [\chi_{12}(l+k_-) - \chi_{12}(l+k_+)]\chi_{22}(l+k_-)\chi_{21}(l+k_-) \\
&+ [\chi_{21}(l+k_-) - \chi_{21}(l+k_+)]\chi_{22}(l+k_-)\chi_{12}(l+k_+) \Big\} [\chi_{22}(l+k_-)\chi_{22}(l+k_+)]^{-1}. \quad \text{(D.33)}
\end{aligned}$$

This form simplifies the problem to computing the vertex insertions into both χ_{12}, χ_{21}, and χ_{22} individually, and then summing the result. Since $\chi_{22}(k) = \chi_{11}(-k)$, we can use the result in Eq. (D.32) to obtain

$$\begin{aligned}
\chi_{22}(l+k_+) - \chi_{22}(l+k_-) = &- \sum_m G(m)G(-l-m-k_-) \\
&\times q_\mu \Gamma^\mu(-l-m-k_-, -l-m-k_+)G(-l-m-k_+).
\end{aligned} \quad \text{(D.34)}$$

We now study the χ_{12} difference term in Eq. (D.33). This difference amounts to performing all possible vertex insertions into χ_{12}. If we write $\chi_{12}(k) = |\Delta_{\rm sc}|^2 \sum_m G_0^\alpha(-m-k)G(m+k)G_0^\alpha(m)G(-m)$, then it is clear there are six possible locations for vertex insertions; two full vertices can be inserted in the full Green's functions, two bare vertices can be inserted in the bare Green's functions, and two collective mode vertices can be inserted in the fluctuating gap $\Delta_{\rm sc}$ or $\Delta_{\rm sc}^*$. For convenience, in this section only, we define $\gamma_\alpha^\mu(k_+, k_-) = \gamma^\mu(k_+, k_-) + \alpha\Lambda^\mu(k_+, k_-)$.

Performing all these vertex insertions then gives the following result:

$$
\begin{aligned}
&2[\chi_{12}(l+k_+) - \chi_{12}(l+k_-)] \\
&= q_\mu \bar{\Pi}^\mu(q) \sum_m G_0^\alpha(m+q) G(-m) F(m+l+k_+) \\
&+ q_\mu \Pi^\mu(q) \sum_m G_0^\alpha(-m-l-k_-) G(m+l+k_+) F^*(m) \\
&+ q_\mu \Pi^\mu(q) \sum_m G_0^\alpha(-m-q) G(m) F^*(m+l+k_+) \\
&+ q_\mu \bar{\Pi}^\mu(q) \sum_m G_0^\alpha(m+l+k_-) G(-m-l-k_+) F(m) \\
&+ \sum_m F^*(m) [G_0^\alpha(-m-l-k_-) q_\mu \gamma_\alpha^\mu(-m-l-k_-, -m-l-k_+) F(m+l+k_+) \\
&\quad - G(m+l+k_+) q_\mu \Gamma^\mu(m+l+k_+, m+l+k_-) F(m+l+k_-)] \\
&+ \sum_m F(m) [G(-m-l-k_+) q_\mu \Gamma^\mu(-m-l-k_-, -m-l-k_+) F^*(m+l+k_-) \\
&\quad - G_0^\alpha(m+l+k_-) q_\mu \gamma_\alpha^\mu(m+l+k_+, m+l+k_-) F^*(m+l+k_+)].
\end{aligned}
\tag{D.35}
$$

Here we have introduced the collective mode vertices $\Pi^\mu(q), \bar{\Pi}^\mu(q)$, which satisfy $q_\mu \Pi^\mu(q) = 2\Delta_{\rm sc}, q_\mu \bar{\Pi}^\mu(q) = -2\Delta_{\rm sc}^*$. These are the collective mode vertices discussed in section (5.2.3). Since $\chi_{12} = \chi_{21}$, the same result derived above holds for χ_{21}.

We can now combine all the previous results from this subsection and define the following vertices

$$v_{11}^{\mu}(l+k_+,l+k_-)=\sum_m G(-m)G(l+m+k_+)\Gamma^{\mu}(l+m+k_+,l+m+k_-)G(l+m+k_-)$$

$$+\sum_m G(l+m+k_+)G(-m)\Gamma^{\mu}(-m,-m-q)G(-m-q), \tag{D.36}$$

$$v_{22}^{\mu}(l+k_+,l+k_-)=-\frac{\chi_{12}(l+k_-)\chi_{21}(l+k_-)}{\chi_{22}(l+k_-)\chi_{22}(l+k_+)}\Bigg\{$$

$$\sum_m G(m)G(-l-m-k_-)\Gamma^{\mu}(-l-m-k_-,-l-m-k_+)G(-l-m-k_+)$$

$$+\sum_m G(-l-m-k_-)G(m)\Gamma^{\mu}(m,m-q)G(m-q)\Bigg\}, \tag{D.37}$$

$$v_{12}^{\mu}(l+k_+,l+k_-)=-\frac{\chi_{21}(l+k_-)}{\chi_{22}(l+k_+)}\Bigg\{\bar{\Pi}^{\mu}(q)\sum_m G_0^{\alpha}(m+q)G(-m)F(m+l+k_+)$$

$$+\Pi^{\mu}(q)\sum_m G_0^{\alpha}(-m-l-k_-)G(m+l+k_+)F^*(m)$$

$$+\Pi^{\mu}(q)\sum_m G_0^{\alpha}(-m-q)G(m)F^*(m+l+k_+)$$

$$+\bar{\Pi}^{\mu}(q)\sum_m G_0^{\alpha}(m+l+k_-)G(-m-l-k_+)F(m)$$

$$+\sum_m F^*(m)[G_0^{\alpha}(-m-l-k_-)\gamma_{\alpha}^{\mu}(-m-l-k_-,-m-l-k_+)F(m+l+k_+)$$

$$-G(m+l+k_+)\Gamma^{\mu}(m+l+k_+,m+l+k_-)F(m+l+k_-)]$$

$$+\sum_m F(m)[G(-m-l-k_+)\Gamma^{\mu}(-m-l-k_-,-m-l-k_+)F^*(m+l+k_-)$$

$$-G_0^{\alpha}(m+l+k_-)\gamma_{\alpha}^{\mu}(m+l+k_+,m+l+k_-)F^*(m+l+k_+)]\Bigg\}, \tag{D.38}$$

$$v_{21}^{\mu}(l+k_+,l+k_-)=\frac{\chi_{12}(l+k_+)}{\chi_{21}(l+k_-)}v_{12}^{\mu}(l+k_+,l+k_-). \tag{D.39}$$

Using the definitions of these vertices, along with Eq. (D.28), finally gives the vertex $\Lambda^{\mu}(k_+, k_-)$ for the t-matrix model of Ref. [Perali et al., 2004]

$$\begin{aligned}\Lambda^{\mu}(k_+, k_-) = &\sum_l t(l)G(l-k_-)\Gamma^{\mu}(l-k_-, l-k_+)G(l-k_+) \\ &+ \sum_l G(l)t(l+k_+)\Big[v^{\mu}_{11}(l+k_+, l+k_-) + v^{\mu}_{12}(l+k_+, l+k_-) \\ &+ v^{\mu}_{21}(l+k_+, l+k_-) + v^{\mu}_{22}(l+k_+, l+k_-)\Big]t(l+k_-). \end{aligned} \tag{D.40}$$

It can be shown this vertex does indeed satisfy $q_{\mu}\Lambda^{\mu}(k_+, k_-) = \Sigma_{\rm corr}(k_-) - \Sigma_{\rm corr}(k_+)$. Diagrammatically, the first term in this expression is a Maki-Thompson (MT) diagram. The first term in the square brackets of the second line represents two identical Aslamazov-Larkin (AL) diagrams [He & Guo, 2015]. Similarly the fourth term in square brackets is similar to two identical Aslamazov-Larkin diagrams. The second and third terms in square brackets are additional diagrams which must be retained in order to satisfy the gauge-invariance condition $q_{\mu}\Lambda^{\mu}(k_+, k_-) = \Sigma_{\rm corr}(k_-) - \Sigma_{\rm corr}(k_+)$.

D.4 f-sum rule and longitudinal sum rule

In this section we show that, given bare and full vertices that satisfy the Ward-Takahashi identity, the density and current response functions satisfy the f- and longitudinal sum rules, respectively.

The exact response function is constructed from a two point correlation function containing one full vertex, $\Gamma^{\mu}(k_+, k_-) = (\Gamma^0(k_+, k_-), \mathbf{\Gamma}(k_+, k_-))$, and one bare vertex $\gamma^{\nu}(k_+, k_-) = (\gamma^0(k_+, k_-), \boldsymbol{\gamma}(k_+, k_-))$:

$$P^{\mu\nu}(q) = 2\sum_k G(k_+)\Gamma^{\mu}(k_+, k_-)G(k_-)\gamma^{\nu}(k_-, k_+). \tag{D.41}$$

To show consistency with sum rules, we use the Ward-Takahashi identity [as in Eq. (D.3)]

$$q_\mu \Gamma^\mu(k_+, k_-) = G^{-1}(k_+) - G^{-1}(k_-). \tag{D.42}$$

Contracting the response function with q_μ, and using the Ward-Takahashi identity, we then have

$$\begin{aligned} q_\mu P^{\mu\nu}(q) &= 2\sum_k G(k_+)[G^{-1}(k_+) - G^{-1}(k_-)]G(k_-)\gamma^\nu(k_-, k_+), \\ &= 2\sum_k G(k)[\gamma^\nu(k, k+q) - \gamma^\nu(k-q, k)]. \end{aligned} \tag{D.43}$$

The $\nu = 0$ component of the bare vertex is equal to one, so that

$$q_\mu P^{\mu 0}(q) = 0 \tag{D.44}$$

On the other hand, the spatial components $\nu = j \in \{1, 2, 3\}$ are

$$\begin{aligned} q_\mu P^{\mu j}(q) &= 2\sum_k G(k)[\boldsymbol{\gamma}(k, k+q) - \boldsymbol{\gamma}(k-q, k)], \\ &= \frac{n}{m}\mathbf{q}. \end{aligned} \tag{D.45}$$

Here we used the fact that $\boldsymbol{\gamma}(k, k+q) - \boldsymbol{\gamma}(k-q, k) = \mathbf{q}/m$ is independent of $\mathbf{k}$, and $2\sum_k G(k) = 2\sum_{\mathbf{k}} n_{\mathbf{k}} = n$.

In terms of components, and real frequencies, these equations become

$$\omega P^{00}(\omega, \mathbf{q}) - \mathbf{q} \cdot \mathbf{P}^{i0}(\omega, \mathbf{q}) = 0, \tag{D.46}$$

$$\omega \mathbf{P}^{0j}(\omega, \mathbf{q}) - \mathbf{q} \cdot \overleftrightarrow{P}^{ij}(\omega, \mathbf{q}) = \frac{n}{m}\mathbf{q}. \tag{D.47}$$

Setting $\omega = 0$ and then operating with $-\mathbf{q}$ (on the right) in Eq. (D.47) gives

$$\mathbf{q} \cdot \overleftrightarrow{P}^{ij}(0, \mathbf{q}) \cdot \mathbf{q} = -\frac{n}{m}\mathbf{q} \cdot \mathbf{q}. \tag{D.48}$$

Now use the identity Im $P^{i0}(\omega, \mathbf{q}) = -\text{Im } P^{0i}(-\omega, -\mathbf{q})$ and Eq. (D.46), Eq. (D.47) to solve for Im P^{00} in terms of Im $\overleftrightarrow{P}^{ij}$. Applying the Kramers-Kronig relations and Eq. (D.48) then gives

$$\begin{aligned}\int \frac{d\omega}{\pi}(-\omega \text{Im } P^{00}(\omega, \mathbf{q})) &= \int \frac{d\omega}{\pi}\left(-\frac{\mathbf{q} \cdot \text{Im } \overleftrightarrow{P}^{ij}(\omega, \mathbf{q}) \cdot \mathbf{q}}{\omega}\right) \\ &= -\mathbf{q} \cdot \text{Re } \overleftrightarrow{P}^{ij}(0, \mathbf{q}) \cdot \mathbf{q} \\ &= \frac{n}{m}\mathbf{q} \cdot \mathbf{q}. \end{aligned} \tag{D.49}$$

The density-density and current-current response functions are respectively defined by $\chi_{\rho\rho}(q) \equiv P^{00}(q)$, $\overleftrightarrow{\chi}_{JJ}(q) \equiv P^{ij}(q), i, j \in \{1, 2, 3\}$. The f-sum rule is then

$$\int \frac{d\omega}{\pi}(-\omega \text{Im } \chi_{\rho\rho}(\omega, \mathbf{q})) = \frac{n}{m}\mathbf{q} \cdot \mathbf{q}. \tag{D.50}$$

Similarly the longitudinal sum rule is

$$\int \frac{d\omega}{\pi}\left(-\frac{\mathbf{q} \cdot \text{Im } \overleftrightarrow{\chi}_{JJ}(\omega, \mathbf{q}) \cdot \mathbf{q}}{\omega}\right) = \frac{n}{m}\mathbf{q} \cdot \mathbf{q}. \tag{D.51}$$

Therefore, provided the full vertex satisfies the Ward-Takahashi identity, both sum rules will hold exactly for all $\mathbf{q}$ in this continuum limit.

APPENDIX E

GOING BEYOND THE BCS LEVEL IN THE SUPERFLUID PATH INTEGRAL: A CONSISTENT TREATMENT OF ELECTRODYNAMICS AND THERMODYNAMICS

E.1 Partition function

We now present a detailed description of the primary result in chapter (6). We start with the path integral representation of the fermionic partition function in the presence of a non-zero vector potential A_μ:

$$\mathcal{Z}[A] = \int \mathcal{D}\left[\psi^\dagger, \psi\right] e^{-S_F\left[\psi^\dagger, \psi, A_\mu\right]}, \tag{E.1}$$

where we assume a general fermionic action for a neutral superfluid

$$S_F\left[\psi^\dagger, \psi, A_\mu\right] = \int dx \int dy\, \psi_s^\dagger(x) \left(G_0^{-1}[A]\right)_{ss'}(x,y)\, \psi_{s'}(y) + g \int dx\, \psi_\uparrow^\dagger \psi_\downarrow^\dagger \psi_\uparrow \psi_\downarrow, \tag{E.2}$$

with an attractive interaction $g > 0$. The fermionic fields $\psi_s^\dagger(x)$ and $\psi_s(x)$ are Grassman fields to be integrated, whereas A_μ is a non-fluctuating external source. The non-interacting inverse Green's function is $G_0^{-1}[A](x,y)$. We assume a neutral s-wave superfluid; in a charged superfluid Coulomb interactions can be straightforwardly included at the level of the RPA [Lutchyn et al., 2008]. The extension to higher order pairings will be left to future work.

We now introduce a Hubbard-Stratonovich (HS) transformation through the identity

$$1 = \int \mathcal{D}[\mathbf{\Delta}] \exp\left[-\int dx\, \frac{|\Delta|^2}{g}\right], \tag{E.3}$$

where the functional integration measure $\int \mathcal{D}[\mathbf{\Delta}]$ is chosen to ensure the integral integrates to unity. The two complex HS fields, represented by $\mathbf{\Delta} = (\Delta, \Delta^*)$, will alternatively be denoted through $\mathbf{\Delta} = (\Delta_1, \Delta_2)$, where $\Delta_a(x)$, $a = 1, 2$ represent the two real fields. These parameterizations are connected by $\Delta_\pm(x) = \Delta_1(x) \pm i\Delta_2(x)$, where the identification $\Delta_- \equiv \Delta$ and

$\Delta_+ \equiv \Delta^*$ is consistent with the standard BCS phase convention. We can then write the partition function as

$$\mathcal{Z}[A] = \int \mathcal{D}\left[\psi^\dagger, \psi, \mathbf{\Delta}\right] e^{-S_{F+\mathrm{HS}}\left[\psi^\dagger, \psi, \mathbf{\Delta}, A_\mu\right]}, \tag{E.4}$$

where the combined fermionic and Hubbard-Stratonovich action

$$\begin{aligned} S_{F+\mathrm{HS}}\left[\psi^\dagger, \psi, \mathbf{\Delta}, A_\mu\right] = \frac{1}{2}\int dx \int dy\, \Psi^\dagger(x)\left(\mathcal{G}_0^{-1}[A](x,y) - \Sigma[\mathbf{\Delta}](x,y)\right)\Psi(y) \\ + \int dx\, \frac{|\Delta|^2}{g} \end{aligned} \tag{E.5}$$

is quadratic in the fermionic fields ψ_s, $\psi_s^\dagger$, after a shift of integration variables $\Delta \to \Delta - g\psi_\uparrow\psi_\downarrow$ and $\Delta^* \to \Delta^* - g\psi_\downarrow^\dagger\psi_\uparrow^\dagger$. Here $\Psi(x)$ is a conventional Nambu spinor and the single particle Nambu Green's function $\mathcal{G}_0^{-1}[A](x,y)$ takes the standard form [Altland & Simons, 2010]. The self-energy is: $\Sigma[\mathbf{\Delta}](x,y) = -\left(\Delta(x)\tau_+ + \Delta^*(x)\tau_-\right)\delta(x-y)$, with τ_+ (τ_-) a raising (lowering) operator in Nambu space. For notational convenience, the self energy can be expressed using the Nambu-Pauli matrices $\tau_{1,2}$ through $\Sigma[\mathbf{\Delta}] = -\left(\Delta_1\tau_1 + \Delta_2\tau_2\right)$.

After applying the HS transformation, the fermionic fields can be integrated out exactly using the standard functional integration formula for Grassman fields. The result is the fermionic partition function expressed exactly as:

$$\mathcal{Z}[A] = \int \mathcal{D}[\mathbf{\Delta}]\, e^{-\int dx\, \frac{|\Delta|^2}{g} + \mathrm{Tr}\ln\left[-\mathcal{G}^{-1}[\mathbf{\Delta}, A]\right]}. \tag{E.6}$$

Here $\mathcal{G}^{-1}[\mathbf{\Delta}, A](x,y) = \mathcal{G}_0^{-1}[A](x,y) - \Sigma[\mathbf{\Delta}](x,y)$ is the inverse Nambu Green's function, which depends on both the HS field $\mathbf{\Delta}$, and on the external vector potential A_μ. The $\mathrm{Tr}[\cdot]$ refers to the trace over both Nambu indices, along with a trace (integral) over position indices. This partition function is the starting point in Eq. (6.2) of section (6.2):

$$\mathcal{Z}[A] = \int \mathcal{D}[\mathbf{\Delta}]\, e^{-S_{\mathrm{HS}}[\mathbf{\Delta}, A]}, \tag{E.7}$$

where we define the HS action:

$$S_{\mathrm{HS}}\left[\mathbf{\Delta}, A\right] = \int dx \, \frac{\left|\Delta\right|^2}{g} - \mathrm{Tr}\ln\left[-\mathcal{G}^{-1}\left[\mathbf{\Delta}, A\right]\right]. \tag{E.8}$$

This is the standard action for a fermionic partition function expressed using the HS transformation.

E.1.1 Saddle point for $A_\mu \neq 0$

The arguments in chapter (6) require that the mean-field gap, $\mathbf{\Delta}^{\mathrm{mf}}\left[A\right]$, be calculated self-consistently in the presence of an arbitrary vector potential $A_\mu \neq 0$. The HS action above can be written as:

$$S_{\mathrm{HS}}\left[\mathbf{\Delta}, A\right] = \int dx \frac{\Delta_1^2\left(x\right) + \Delta_2^2\left(x\right)}{g} - \mathrm{Tr}\ln\left[-\mathcal{G}^{-1}\left[\mathbf{\Delta}, A\right]\left(x, x'\right)\right], \tag{E.9}$$

where the Nambu Green's function $\mathcal{G}\left[\mathbf{\Delta}, A\right]\left(x, x'\right)$ is not diagonal in position space. To derive the gap equation, one takes the saddle-point condition and evaluates at the mean-field solution $\mathbf{\Delta}^{\mathrm{mf}}\left[A\right](x)$:

$$\left.\frac{\delta S_{\mathrm{HS}}}{\delta \Delta_a\left(x\right)}\right|_{\mathbf{\Delta}^{\mathrm{mf}}[A]} = 0 = 2\frac{\Delta_a^{\mathrm{mf}}\left[A\right](x)}{g} - \mathrm{tr}\left[\mathcal{G}\left[\mathbf{\Delta}^{\mathrm{mf}}\left[A\right], A\right](x, x)\,\tau_a\right], \tag{E.10}$$

where $\mathrm{tr}\left[\cdot\right]$ refers to a trace over Nambu indices only. While a solution to this equation is not tractable in general, the non-zero vector potential dependence will be used only to determine how the gap fluctuates with respect to a change in A_μ. At the end of the calculation $A_\mu \to 0$; this allows for the mean-field gap to be calculated for $A_\mu = 0$, and no additional computational complexities arise from this formalism as compared to gauge restoring Gaussian fluctuations (GRGF.)

Alternative parameterizations

It is instructive to consider alternative parameterizations of the mean-field degrees of freedom. The above mean-field equations are two simultaneous equations for the gaps Δ_1 and Δ_2. By taking the superposition of these two equations

$$\frac{1}{2}\left(\frac{\delta S_{\mathrm{HS}}}{\delta\Delta_1(x)} \pm i\frac{\delta S_{\mathrm{HS}}}{\delta\Delta_2(x)}\right)_{\mathbf{\Delta}^{\mathrm{mf}}[A]} = \frac{\Delta_{\pm}^{\mathrm{mf}}[A](x)}{g} - \mathrm{tr}\left[\mathcal{G}\left[\mathbf{\Delta}^{\mathrm{mf}}[A], A\right](x,x)\,\tau_{\pm}\right] \tag{E.11}$$

we arrive at the well known form of the BCS gap equation for Δ^{mf} [and similarly $(\Delta^{\mathrm{mf}})^*$].

Another common parameterization of the mean-field degrees of freedom is $\Delta^{\mathrm{mf}} = \rho e^{i2\phi}$, where $\rho = \left|\Delta^{\mathrm{mf}}\right|$, and $2\phi = \arg\left(\Delta^{\mathrm{mf}}\right)$ are respectively the amplitude and phase of the mean-field gap. (We will suppress the mf superscript on ρ and ϕ for notational convenience.) Using this parameterization the Green's function can be expressed as $\mathcal{G}\left[\mathbf{\Delta}^{\mathrm{mf}}[A], A\right] = \mathcal{G}[\rho[A], \phi[A], A]$. A gauge transformation gives yet another parameterization:

$$\mathcal{G}[\rho[A], \phi[A], A](x,y) \to U(x)\,\mathcal{G}\left[\rho[A], 0, A_\mu + \partial_\mu\phi[A]\right](x,y)\,U^\dagger(y), \tag{E.12}$$

where $U(x) = \exp[-i\phi(x)\tau_z]$ is a gauge transformation matrix which "dresses" the vector potential with the phase of the mean-field gap. The variational condition can then be expressed as:

$$\frac{\delta S_{\mathrm{mf}}}{\delta\rho(x)} = 0 = 2\frac{\rho(x)}{g} - \mathrm{Tr}\left[\mathcal{G}\left[\rho[A], 0, A_\mu + \partial_\mu\phi[A]\right]\tau_1\right](x), \tag{E.13}$$

$$-\partial_\mu\frac{\delta S_{\mathrm{mf}}}{\delta\left(\partial_\mu\phi(x)\right)} = 0 = \partial_\mu \mathrm{Tr}\left[\mathcal{G}\left[\rho[A], 0, A_\mu + \partial_\mu\phi[A]\right](y,y')\,\gamma^\mu\left(y', y, x\right)\right], \tag{E.14}$$

where the current operator, or vertex function, is $\gamma^\mu\left(y', y, x\right) = \delta\mathcal{G}_0^{-1}\left(y', y\right)/\delta A_\mu(x)$. The first line is the gap equation for the amplitude of the mean-field order parameter. The second equation is the four-divergence of the average current; this gap condition is conceptually understood as the absence of currents in equilibrium.

Equations (E.13) and (E.14) follow from the functional derivative relations:

$$\frac{\delta S_{\mathrm{mf}}}{\delta A_\mu} = \frac{\delta S_{\mathrm{mf}}}{\delta\left(\partial_\mu \phi\right)}, \qquad \partial_\mu \frac{\delta S_{\mathrm{mf}}}{\delta\left(\partial_\mu \phi\right)} = -\frac{\delta S_{\mathrm{mf}}}{\delta \phi}. \tag{E.15}$$

We emphasize these relations are not generic operator identities, but are specific to gauge-invariant actions such as S_{mf}. Similar results will hold in related structures below; see discussion of Eq. (E.46) for details.

Recall that invoking the saddle-point condition requires the breaking of a *global* $\mathrm{U}(1)$ symmetry (although gauge invariance is of course preserved [Greiter, 2005].) If one uses the convention that $\Delta^{\mathrm{mf}}[0]$ is purely real then $\Delta_2^{\mathrm{mf}}[0] = 0$. It follows that the functional derivatives $\delta/\delta\Delta_1^{\mathrm{mf}} = \delta/\delta\rho$ corresponds to amplitude fluctuations, whereas $\delta/\delta\Delta_2^{\mathrm{mf}} = \rho^{-1}\,\delta/\delta\phi$ corresponds to phase fluctuations. In the limit that $\rho/E_F \ll 1$, it is known that the amplitude and phase modes decouple. However, for a non-relativistic scalar theory the Bogoliubov and Higgs modes are generically coupled for a finite mean-field amplitude [Cea et al., 2015, Zee, 2010]. Therefore, both amplitude and phase fluctuations of the gap are induced by A_μ (and therefore contribute to response.) However, phase fluctuations are necessary as well as sufficient to ensure gauge invariance of the response kernel.

E.1.2 Beyond saddle point

In order to calculate response beyond saddle point, it is necessary to calculate the partition function at the corresponding level. We generically expand the HS field through

$$\boldsymbol{\Delta} = \boldsymbol{\Delta}^{\mathrm{mf}}[A] + \boldsymbol{\eta}, \tag{E.16}$$

where $\boldsymbol{\eta} = (\eta_1, \eta_2)$ is a fluctuation around the mean-field solution. (Similar to $\boldsymbol{\Delta}$, we can also use the $\eta_\pm = \eta_1 \pm i\eta_2$ parameterization.) No assumptions are made about the size of $\boldsymbol{\eta}$ yet, but we note that it is a dynamic variable so it does not contain dependence on either the vector potential A_μ, or the mean-field solution $\boldsymbol{\Delta}^{\mathrm{mf}}[A]$. The partition function can be exactly factorized

as $\mathcal{Z}[A] = \mathcal{Z}_{\rm mf}\left[\mathbf{\Delta}^{\rm mf}[A], A\right]\mathcal{Z}_{\rm fl}\left[\mathbf{\Delta}^{\rm mf}[A], A\right]$, where

$$\mathcal{Z}_{\rm fl}\left[\mathbf{\Delta}^{\rm mf}[A], A\right] = \int \mathcal{D}[\boldsymbol{\eta}]\, e^{-S_\eta\left[\mathbf{\Delta}^{\rm mf}[A], A, \boldsymbol{\eta}\right]} \tag{E.17}$$

is the partition function describing beyond-saddle-point fluctuations, and

$$S_\eta\left[\mathbf{\Delta}^{\rm mf}[A], A, \boldsymbol{\eta}\right] = S_{\rm HS}\left[\mathbf{\Delta}^{\rm mf}[A] + \boldsymbol{\eta}, A\right] - S_{\rm HS}\left[\mathbf{\Delta}^{\rm mf}[A], A\right] \tag{E.18}$$

is the action of a fluctuation $\boldsymbol{\eta}$ around the mean-field solution. While this action is not assumed to be small, the lowest order correction is $\mathcal{O}\left(\boldsymbol{\eta}^2\right)$, since the term linear in $\boldsymbol{\eta}$ exactly vanishes by the saddle-point condition. Note also that under a gauge transformation $A_\mu \to A_\mu + \partial_\mu\alpha$, the mean-field gap transforms as $\mathbf{\Delta}^{\rm mf}[A] \to e^{2i\alpha}\mathbf{\Delta}^{\rm mf}[A]$. Therefore, after a change of variables in $\boldsymbol{\eta}$, both $\mathcal{Z}_{\rm mf}$ and $\mathcal{Z}_{\rm fl}$ are gauge invariant, provided the mean-field solution is properly gauge transformed.

If the partition function is desired at the Gaussian-fluctuation level, then the action S_η can be expanded to second order to give

$$S_\eta\left[\mathbf{\Delta}^{\rm mf}[A], A, \boldsymbol{\eta}\right] \approx \frac{1}{2}\int dx \int dy \sum_{ab} \eta_a(x)\, \widetilde{Q}^{ab}_{\rm mf}(x,y)\, \eta_b(y), \tag{E.19}$$

where $\widetilde{Q}^{ab}_{\rm mf} = \widetilde{Q}^{ab}_{\rm mf}\left[\mathbf{\Delta}^{\rm mf}[A], A\right]$ is the conventional mean-field propagator, except calculated at a gap $\mathbf{\Delta}^{\rm mf}[A]$ and non-zero A_μ. We can then integrate out the fluctuation field $\boldsymbol{\eta}$ explicitly, giving

$$\mathcal{Z}_{\rm fl}\left[\mathbf{\Delta}^{\rm mf}[A], A\right] \approx e^{-S^{(2)}_{\rm fl}\left[\mathbf{\Delta}^{\rm mf}[A], A\right]}, \tag{E.20}$$

where the well-known Gaussian-fluctuation action

$$S^{(2)}_{\rm fl}\left[\mathbf{\Delta}^{\rm mf}[A], A\right] = \frac{1}{2}{\rm Tr}\ln\left[\widetilde{Q}^{ab}_{\rm mf}\right] \tag{E.21}$$

depends on the mean-field solution $\mathbf{\Delta}^{\rm mf}[A]$ and the vector potential A_μ.

E.2 General response kernel

In chapter (6) we are interested in the gauge-invariant response kernels for both the mean-field and beyond-mean-field response. We note that a general response function is found from expanding the effective action $S_{\text{eff}}[A] = -\ln \mathcal{Z}[A]$ to second order in the vector potential A_μ [Fradkin, 2013]. From the above parameterization of the mean-field/fluctuation partition function, we find that the total effective action is linear in the saddle-point and fluctuation actions: $S_{\text{eff}}[A] = S_{\text{mf}}[A] + S_{\text{fl}}[A]$. As a result, the response kernel will also be linear in the successive approximations for $\mathcal{Z}[A]$. We write a generic effective action as $S_i[A] = -\ln \mathcal{Z}_i[A]$, where i can be eff, mf, or fl above, and expand to second order in A_μ to obtain the general response kernel, defined through:

$$K_i^{\mu\nu}(x, x') = \left.\frac{\delta^2 S_i[A]}{\delta A_\mu(x)\,\delta A_\nu(x')}\right|_{A\to 0}. \tag{E.22}$$

In what follows we will show this has the form presented in Eq. (6.5) of section (6.3).

E.2.1 Functional chain rule

By invoking the saddle-point condition, the partition function depends on the vector potential through the mean-field solution, so $\mathcal{Z}_i[A] = \mathcal{Z}_i\left[\boldsymbol{\Delta}^{\text{mf}}[A], A\right]$, where $\boldsymbol{\Delta}^{\text{mf}}[A]$ is a self-consistent mean-field gap. When taking the second order functional derivatives of S_i, an additional contribution appears due to a "functional chain rule" [Altland & Simons, 2010] arising from the dependence of the mean-field gap on the vector potential. These contributions will emerge as follows:

$$\frac{\delta S_i\left[\boldsymbol{\Delta}^{\text{mf}}[A], A\right]}{\delta A_\mu(x)} = \left(\frac{\delta S_i[\boldsymbol{\Delta}, A]}{\delta A_\mu(x)}\right)_{\boldsymbol{\Delta}^{\text{mf}}[A]} + \int dy \frac{\delta \Delta_a^{\text{mf}}[A](y)}{\delta A_\mu(x)} \left(\frac{\delta S_i[\boldsymbol{\Delta}, A]}{\delta \Delta_a(y)}\right)_{\boldsymbol{\Delta}^{\text{mf}}[A]}. \tag{E.23}$$

In this expression and below, terms such as $\left(\delta S_i[\boldsymbol{\Delta}, A]/\delta A_\mu\right)_{\boldsymbol{\Delta}^{\text{mf}}[A]}$ or $\left(\delta S_i[\boldsymbol{\Delta}, A]/\delta \Delta_a\right)_{\boldsymbol{\Delta}^{\text{mf}}[A]}$ are evaluated by differentiating only the explicit A_μ or Δ_a dependence, and then evaluating the result at $\boldsymbol{\Delta} = \boldsymbol{\Delta}^{\text{mf}}[A]$. In this way, these can be interpreted as "partial functional derivatives." We have not yet taken the $A_\mu \to 0$ limit; taking the second functional derivative, a similar procedure

results in:

$$\begin{aligned}\frac{\delta^2 S_i\left[\mathbf{\Delta}^{\mathrm{mf}}[A],A\right]}{\delta A_\mu(x)\,\delta A_\nu(x')} &= \left(\frac{\delta^2 S_i[\mathbf{\Delta},A]}{\delta A_\mu(x)\,\delta A_\nu(x')}\right)_{\mathbf{\Delta}^{\mathrm{mf}}[A]} \\ &+ \int dy \int dy' \frac{\delta\Delta_a^{\mathrm{mf}}[A](y)}{\delta A_\mu(x)} \left(\frac{\delta^2 S_i[\mathbf{\Delta},A]}{\delta\Delta_a(y)\,\delta\Delta_b(y')}\right)_{\mathbf{\Delta}^{\mathrm{mf}}[A]} \frac{\delta\Delta_b^{\mathrm{mf}}[A](y')}{\delta A_\nu(x')} \\ &+ \int dy \frac{\delta\Delta_a^{\mathrm{mf}}[A](y)}{\delta A_\mu(x)} \left(\frac{\delta^2 S_i[\mathbf{\Delta},A]}{\delta\Delta_a(y)\,\delta A_\nu(x')}\right)_{\mathbf{\Delta}^{\mathrm{mf}}[A]} \\ &+ \int dy \left(\frac{\delta^2 S_i[\mathbf{\Delta},A]}{\delta A_\mu(x)\,\delta\Delta_a(y)}\right)_{\mathbf{\Delta}^{\mathrm{mf}}[A]} \frac{\delta\Delta_a^{\mathrm{mf}}[A](y)}{\delta A_\nu(x')} \\ &+ \int dy \left(\frac{\delta S_i[\mathbf{\Delta},A]}{\delta\Delta_a(y)}\right)_{\mathbf{\Delta}^{\mathrm{mf}}[A]} \frac{\delta^2\Delta_a^{\mathrm{mf}}[A](y)}{\delta A_\mu(x)\,\delta A_\nu(x')}. \end{aligned} \tag{E.24}$$

The response is then found by applying the $A_\mu \to 0$ limit to the above equation. The result is Eq. (6.5) in section (6.3) for $i = \mathrm{mf}$, along with the functional equivalent for $i = \mathrm{fl}$.

To reproduce Eq. (6.7) of section (6.3), it is convenient to define a set of two-point correlation functions

$$\mathcal{Q}_i^{\alpha\beta}(x,x') = \left.\frac{\delta^2 S_i\left[\mathbf{\Delta}^{\mathrm{mf}},A\right]}{\delta\mathcal{A}_\alpha(x)\,\delta\mathcal{A}_\beta(x')}\right|_{A\to 0}, \tag{E.25}$$

with a generalized response vector $\mathcal{A}_\alpha = \left(\Delta_1^{\mathrm{mf}}, \Delta_2^{\mathrm{mf}}, A_\mu\right)$ which combines simultaneous gap and vector potential fluctuations. Due to the order of limits, we take $\mathbf{\Delta}^{\mathrm{mf}} \equiv \mathbf{\Delta}^{\mathrm{mf}}[0]$, and do not include any chain rule terms arising from $\mathbf{\Delta}^{\mathrm{mf}}[A]$. From here, the two-point functions in chapter (6) are $K_{0,i}^{\mu\nu} = \mathcal{Q}_i^{\mu\nu}$,$Q_i^{\mu a} = \mathcal{Q}_i^{\mu a}$, and $Q_i^{ab} = \mathcal{Q}_i^{ab}$. It is also helpful to define the first and second order gap fluctuations

$$\begin{aligned}\Pi_a^\mu(x,x') &= \left.\frac{\delta\Delta_a^{\mathrm{mf}}[A](x')}{\delta A_\mu(x)}\right|_{A\to 0}, \\ \Xi_a^{\mu\nu}(x,x',x'') &= \left.\frac{\delta^2\Delta_a^{\mathrm{mf}}[A](x')}{\delta A_\mu(x)\,\delta A_\nu(x'')}\right|_{A\to 0}, \end{aligned} \tag{E.26}$$

whose form will be calculated explicitly below.

Using these expressions, the full gauge-invariant response kernel for an action $S_i\left[\mathbf{\Delta}^{\mathrm{mf}}\left[A\right],A\right]$ is

$$\begin{aligned}
K_i^{\mu\nu}\left(x,x'\right) &= \left.\frac{\delta^2 S_i\left[\mathbf{\Delta}^{\mathrm{mf}}\left[A\right],A\right]}{\delta A_\mu\left(x\right)\delta A_\nu\left(x'\right)}\right|_{A\to 0}, \\
&= K_{0,i}^{\mu\nu}\left(x,x'\right) + \int dy \int dy' \Pi_a^\mu\left(x,y\right) Q_i^{ab}\left(y,y'\right) \Pi_b^\nu\left(x',y'\right) \\
&\quad + \int dy \left(\Pi_a^\mu\left(x,y\right) Q_i^{a\nu}\left(y,x'\right) + Q_i^{\mu a}\left(x,y\right)\Pi_a^\nu\left(x',y\right)\right) \\
&\quad + \int dy \frac{\delta S_i\left[\mathbf{\Delta}^{\mathrm{mf}},0\right]}{\delta\Delta_a^{\mathrm{mf}}\left(y\right)} \Xi_a^{\mu\nu}\left(x,y,x'\right). \qquad \text{(E.27)}
\end{aligned}$$

Since the i-index is general, this equation produces the mean-field response as derived in chapter (6) for $i=\mathrm{mf}$, where the stationary condition causes the last line in Eq. (E.27) to vanish. For a generic fluctuation action, the stationary condition may not be satisfied, and the last line may be non-zero. In this case, the second order gap fluctuation will contribute and this term is key to maintaining gauge invariance for non-stationary actions. This will be explicitly shown below.

E.2.2 Gap equation and collective mode vertices

We now use the gap equation, or saddle-point condition, to calculate the collective mode terms $\Pi_a^\mu\left(x,x'\right) = \delta\Delta_a^{\mathrm{mf}}\left[A\right]\left(x'\right)/\delta A_\mu\left(x\right)\Big|_{A\to 0}$. We start by using the saddle-point condition for the gap equation in the presence of $A_\mu \neq 0$:

$$0 = \frac{\delta S_{\mathrm{mf}}\left[\mathbf{\Delta}^{\mathrm{mf}}\left[A\right],A\right]}{\delta\Delta_a^{\mathrm{mf}}\left[A\right]\left(x'\right)}. \qquad \text{(E.28)}$$

Now take the functional derivative with respect to $\delta/\delta A_\mu\left(x\right)$ and invoke the functional chain rule:

$$\begin{aligned}
0 &= \frac{\delta}{\delta A_\mu\left(x\right)}\left(\frac{\delta S_{\mathrm{mf}}\left[\mathbf{\Delta},A\right]}{\delta\Delta_a\left(x'\right)}\right)_{\mathbf{\Delta}^{\mathrm{mf}}[A]}, \\
&= \left(\frac{\delta^2 S_{\mathrm{mf}}\left[\mathbf{\Delta},A\right]}{\delta A_\mu\left(x\right)\delta\Delta_a\left(x'\right)}\right)_{\mathbf{\Delta}^{\mathrm{mf}}[A]} + \int dy \frac{\delta\Delta_b^{\mathrm{mf}}\left[A\right]\left(y\right)}{\delta A_\mu\left(x\right)}\left(\frac{\delta^2 S_{\mathrm{mf}}\left[\mathbf{\Delta},A\right]}{\delta\Delta_b\left(y\right)\delta\Delta_a\left(x'\right)}\right)_{\mathbf{\Delta}^{\mathrm{mf}}[A]}. \qquad \text{(E.29)}
\end{aligned}$$

After taking the $A_\mu \to 0$ limit, this is expressed using the notation introduced above as:

$$0 = Q^{\mu a}_{\rm mf}\left(x, x'\right) + \int dy\, \Pi^{\mu}_{b}\left(x, y\right) Q^{ba}_{\rm mf}\left(y, x'\right). \tag{E.30}$$

This is a linear equation which can be expressed in the form $M\mathbf{x} = \mathbf{b}$; schematically $Q^{ab}_{\rm mf}(x, y)$, $\Pi^{\mu}_{b}(x, y)$, and $Q^{\mu a}_{\rm mf}\left(x, x'\right)$ take the role of the matrix M, $\mathbf{x}$, and $\mathbf{b}$ respectively. Therefore, provided $Q^{ab}_{\rm mf}(x, y)$ is invertible, we can write:

$$\Pi^{\mu}_{a}\left(x, x'\right) = -\int dy\, \left[Q^{-1}_{\rm mf}\right]_{ab}\left(x', y\right) Q^{b\mu}_{\rm mf}\left(y, x\right), \tag{E.31}$$

where $\left[Q^{-1}_{\rm mf}\right]_{ab}(x, y)$ is the inverse of the bosonic fluctuation propagator with respect to both Nambu matrix elements a, b and position matrix elements x, y, and for notational clarity we have used the relation $Q^{b\mu}_{\rm mf}(y, x) = Q^{\mu b}_{\rm mf}(x, y)$.

Note that the inverse of the two-point function $Q^{ab}_{\rm mf}(x, y)$, which can be interpreted as a bosonic propagator [Chen et al., 2005, Diener et al., 2008], will have a pole corresponding to the gap equation [Boyack et al., 2016, Guo et al., 2013a, Kosztin et al., 2000]. The collective mode terms can therefore be calculated using the textbook resolvent method [Altland & Simons, 2010] for finding Green's functions. For a translationally invariant system, it is useful to convert to momentum space: $Q^{ab}_{\rm mf}\left(q, q'\right) = Q^{ab}_{\rm mf}(q)\,\delta_{qq'} = \int dx dx'\, e^{i(qx - q'x')} Q^{ab}_{\rm mf}\left(x, x'\right)$. The inverse propagator then becomes $\left[Q^{-1}_{\rm mf}\right]_{ab}\left(q, q'\right) = \left[Q^{ab}_{\rm mf}(q)\right]^{-1}\delta_{qq'}$, that is, the matrix elements of the inverse of the propagator are given by the inverse of the 2×2 matrix $Q^{ab}_{\rm mf}(q)$ for each $q_\mu \neq 0$; the limit $q_\mu \to 0$ gives the BCS gap equation. Converting $\left[Q^{ab}_{\rm mf}(q)\right]^{-1}$ back to position space gives the inverse propagator $[Q_{\rm mf}]^{-1}_{ab}(x, y)$.

To understand the $q_\mu \to 0$ pole of the bosonic propagator, note that the collective modes must be singular in that limit. This should not be surprising since it is well known [Boyack et al., 2016, Guo et al., 2013a, Kosztin et al., 2000] that the collective modes satisfy $q_\mu \Pi^{\mu}_{a}(q) = 2i\epsilon_{ab}\Delta_b$ for all q_μ. Therefore, as $q_\mu \to 0$, $\Pi^{\mu}_{a} \sim q^\mu/q^2$ must have a simple pole to maintain a finite contraction at $q_\mu = 0$. While the collective modes for finite A_μ are in general complicated, taking $A_\mu \to 0$ in

a translationally invariant system produces the well known result:

$$\Pi_a^{\mu}\left(q\right) = -\left[Q_{\mathrm{mf}}^{ab}\left(q\right)\right]^{-1} Q_{\mathrm{mf}}^{b\mu}\left(q\right). \tag{E.32}$$

In this case, the simple pole in $\Pi_a^{\mu}\left(q\right)$ is directly inherited from the bosonic propagator $\left[Q_{\mathrm{mf}}^{ab}\left(q\right)\right]^{-1}$.

E.2.3 Second order fluctuation of $\Delta^{\mathrm{mf}}\left[A\right]$

We can calculate the second order fluctuation of the gap, denoted $\Xi_a^{\mu\nu}\left(x,x',x''\right)$, in a manner similar to that done above for $\Pi_a^{\mu}(x,y)$. The general expression involves three derivatives of the saddle-point action with respect to A_μ or Δ_a^{mf}. The calculation is a straightforward extension of the one in the previous section. The result is given by:

$$\Xi_a^{\mu\nu}\left(x,x',x''\right) \equiv \left.\frac{\delta^2\Delta_a^{\mathrm{mf}}\left[A\right]\left(x'\right)}{\delta A_\mu\left(x\right)\delta A_\nu\left(x''\right)}\right|_{A\to 0}, \tag{E.33}$$

$$\begin{aligned}
&= -\int d\xi\left[Q_{\mathrm{mf}}\right]_{aa'}^{-1}\left(x',\xi\right)\left(Q_{\mathrm{mf}}^{\mu a'\nu}\left(x,\xi,x''\right) + \int dy\Pi_b^{\mu}\left(x,y\right)Q_{\mathrm{mf}}^{ba'\nu}\left(y,\xi,x''\right)\right)\\
&\quad -\int d\xi\left[Q_{\mathrm{mf}}\right]_{aa'}^{-1}\left(x',\xi\right)\int dy'\Bigg(Q_{\mathrm{mf}}^{\mu a'b}\left(x,\xi,y'\right)\\
&\quad +\int dy\Pi_c^{\mu}\left(x,y\right)Q_{\mathrm{mf}}^{ca'b}\left(y,\xi,y'\right)\Bigg)\Pi_b^{\nu}\left(x'',y'\right),
\end{aligned} \tag{E.34}$$

where we define the three-point functions

$$Q_{\mathrm{mf}}^{\alpha\beta\gamma}\left(x,x',x''\right) = \left.\frac{\delta^3 S_{\mathrm{mf}}\left[\boldsymbol{\Delta}^{\mathrm{mf}},A\right]}{\delta\mathcal{A}_\alpha\left(x\right)\delta\mathcal{A}_\beta\left(x'\right)\delta\mathcal{A}_\gamma\left(x''\right)}\right|_{A\to 0}, \tag{E.35}$$

similarly to the two-point correlation functions in Eq. (E.25).

E.3 Proving gauge invariance

We now prove the gauge invariance of the response kernel in Eq. (E.27) for an arbitrary action $S_i\left[\mathbf{\Delta}^{\mathrm{mf}}\left[A\right],A\right]$. Before we do this, we note that by construction the effective action is gauge invariant. Therefore, a proper $A_\mu \to 0$ expansion will automatically maintain gauge invariance. Any violation of gauge invariance must be a result of an improperly calculated functional expansion. In linear response theory, the condition

$$\partial_\mu^x K_i^{\mu\nu}\left(x,x'\right)=0 \tag{E.36}$$

is necessary and sufficient for gauge invariance of a given response kernel [Fradkin, 2013].

To check the calculated response kernel in Eq. (E.27) satisfies the gauge-invariant condition above, it is useful to write:

$$\begin{aligned}K_i^{\mu\nu}\left(x,x'\right)=K_{0,i}^{\mu\nu}\left(x,x'\right)&+\int dy\,\Pi_a^\mu\left(x,y\right)Q_i^{a\nu}\left(y,x'\right)\\&+\int dy'\left(Q_i^{\mu b}\left(x,y'\right)+\int dy\,\Pi_a^\mu\left(x,y\right)Q_i^{ab}\left(y,y'\right)\right)\Pi_b^\nu\left(x',y'\right)\\&+\int dy\,\frac{\delta S_i}{\delta\Delta_a^{\mathrm{mf}}\left(y\right)}\Xi_a^{\mu\nu}\left(x,y,x'\right).\end{aligned} \tag{E.37}$$

For the $i=\mathrm{mf}$ action only, the second and third lines vanish explicitly without any contraction. If the saddle-point action is not considered, calculations of the contractions is technically involved. The calculations are presented in detail in the next section. We now present the line-by-line results of the contractions of the full response above:

$$\partial_\mu^x\left(K_{0,i}^{\mu\nu}\left(x,x'\right)+\int dy\,\Pi_a^\mu\left(x,y\right)Q_i^{a\nu}\left(y,x'\right)\right)=0, \tag{E.38}$$

$$\partial_\mu^x\left(Q_i^{\mu b}\left(x,y'\right)+\int dy\,\Pi_a^\mu\left(x,y\right)Q_i^{ab}\left(y,y'\right)\right)=-2\frac{\delta S_i}{\delta\Delta_a^{\mathrm{mf}}\left(x\right)}\epsilon_{ab}\delta\left(x-y'\right), \tag{E.39}$$

$$\partial_\mu^x\Xi_a^{\mu\nu}\left(x,y,x'\right)=2\epsilon_{ab}\delta\left(x-y\right)\Pi_b^\nu\left(x',y\right). \tag{E.40}$$

Substituting these relations into Eq. (E.37) gives the contraction of the response kernel:

$$\begin{aligned}\partial_{\mu}^{x} K_{i}^{\prime\mu\nu}\left(x,x'\right) &= \int dy' \left(-2\frac{\delta S_i}{\delta\Delta_a^{\mathrm{mf}}\left(x\right)}\epsilon_{ab}\delta\left(x-y'\right)\right)\Pi_b^{\nu}\left(x',y'\right) \\ &\quad + \int dy\, \frac{\delta S_i}{\delta\Delta_a^{\mathrm{mf}}\left(y\right)}\left(2\epsilon_{ab}\delta\left(x-y\right)\Pi_b^{\nu}\left(x',y\right)\right), \\ &= 0. \end{aligned} \tag{E.41}$$

Therefore, provided the relations in Eqs. (E.38-E.40) hold, the contraction of the response kernel vanishes, and we conclude that the general response kernel in Eq. (E.27) is gauge invariant.

E.3.1 Useful contraction formulas

This section systematically derives the contraction relations in Eqs. (E.38-E.40). In order to derive these identities, we first consider a set of formulas for the contraction of a general n-point correlation function, as calculated from functional derivatives of the gauge-invariant action with respect to either A_μ, or $\Delta_a^{\mathrm{mf}}\left[0\right]$. The desired contraction relations will immediately follow from limiting cases. The relevant correlation functions, such as those in Eq. (E.38), are all partial derivatives calculated with $\boldsymbol{\Delta} = \boldsymbol{\Delta}^{\mathrm{mf}}\left[0\right]$. Since the gap in these functions is independent of A_μ, the functional chain rule should not be invoked. In order to simplify notation, *in this section only*, we will drop the mf superscript on the mean-field gaps, so that $\boldsymbol{\Delta} = \boldsymbol{\Delta}^{\mathrm{mf}}\left[0\right]$.

Generic contracted n-point function

All correlation functions of interest will be of the form

$$\mathcal{Q}_i^{\alpha_1\ldots\alpha_n}\left(x_1\ldots x_n\right) \equiv \left.\frac{\delta^n S_i\left[\boldsymbol{\Delta},A\right]}{\delta\mathcal{A}_1\ldots\delta\mathcal{A}_n}\right|_{A\to 0}, \tag{E.42}$$

where $\mathcal{A}_m = \mathcal{A}_{\alpha_m}\left(x_m\right)$ is a generalized response vector that contains both the gap and vector potential, as defined below Eq. (E.25). Since the gauge invariance condition requires the contraction

of an index, it will be helpful to calculate a series of contraction formulas:

$$\partial_\mu^x \frac{\delta}{\delta A_\mu(x)} \mathcal{Q}_i^{\{\alpha_n\}}(\{x_n\}), \tag{E.43}$$

where the shorthand $\{x_n\} = x_1 \dots x_n$ and $\{\alpha_n\} = \alpha_1 \dots \alpha_n$. In order to calculate these contraction formulas, first note that all functional derivatives with respect to Δ_{a_n} and A_{μ_n} commute. We also assume $x_m \neq x$ for any m, so the partial derivative ∂_x can be commuted through the functional derivatives. The contracted correlation function is equivalently expressed as:

$$\partial_\mu^x \frac{\delta}{\delta A_\mu(x)} \mathcal{Q}_i^{\{\alpha_n\}}(\{x_n\}) = \frac{\delta^n}{\delta \mathcal{A}_1 \dots \delta \mathcal{A}_n} \left(\partial_\mu^x \frac{\delta S_i[\mathbf{\Delta}, A]}{\delta A_\mu(x)} \right). \tag{E.44}$$

In the path integral, the actions $S_i[\mathbf{\Delta}, A] = S_i[\rho, \phi, A]$ are manifestly gauge invariant. Therefore, we can apply a gauge transformation $\Delta = \rho e^{2i\phi} \to \rho$ and $A_\mu \to A_\mu + \partial_\mu \phi$ to move all phase dependence of the order parameter into a "dressed" vector potential $\widetilde{A}_\mu = A_\mu + \partial_\mu \phi$ [Lutchyn et al., 2008, Ojanen & Kitagawa, 2013]. Under this transformation, the gauge-invariant action must not change, and the three parameterizations of the action

$$S_i[\mathbf{\Delta}, A] = S_i[\rho, \phi, A] = S_i[\rho, 0, A + \partial\phi] \tag{E.45}$$

are equivalent for both a saddle-point and a generic fluctuation action. Returning to the contraction formulas, the above gauge-invariant reparameterizations of the action S_i then imply

$$\partial_\mu^x \frac{\delta S_i[\mathbf{\Delta}, A]}{\delta A_\mu(x)} = \partial_\mu^x \frac{\delta S_i[\rho, 0, A + \partial\phi]}{\delta\left(\partial_\mu^x \phi(x)\right)} = -\frac{\delta S_i[\rho, 0, A + \partial\phi]}{\delta \phi(x)} = -\frac{\delta S_i[\rho, \phi, A]}{\delta \phi(x)}. \tag{E.46}$$

The first equality follows from gauge invariance and the functional chain rule. The second equality is a result of the functional derivative identity $\frac{\delta F[\partial\phi]}{\delta\phi} = -\partial \frac{\delta F[\partial\phi]}{\delta(\partial\phi)}$, which is true if $F[\partial\phi]$ is a functional of *only* $\partial_\mu\phi$ (and not ϕ and $\partial_\mu\phi$ simultaneously.) This condition is satisfied when the action is expressed as $S_i[\rho, 0, A + \partial\phi]$, so the vector potential is dressed with the mean-field phase.

The last equality used the property of gauge invariance in the choice of the parameterization of the action in Eq. (E.45).

The contraction formula can then be expressed as:

$$\partial_{\mu}^{x}\frac{\delta}{\delta A_{\mu}\left(x\right)}\mathcal{Q}_{i}^{\alpha_{1}\ldots\alpha_{n}}\left(x_{1}\ldots x_{n}\right)=-\frac{\delta^{n}}{\delta\mathcal{A}_{1}\ldots\delta\mathcal{A}_{n}}\frac{\delta S_{i}}{\delta\phi}=-\frac{\delta^{n}}{\delta\mathcal{A}_{1}\ldots\delta\mathcal{A}_{n}}\frac{\delta\Delta_{a}}{\delta\phi}\frac{\delta S_{i}}{\delta\Delta_{a}}, \tag{E.47}$$

where we henceforth suppress the functional argument on the action S_i. While the functional derivatives $\delta/\delta\mathcal{A}_{\alpha}$ commute between themselves, note that $\delta/\delta\Delta_{a}^{\mathrm{mf}}$ and $\delta/\delta\phi$ do not commute, nor do they commute with $\delta\Delta_{a}/\delta\phi$. This will lead to a product rule with respect to the n functional derivatives of $\mathcal{A}_{\alpha}$. Since $\delta\Delta_{a}/\delta\phi=2\epsilon_{ab}\Delta_{b}$ is linear in the gap Δ_b, only terms with a single functional derivative applied to $\delta\Delta_{a}/\delta\phi$ will contribute:

$$\begin{aligned}\frac{\delta^{n}}{\delta\mathcal{A}_{1}\ldots\delta\mathcal{A}_{n}}\frac{\delta\Delta_{a}}{\delta\phi}\frac{\delta S_{i}}{\delta\Delta_{a}}&=\frac{\delta\Delta_{a}}{\delta\phi}\frac{\delta^{n+1}S_{i}}{\delta\mathcal{A}_{1}\ldots\delta\mathcal{A}_{n}\delta\Delta_{a}}+\sum_{m=1}^{n}\left(\frac{\delta}{\delta\mathcal{A}_{\alpha_{m}}}\frac{\delta\Delta_{a}}{\delta\phi}\right)\frac{\delta^{n}S_{i}}{\prod_{k\neq m}\delta\mathcal{A}_{k}\delta\Delta_{a}},\\&=\frac{\delta\mathcal{Q}_{i}^{\{\alpha_{n}\}}\left(\{x_{n}\}\right)}{\delta\phi\left(x\right)}+2\sum_{m=1}^{n}\epsilon_{ab}\delta_{b\alpha_{m}}\delta\left(x-x_{m}\right)\mathcal{Q}_{i}^{\left\{\alpha_{n\neq m},a\right\}}\left(\left\{x_{n\neq m},x\right\}\right).\end{aligned} \tag{E.48}$$

The contraction of an arbitrary correlation function is therefore given by

$$\begin{aligned}\partial_{\mu}^{x}\frac{\delta}{\delta A_{\mu}\left(x\right)}\mathcal{Q}_{i}^{\{\alpha_{n}\}}\left(\{x_{n}\}\right)=&-\frac{\delta\mathcal{Q}_{i}^{\{\alpha_{n}\}}\left(\{x_{n}\}\right)}{\delta\phi}\\&-2\sum_{m=1}^{n}\epsilon_{ab}\delta_{b\alpha_{m}}\delta\left(x-x_{m}\right)\mathcal{Q}_{i}^{\left\{\alpha_{n\neq m},a\right\}}\left(\left\{x_{n\neq m},x\right\}\right),\end{aligned} \tag{E.49}$$

for any set of arbitrary n-point correlation functions calculated from an effective action $S_i\left[\boldsymbol{\Delta},A\right]$.

Contractions in two-point functions

This contraction formula immediately produces the two contractions $\partial_{\mu}K_{0,i}^{\mu\nu}$ and $\partial_{\mu}Q_{i}^{\mu a}$; both contractions correspond to the operator $\partial_{\mu}\frac{\delta}{\delta A_{\mu}}$ applied to the one-point correlation function $\mathcal{Q}_{i}^{\alpha}\left(y\right)$.

Directly applying the above formula gives:

$$\partial_{\mu}^{x}\frac{\delta}{\delta A_{\mu}\left(x\right)}\mathcal{Q}_{i}^{\alpha}\left(y\right)=-\frac{\delta\mathcal{Q}_{i}^{\alpha}\left(y\right)}{\delta\phi}-2\epsilon_{bc}\delta_{c\alpha}\mathcal{Q}_{i}^{b}\left(x\right)\delta\left(x-y\right). \tag{E.50}$$

The bubble response kernel is $\alpha=\nu$, and the $\delta_{c\nu}=0$ Kronecker delta causes the term to the right to vanish. For the $Q_{i}^{\mu a}$ term, the Kronecker delta δ_{ca} does not vanish. The two contractions are generically expressed as:

$$\begin{aligned}\partial_{\mu}^{x}K_{0,i}^{\mu\nu}\left(x,y\right) &= -\frac{\delta\mathcal{Q}_{i}^{\nu}\left(y\right)}{\delta\phi\left(x\right)}, &\text{(E.51)}\\ \partial_{\mu}^{x}Q_{i}^{\mu a}\left(x,y\right) &= -\frac{\delta\mathcal{Q}_{i}^{a}\left(y\right)}{\delta\phi\left(x\right)}-2\epsilon_{ba}\mathcal{Q}_{i}^{b}\left(x\right)\delta\left(x-y\right). &\text{(E.52)}\end{aligned}$$

If $i=\mathrm{mf}$, the $\mathcal{Q}_{i}^{b}\left(x\right)$ term on the second line corresponds to the saddle-point condition, and therefore vanishes. Otherwise, this term needs to be kept, and it will be shown that this is an important contribution in maintaining gauge invariance of $K^{\mu\nu}$ for non-stationary actions $\delta S_{i}/\delta\Delta_{a}\neq0$.

Of special interest is the contraction $\partial_{\mu}^{x}Q_{\mathrm{mf}}^{\mu a}$, which evaluates to:

$$\partial_{\mu}^{x}Q_{\mathrm{mf}}^{\mu a}\left(x,x'\right)=-2\epsilon_{cb}\Delta_{b}\left(x\right)Q_{\mathrm{mf}}^{ca}\left(x,x'\right) \tag{E.53}$$

after using the functional identity

$$\frac{\delta}{\delta\phi}=\frac{\delta\Delta_{a}}{\delta\phi}\frac{\delta}{\delta\Delta_{a}}=2\epsilon_{ba}\Delta_{a}\frac{\delta}{\delta\Delta_{b}}. \tag{E.54}$$

Using Eq. (E.53) and Eq. (E.29), the contraction $\partial_{\mu}^{x}\Pi_{a}^{\mu}\left(x,x'\right)$ over the collective mode vertices follows straightforwardly:

$$\begin{aligned}\partial_{\mu}^{x}\Pi_{a}^{\mu}\left(x,x'\right) &= -\int dy\ \left[Q_{\mathrm{mf}}\right]_{ab}^{-1}\left(x',y\right)\left(\partial_{\mu}^{x}Q_{\mathrm{mf}}^{b\mu}\left(y,x\right)\right),\\ &= 2\epsilon_{ab}\Delta_{b}\left(x\right)\delta\left(x-x'\right). &\text{(E.55)}\end{aligned}$$

A related set of contraction formulas will also be helpful

$$\begin{aligned}\partial_\mu \int dy\, \Pi_a^\mu(x,y)\, \mathcal{Q}_i^{\{a\alpha_n\}}(y,\{x_n\}) &= \int dy\, \left(2\epsilon_{ab}\Delta_b(x)\,\delta(x-y)\right) \mathcal{Q}_i^{\{a\alpha_n\}}(y,\{x_n\}), \\ &= 2\Delta_b(x)\,\epsilon_{ab}\frac{\delta}{\delta\Delta_a(x)}\mathcal{Q}_i^{\{\alpha_n\}}(\{x_n\}), \\ &= \frac{\delta}{\delta\phi(x)}\mathcal{Q}_i^{\{\alpha_n\}}(\{x_n\}). \end{aligned} \tag{E.56}$$

This shows that the contraction of a collective mode propagator acts as a ϕ-derivative, but with the opposite sign as a generic correlation function $\mathcal{Q}^{\{\alpha_n\}}(\{x_n\})$. On a physical level, this can be interpreted as an equivalence between "pure gauge" fluctuations and phase fluctuations of the order parameter. From a similar standpoint, we note that amplitude collective modes are not responsible for the restoration of gauge invariance, even though they contribute to response. Combined with Eq. (E.49) above, we find the functional identity:

$$\begin{aligned}&\partial_\mu^x\left(\mathcal{Q}_i^{\{\mu\alpha_n\}}(x,\{x_n\}) + \int dy\,\Pi_a^\mu(x,y)\,\mathcal{Q}_i^{\{a\alpha_n\}}(y,\{x_n\})\right) \\ &= -2\sum_{m=1}^{n}\epsilon_{ab}\delta_{b\alpha_m}\delta(x-x_m)\,\mathcal{Q}_i^{\left\{\alpha_{n\neq m},a\right\}}\left(\left\{x_{n\neq m},x\right\}\right). \end{aligned} \tag{E.57}$$

Specific contractions in the gauge-invariant response kernel

These results are now sufficient to show the full response is gauge invariant, $\partial_\mu K_i^{\mu\nu} = 0$. We examine the three lines in Eqs. (E.38-E.40) above in the contracted response. The contraction of Eq. (E.38)

$$\partial_\mu^x\left(K_{0,i}^{\mu\nu}(x,x') + \int dy\,\Pi_a^\mu(x,y)\,Q_i^{a\nu}(y,x')\right) = 0 \tag{E.58}$$

vanishes explicitly. When contracting the correlation functions in Eq. (E.39), the term in the parentheses does not vanish due to the non-commutativity of $\delta/\delta\phi$ and $\delta/\delta\Delta_a$:

$$\partial_\mu^x\left(Q_i^{\mu b}(x,y') + \int dy\,\Pi_a^\mu(x,y)\,Q_i^{ab}(y,y')\right) = -2\epsilon_{ab}\mathcal{Q}_i^a(y')\,\delta(x-y').$$

This reproduces the contraction identity Eq. (E.39), since by definition $\mathcal{Q}_i^b(y) = \delta S_i/\delta\Delta_a^{\rm mf}(y)$. Therefore, the second line of Eq. (E.27) gives

$$\begin{aligned}
&\partial_\mu^x \int dy' \left(Q_i^{\mu b}\left(x,y'\right) + \int dy\, \Pi_a^\mu(x,y)\, Q_i^{ab}\left(y,y'\right)\right) \Pi_b^\nu\left(x',y'\right) \\
&= -2\epsilon_{ab} \int dy' \left(\mathcal{Q}_i^a\left(y'\right)\delta\left(x-y'\right)\right) \Pi_b^\nu\left(x',y'\right), \\
&= -2\mathcal{Q}_i^a(x)\,\epsilon_{ab}\Pi_b^\nu\left(x',x\right). \qquad \text{(E.59)}
\end{aligned}$$

Finally, we need to reproduce the contraction of the second-order fluctuation found in Eq. (E.40):

$$\partial_\mu^x \Xi_a^{\mu\nu}\left(x,y,x'\right) = 2\epsilon_{ab}\delta(x-y)\left.\frac{\delta\Delta_b(x)}{\delta A_\nu(x')}\right|_{A\to 0} = 2\epsilon_{ab}\delta(x-y)\,\Pi_b^\nu\left(x',x\right). \qquad \text{(E.60)}$$

An alternative derivation of this result will follow from the contraction of Eq. (E.33) after repeated application of the formula in Eq. (E.57). Combined with the relation $\mathcal{Q}_i^b(y) = \delta S_i/\delta\Delta_a^{\rm mf}(y)$, the third line of Eq. (E.27) is

$$\begin{aligned}
\partial_\mu^x \int dy\, \frac{\delta S_i}{\delta\Delta_a^{\rm mf}(y)} \Xi_a^{\mu\nu}\left(x,y,x'\right) &= \int dy\, \mathcal{Q}_i^a(y)\left(\partial_\mu^x \Xi_a^{\mu\nu}\left(x,y,x'\right)\right), \\
&= 2\mathcal{Q}_i^a(x)\,\epsilon_{ab}\Pi_b^\nu\left(x',x\right). \qquad \text{(E.61)}
\end{aligned}$$

This contraction has the same magnitude, but inverted sign, compared to the contraction of the second line of Eq. (E.27). Therefore, this term is necessary to maintain gauge invariance for a non-stationary action.

Thus, we have derived the relations presented in the previous section, and consequently the full response is gauge invariant.

APPENDIX F

COLLECTIVE MODE CONTRIBUTIONS TO THE MEISSNER EFFECT: FULDE-FERRELL AND PAIR-DENSITY-WAVE SUPERFLUIDS

F.1 Mean-field formalism

F.1.1 Green's functions

The starting point for our study of Fulde-Ferrell (FF) superfluids is the mean-field Hamiltonian [Chen et al., 2007]:

$$H_{\rm FF} = \sum_{\mathbf{k}} \Big[\xi_{\mathbf{k},\uparrow} c^\dagger_{\mathbf{k},\uparrow} c_{\mathbf{k},\uparrow} + \xi_{\mathbf{k}-\mathbf{Q},\downarrow} c^\dagger_{-\mathbf{k}+\mathbf{Q},\downarrow} c_{-\mathbf{k}+\mathbf{Q},\downarrow} + \Delta c^\dagger_{-\mathbf{k}+\mathbf{Q},\downarrow} c^\dagger_{\mathbf{k},\uparrow} + \Delta^* c_{\mathbf{k},\uparrow} c_{-\mathbf{k}+\mathbf{Q},\downarrow} \Big]. \tag{F.1}$$

The matrix representation of this Hamiltonian, in the $\psi^\dagger_{\mathbf{k}} = (c_{\mathbf{k},\uparrow}, c^\dagger_{-\mathbf{k}+\mathbf{Q},\downarrow})$ basis, is $H_{\rm FF} = \sum_{\mathbf{k}} \psi^\dagger_{\mathbf{k}} \mathcal{H}_{\rm FF} \psi_{\mathbf{k}}$, where

$$\mathcal{H}_{\rm FF} = \begin{pmatrix} \xi_{\mathbf{k},\uparrow} & -\Delta \\ -\Delta^* & -\xi_{\mathbf{k}-\mathbf{Q},\downarrow} \end{pmatrix}. \tag{F.2}$$

Here we have ignored an irrelevant constant $-\sum_{\mathbf{k}} \xi_{\mathbf{k}-\mathbf{Q},\downarrow}$. The inverse Nambu Green's function is then $\mathcal{G}^{-1} = i\omega_n - \mathcal{H}_{\rm FF}$, where $i\omega_n$ is a fermionic Matsubara frequency. Performing the matrix inverse we obtain

$$\mathcal{G}(k) = \frac{1}{\left(i\omega_n - \xi_{\mathbf{k},\uparrow}\right)\left(i\omega_n + \xi_{\mathbf{k}-\mathbf{Q},\downarrow}\right) - |\Delta|^2} \begin{pmatrix} i\omega_n + \xi_{\mathbf{k}-\mathbf{Q},\downarrow} & -\Delta \\ -\Delta^* & i\omega_n - \xi_{\mathbf{k},\uparrow} \end{pmatrix}. \tag{F.3}$$

If we shift $\mathbf{k} \to \mathbf{k} + \mathbf{Q}/2$, then redefine $\mathbf{Q} \to 2\mathbf{Q}$, this Nambu Green's function agrees with Eq. (3) of Ref. [Yin et al., 2014]. The single particle Green's function can then be found from the above equation. Namely, $G_\uparrow(k) = \mathcal{G}_{11}(k)$ and $-G_\downarrow(-k+Q) = \mathcal{G}_{22}(k)$. If we perform this inversion,

and define the bare Green's function by $G_{0,\sigma}^{-1}(k) = i\omega_n - \xi_{\mathbf{k},\sigma}$, then the full (inverse) Green's function is

$$G_{\sigma}^{-1}(k) = G_{0,\sigma}^{-1}(k) - \Sigma_{\sigma}(k), \tag{F.4}$$

where the self energy is given by

$$\Sigma_{\sigma}(k) = -|\Delta|^2 G_{0,\bar{\sigma}}(-k+Q) = \frac{|\Delta|^2}{i\omega_n + \xi_{\mathbf{k}-\mathbf{Q},\bar{\sigma}}}. \tag{F.5}$$

Here $k^{\mu} = (i\omega_n, \mathbf{k})$, $Q^{\mu} = (0, \mathbf{Q})$ and without loss of generality the FF pairing vector is assumed to be along the $\hat{z}$-direction: $\mathbf{Q} = Q\hat{z}$. The full Green's function is thus

$$G_{\sigma}(k) = \frac{\left(i\omega_n + \xi_{\mathbf{k}-\mathbf{Q},\bar{\sigma}}\right)}{\left(i\omega_n - \xi_{\mathbf{k},\sigma}\right)\left(i\omega_n + \xi_{\mathbf{k}-\mathbf{Q},\bar{\sigma}}\right) - |\Delta|^2}. \tag{F.6}$$

Similarly, from the Nambu Green's function in Eq. (F.3), one has $\mathcal{G}_{12}(k) = \Delta G_{0,\downarrow}(-k+Q)G_{\uparrow}(k) = \Delta G_{0,\uparrow}(k)G_{\downarrow}(-k+Q)$. It will prove convenient to express the Gorkov function symmetrically by

$$\mathcal{G}_{12}(k+Q/2) = \Delta G_{0,\downarrow}(-k+Q/2)G_{\uparrow}(k+Q/2) = \Delta G_{0,\uparrow}(k+Q/2)G_{\downarrow}(-k+Q/2). \tag{F.7}$$

For a polarized superfluid we define the chemical potential and effective magnetic field by

$$\mu = \frac{1}{2}\left(\mu_{\uparrow} + \mu_{\downarrow}\right), \tag{F.8}$$

$$h = \frac{1}{2}\left(\mu_{\uparrow} - \mu_{\downarrow}\right). \tag{F.9}$$

For convenience we shall need the following dispersion relations

$$\xi_{\mathbf{kQ}} = \frac{1}{2m}\left[\mathbf{k}^2 + (\mathbf{Q}/2)^2\right] - \mu, \tag{F.10}$$

$$E^2_{\mathbf{kQ}} = \xi^2_{\mathbf{kQ}} + |\Delta|^2, \tag{F.11}$$

$$h_{\mathbf{kQ}} = h - \frac{\mathbf{k}\cdot\mathbf{Q}/2}{m}, \tag{F.12}$$

$$g_{\mathbf{kQ}} = h + \frac{\mathbf{k}\cdot\mathbf{Q}/2}{m} = h_{-\mathbf{k},\mathbf{Q}}. \tag{F.13}$$

The coherence factors of the Green's functions are then defined by

$$u^2_{\mathbf{kQ}} = \frac{1}{2}\left(1 + \frac{\xi_{\mathbf{kQ}}}{E_{\mathbf{kQ}}}\right), \tag{F.14}$$

$$v^2_{\mathbf{kQ}} = \frac{1}{2}\left(1 - \frac{\xi_{\mathbf{kQ}}}{E_{\mathbf{kQ}}}\right). \tag{F.15}$$

Similarly the poles of the Green's functions are defined by

$$x_{1,\uparrow} = E_{\mathbf{kQ}} - h_{\mathbf{kQ}}, \tag{F.16}$$

$$x_{2,\uparrow} = E_{\mathbf{kQ}} + h_{\mathbf{kQ}}, \tag{F.17}$$

$$x_{1,\downarrow} = E_{\mathbf{kQ}} + g_{\mathbf{kQ}}, \tag{F.18}$$

$$x_{2,\downarrow} = E_{\mathbf{kQ}} - g_{\mathbf{kQ}}. \tag{F.19}$$

With the above definitions, it follows that the spin up and spin down Green's functions are

$$G_\uparrow(k+Q/2) = \frac{u^2_{\mathbf{kQ}}}{i\omega_n - x_{1,\uparrow}} + \frac{v^2_{\mathbf{kQ}}}{i\omega_n + x_{2,\uparrow}}, \tag{F.20}$$

$$G_\downarrow(k+Q/2) = \frac{u^2_{\mathbf{kQ}}}{i\omega_n - x_{1,\downarrow}} + \frac{v^2_{\mathbf{kQ}}}{i\omega_n + x_{2,\downarrow}}. \tag{F.21}$$

In terms of the coherence factors, the Gorkov function is

$$\mathcal{G}_{12}(k+Q/2) = -u_{\mathbf{kQ}}v_{\mathbf{kQ}}\left(\frac{1}{i\omega_n - x_{1,\uparrow}} - \frac{1}{i\omega_n + x_{2,\uparrow}}\right). \tag{F.22}$$

Finally, it will prove convenient when evaluating the superfluid density to define the following expressions

$$W_{\mathbf{k}} \equiv \frac{\sinh(\beta h_{\mathbf{kQ}})}{\cosh(\beta E_{\mathbf{kQ}}) + \cosh(\beta h_{\mathbf{kQ}})}, \tag{F.23}$$

$$X_{\mathbf{k}} \equiv \frac{\sinh(\beta E_{\mathbf{kQ}})}{\cosh(\beta E_{\mathbf{kQ}}) + \cosh(\beta h_{\mathbf{kQ}})}, \tag{F.24}$$

$$Y_{\mathbf{k}} \equiv \frac{1 + \cosh(\beta E_{\mathbf{kQ}})\cosh(\beta h_{\mathbf{kQ}})}{\left[\cosh(\beta E_{\mathbf{kQ}}) + \cosh(\beta h_{\mathbf{kQ}})\right]^2}, \tag{F.25}$$

$$Z_{\mathbf{k}} \equiv \frac{\sinh(\beta E_{\mathbf{kQ}})\sinh(\beta h_{\mathbf{kQ}})}{\left[\cosh(\beta E_{\mathbf{kQ}}) + \cosh(\beta h_{\mathbf{kQ}})\right]^2}. \tag{F.26}$$

The $X_{\mathbf{k}}$ and $Y_{\mathbf{k}}$ expressions are the same definitions as given in Ref. [Yin et al., 2014], however, the $Z_{\mathbf{k}}$ expression is slightly modified. The $W_{\mathbf{k}}$ expression is our own definition.

F.1.2 Mean-field equations

For completeness here we summarize the four mean-field equations in Fermi units. The mean-field equation for the gap Δ [defined in Eq. (F.40)] is

$$\frac{\Delta}{g} = \Delta\sum_{k} G_{0,\downarrow}(-k+Q)G_{\uparrow}(k) = \Delta\sum_{\mathbf{k}}\frac{X_{\mathbf{k}}}{2E_{\mathbf{kQ}}}. \tag{F.27}$$

Regularizing this equation using $m/(4\pi a) = -1/g + \sum_{\mathbf{k}}(1/2\epsilon_{\mathbf{k}})$, and converting it into dimensionless form, then gives

$$0 = \Delta\left\{(k_F a)^{-1} + \frac{1}{\pi}\int_0^\infty dx\, x^2 \int_0^\pi d\theta\, \sin(\theta)\left[\frac{\widetilde{X}_{\mathbf{k}}}{\widetilde{E}_{\mathbf{kQ}}} - \frac{1}{\widetilde{\epsilon_{\mathbf{k}}}}\right]\right\}. \tag{F.28}$$

Here we defined $x = k/k_F$, $\widetilde{E}_{\mathbf{kQ}} = E_{\mathbf{kQ}}/E_F, \widetilde{h}_{\mathbf{kQ}} = h_{\mathbf{kQ}}/E_F, \widetilde{\epsilon}_{\mathbf{k}} = \epsilon_{\mathbf{k}}/E_F$, where E_F is the Fermi energy and k_F is the Fermi wave vector. All expressions with a tilde (such as $\widetilde{X}_{\mathbf{k}}$) are to be interpreted as having their dependent variables normalized to Fermi units.

The mean-field equation for the FF pairing vector Q [defined in Eq. (F.78)] is

$$0 = \sum_{\sigma}\sum_{k}\left(\frac{k+Q/2}{m}\right)^{z} G_{\sigma}(k+Q/2) = \sum_{\mathbf{k}}\frac{Q/2}{m}\left[1 - \frac{\xi_{\mathbf{kQ}}}{E_{\mathbf{kQ}}}X_{\mathbf{k}} + \frac{k^z}{Q/2}W_{\mathbf{k}}\right]. \tag{F.29}$$

In terms of dimensionless variables, this equation becomes

$$0 = \widetilde{Q}\int_0^{\infty} dx\; x^2 \int_0^{\pi} d\theta\; \sin(\theta)\left[1 - \frac{\widetilde{\xi}_{\mathbf{kQ}}}{\widetilde{E}_{\mathbf{kQ}}}\widetilde{X}_{\mathbf{k}} + \frac{\widetilde{k}_z}{\widetilde{Q}/2}\widetilde{W}_{\mathbf{k}}\right]. \tag{F.30}$$

The number equations are

$$n_{\sigma} = \sum_{k} G_{\sigma}(k+Q/2) = \frac{1}{2}\sum_{\mathbf{k}}\left\{\left[1 + f(x_{1,\sigma}) - f(x_{2,\sigma})\right] - \frac{\xi_{\mathbf{kQ}}}{E_{\mathbf{kQ}}}\left[1 - f(x_{1,\sigma}) - f(x_{2,\sigma})\right]\right\}. \tag{F.31}$$

In terms of dimensionless variables these become

$$\frac{n_{\sigma}}{n} = \frac{3}{8}\int_0^{\infty} dx\; x^2 \int_0^{\pi} d\theta\; \sin(\theta)\left\{\left[1 + f(x_{1,\sigma}) - f(x_{2,\sigma})\right] - \frac{\widetilde{\xi}_{\mathbf{kQ}}}{\widetilde{E}_{\mathbf{kQ}}}\left[1 - f(x_{1,\sigma}) - f(x_{2,\sigma})\right]\right\}. \tag{F.32}$$

Here we used $k_F^3 = 3\pi^2 n$ as the relation between particle number and the Fermi wave vector. The two number equations can be rewritten as $n = \sum_{\sigma} n_{\sigma}$ and $p = (n_{\uparrow} - n_{\downarrow})/(n_{\uparrow} + n_{\downarrow})$. By taking the sum and difference of Eq. (F.32), we can then express these as two number equations:

$$\frac{4}{3} = \int_0^{\infty} dx\; x^2 \int_0^{\pi} d\theta\; \sin(\theta)\left[1 - \frac{\widetilde{\xi}_{\mathbf{kQ}}}{\widetilde{E}_{\mathbf{kQ}}}\widetilde{X}_{\mathbf{k}}\right], \tag{F.33}$$

$$\frac{4}{3}p = \int_0^{\infty} dx\; x^2 \int_0^{\pi} d\theta\; \sin(\theta)\widetilde{W}_{\mathbf{k}}. \tag{F.34}$$

There are now four equations: Eq. (F.28), Eq. (F.30), Eq. (F.33), and Eq. (F.34) in four unknowns:

μ, Δ, h, Q. Thus for fixed scattering length $(1/k_F a)$ and fixed polarization (p) we have a well-defined system of equations. To obtain the correct ground state, the thermodynamic potential in Eq. (F.93) must also be minimized. Hence one can solve the mean-field equations, and then restrict the region of parameter space to those solutions that minimize Ω.

F.2 Full vertex and Ward-Takahashi identity

In order to determine the full vertex and the response functions in the superfluid phase, we apply the Ward-Takahashi identity (WTI). The Ward-Takahashi identity for the full vertex $\Gamma^{\mu}_{\sigma}(k_+, k_-)$ is [Ryder, 1996]

$$\begin{aligned} q_\mu \Gamma^{\mu}_{\sigma}(k_+, k_-) &= G^{-1}_{\sigma}(k_+) - G^{-1}_{\sigma}(k_-), \\ &= q_\mu \gamma^{\mu}_{\sigma}(k_+, k_-) + \Sigma_\sigma(k_-) - \Sigma_\sigma(k_+). \end{aligned} \tag{F.35}$$

Here $k^{\mu}_{\pm} = k^{\mu} \pm q^{\mu}/2$, where $q^{\mu} = (i\Omega_m, \mathbf{q})$ with $i\Omega_m$ being a bosonic Matsubara frequency. This is an exact relation in quantum field theory which relates the single particle Green's function to the full vertex. It is a gauge-invariant statement and here it reflects the underlying global $\mathrm{U}(1)$ symmetry. The bare WTI identity, $q_\mu \gamma^{\mu}_{\sigma}(k_+, k_-) = G^{-1}_{0,\sigma}(k_+) - G^{-1}_{0,\sigma}(k_-)$, is satisfied by the bare vertex $\gamma^{\mu}_{\sigma}(k_+, k_-) = \left(1, \frac{\mathbf{k}}{m}\right)$. In order to satisfy the WTI one must perform all possible vertex insertions in the self energy Feynman diagram [Nambu, 1960, Ryder, 1996]. In Fig. (F.1) the self energy Feynman diagram for Eq. (F.5) is shown. Note that, the external lines for Δ and Δ^* are merely for illustration. They carry no external momentum, and the self energy is indeed a two point function.

The self energy Feynman diagram of Fig. (F.1) has three possible positions where vertices can be inserted: the bare Green's function and the two gaps Δ and Δ^*. Inserting current in the bare Green's function gives rise to a bare vertex. In the superfluid phase there are collective mode vertices $\Pi^{\mu}(q)$ and $\bar{\Pi}^{\mu}(q)$ due to the spontaneously broken global $\mathrm{U}(1)$ symmetry. Inserting the bare vertex in all possible places in the gaps Δ and Δ^* thus leads to collective mode vertices.

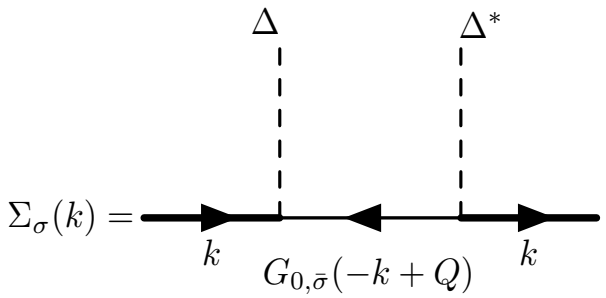

Figure F.1: Feynman diagram for the self energy $\Sigma_\sigma(k) = -|\Delta|^2 G_{0,\bar{\sigma}}(-k+Q)$.

Therefore, the full vertex is

$$\begin{aligned}\Gamma^{\mu}_{\sigma}(k_+,k_-) &= \gamma^{\mu}_{\sigma}(k_+,k_-) \\ &- \left[\Delta^* \Pi^{\mu}(q) G_{0,\bar{\sigma}}(-k_- + Q) + \Delta \bar{\Pi}^{\mu}(q) G_{0,\bar{\sigma}}(-k_+ + Q)\right] \\ &- |\Delta|^2 G_{0,\bar{\sigma}}(-k_- + Q)\gamma^{\mu}_{\bar{\sigma}}(-k_- + Q, -k_+ + Q) G_{0,\bar{\sigma}}(-k_+ + Q). \end{aligned} \tag{F.36}$$

The Feynman diagrams for the full vertex are expressed in Fig. (F.2).

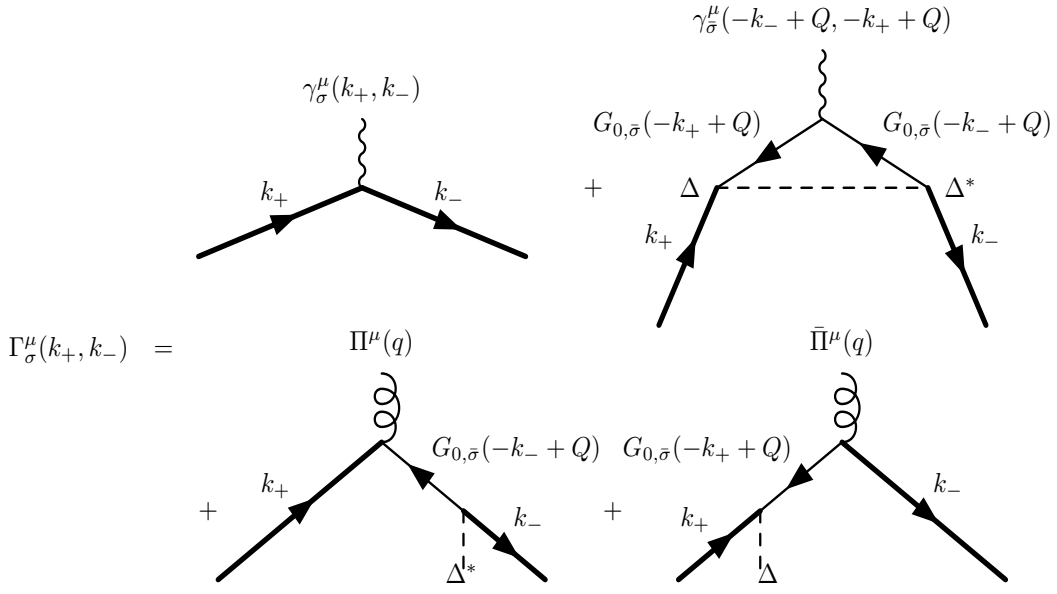

Figure F.2: Feynman diagrams for the full vertex $\Gamma^{\mu}_{\sigma}(k_+, k_-)$ appearing in response functions.

In the next section we shall verify that, for $q^\mu \neq 0$, the collective mode vertices satisfy $q_\mu \Pi^\mu(q) = 2\Delta$ and $q_\mu \bar{\Pi}^\mu(q) = -2\Delta^*$. Given these relations, we now verify that the WTI is satisfied by the full vertex appearing in Eq. (F.36). Taking the contraction of the full vertex gives

$$\begin{aligned} q_\mu \Gamma^\mu_\sigma(k_+, k_-) &= G^{-1}_{0,\sigma}(k_+) - G^{-1}_{0,\sigma}(k_-) \\ &\quad - 2|\Delta|^2 \left[G_{0,\bar{\sigma}}(-k_- + Q) - G_{0,\bar{\sigma}}(-k_+ + Q) \right] \\ &\quad - |\Delta|^2 G_{0,\bar{\sigma}}(-k_- + Q) \left[G^{-1}_{0,\bar{\sigma}}(-k_- + Q) - G^{-1}_{0,\bar{\sigma}}(-k_+ + Q) \right] G_{0,\bar{\sigma}}(-k_+ + Q). \end{aligned} \tag{F.37}$$

Collecting terms we then have

$$\begin{aligned} q_\mu \Gamma^\mu_\sigma(k_+, k_-) &= G^{-1}_{0,\sigma}(k_+) - G^{-1}_{0,\sigma}(k_-) + 2\left[\Sigma_\sigma(k_-) - \Sigma_\sigma(k_+)\right] \\ &\quad - |\Delta|^2 \left[G_{0,\bar{\sigma}}(-k_+ + Q) - G_{0,\bar{\sigma}}(-k_- + Q) \right], \\ &= G^{-1}_{0,\sigma}(k_+) - G^{-1}_{0,\sigma}(k_-) + 2\left[\Sigma_\sigma(k_-) - \Sigma_\sigma(k_+)\right] - \left[\Sigma_\sigma(k_-) - \Sigma_\sigma(k_+)\right], \\ &= G^{-1}_{\sigma}(k_+) - G^{-1}_{\sigma}(k_-). \end{aligned} \tag{F.38}$$

Thus the Ward-Takahashi identity is indeed satisfied by the full vertex in Eq. (F.36). The exact response functions are then given by

$$P^{\mu\nu}(q) = \sum_\sigma \sum_k G_\sigma(k_+) \Gamma^\mu_\sigma(k_+, k_-) G_\sigma(k_-) \gamma^\nu_\sigma(k_-, k_+). \tag{F.39}$$

F.3 Gap equation and collective mode vertices

In this section the explicit form of the collective mode vertices is determined. To do this, it is crucial to ensure that they are consistent with the mean-field gap equation. The gap equation is given by [Chen et al., 2007]

$$\frac{\Delta}{g} = \sum_k \mathcal{G}_{12}(k) = \sum_k \Delta G_{0,\downarrow}(-k + Q) G_\uparrow(k). \tag{F.40}$$

Here $g > 0$ is an s-wave interaction constant. This equation is equivalent to the statement that the mean-field thermodynamic potential is stationary with respect to Δ. In Fig. (F.3) the gap equation is expressed as a Feynman diagram.

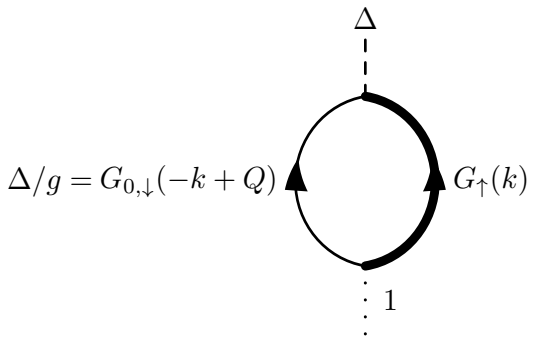

Figure F.3: Feynman diagram for the gap equation $\Delta/g = \sum_k \Delta G_{0,\downarrow}(-k+Q)G_\uparrow(k)$.

To derive the collective mode vertices, we perform all possible vertex insertions in the gap equation. In Fig. (F.3) there are three possible vertex insertions: a collective mode vertex can be inserted in the gap Δ, a bare vertex can be inserted in the bare Green's function, and a full vertex can be inserted in the full Green's function. After performing all these possible vertex insertions in the gap equation, we obtain the Feynman diagrams in Fig. (F.4).

Mathematically these Feynman diagrams are expressed as

$$\begin{aligned}\Pi^\mu/g = \Pi^\mu &\sum_k G_{0,\downarrow}(-k+Q)G_\uparrow(k+q) \\ &+ \Delta\sum_k G_{0,\downarrow}(-k+Q)G_\uparrow(k+q)\Gamma^\mu_\uparrow(k+q,k)G_\uparrow(k) \\ &+ \Delta\sum_k G_\uparrow(k+q)G_{0,\downarrow}(-k+Q)\gamma^\mu_\downarrow(-k+Q,-k-q+Q)G_{0,\downarrow}(-k-q+Q). \quad \text{(F.41)}\end{aligned}$$

Notice that the full vertex appears in this expression. If we insert the full vertex from Eq. (F.36)

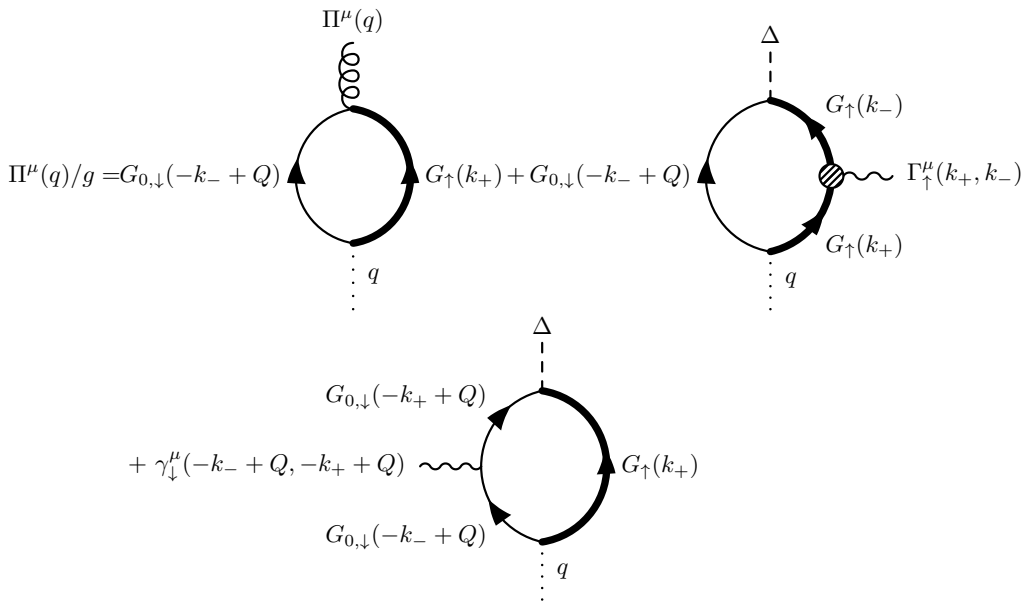

Figure F.4: Self-consistent equation for collective mode vertices after performing all possible vertex insertions in the gap equation.

into Eq. (F.41), and then shift $k \to k + Q/2$, then we obtain the following expression:

$$\begin{aligned}
&\Pi^\mu \left[1/g - \sum_k G_{0,\downarrow}(-k + Q/2) G_\uparrow(k + q + Q/2) \left(1 - |\Delta|^2 G_{0,\downarrow}(-k + Q/2) G_\uparrow(k + Q/2) \right) \right] \\
&= -\bar{\Pi}^\mu \sum_k \mathcal{G}_{12}(k + Q/2) \mathcal{G}_{12}(k + q + Q/2) \\
&+ \sum_k G_\uparrow(k + q + Q/2) \gamma^\mu_\uparrow(k + q + Q/2, k + Q/2) \mathcal{G}_{12}(k + Q/2) \\
&+ \sum_k G_{0,\downarrow}(-k + Q/2) \gamma^\mu_\downarrow(-k + Q/2, -k - q + Q/2) \mathcal{G}_{12}(k + q + Q/2) \\
&\quad \times \left(1 - |\Delta|^2 G_{0,\downarrow}(-k + Q/2) G_\uparrow(k + Q/2) \right).
\end{aligned} \tag{F.42}$$

Using the property derived in Eq. (F.7), along with Eq. (F.4) and Eq. (F.5), we obtain

$$\left(1 - |\Delta|^2 G_{0,\downarrow}(-k + Q/2) G_\uparrow(k + Q/2) \right) = G_\downarrow(-k + Q/2) / G_{0,\downarrow}(-k + Q/2). \tag{F.43}$$

Therefore Eq. (F.42) can be simplified to

$$\Pi^{\mu}\left[1/g-\sum_{k}G_{\downarrow}(-k+Q/2)G_{\uparrow}(k+q+Q/2)\right]+\bar{\Pi}^{\mu}\sum_{k}\mathcal{G}_{12}(k+Q/2)\mathcal{G}_{12}(k+q+Q/2)$$
$$=\sum_{\sigma}\sum_{k}G_{\sigma}(k+q+Q/2)\gamma_{\sigma}^{\mu}(k+q+Q/2,k+Q/2)\Delta G_{0,\bar{\sigma}}(-k+Q/2)G_{\sigma}(k+Q/2). \tag{F.44}$$

Performing the same analysis on the conjugate gap equation, $\Delta^{*}/g=\sum_{k}\Delta^{*}G_{0,\downarrow}(-k+Q)G_{\uparrow}(k)$, leads to

$$\bar{\Pi}^{\mu}\left[1/g-\sum_{k}G_{\downarrow}(-k-q+Q/2)G_{\uparrow}(k+Q/2)\right]+\Pi^{\mu}\sum_{k}\mathcal{G}_{12}^{*}(-k-Q/2)\mathcal{G}_{12}^{*}(-k-q-Q/2)$$
$$=\sum_{\sigma}\sum_{k}\Delta^{*}G_{0,\bar{\sigma}}(-k-q+Q/2)G_{\sigma}(k+q+Q/2)\gamma_{\sigma}^{\mu}(k+q+Q/2,k+Q/2)G_{\sigma}(k+Q/2). \tag{F.45}$$

The collective mode vertices can thus be written as the following matrix equation (for $q^{\mu}\neq 0$):

$$\begin{pmatrix}\Pi^{\mu}\\ \bar{\Pi}^{\mu}\end{pmatrix}=\begin{pmatrix}M_{+-} & M_{++}\\ M_{--} & M_{-+}\end{pmatrix}^{-1}\begin{pmatrix}P_{+}^{\mu}\\ P_{-}^{\mu}\end{pmatrix}. \tag{F.46}$$

Here the response functions entering into the above equation are

$$M_{+-}(q)=1/g-\sum_{k}G_{\uparrow}(k+q+Q/2)G_{\downarrow}(-k+Q/2), \tag{F.47}$$

$$M_{-+}(q)=1/g-\sum_{k}G_{\uparrow}(k+Q/2)G_{\downarrow}(-k-q+Q/2), \tag{F.48}$$

$$M_{++}(q)=\sum_{k}\mathcal{G}_{12}(k+Q/2)\mathcal{G}_{12}(k+q+Q/2), \tag{F.49}$$

$$M_{--}(q)=\sum_{k}\mathcal{G}_{12}^{*}(-k-Q/2)\mathcal{G}_{12}^{*}(-k-q-Q/2). \tag{F.50}$$

$$P_+^\mu(q) = \sum_\sigma \sum_k G_\sigma(k+q+Q/2)\gamma_\sigma^\mu(k+q+Q/2, k+Q/2)$$
$$\times \Delta G_{0,\bar{\sigma}}(-k+Q/2)G_\sigma(k+Q/2), \tag{F.51}$$
$$P_-^\mu(q) = \sum_\sigma \sum_k \Delta^* G_{0,\bar{\sigma}}(-k-q+Q/2)G_\sigma(k+q+Q/2)$$
$$\times \gamma_\sigma^\mu(k+q+Q/2, k+Q/2)G_\sigma(k+Q/2). \tag{F.52}$$

Note that, Eq. (F.46) cannot be inverted at $q^\mu = 0$. This is because of the poles of the collective mode vertices; this singularity is associated with the Nambu-Goldstone mode which restores the global $\mathrm{U}(1)$ symmetry. It will prove convenient later to study the collective modes at $q^\mu = 0$. At $q^\mu = 0$, the collective modes obey

$$\begin{pmatrix} M_{+-}(0) & M_{++}(0) \\ M_{--}(0) & M_{-+}(0) \end{pmatrix} \begin{pmatrix} \Pi^\mu(0) \\ \bar{\Pi}^\mu(0) \end{pmatrix} = \begin{pmatrix} P_+^\mu(0) \\ P_-^\mu(0) \end{pmatrix}. \tag{F.53}$$

Inserting $q^\mu = 0$ into Eqs. (F.47-F.52), we find that $P_+^\mu(0)/\Delta = P_-^\mu(0)/\Delta^* = P_0^\mu$, and $M_{++}(0)/\Delta^2 = M_{+-}(0)/|\Delta|^2 = M_{-+}(0)/|\Delta|^2 = M_{--}(0)/\left(\Delta^*\right)^2 = M_0$, where P_0^μ and M_0 are defined by

$$P_0^\mu = \sum_\sigma \sum_k G_\sigma(k+Q/2)\gamma_\sigma^\mu(k+Q/2, k+Q/2)G_{0,\bar{\sigma}}(-k+Q/2)G_\sigma(k+Q/2), \tag{F.54}$$
$$M_0 = \sum_k G_{0,\downarrow}^2(-k+Q/2)G_\uparrow^2(k+Q/2). \tag{F.55}$$

Explicit calculation shows that $P_0^x = P_0^y = 0$. For the z-component, Eq. (F.53) gives the following equation

$$M_0\left(\Delta^*\Pi^z(0) + \Delta\bar{\Pi}^z(0)\right)\begin{pmatrix} \Delta \\ \Delta^* \end{pmatrix} = P_0^z \begin{pmatrix} \Delta \\ \Delta^* \end{pmatrix}. \tag{F.56}$$

For $\Delta \neq 0$, this equation then implies that

$$\Delta^* \Pi^z(0) + \Delta \bar{\Pi}^z(0) = \frac{P_0^z}{M_0}. \tag{F.57}$$

Returning to the general $q^\mu \neq 0$ case, the final task is to check the property of the collective mode vertices: $q_\mu \Pi^\mu(q) = 2\Delta$ and $q_\mu \bar{\Pi}^\mu(q) = -2\Delta^*$, which was used in verifying the WTI for the full vertex. To do this we contract each side of Eq. (F.46) with q_μ. In order to calculate the right-hand side, we calculate the contraction $q_\mu P_\pm^\mu(q)$: explicit calculation shows that

$$q_\mu P_+^\mu(q) = 2\left(\Delta M_{+-} - \Delta^* M_{++}\right). \tag{F.58}$$

Similarly, since $\Delta^* P_+^\mu(q) = \Delta P_-^\mu(-q)$, we also find $q_\mu P_-^\mu(q) = -\left(q_\mu P_+^\mu(q)\right)^*$. The contractions of the collective mode vertices are then

$$\begin{pmatrix} q_\mu \Pi^\mu \\ q_\mu \bar{\Pi}^\mu \end{pmatrix} = \begin{pmatrix} M_{+-} & M_{++} \\ M_{--} & M_{-+} \end{pmatrix}^{-1} \begin{pmatrix} 2\left(\Delta M_{+-} - \Delta^* M_{++}\right) \\ -2\left(\Delta^* M_{-+} - \Delta M_{--}\right) \end{pmatrix} = \begin{pmatrix} 2\Delta \\ -2\Delta^* \end{pmatrix}. \tag{F.59}$$

This confirms that, for all $q^\mu \neq 0$, we have the desired relations

$$q_\mu \Pi^\mu(q) = 2\Delta, \quad q_\mu \bar{\Pi}^\mu(q) = -2\Delta^*. \tag{F.60}$$

F.4 Superfluid density derivation via Kubo formula

F.4.1 Kubo formula analysis

This section derives the explicit formula for the superfluid density tensor derived in Eq. (7.11) of section (7.3). The superfluid density tensor is defined by

$$\left(n_s^{ij}/m\right) = (n/m)\,\delta^{ij} + P^{ij}(\omega = 0, \mathbf{q} \to 0). \tag{F.61}$$

The particle number is

$$n/m = (1/m)\sum_{\sigma}\sum_{k} G_{\sigma}(k). \tag{F.62}$$

It is convenient to perform an integration by parts on the above expression as follows:

$$\begin{aligned}
(n/m)\,\delta^{ij} &= -\sum_{\sigma}\sum_{k}\gamma^{j}_{\sigma}(k,k)\frac{d}{dk^{i}}G_{\sigma}(k), \\
&= \sum_{\sigma}\sum_{k}\gamma^{j}_{\sigma}(k,k)G^{2}_{\sigma}(k)\frac{d}{dk^{i}}G^{-1}_{\sigma}(k), \\
&= \sum_{\sigma}\sum_{k}\gamma^{j}_{\sigma}(k,k)G^{2}_{\sigma}(k)\frac{d}{dk^{i}}\left(G^{-1}_{0,\sigma}(k)-\Sigma_{\sigma}(k)\right), \\
&= -\sum_{\sigma}\sum_{k}\gamma^{j}_{\sigma}(k,k)G^{2}_{\sigma}(k)\left(\gamma^{i}_{\sigma}(k,k)+|\Delta|^{2}G^{2}_{0,\bar{\sigma}}(-k+Q)\gamma^{i}_{\bar{\sigma}}(-k+Q,-k+Q)\right).
\end{aligned} \tag{F.63}$$

Combining this expression with that for the response function in Eq. (F.39), and using Eq. (F.7), we then obtain

$$\begin{aligned}
\left(\frac{n_s^{ij}}{m}\right) &= 4\sum_{k}\mathcal{G}_{12}(k+Q/2)\left(\frac{k^{i}-Q/2\delta^{iz}}{m}\right)\mathcal{G}^{*}_{12}(-k-Q/2)\left(\frac{k^{j}+Q/2\delta^{jz}}{m}\right) \\
&\quad - \lim_{q^{k}\to 0, q^{i}=q^{j}=0,\omega=0}\left[\Pi^{i}(q)P^{j}_{-}(-q)+\bar{\Pi}^{i}(q)P^{j}_{+}(-q)\right].
\end{aligned} \tag{F.64}$$

The first term represents a "bubble" contribution whereas the second terms represent the collective mode contribution. Here the order of limits is crucial. For instance, to compute n_s^{ij}, first set $\omega = 0$ and $q^i = q^j = 0$, then finally take $q^k \to 0$, where $k \neq i, k \neq j$.

Using the Gorkov function derived in Eq. (F.22), and then performing the Matsubara frequency summation in the bubble term in Eq. (F.64), the superfluid density becomes

$$\begin{aligned}
\left(\frac{n_s^{ij}}{m}\right) &= \sum_{\mathbf{k}}\frac{|\Delta|^{2}}{E^{2}_{\mathbf{kQ}}}\left(\frac{X_{\mathbf{k}}}{E_{\mathbf{kQ}}}-\beta Y_{\mathbf{k}}\right)\left(\frac{k^{i}-Q/2\delta^{iz}}{m}\right)\left(\frac{k^{j}+Q/2\delta^{jz}}{m}\right) \\
&\quad - \lim_{q^{k}\to 0, q^{i}=q^{j}=0,\omega=0}\left[\Pi^{i}(q)P^{j}_{-}(-q)+\bar{\Pi}^{i}(q)P^{j}_{+}(-q)\right].
\end{aligned} \tag{F.65}$$

As noted previously, $P_0^x = P_0^y = 0$. By taking the limit in Eq. (F.65) in the appropriate order, and using Eq. (F.57), the superfluid density then becomes

$$\left(\frac{n_s^{ij}}{m}\right) = \sum_{\mathbf{k}} \frac{|\Delta|^2}{E_{\mathbf{kQ}}^2}\left(\frac{X_{\mathbf{k}}}{E_{\mathbf{kQ}}} - \beta Y_{\mathbf{k}}\right)\left(\frac{k^i - Q/2\delta^{iz}}{m}\right)\left(\frac{k^j + Q/2\delta^{jz}}{m}\right) - \delta^{iz}\delta^{jz}\frac{\left(P_0^z\right)^2}{M_0}. \quad \text{(F.66)}$$

This produces Eq. (7.11) of section (7.3). Note that, when $\Delta = 0$, $P_0^z = 0$ so that the above expression does indeed vanish in the normal state. Similarly, for a non-FF superfluid, where $Q = 0$, $P_0^z = 0$ so that the above expression also reduces to the known result [Chien et al., 2006] in this limit. For a complete expression for the superfluid density, it only remains to compute P_0^z and M_0. The definitions of these quantities appears in Eqs. (F.54-F.55). Evaluating those expressions gives

$$P_0^z = \sum_{\mathbf{k}} \frac{1}{2E_{\mathbf{kQ}}}\left[\beta Z_{\mathbf{k}}\frac{k^z}{m} + \frac{\xi_{\mathbf{kQ}}}{E_{\mathbf{kQ}}}\left(\beta Y_{\mathbf{k}} - \frac{X_{\mathbf{k}}}{E_{\mathbf{kQ}}}\right)\frac{Q/2}{m}\right], \quad \text{(F.67)}$$

$$M_0 = \sum_{\mathbf{k}} \frac{1}{4E_{\mathbf{kQ}}^2}\left(\frac{X_{\mathbf{k}}}{E_{\mathbf{kQ}}} - \beta Y_{\mathbf{k}}\right). \quad \text{(F.68)}$$

The bubble term in Eq. (F.66) is in agreement with Eq. (16) of Ref. [Yin et al., 2014], as we will show in the next section. However, our complete expression has the inclusion of collective modes.

F.4.2 Comparison of bubble term with the literature

In this section we compare our expression for the superfluid density with that appearing in Ref. [Yin et al., 2014]. The superfluid density is defined in Eq. (F.61). Performing the Matsubara frequency summation in Eq. (F.62) gives the particle number as follows

$$\left(\frac{n}{m}\right)\delta^{ij} = \sum_{\mathbf{k}}\left(1 - \frac{\xi_{\mathbf{kQ}}}{E_{\mathbf{kQ}}}X_{\mathbf{k}}\right)\frac{\delta^{ij}}{m}. \quad \text{(F.69)}$$

Using Eq. (F.39), and performing the Matsubara frequency summation, for $P^{ij}(0)$ we find

$$P^{ij}(0) = -\sum_{\mathbf{k}} \Bigg\{ \left(\frac{k^i}{m}\right)^2 \delta^{ij} \beta Y_{\mathbf{k}} + 2\frac{k^z}{m}\frac{Q/2}{m}\delta^{iz}\delta^{jz}\beta\frac{\xi_{\mathbf{kQ}}}{E_{\mathbf{kQ}}}Z_{\mathbf{k}} + \left(\frac{Q/2}{m}\right)^2 \delta^{iz}\delta^{jz}\left[\left(\frac{\xi_{\mathbf{kQ}}}{E_{\mathbf{kQ}}}\right)^2 \beta Y_{\mathbf{k}} + \frac{|\Delta|^2}{E_{\mathbf{kQ}}^2}\frac{X_{\mathbf{k}}}{E_{\mathbf{kQ}}}\right]\Bigg\} - \delta^{iz}\delta^{jz}\frac{\left(P_0^z\right)^2}{M_0}. \tag{F.70}$$

Combining Eq. (F.69) and Eq. (F.70) then gives the superfluid density tensor

$$\left(\frac{n_s^{ij}}{m}\right) = \sum_{\mathbf{k}}\left(1 - \frac{\xi_{\mathbf{kQ}}}{E_{\mathbf{kQ}}}X_{\mathbf{k}}\right)\frac{\delta^{ij}}{m} - \sum_{\mathbf{k}} \Bigg\{ \left(\frac{k^i}{m}\right)^2 \delta^{ij} \beta Y_{\mathbf{k}} + 2\frac{k^z}{m}\frac{Q/2}{m}\delta^{iz}\delta^{jz}\beta\frac{\xi_{\mathbf{kQ}}}{E_{\mathbf{kQ}}}Z_{\mathbf{k}} + \left(\frac{Q/2}{m}\right)^2 \delta^{iz}\delta^{jz}\left[\left(\frac{\xi_{\mathbf{kQ}}}{E_{\mathbf{kQ}}}\right)^2 \beta Y_{\mathbf{k}} + \frac{|\Delta|^2}{E_{\mathbf{kQ}}^2}\frac{X_{\mathbf{k}}}{E_{\mathbf{kQ}}}\right]\Bigg\} - \delta^{iz}\delta^{jz}\frac{\left(P_0^z\right)^2}{M_0}. \tag{F.71}$$

This is in agreement with Eq. (16) of Ref. [Yin et al., 2014], up to our inclusion of collective modes, and a factor of 1/4 in the first two summations, which arises from our $Q/2$ being the Q of Ref. [Yin et al., 2014]. It only remains to prove the equivalence between Eq. (F.66) and Eq. (F.71). By performing integration by parts on the number equation in Eq. (F.69), we have

$$\left(\frac{n}{m}\right)\delta^{ij} = \sum_{\mathbf{k}} \frac{k^j}{m}\frac{d}{dk^i}\left(\frac{\xi_{\mathbf{kQ}}}{E_{\mathbf{kQ}}}X_{\mathbf{k}}\right). \tag{F.72}$$

Computing the derivative then gives

$$\left(\frac{n}{m}\right)\delta^{ij} = \sum_{\mathbf{k}} \left\{ \left[\frac{|\Delta|^2}{E_{\mathbf{kQ}}^2}\frac{X_{\mathbf{k}}}{E_{\mathbf{kQ}}} + \beta Y_{\mathbf{k}}\left(1 - \frac{|\Delta|^2}{E_{\mathbf{kQ}}^2}\right)\right]\frac{k^i}{m}\frac{k^j}{m} + \frac{k^z}{m}\frac{Q/2}{m}\delta^{iz}\delta^{jz}\beta\frac{\xi_{\mathbf{kQ}}}{E_{\mathbf{kQ}}}Z_{\mathbf{k}}\right\}. \tag{F.73}$$

The superfluid density thus becomes

$$\left(\frac{n_s^{ij}}{m}\right) = \sum_{\mathbf{k}} \frac{|\Delta|^2}{E_{\mathbf{kQ}}^2}\left(\frac{X_{\mathbf{k}}}{E_{\mathbf{kQ}}} - \beta Y_{\mathbf{k}}\right)\left(\frac{k^i - Q/2\delta^{iz}}{m}\right)\left(\frac{k^j + Q/2\delta^{jz}}{m}\right) - \sum_{\mathbf{k}}\left[\frac{k^z}{m}\frac{Q/2}{m}\delta^{iz}\delta^{jz}\beta\frac{\xi_{\mathbf{kQ}}}{E_{\mathbf{kQ}}}Z_{\mathbf{k}} + \left(\frac{Q/2}{m}\right)^2\delta^{iz}\delta^{jz}\beta Y_{\mathbf{k}}\right] - \delta^{iz}\delta^{jz}\frac{\left(P_0^z\right)^2}{M_0}. \tag{F.74}$$

Using the $W_{\mathbf{k}}$ function from Eq. (F.23), the superfluid density can be written as

$$\left(\frac{n_s^{ij}}{m}\right) = \sum_{\mathbf{k}} \frac{|\Delta|^2}{E_{\mathbf{kQ}}^2}\left(\frac{X_{\mathbf{k}}}{E_{\mathbf{kQ}}} - \beta Y_{\mathbf{k}}\right)\left(\frac{k^i - Q/2\delta^{iz}}{m}\right)\left(\frac{k^j + Q/2\delta^{jz}}{m}\right) + \frac{Q/2}{m}\delta^{iz}\delta^{jz}\sum_{\mathbf{k}}\frac{dW_{\mathbf{k}}}{dk^z} - \delta^{iz}\delta^{jz}\frac{\left(P_0^z\right)^2}{M_0}. \tag{F.75}$$

The second term gives zero contribution. Therefore the superfluid density reduces to

$$\left(\frac{n_s^{ij}}{m}\right) = \sum_{\mathbf{k}} \frac{|\Delta|^2}{E_{\mathbf{kQ}}^2}\left(\frac{X_{\mathbf{k}}}{E_{\mathbf{kQ}}} - \beta Y_{\mathbf{k}}\right)\left(\frac{k^i - Q/2\delta^{iz}}{m}\right)\left(\frac{k^j + Q/2\delta^{jz}}{m}\right) - \delta^{iz}\delta^{jz}\frac{\left(P_0^z\right)^2}{M_0}. \tag{F.76}$$

This proves the equivalence between Eq. (F.66) and Eq. (F.71).

F.5 Superfluid density derivation via equilibrium current

F.5.1 Equilibrium current analysis

The equilibrium current in the z-direction is

$$j^z = \sum_{\sigma}\sum_{k}\left(\frac{k + Q/2}{m}\right)^z G_\sigma(k + Q/2). \tag{F.77}$$

The Feynman diagram for this equilibrium current is given in Fig. (F.5).

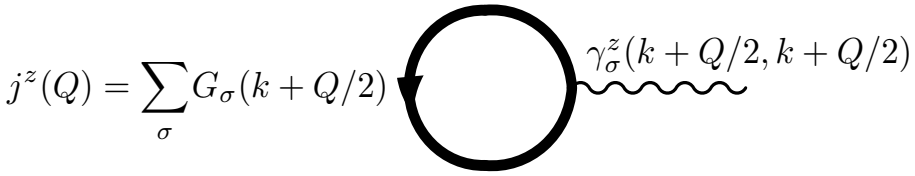

Figure F.5: Feynman diagram for the equilibrium current $j^z(Q)$.

After performing the Matsubara frequency summation, the current becomes

$$j^z = \sum_{\mathbf{k}} \frac{Q/2}{m} \left[1 - \frac{\xi_{\mathbf{kQ}}}{E_{\mathbf{kQ}}} X_{\mathbf{k}} + \frac{k^z}{Q/2} W_{\mathbf{k}} \right], \tag{F.78}$$

which is in agreement with Eq. (20) of Ref. [Yin et al., 2014] (up to a factor of 1/2 discussed earlier). The self-consistent condition for the FF pairing vector $\mathbf{Q} = Q\hat{\mathbf{z}}$ is that $j^z = 0$. This condition is equivalent to the statement that the mean-field thermodynamic potential is stationary with respect to Q. In what follows we will need the derivative of Eq. (F.77) with respect to Q, with μ and h fixed at their mean-field values. This will require the following lemma:

$$\frac{\partial}{\partial Q} G_\sigma^{-1}(k+Q/2)\bigg|_{\mu,h} = -\frac{1}{2}\Gamma^z_\sigma(k+Q/2, k+Q/2). \tag{F.79}$$

This result is proved as follows:

$$\begin{aligned}
\frac{\partial}{\partial Q} G_\sigma^{-1}(k+Q/2)\bigg|_{\mu,h} &= \frac{\partial}{\partial Q}\left(G_{0,\sigma}^{-1}(k+Q/2) - \Sigma_\sigma(k+Q/2) \right)\bigg|_{\mu,h}, \\
&= \frac{\partial}{\partial Q}\left(i\omega - \xi_{\mathbf{k}+\mathbf{Q}/2,\sigma} + |\Delta|^2 G_{0,\bar{\sigma}}(-k+Q/2) \right)\bigg|_{\mu,h}, \\
&= -\frac{1}{2m}(k+Q/2)^z + \frac{\partial |\Delta|^2}{\partial Q}\bigg|_{\mu,h} G_{0,\bar{\sigma}}(-k+Q/2) \\
&\quad - |\Delta|^2 G_{0,\bar{\sigma}}^2(-k+Q/2)\, \frac{\partial}{\partial Q} G_{0,\bar{\sigma}}^{-1}(-k+Q/2)\bigg|_{\mu,h}.
\end{aligned} \tag{F.80}$$

Inserting the expressions for the bare vertices then gives

$$\frac{\partial}{\partial Q}G_\sigma^{-1}(k+Q/2)\bigg|_{\mu,h} = -\frac{1}{2}\bigg[\gamma_\sigma^z(k+Q/2,k+Q/2) - 2\frac{\partial|\Delta|^2}{\partial Q}\bigg|_{\mu,h} G_{0,\bar\sigma}(-k+Q/2) \\ - |\Delta|^2 G_{0,\bar\sigma}^2(-k+Q/2)\gamma_{\bar\sigma}^z(-k+Q/2,-k+Q/2)\bigg]. \tag{F.81}$$

From the gap equation in Eq. (F.40) and the collective mode equation in Eq. (F.57) it follows that

$$2\frac{\partial|\Delta|^2}{\partial Q}\bigg|_{\mu,h} = \frac{P_0^z}{M_0} = \Delta^*\Pi^z(0) + \Delta\bar\Pi^z(0). \tag{F.82}$$

Inserting this relation into Eq. (F.81), and then using Eq. (F.36), gives

$$\begin{aligned}\frac{\partial}{\partial Q}G_\sigma^{-1}(k+Q/2)\bigg|_{\mu,h} &= -\frac{1}{2}\bigg[\gamma_\sigma^z(k+Q/2,k+Q/2) - \left(\Delta^*\Pi^z(0)+\Delta\bar\Pi^z(0)\right) G_{0,\bar\sigma}(-k+Q/2) \\ &\quad - |\Delta|^2 G_{0,\bar\sigma}^2(-k+Q/2)\gamma_{\bar\sigma}^z(-k+Q/2,-k+Q/2)\bigg] \\ &= -\frac{1}{2}\Gamma_\sigma^z(k+Q/2,k+Q/2).\end{aligned} \tag{F.83}$$

Thus the lemma is proved.

Taking the derivative of Eq. (F.77) gives

$$\begin{aligned}\frac{\partial j^z}{\partial Q}\bigg|_{\mu,h} &= \frac{\partial}{\partial Q}\sum_\sigma\sum_k\left(\frac{k+Q/2}{m}\right)^z G_\sigma(k+Q/2), \\ &= \frac{1}{2m}\sum_\sigma\sum_k G_\sigma(k+Q/2) + \sum_\sigma\sum_k\left(\frac{k+Q/2}{m}\right)^z \frac{\partial}{\partial Q}G_\sigma(k+Q/2)\bigg|_{\mu,h}, \\ &= \frac{n}{2m} - \sum_\sigma\sum_k\left(\frac{k+Q/2}{m}\right)^z G_\sigma^2(k+Q/2)\,\frac{\partial}{\partial Q}G_\sigma^{-1}(k+Q/2)\bigg|_{\mu,h}.\end{aligned} \tag{F.84}$$

Using the lemma in Eq. (F.79), the above expression simplifies to

$$\begin{aligned}\left.\frac{\partial j^z}{\partial Q}\right|_{\mu,h} &= \frac{1}{2}\Bigg(\frac{n}{m} + \sum_\sigma \sum_k G_\sigma(k+Q/2)\Gamma^z_\sigma(k+Q/2,k+Q/2) \\ &\qquad \times G_\sigma(k+Q/2)\gamma^z_\sigma(k+Q/2,k+Q/2)\Bigg), \\ &= \frac{1}{2}\left(\frac{n}{m} + P^{zz}(0)\right), \\ &= \frac{1}{2}\left(\frac{n_s^{zz}}{m}\right). \end{aligned} \tag{F.85}$$

Thus, the z,z-component of the superfluid density tensor is the derivative of j^z with respect to Q, at fixed μ and h.

Performing the derivative of the equilibrium current, with respect to Q, can also be understood diagrammatically. The Feynman diagram for the current in Fig. (F.5) has Q dependence in two locations: the full Green's function $G_\sigma(k+Q/2)$ and the bare vertex $\gamma^z_\sigma(k+Q/2,k+Q/2)$. Differentiating the Green's function corresponds to the insertion of the full vertex $\Gamma^z_\sigma(k+Q/2,k+Q/2)$, whereas differentiating the bare vertex corresponds to removing the external line in the tadpole diagram, which gives a bubble diagram. This procedure then gives the Feynman diagrams for the derivative of the equilibrium current as shown in Fig. (F.6). As outlined above, the derivative of the equilibrium current, with respect to Q, exactly reproduces the diagrammatic form of the response kernel.

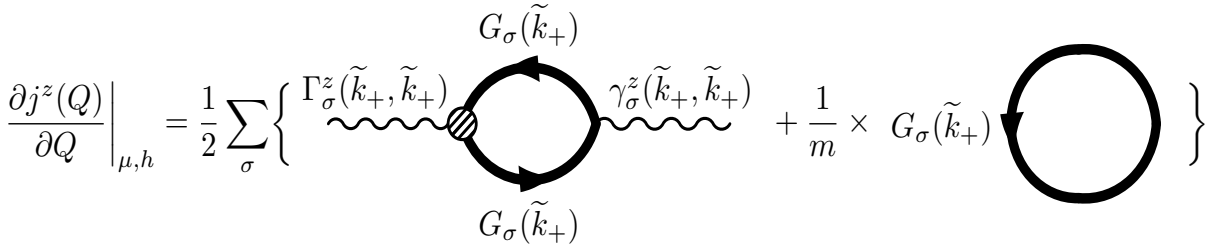

Figure F.6: Feynman diagrams of the derivative of the equilibrium current, $j^z(Q)$, with respect to Q. For convenience, here $\widetilde{k}_+ = k + Q/2$ has been used.

The explicit Q-derivative of Eq. (F.78), with μ and h fixed at their mean-field values, is

$$\left.\frac{\partial j^z}{\partial Q}\right|_{\mu,h} = \sum_{\mathbf{k}} \frac{Q/2}{m}\frac{\partial}{\partial Q}\left[1 - \frac{\xi_{\mathbf{kQ}}}{E_{\mathbf{kQ}}}X_{\mathbf{k}} + \frac{k^z}{Q/2}W_{\mathbf{k}}\right]\Bigg|_{\mu,h}. \tag{F.86}$$

Here the saddle point equation $j^z = 0$ has been used to simplify the above expression. Performing the remaining Q-derivative, and accounting for the Q-dependence in the gap Δ through Eq. (F.82), we obtain

$$\begin{aligned}\left.\frac{\partial j^z}{\partial Q}\right|_{\mu,h} = \frac{1}{2}\sum_{\mathbf{k}}\left(1 - \frac{\xi_{\mathbf{kQ}}}{E_{\mathbf{kQ}}}X_{\mathbf{k}}\right)\frac{1}{m} - \frac{1}{2}\sum_{\mathbf{k}}\Bigg\{\left(\frac{k^z}{m}\right)^2\beta Y_{\mathbf{k}} + 2\frac{k^z}{m}\frac{Q/2}{m}\beta\frac{\xi_{\mathbf{kQ}}}{E_{\mathbf{kQ}}}Z_{\mathbf{k}} \\ + \left(\frac{Q/2}{m}\right)^2\left[\left(\frac{\xi_{\mathbf{kQ}}}{E_{\mathbf{kQ}}}\right)^2\beta Y_{\mathbf{k}} + \frac{|\Delta|^2}{E_{\mathbf{kQ}}^2}\frac{X_{\mathbf{k}}}{E_{\mathbf{kQ}}}\right]\Bigg\} - \frac{1}{2}\frac{\left(P_0^z\right)^2}{M_0}.\end{aligned} \tag{F.87}$$

Thus, from Eq. (F.85), it follows that the superfluid density is

$$\begin{aligned}\left(\frac{n_s^{zz}}{m}\right) = \sum_{\mathbf{k}}\left(1 - \frac{\xi_{\mathbf{kQ}}}{E_{\mathbf{kQ}}}X_{\mathbf{k}}\right)\frac{1}{m} - \sum_{\mathbf{k}}\Bigg\{\left(\frac{k^z}{m}\right)^2\beta Y_{\mathbf{k}} + 2\frac{k^z}{m}\frac{Q/2}{m}\beta\frac{\xi_{\mathbf{kQ}}}{E_{\mathbf{kQ}}}Z_{\mathbf{k}} \\ + \left(\frac{Q/2}{m}\right)^2\left[\left(\frac{\xi_{\mathbf{kQ}}}{E_{\mathbf{kQ}}}\right)^2\beta Y_{\mathbf{k}} + \frac{|\Delta|^2}{E_{\mathbf{kQ}}^2}\frac{X_{\mathbf{k}}}{E_{\mathbf{kQ}}}\right]\Bigg\} - \frac{\left(P_0^z\right)^2}{M_0}.\end{aligned} \tag{F.88}$$

This reproduces the result in Eq. (F.71), which was shown in appendix (F.4.2) to be equivalent to Eq. (F.66).

F.5.2 Vanishing of the superfluid density in directions transverse to Q

Interestingly, due to the underlying rotational invariance of the FF state [Radzihovsky, 2011], the perpendicular components of the superfluid density tensor vanish: $n_s^{xx} = n_s^{yy} = 0$. This result was proved, analytically for $T = 0$ and numerically for finite T, in Ref. [Yin et al., 2014]. Here we analytically prove that $n_s^{xx} = 0$ for all temperatures. Setting $i = j = x$ in Eq. (F.65) gives zero

collective mode contribution; thus we obtain

$$\left(\frac{n_s^{xx}}{m}\right) = \sum_{\mathbf{k}} \frac{|\Delta|^2}{E_{\mathbf{kQ}}^2} \left(\frac{X_{\mathbf{k}}}{E_{\mathbf{kQ}}} - \beta Y_{\mathbf{k}}\right) \left(\frac{k^x}{m}\right)^2. \tag{F.89}$$

The self-consistent equation for Q is given in Eq. (F.78). After performing integration by parts on the expression in Eq. (F.78), we obtain

$$j^z = -(Q/2) \sum_{\mathbf{k}} \frac{k^x}{m} \frac{d}{dk^x} \left[1 - \frac{\xi_{\mathbf{kQ}}}{E_{\mathbf{kQ}}} X_{\mathbf{k}} + \frac{k^z}{Q/2} W_{\mathbf{k}}\right]. \tag{F.90}$$

Evaluating the derivatives and simplifying then gives

$$j^z = (Q/2) \left(\frac{n_s^{xx}}{m}\right) - m \sum_{\mathbf{k}} \left(\frac{k^x}{m}\right)^2 \frac{dW_{\mathbf{k}}}{dk^z}. \tag{F.91}$$

The second term gives zero contribution, and thus

$$\left(\frac{n_s^{xx}}{m}\right) = \frac{j^z}{Q/2} = 0. \tag{F.92}$$

In the last step the saddle-point condition $j^z = 0$ has been used. Thus the x, x-component (and similarly the y, y-component) of the superfluid density tensor vanishes as a result of the self-consistent condition for the pairing vector Q.

F.6 Thermodynamic potential and stability criteria

In Eq. (F.85) it was shown that the superfluid density is related to the partial derivative of the z-component of the equilibrium current with μ and h fixed at their mean-field values. This equation can be expressed in terms of the thermodynamic potential, which then allows constraints on the stability of the FF phase to be studied.

The mean-field thermodynamic potential is given by [Chen et al., 2007, Yin et al., 2014]

$$\Omega = \frac{|\Delta|^2}{g} - \beta^{-1} \sum_{\mathbf{k}} \left\{ \log \left[2\cosh(\beta E_{\mathbf{kQ}}) + 2\cosh(\beta h_{\mathbf{kQ}}) \right] - \beta \xi_{\mathbf{kQ}} \right\}. \tag{F.93}$$

The saddle-point conditions are given by

$$\left.\frac{\partial \Omega}{\partial \Delta}\right|_{\mu,h,Q} = 0, \quad \left.\frac{\partial \Omega}{\partial \Delta^*}\right|_{\mu,h,Q} = 0, \quad \left.\frac{\partial \Omega}{\partial Q}\right|_{\mu,h,\Delta,\Delta^*} = 0. \tag{F.94}$$

The first two of these conditions can be combined to give the following gap equation

$$\left.\frac{\partial \Omega}{\partial |\Delta|}\right|_{\mu,h,Q} = 0. \tag{F.95}$$

Explicit calculation then gives

$$2|\Delta| \left(\frac{1}{g} - \sum_{\mathbf{k}} \frac{X_{\mathbf{k}}}{2E_{\mathbf{kQ}}} \right) = 0, \tag{F.96}$$

The third condition in Eq. (F.94) reproduces the constraint that the equilibrium current j^z vanishes

$$\frac{1}{2} \sum_{\mathbf{k}} \frac{Q/2}{m} \left[1 - \frac{\xi_{\mathbf{kQ}}}{E_{\mathbf{kQ}}} X_{\mathbf{k}} + \frac{k^z}{Q/2} W_{\mathbf{k}} \right] = 0. \tag{F.97}$$

The partial derivative of j^z at fixed μ and h is given by

$$\left.\frac{\partial j^z}{\partial Q}\right|_{\mu,h} = \left.\frac{\partial j^z}{\partial Q}\right|_{\mu,h,|\Delta|} + \left.\frac{\partial j^z}{\partial |\Delta|}\right|_{\mu,h,Q} \left.\frac{\partial |\Delta|}{\partial Q}\right|_{\mu,h}. \tag{F.98}$$

The equilibrium current is related to the thermodynamic potential by $j^z = 2\,(\partial\Omega/\partial Q)|_{\mu,h,|\Delta|}$; thus Eq. (F.98) can be expressed as

$$\frac{1}{2} \left.\frac{\partial j^z}{\partial Q}\right|_{\mu,h} = \left.\frac{\partial^2 \Omega}{\partial Q^2}\right|_{\mu,h,|\Delta|} + \left[\left.\frac{\partial}{\partial |\Delta|} \left(\left.\frac{\partial \Omega}{\partial Q}\right|_{\mu,h,|\Delta|} \right) \right|_{\mu,h,|\Delta|} \right]_{\mu,h,Q} \left.\frac{\partial |\Delta|}{\partial Q}\right|_{\mu,h}. \tag{F.99}$$

To compute the remaining term, $(\partial|\Delta|/\partial Q)|_{\mu,h}$, we first consider the gap equation in Eq. (F.95):

$$\left.\frac{\partial\Omega}{\partial|\Delta|}\right|_{\mu,h,Q} = 0. \tag{F.95}$$

Differentiating this equation with respect to Q, at fixed μ and h, then gives

$$\left.\frac{\partial}{\partial Q}\left[\left.\frac{\partial\Omega}{\partial|\Delta|}\right|_{\mu,h,Q}\right]\right|_{\mu,h} = 0, \tag{F.100}$$

$$\Rightarrow \left.\left[\frac{\partial}{\partial Q}\left(\left.\frac{\partial\Omega}{\partial|\Delta|}\right)\right|_{\mu,h,Q}\right]\right|_{\mu,h,|\Delta|} + \left.\frac{\partial^2\Omega}{\partial|\Delta|^2}\right|_{\mu,h,Q}\left.\frac{\partial|\Delta|}{\partial Q}\right|_{\mu,h} = 0. \tag{F.101}$$

Rearranging then gives

$$\left.\frac{\partial|\Delta|}{\partial Q}\right|_{\mu,h} = -\left.\left[\frac{\partial}{\partial Q}\left(\left.\frac{\partial\Omega}{\partial|\Delta|}\right)\right|_{\mu,h,Q}\right]\right|_{\mu,h,|\Delta|} \Bigg/ \left.\frac{\partial^2\Omega}{\partial|\Delta|^2}\right|_{\mu,h,Q}. \tag{F.102}$$

Inserting this into Eq. (F.99), and then using the fact that the second order partial derivatives of Ω with respect to Q and $|\Delta|$ are symmetric in one another, we obtain

$$\frac{1}{4}\left(\frac{n_s^{zz}}{m}\right) = \frac{1}{2}\left.\frac{\partial j^z}{\partial Q}\right|_{\mu,h} = \left.\frac{\partial^2\Omega}{\partial Q^2}\right|_{\mu,h,|\Delta|} - \left\{\left.\left[\frac{\partial}{\partial|\Delta|}\left(\left.\frac{\partial\Omega}{\partial Q}\right)\right|_{\mu,h,|\Delta|}\right]\right|_{\mu,h,Q}\right\}^2 \Bigg/ \left.\frac{\partial^2\Omega}{\partial|\Delta|^2}\right|_{\mu,h,Q}. \tag{F.103}$$

Thus, by taking various partial derivatives of the thermodynamic potential Ω, one can compute the superfluid density in the z,z-direction, with the collective mode contribution incorporated. The first term is the bubble contribution while the second term is the collective mode contribution.

By explicit calculation, we obtain

$$\left.\frac{\partial^2\Omega}{\partial Q^2}\right|_{\mu,h,|\Delta|} = \frac{1}{4}\sum_{\mathbf{k}}\left(1-\frac{\xi_{\mathbf{kQ}}}{E_{\mathbf{kQ}}}X_{\mathbf{k}}\right)\frac{1}{m} - \frac{1}{4}\sum_{\mathbf{k}}\Bigg\{\left(\frac{k^z}{m}\right)^2\beta Y_{\mathbf{k}} + 2\frac{k^z}{m}\frac{Q/2}{m}\beta\frac{\xi_{\mathbf{kQ}}}{E_{\mathbf{kQ}}}Z_{\mathbf{k}} + \left(\frac{Q/2}{m}\right)^2\left[\left(\frac{\xi_{\mathbf{kQ}}}{E_{\mathbf{kQ}}}\right)^2\beta Y_{\mathbf{k}} + \frac{|\Delta|^2}{E_{\mathbf{kQ}}^2}\frac{X_{\mathbf{k}}}{E_{\mathbf{kQ}}}\right]\Bigg\}, \tag{F.104}$$

$$\left[\frac{\partial}{\partial|\Delta|}\left(\frac{\partial\Omega}{\partial Q}\right)\Big|_{\mu,h,|\Delta|}\right]\Bigg|_{\mu,h,Q} = -|\Delta|P_0^z, \tag{F.105}$$

$$\left.\frac{\partial^2\Omega}{\partial|\Delta|^2}\right|_{\mu,h,Q} = 4|\Delta|^2 M_0, \tag{F.106}$$

where P_0^z and M_0 are defined in Eqs. (F.67-F.68). Inserting these definitions into Eq. (F.103) and simplifying then reproduces

$$\left(\frac{n_s^{zz}}{m}\right) = \sum_{\mathbf{k}}\left(1-\frac{\xi_{\mathbf{kQ}}}{E_{\mathbf{kQ}}}X_{\mathbf{k}}\right)\frac{1}{m} - \sum_{\mathbf{k}}\Bigg\{\left(\frac{k^z}{m}\right)^2\beta Y_{\mathbf{k}} + 2\frac{k^z}{m}\frac{Q/2}{m}\beta\frac{\xi_{\mathbf{kQ}}}{E_{\mathbf{kQ}}}Z_{\mathbf{k}} + \left(\frac{Q/2}{m}\right)^2\left[\left(\frac{\xi_{\mathbf{kQ}}}{E_{\mathbf{kQ}}}\right)^2\beta Y_{\mathbf{k}} + \frac{|\Delta|^2}{E_{\mathbf{kQ}}^2}\frac{X_{\mathbf{k}}}{E_{\mathbf{kQ}}}\right]\Bigg\} - \frac{\left(P_0^z\right)^2}{M_0}, \tag{F.107}$$

which is the expression for n_s^{zz} obtained in Eq. (F.71) and is equivalent to Eq. (F.66).

The stability criteria for the FF superfluid are [Wang et al., 2017]

$$\left.\frac{\partial^2\Omega}{\partial Q^2}\right|_{\mu,h,|\Delta|} - \left\{\left[\frac{\partial}{\partial|\Delta|}\left(\frac{\partial\Omega}{\partial Q}\right)\Big|_{\mu,h,|\Delta|}\right]\Bigg|_{\mu,h,Q}\right\}^2 \Bigg/ \left.\frac{\partial^2\Omega}{\partial|\Delta|^2}\right|_{\mu,h,Q} > 0, \tag{F.108}$$

$$\left.\frac{\partial^2\Omega}{\partial|\Delta|^2}\right|_{\mu,h,Q} > 0. \tag{F.109}$$

The first expression is related to n_s^{zz} by Eq. (F.103). Thus the FF phase is stable if the following two conditions are satisfied: $n_s^{zz} > 0$, $\left.\frac{\partial^2\Omega}{\partial|\Delta|^2}\right|_{\mu,h,Q} > 0$.

BIBLIOGRAPHY

Abrikosov, A. A., Gorkov, L. P., & Dzyaloshinskii, I. E. 1975, Methods of quantum field theory in statistical physics, Dover books on physics series (Dover publications)

Alicea, J. 2012, Reports on Progress in Physics, 75, 076501

Altland, A., & Simons, B. D. 2010, Condensed matter field theory (Cambridge University Press)

Ambegaokar, V., & Kadanoff, L. P. 1961, Nuovo Cimento, 22, 914

Anderson, B. M., Boyack, R., Wu, C.-T., & Levin, K. 2016, Phys. Rev. B, 93, 180504

Anderson, B. M., Wu, C.-T., Boyack, R., & Levin, K. 2015, Phys. Rev. B, 92, 134523

Anderson, P. W. 1958, Phys. Rev., 110, 827

—. 1963, Phys. Rev., 130, 439

Andrenacci, N., Pieri, P., & Strinati, G. C. 2003, Phys. Rev. B, 68, 144507

Arseev, P. I., Loiko, S. O., & Fedorov, N. K. 2006, Physics-Uspekhi, 49, 1

Bardeen, J., Cooper, L. N., & Schrieffer, J. R. 1957a, Phys. Rev., 106, 162

—. 1957b, Phys. Rev., 108, 1175

Baym, G. 1962, Phys. Rev., 127, 1391

Baym, G., & Kadanoff, L. P. 1961, Phys. Rev., 124, 287

Bergeron, D., Hankevych, V., Kyung, B., & Tremblay, A.-M. S. 2011, Phys. Rev. B, 84, 085128

Bogoliubov, N. N. 1958, JETP, 7, 41

Boyack, R., Anderson, B. M., Wu, C.-T., & Levin, K. 2016, Phys. Rev. B, 94, 094508

Boyack, R., Wu, C.-T., Anderson, B. M., & Levin, K. 2017a, Phys. Rev. B, 95, 214501

Boyack, R., Wu, C.-T., Scherpelz, P., & Levin, K. 2014, Phys. Rev. B, 90, 220513

—. 2017b, Phys. Rev. B, 95, 099904

Brinckmann, J., & Lee, P. A. 1999, Phys. Rev. Lett., 82, 2915

Browne, D. A., & Levin, K. 1983, Phys. Rev. B, 28, 4029

Casalbuoni, R., & Nardulli, G. 2004, Rev. Mod. Phys., 76, 263

Cea, T., Castellani, C., Seibold, G., & Benfatto, L. 2015, Phys. Rev. Lett., 115, 157002

Chen, H.-D., Vafek, O., Yazdani, A., & Zhang, S.-C. 2004, Phys. Rev. Lett., 93, 187002

Chen, Q., He, Y., Chien, C.-C., & Levin, K. 2007, Phys. Rev. B, 75, 014521

Chen, Q., Kosztin, I., Jankó, B., & Levin, K. 1999, Phys. Rev. B, 59, 7083

Chen, Q., Stajic, J., Tan, S., & Levin, K. 2005, Phys. Rep., 412, 1

Cheuk, L. W., Sommer, A. T., Hadzibabic, Z., Yefsah, T., Bakr, W. S., & Zwierlein, M. W. 2012, Phys. Rev. Lett., 109, 095302

Chien, C.-C., Chen, Q., He, Y., & Levin, K. 2006, Phys. Rev. Lett., 97, 090402

Chung, S., & Roy, R. 2014, Phys. Rev. B, 90, 224510

Comin, R. et al. 2014, Science, 343, 390

Cooper, L. N. 1956, Phys. Rev., 104, 1189

Corson, J., Mallozzi, R., Orenstein, J., Eckstein, J. N., & Bozovic, I. 1999, Nature, 398, 221

Dai, P., Mook, H. A., Hayden, S. M., Aeppli, G., Perring, T. G., Hunt, R. D., & Doğan, F. 1999, Science, 284, 1344

Diener, R. B., Sensarma, R., & Randeria, M. 2008, Phys. Rev. A, 77, 023626

Drummond, P. D., Hu, H., & Liu, X. J. 2009, J. Mod. Opt., 56, 2076

Eagles, D. M. 1969, Phys. Rev., 186, 456

Eliashberg, G. 1960, Sov. Phys. JETP, 11, 696

Elitzur, S. 1975, Phys. Rev. D, 12, 3978

Endres, M. et al. 2012, Nature, 487, 454

Engelbrecht, J. R., Randeria, M., & Sáde Melo, C. A. R. 1997, Phys. Rev. B, 55, 15153

Englert, F., & Brout, R. 1964, Phys. Rev. Lett., 13, 321

Ercolessi, E., Morandi, G., Pieri, P., & Roncaglia, M. 2000, Phys. Rev. B, 62, 14860

Förster, D. 1975, Hydrodynamic fluctuations, broken symmetry and correlation functions (Reading, MA : Benjamin)

Fradkin, E. 2012, Electronic liquid crystal phases in strongly correlated systems (Springer), 53–116

—. 2013, Field theories of condensed matter physics (Cambridge University Press)

Fradkin, E., Kivelson, S. A., Lawler, M. J., Esisenstein, J. P., & Mackenzie, A. P. 2010, Annu. Rev. Condens. Matter Phys., 78, 153

Fradkin, E., Kivelson, S. A., & Tranquada, J. M. 2015, Rev. Mod. Phys., 87, 457

Fu, L., & Kane, C. L. 2008, Phys. Rev. Lett., 100, 096407

Fu, Z., Huang, L., Meng, Z., Wang, P., Liu, X.-J., Pu, H., Hu, H., & Zhang, J. 2013, Phys. Rev. A, 87, 053619

Fukushima, N., Ohashi, Y., Taylor, E., & Griffin, A. 2007, Phys. Rev. A, 75, 033609

Fulde, P., & Ferrell, R. A. 1964, Phys. Rev., 135, A550

Ghiringhelli, G. et al. 2012, Science, 337, 821

Gilbert, W. 1964, Phys. Rev. Lett., 12, 713

Giorgini, S., Pitaevskii, L. P., & Stringari, S. 2008, Rev. Mod. Phys., 80, 1215

Goldman, N., Juzeliūnas, G., Öhberg, P., & Spielman, I. B. 2014, Reports on Progress in Physics, 77, 126401

Goldstone, J. 1961, Il Nuovo Cimento (1955-1965), 19, 154

Goldstone, J., Salam, A., & Weinberg, S. 1962, Phys. Rev., 127, 965

Gong, M., Tewari, S., & Zhang, C. 2011, Phys. Rev. Lett., 107, 195303

Goryo, J., & Ishikawa, K. 1999, Phys. Lett. A, 260, 294

Greiter, M. 2005, Annals of Physics, 319, 217

Guo, H., Chien, C.-C., & He, Y. 2013a, J. Low Temp. Phys., 172, 5

Guo, H., Chien, C.-C., & Levin, K. 2010, Phys. Rev. Lett., 105, 120401

Guo, H., He, Y., Chien, C.-C., & Levin, K. 2013b, Phys. Rev. A, 88, 043644

Guralnik, G. S., Hagen, C. R., & Kibble, T. W. B. 1964, Phys. Rev. Lett., 13, 585

—. 1968, Advances in Particle Physics, 2, 567

Hamidian, M. H. et al. 2016, Nature, 532, 343

Han, L., & Sá de Melo, C. A. R. 2012, Phys. Rev. A, 85, 011606

Hasan, M. Z., & Kane, C. L. 2010, Rev. Mod. Phys., 82, 3045

Haussmann, R., Rantner, W., Cerrito, S., & Zwerger, W. 2007, Phys. Rev. A, 75, 023610

He, L. 2016, Annals of Physics, 373, 470

He, L., & Huang, X.-G. 2012, Phys. Rev. Lett., 108, 145302

—. 2013, Annals of Physics, 337, 163

He, L., Huang, X.-G., Hu, H., & Liu, X.-J. 2013, Phys. Rev. A, 87, 053616

He, L., Lü, H., Cao, G., Hu, H., & Liu, X.-J. 2015, Phys. Rev. A, 92, 023620

He, Y., Chien, C.-C., Chen, Q., & Levin, K. 2007a, Phys. Rev. A, 75, 021602

—. 2007b, Phys. Rev. B, 76, 224516

He, Y., & Guo, H. 2015, ArXiv e-prints

Henrici, P., ed. 1986, Applied and computational complex analysis. Vol. 3: Discrete Fourier analysis–Cauchy integrals–construction of conformal maps—univalent functions (New York, NY, USA: John Wiley & Sons, Inc.)

Higbie, J., & Stamper-Kurn, D. M. 2004, Phys. Rev. A, 69, 053605

Higgs, P. W. 1964, Phys. Rev. Lett., 13, 508

Hinkov, V. et al. 2007, Nature Physics, 3, 780

Hu, H. 2012, Front. Phys., 7, 98

Hu, H., Drummond, P. D., & Liu, X.-J. 2007, Nature Physics, 3, 469

Hu, H., Jiang, L., Liu, X.-J., & Pu, H. 2011, Phys. Rev. Lett., 107, 195304

Hu, H., Liu, X.-J., & Drummond, P. D. 2006, Europhys. Lett., 74, 574

Huang, L. et al. 2016, Nature Physics, 12, 540

Hur, K. L., & Maurice Rice, T. 2009, Ann. Phys., 324, 1452

Iskin, M., & Subaşı, A. L. 2011, Phys. Rev. Lett., 107, 050402

James, A. J. A., Konik, R. M., & Rice, T. M. 2012a, Phys. Rev. B, 86, 100508

—. 2012b, Phys. Rev. B, 86, 100508(R)

Jiang, L., Liu, X.-J., Hu, H., & Pu, H. 2011, Phys. Rev. A, 84, 063618

Kadanoff, L. P., & Martin, P. C. 1961, Phys. Rev., 124, 670

Kamenev, A., & Andreev, A. 1999, Phys. Rev. B, 60, 2218

Kao, Y.-J., Si, Q., & Levin, K. 2000, Phys. Rev. B, 61, R11898

Ketterle, W., & Zwierlein, M. W. 2008, Rivista del Nuovo Cimento, 31, 247

Kivelson, S. A., Fradkin, E., & Emery, V. J. 1998, Nature, 393, 550

Kosztin, I., Chen, Q., Kao, Y.-J., & Levin, K. 2000, Phys. Rev. B, 61, 11662

Kulik, I. O., Entin-Wohlman, O., & Orbach, R. 1981, Journal of Low Temperature Physics, 43, 591

Larkin, A., & Ovchinnikov, I. 1965, Soviet Physics-JETP, 20, 762

Le Tacon, M. et al. 2011, Nature Physics, 7, 725

Lee, P. A. 2014, Phys. Rev. X, 4, 031017

Leggett, A. J. 1980, Diatomic molecules and cooper pairs (Berlin, Heidelberg: Springer Berlin Heidelberg), 13–27

Li, L., Wang, Y., Komiya, S., Ono, S., Ando, Y., Gu, G. D., & Ong, N. P. 2010, Phys. Rev. B, 81, 054510

Lin, Y. J., Jimenez-Garcia, K., & Spielman, I. B. 2011, Nature, 471, 83

Littlewood, P. B., & Varma, C. M. 1981, Phys. Rev. Lett., 47, 811

Liu, D. Z., Zha, Y., & Levin, K. 1995, Phys. Rev. Lett., 75, 4130

Loeser, A. G., Shen, Z.-X., Dessau, D. S., Marshall, D. S., Park, C. H., Fournier, P., & Kapitulnik, A. 1996, Science, 273, 325

Loktev, V. M., Quick, R. M., & Sharapov, S. G. 2001, Phys. Rep., 349, 1

Lutchyn, R. M., Nagornykh, P., & Yakovenko, V. M. 2008, Phys. Rev. B, 77, 144516

Lykken, J., & Spiropulu, M. 2013, Phys. Today, 66, 26

Maly, J., Jankó, B., & Levin, K. 1999, Physica C: Superconductivity, 321, 113

Matsunaga, R., Hamada, Y. I., Makise, K., Uzawa, Y., Terai, H., Wang, Z., & Shimano, R. 2013, Phys. Rev. Lett., 111, 057002

Millis, A. J. 1987, Phys. Rev. B, 35, 151

Nambu, Y. 1960, Phys. Rev., 117, 648

Nambu, Y., & Jona-Lasinio, G. 1961a, Phys. Rev., 122, 345

—. 1961b, Phys. Rev., 124, 246

Nayak, C., Simon, S. H., Stern, A., Freedman, M., & Das Sarma, S. 2008, Rev. Mod. Phys., 80, 1083

Norman, M. R. 2000, Phys. Rev. B, 61, 14751

Norman, M. R., Randeria, M., Ding, H., & Campuzano, J. C. 1998, Phys. Rev. B, 57, R11093

Nozières, P. 1964, Theory of interacting Fermi systems (Benjamin)

Nozières, P., & Schmitt-Rink, S. 1985, J. Low Temp. Phys., 59, 195

Ojanen, T., & Kitagawa, T. 2013, Phys. Rev. B, 87, 014512

Pan, S. H., Hudson, E. W., Gupta, A. K., Ng, K.-W., Eisaki, H., Uchida, S., & Davis, J. C. 2000, Phys. Rev. Lett., 85, 1536

Parks, R. 1969, Superconductivity: Part 1 (In Two Parts), Superconductivity (Taylor & Francis)

Patton, B. R. 1971, The effect of fluctuations in superconducting alloys above the transition temperature. Ph.D Thesis. (Unpublished, Cornell University)

Pekker, D., & Varma, C. M. 2015, Annual Review of Condensed Matter Physics, 6, 269

Perali, A., Pieri, P., Pisani, L., & Strinati, G. C. 2004, Phys. Rev. Lett., 92, 220404

Pieri, P., Pisani, L., & Strinati, G. C. 2004, Phys. Rev. B, 70, 094508

Pieri, P., & Strinati, G. C. 2005, Phys. Rev. B, 71, 094520

Pines, D., & Nozières, P. 1966, The theory of quantum liquids. Vol. 1: Normal Fermi liquids (New York)

Pollet, L., & Prokof'ev, N. 2012, Phys. Rev. Lett., 109, 010401

Pomeranchuk, I. Y. 1958, Sov. Phys. JETP, 8, 361

Qi, X.-L., & Zhang, S.-C. 2011, Rev. Mod. Phys., 83, 1057

Radzihovsky, L. 2011, Phys. Rev. A, 84, 023611

Radzihovsky, L., & Sheehy, D. E. 2010, Reports on Progress in Physics, 73, 076501

Randeria, M., Griffin, A., & Snoke, D. 1995, Bose-Einstein Condensation (Cambridge University Press Cambridge), 355–392

Read, N., & Green, D. 2000, Phys. Rev. B, 61, 10267

Rickayzen, G. 1959, Phys. Rev., 115, 795

—. 1965, Interscience monographs and texts in physics and astronomy, Vol. 14, Theory of superconductivity (Interscience Publishers)

Roy, R., & Kallin, C. 2008, Phys. Rev. B, 77, 174513

Ryder, L. H. 1996, Quantum field theory, 2nd edn. (Cambridge University Press)

Sakai, S., Civelli, M., & Imada, M. 2016, Phys. Rev. Lett., 116, 057003

Salasnich, L., Marchetti, P. A., & Toigo, F. 2013, Phys. Rev. A, 88, 053612

Samokhin, K. V. 2010, Phys. Rev. B, 81, 224507

Sato, M., Takahashi, Y., & Fujimoto, S. 2009, Phys. Rev. Lett., 103, 020401

Schafroth, M. R. 1958, Phys. Rev., 111, 72

Scherpelz, P., Rançon, A., He, Y., & Levin, K. 2014, Phys. Rev. B, 90, 060506

Schrieffer, J. R. 1964, Theory of superconductivity, 1st edn. (W.A. Benjamin, Inc.)

Seo, K., Han, L., & Sá de Melo, C. A. R. 2012, Phys. Rev. A, 85, 033601

Seo, K., Zhang, C., & Tewari, S. 2013, Phys. Rev. A, 87, 063618

Serene, J. W. 1989, Phys. Rev. B, 40, 10873

Sherman, D. et al. 2015, Nature Physics, 11, 188

Si, Q., Lu, J. P., & Levin, K. 1992, Phys. Rev. B., 45, 4930

Si, Q., Zha, Y., Levin, K., & Lu, J. P. 1993, Phys. Rev. B, 47, 9055

Soto-Garrido, R., & Fradkin, E. 2014, Phys. Rev. B, 89, 165126

Soto-Garrido, R., Wang, Y., Fradkin, E., & Cooper, S. L. 2017, Phys. Rev. B, 95, 214502

Stajic, J., Milstein, J. N., Chen, Q. J., Chiofalo, M. L., Holland, M. J., & Levin, K. 2004, Phys. Rev. A, 69, 063610

Stemmann, G., Pépin, C., & Lavagna, M. 1994, Phys. Rev. B, 50, 4075

Sterman, G. 1993, An introduction to quantum field theory (Cambridge University Press)

Stewart, J. T., Gaebler, J. P., & Jin, D. S. 2008, Nature Physics, 454, 744

Stock, C., Buyers, W. J. L., Liang, R., Peets, D., Tun, Z., Bonn, D., Hardy, W. N., & Birgeneau, R. J. 2004, Phys. Rev. B, 69, 014502

Sun, K., Fregoso, B. M., Lawler, M. J., & Fradkin, E. 2008, Phys. Rev. B, 78, 085124

Taylor, E., Griffin, A., Fukushima, N., & Ohashi, Y. 2006, Phys. Rev. A, 74, 063626

Taylor, E., Griffin, A., & Ohashi, Y. 2007, Phys. Rev. A, 76, 023614

Veeravalli, G., Kuhnle, E., Dyke, P., & Vale, C. J. 2008, Phys. Rev. Lett., 101, 250403

Vollhardt, D., & Wolfle, P. 2013, The superfluid phases of helium 3 (Courier Corporation)

Vyasanakere, J. P., & Shenoy, V. B. 2011, Phys. Rev. B, 83, 094515

—. 2015, Phys. Rev. B, 92, 121111

Vyasanakere, J. P., Zhang, S., & Shenoy, V. B. 2011, Phys. Rev. B, 84, 014512

Wang, C.-Y., & He, Y. 2015, Physics Letters A, 379, 3089

Wang, J., Che, Y., Zhang, L., & Chen, Q. 2017, Scientific Reports, 7

Wang, P., Yu, Z.-Q., Fu, Z., Miao, J., Huang, L., Chai, S., Zhai, H., & Zhang, J. 2012, Phys. Rev. Lett., 109, 095301

Wise, W. D., Boyer, M. C., Chatterjee, K., Kondo, T., Takeuchi, T., Ikuta, H., Wang, Y., & Hudson, E. W. 2008, Nature Physics, 4, 696

Wu, C., Sun, K., Fradkin, E., & Zhang, S.-C. 2007, Phys. Rev. B, 75, 115103

Wu, C.-T., Anderson, B. M., Boyack, R., & Levin, K. 2015, Phys. Rev. B, 91, 220504

Yang, K.-Y., Rice, T. M., & Zhang, F.-C. 2006, Phys. Rev. B, 73, 174501

Yi, W., & Guo, G.-C. 2011, Phys. Rev. A, 84, 031608

Yin, S., Martikainen, J.-P., & Törmä, P. 2014, Phys. Rev. B, 89, 014507

Yu, Z., Bruun, G. M., & Baym, G. 2009, Phys. Rev. A, 80, 023615

Yu, Z.-Q. 2014, Phys. Rev. A, 90, 053608

Yu, Z.-Q., & Zhai, H. 2011, Phys. Rev. Lett., 107, 195305

Zee, A. 2010, Quantum field theory in a nutshell, 2nd edn. (Princeton University Press)

Zha, Y., Levin, K., & Si, Q. 1993a, Phys. Rev. B, 47, 9124

Zha, Y., Si, Q., & Levin, K. 1993b, Physica C, 212, 413

Zhai, H. 2015, Reports on Progress in Physics, 78, 026001

Zhang, C., Tewari, S., Lutchyn, R. M., & Das Sarma, S. 2008, Phys. Rev. Lett., 101, 160401

Zheng, Z., Pu, H., Zou, X., & Guo, G. 2014, Phys. Rev. A, 90, 063623

Zhou, J., Zhang, W., & Yi, W. 2011, Phys. Rev. A, 84, 063603

Zhou, K., & Zhang, Z. 2012, Phys. Rev. Lett., 108, 025301

Zwerger, W. 2011, The BCS-BEC Crossover and the Unitary Fermi Gas, Lecture Notes in Physics (Springer Berlin Heidelberg)